IC 8818

Bureau of Mines Information Circular/1980

The Physical Chemistry of Mineral-Reagent Interactions in Sulfide Flotation

Proceedings of Symposium
Held at College Park, Md., April 6-7, 1978

Compiled by Paul E. Richardson, Garrett R. Hyde,
and Morris S. Ojalvo

NEWARK PUBLIC LIBRARY

JUN 20 1980

U. S. GOVT. PUBS.
DEPOSITORY 375

UNITED STATES DEPARTMENT OF THE INTERIOR

I 28.27:

Information Circular 8818

The Physical Chemistry of Mineral-Reagent Interactions in Sulfide Flotation

Proceedings of Symposium
Held at College Park, Md., April 6-7, 1978

Compiled by Paul E. Richardson, Garrett R. Hyde,
and Morris S. Ojalvo

March 3, 1849

UNITED STATES DEPARTMENT OF THE INTERIOR
Cecil D. Andrus, Secretary

BUREAU OF MINES
Lindsay D. Norman, Acting Director

READEX
FICHE

This publication has been cataloged as follows:

The Physical chemistry of mineral-reagent interactions in sulfide flotation, proceedings of symposium held at College Park, Md., April 6-7, 1978.

(Information Circular)

Meeting held at the College Park Campus of the University of Maryland, April 6-7, 1978 and sponsored by the United States Bureau of Mines.

Bibliography: p.

1. Flotation--Congresses. 2. Flotation reagents--Congresses. 3. Sulphides--Metallurgy--Congresses. 4. Chemistry, Physical and theoretical--Congresses. I. Richardson, Paul E. II. Hyde, Garrett R. III. Ojalvo, Morris S. IV. United States. Bureau of Mines. V. Series: United States. Bureau of Mines. Information Circular.

TN295.U4 [TN523] 622'.08s [622'.752] 79-22025

PREFACE

The purpose of this symposium on the "Physical Chemistry of Mineral-Reagent Interactions in Sulfide Flotation" was to critically examine the current state-of-the-art in sulfide flotation and to define areas that need to be emphasized in future fundamental research. In considering this objective, it should be recognized that new and changing stimuli for research in minerals processing in general, and flotation in particular, have evolved during the past several decades. As the symposium participants were reminded by the banquet speaker, Mr. Carl Rampacek,

"With the depletion of our higher grade and readily available ores, our industry now is faced with producing an increasing quantity of minerals and resources; and this must be achieved within the constraints of more stringent environmental controls and the changing energy situation."

We are all acutely aware of the three challenges to the minerals industry contained in this sentence--the development of new processes to recover minerals from low-grade resources; the practice of energy efficiency and conservation; and safeguards to protect the environment. These challenges may be met in many different ways, but as pointed out by Mr. Rampacek, it is easy to visualize that flotation will assume an increasingly important role in recovering the maximum values from low-grade resources. This can be believed with some confidence because the 70-year history of flotation has shown that it is an extremely successful industrial process and applicable to most minerals, it consumes a relatively small quantity of energy, and it is not highly polluting, although in the future more consideration will have to be given to tailing and water disposal.

Flotation is accomplished through an exceedingly complex set of interrelated processes that depend on a host of variables, encompassing and crossing many scientific and engineering disciplines. In organizing this symposium, one of the earliest and more difficult decisions was to restrict the papers to those dealing with the physical chemistry of mineral-reagent interactions in sulfide flotation, which subsequently became the title of the meeting. This restricted forum is a departure from most other symposiums dealing with flotation, which generally treat all aspects of the process. Typically covered would be metallic and nonmetallic ore flotation and papers on kinetics and cell design, mathematical modeling, circuits and automatic control, plant practice, bubble-particle collision mechanisms, as well as the fundamentals of reaction and adsorption phenomena. The decision to limit the symposium to the last-mentioned topic was not based on any profound insight that mineral-reagent interactions are any more important than other phenomena in determining the success of a practical flotation process. Rather, it was felt that with the progress in recent years in understanding reactions in sulfide-flotation reagent interactions, the time appeared ripe for a separate conference to review the current state-of-the-art and to assess the directions for future research.

The organizers wish to express their thanks to the program participants for their contributions to this meeting, and especially to the program speakers for their extra effort in preparing their talks and manuscripts for this publication. We also owe a special debt of gratitude to the Washington, D.C., section of the American Institute of Mining, Metallurgical, and Petroleum Engineers for cosponsoring a most enjoyable and informative banquet for this meeting, and to the staff of the Conferences and Institutes Division of the University of Maryland, especially Ms. Judith Orth, for capable assistance in managing this conference.

CONTENTS

Page

Preface.......... i

Abstract.......... 1

Flotation Research and Our National Mineral Requirements, by Carl Rampacek.......... 2

Thiol Collector Adsorption Processes, by M. C. Fuerstenau.......... 7

Effects of Point Defects on Flotation, by F. F. Aplan, G. Simkovich, E. Y. Spearin, and K. C. Thompson.......... 25

Thermodynamics of Sulfide Mineral Flotation Systems, by Douglas W. Fuerstenau.......... 35

Flotation Research at the Avondale Research Center: An Introduction, by Garrett R. Hyde.......... 63

The Effect of the Space Charge Layer of Galena on the Kinetics of the Oxygen Reduction Reaction, by Paul E. Richardson and Daniel L. Edelstein.......... 72

Activation and Deactivation in the Flotation of Sulfide Minerals, by Douglas W. Fuerstenau.......... 100

Environmental Considerations in Tailing Disposal, by G. W. Poling.... 121

Industrial Flotation Research and Its Interface with Academics, by Nathaniel Arbiter.......... 144

Selective Flocculation of Fines, by P. Somasundaran.......... 150

Summary of Symposium, by Maurice C. Fuerstenau and Booker W. Morey... 168

THE PHYSICAL CHEMISTRY OF MINERAL-REAGENT INTERACTIONS IN SULFIDE FLOTATION

Proceedings of Symposium Held at College Park, Md., April 6-7, 1978

compiled by

Paul E. Richardson[1], Garrett R. Hyde[2], and Morris S. Ojalvo[3]

ABSTRACT

This symposium was sponsored by the Bureau of Mines, U.S. Department of the Interior, in order to critically examine the state-of-the-art of sulfide flotation chemistry and to define current and emerging problems that should be emphasized in future fundamental research. The topics covered through invited papers include both reviews and recent research results in the areas of thermodynamics of reagent-mineral interactions; collector adsorption processes; the effects of solid-state point defects on flotation; activation and deactivation phenomena; the electrochemical role of oxygen in sulfide flotation; environmental problems in flotation; and selective flocculation of fines. Papers giving perspectives on flotation research in relationship to our national mineral requirements and the relationships between industrial flotation research and academics are also presented. An edited summary of the symposium follows the papers.

---

[1] Supervisory research physicist, Avondale Research Center, Bureau of Mines, Avondale, Md.

[2] Research physicist, Avondale Research Center, Bureau of Mines, Avondale, Md.

[3] Program Director, Particulate and Multiphase Processes, Division of Engineering, National Science Foundation, Washington, D.C.

FLOTATION RESEARCH AND OUR NATIONAL MINERAL REQUIREMENTS

by

Carl Rampacek[1]

ABSTRACT

The United States has an insatiable appetite for minerals. With but 6 percent of the world's population and only 6 percent of the world's land area, we consume 30 percent of the world's fuels and 23 percent of its nonenergy minerals--and this pattern of usage is not changing appreciably. Currently, U.S. consumption of nonenergy minerals is about 22,000 pounds per person annually, and, by the year 2000, we expect this figure to at least double.

The strength and wealth of our American Nation have been built from its natural resources--land, water, forests, minerals, and fuels. Of these, minerals and fuels--which I think are the essence of our machine civilization--are the multipliers that, over the years, have enabled U.S. industry to produce more goods and services at least cost and effort. But in the past three decades, this enviable position has been changing drastically. With the depletion of our higher grade and readily available ores, our industry now is faced with producing an increasing quantity of minerals and metals from lower grade, more complex, deeper buried, and less accessible resources; this must be achieved within the constraints of ever more stringent environmental controls and the changing energy situation.

Until the early 20th century, all mineral processing of ores was by gravity separation methods. These methods recovered the coarse mineral particles, but not the extremely fine or slimed minerals. A whole new dimension to minerals separation and concentration was added with the discovery in 1905[2] of froth flotation. Introduced into the United States in 1911, flotation techniques have had an impact on every segment of metal and nonmetal

---

[1] Director, Mineral Resources Institute, University of Alabama, Tuscaloosa, Ala.

[2] Hines, Pierre R. Before Flotation. Ch. in Froth Flotation, ed. by D. W. Fuerstenau. AIME, New York, 1962, pp. 5-10.

mining industry. Without these techniques there would be no mining industry as we know it today, a fact that has been clearly enunciated by Milliken[3] as follows:

> "Flotation has permitted the mining of low-grade and complex ores which would have been worthless if it had been necessary to rely on the time honored method of gravity concentration. It has meant the conversion of tailing dumps into mines. In fact, the tailings of some previous gravity operations were higher grade than the ore in many mines today. To a mineral hungry world, flotation has provided millions of tons of material that otherwise would not have been economically available."

Since 1911, froth flotation technology has undergone significant refinements in response to the need to devise lower cost and more efficient operations aimed at better mineral recoveries and lower energy requirements. A better understanding of the chemistry of flotation and the properties of mineral surfaces, together with adoption of sophisticated flowsheets, has led to improved flotation systems, but engineering advances in the development of larger size equipment (such as grinding mills and flotation cells) and changes in equipment design probably have had the major impact on improving milling operations and reducing costs. The trend toward larger size equipment probably will continue as long as ore grades are sufficient to justify the processing costs, but at some point the need for more efficient processing with minimal energy requirements will shift attention towards improving cell and equipment design.

Let's look at the role now being played by froth flotation as a first step in supplying our Nation's mineral requirements. In 1975, there were 252 flotation plants operating in the United States.[4] These plants treated nearly 423 million tons of ore, from which 60 million tons of concentrates were recovered. Of the total ore treated, 66 percent was metal sulfides, principally copper and copper-molybdenum ores; 7 percent was oxides and carbonates, mostly iron ores; 24 percent was nonmetallic minerals, chiefly potash and phosphate ores; and 3 percent was coal. Massive quantities of power, water, and reagents were consumed in processing these ores. The impact of flotation on our economy in terms of employment and supporting industries is obvious.

But, enough of that. I visualize that as we are confronted with mining and processing lower grade and refractory ores, flotation will assume an ever-increasing importance in deriving from these resources the maximum metal and mineral values. The recovery of high-grade concentrates will remain the primary objective of the flotation engineer, but more and more frequently complex bulk concentrates will be recovered for further processing by hydrometallurgical or pyrometallurgical methods. This trend already is evident in research underway by the Bureau of Mines on the Duluth, Minn., copper-nickel gabbros, in which a bulk copper-nickel-cobalt sulfide flotation concentrate is being further processed by combined pyrometallurgical and hydrometallurgical treatment.

---

[3] Milliken, Frank R. The Early Days of Froth Flotation. Introductory chapter in Froth Flotation, ed. by D. W. Fuerstenau. AIME, New York, 1962, pp. 1-3.

[4] Greenspoon, Gertrude, and John Morning, Flotation Trends. BuMines Minerals Yearbook 1975, v. I, 1977, pp. 96-124.

This conference is focusing on sulfide mineral flotation. There is not much I can add to what already is being discussed, so I am going to direct most of my remarks to some challenges facing you in the field of froth flotation in general. Sulfide mineral flotation has reached a high degree of technical efficiency. As a result, our industry can treat copper and copper-molybdenum ores containing as little as 0.4 to 0.5 percent copper at minimum cost and with excellent mineral recoveries. Much of the success can be attributed to the development of sulfide-specific reagents such as the xanthates and to the wealth of basic scientific information available on the chemistry of xanthate flotation. Despite progress in gaining a better understanding of sulfide mineral flotation, however, a universally accepted flotation theory still is lacking for the xanthate-sulfide mineral system. We still haven't sorted out completely the complex nature of the liquid-liquid, liquid-gas interfaces with the mineral particles, and the flotation reagents. Sutherland and Wark[5] have listed 32 variables in sulfide flotation, of which perhaps only 22 can be controlled by the metallurgist. Therefore, we are still far from the state where a process can be designed or can be optimized from first principles.

In nonsulfide ore processing, our understanding of the basic principles involved in floating oxides and nonmetallics is sadly deficient. More often than not we are content to reject as much as 15 to 25 percent of the mineral values in the flotation tailings owing to our limited knowledge of the chemical and physical properties of the oxide and silicate minerals with which we deal. Developing a fundamental scientific understanding of the solid state properties of these minerals and how they relate to the floatability of the minerals will tax the ingenuity of the researcher. The advances in colloid science, solid state physics, electrochemistry, and the chemistry and physics of surfaces, which you have learned to apply in studies with sulfide minerals, should be valuable techniques for determining the mechanisms and kinetics of the micro processes involved in the flotation of the complex nonsulfide minerals.

Perhaps through such intensive research it will be possible to develop tailor-made collectors that have the properties to react with specific mineral species by chemisorption. This, of course, will require much more knowledge than we have now about the solution chemistry of available flotation reagents. But, a free interchange of new ideas at more meetings, such as the one here at College Park, can provide needed scientific data and in the process finally lay to rest the old adage that "flotation is more of an art than a science."

From a practical operating standpoint, the problem of slime flotation still faces us. At present we avoid it by removing the slimes before flotation and discarding them along with their mineral values. In phosphate flotation, for example, wouldn't it be nice if we had a practical flotation process for recovering the 25 percent of phosphate mineral values in the slimes now being discarded and impounded. Here is a challenge in ultrafine particle flotation. In potash ore processing, flotation of the sylvite is seriously impaired when the pulps contain more than about 3 percent clay constituents. It is a problem of concern to the potash industry to which insufficient attention has been given.

---

[5] Sutherland, K. L., and I. W. Wark. Principles of Flotation, Australasian Institute of Mining and Metallurgy, 1955, pp. 13-23.

Some progress is being made in handling slimes concurrently with the sand fractions in flotation. The selective flocculation-flotation process developed for Tilden, Mich., nonmagnetic taconite ore is an example of what an intensive scientific and technical research program has achieved in solving a specific problem. This process, developed as a cooperative effort between the Bureau of Mines and the Cleveland Cliffs Iron Co., has resulted in the construction and operation of a plant now producing 4 million tons of high-grade iron ore pellets annually. Four features of the process are--

1. Extremely fine grinding.

2. The application of selective flocculation of the iron oxide slimes.

3. Flotation of the gangue minerals from a pulp containing the flocculated slime, together with the more granular portions of the ore.

4. Effective recycling of the water.

Although the process has proved successful for the Tilden, Mich., taconites, it is not applicable to the taconites of the western Mesabi range, owing to their different mineralogical compositions. Hopefully, further research will refine and modify the process so that it will apply to the variety of nonmagnetic ores in the region.

In studying the beneficiation of the nonsulfides by flotation, we tend to focus our attention on the bulk commodities such as iron, phosphate, and potash. This is as it should be, but also there is a need to give more attention to flotation of other types of nonsulfides. For example, more intensive research is needed to improve flotation separations of barite, fluorspar, kyanite, calcite, mica, and other nonmetallic ores.

In conclusion, I emphasize that U.S. demand for minerals and metals is expected to double by the end of this century. Adding to the seriousness of the situation is the fact that the domestic supply of raw mineral materials is not keeping pace with demand. If we intend to maintain some reasonable balance between domestic production and imported supplies of a number of our important mineral raw materials, we will be forced to treat greater quantities of our lower grade and more refractory resources. Economics will dictate a need for more efficient and effective froth flotation processes that will allow us to achieve maximum recovery of the economic minerals at acceptable costs. Maximum future progress in developing and improving the flotation process will require a full merging of scientific principles with applied approaches. A better understanding of the complex chemical and physical phenomena involved in flotation will materially provide the scientific principles that are needed. We have no choice but to continue our efforts in that direction.

THIOL COLLECTOR ADSORPTION PROCESSES

by

M. C. Fuerstenau[1]

Thiol collectors exhibit three important properties that account for their uniqueness in adsorption phenomena: (1) the insoluble nature of heavy-metal, short-chain thiol salts; (2) the weak acid characteristics of some of the dissolved thiol acids; and (3) the ability of some of the thiols to oxidize to a neutral dimer.

The stability of some of the heavy-metal thiol salts can be seen from the solubility products listed in table 1. In general, the dithiophosphate salts possess greater solubility than their xanthate counterparts. Also, the copper salts of thiol collectors are more stable than lead salts, which in turn are more stable than zinc salts.

TABLE 1. - Solubility products of selected metal thiol salts (20)

(Courtesy, Butterworths & Co.)

Species	Solubility product
Zinc ethyl xanthate	4.9×10^{-9}
Zinc amyl xanthate	1.6×10^{-12}
Lead ethyl xanthate	2.1×10^{-17}
Lead amyl xanthate	1.0×10^{-24}
Cuprous ethyl xanthate	5.2×10^{-20}
Zinc ethyl dithiophosphate	1.5×10^{-2}
Lead ethyl dithiophosphate	7.5×10^{-12}
Cupric ethyl dithiophosphate	1.4×10^{-16}

The dissociation constants of short-chain xanthic acids are presented in table 2. As can be noted from these values, the predominant xanthate species is xanthate ion above about pH 5 and xanthic acid below pH 5.

---

[1] Professor and Chairman, Department of Metallurgical Engineering, South Dakota School of Mines and Technology, Rapid City, S. Dak.

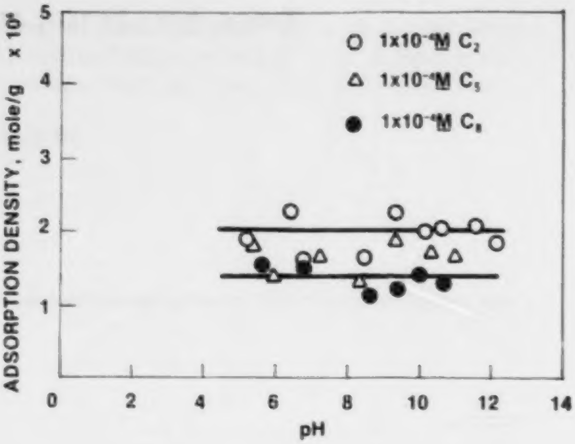

FIGURE 1. - Adsorption density of various xanthates on galena as a function of pH in the virtual absence of oxygen. Surface area of galena: 0.243 m^2/g (15).

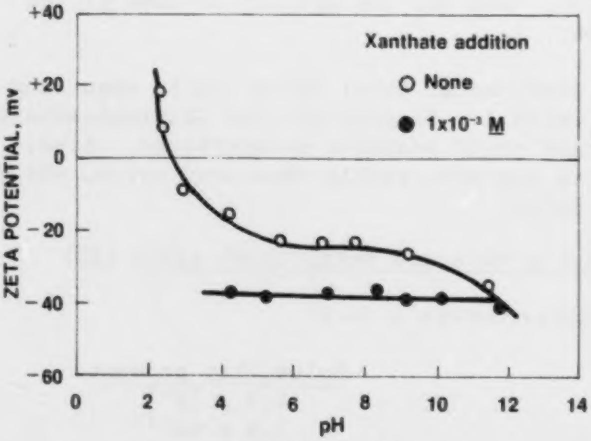

FIGURE 2. - Zeta potential of galena as a function of pH in the absence and presence of ethyl xanthate in the virtual absence of oxygen (15).

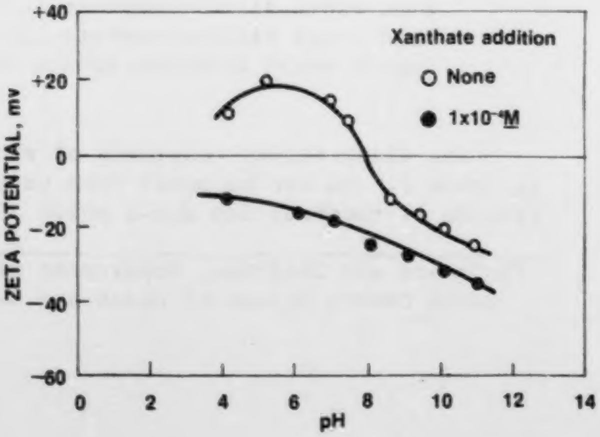

FIGURE 3. - Zeta potential of galena as a function of pH in the absence and presence of ethyl xanthate in the presence of oxygen (14).

TABLE 2. - Dissociation constants of various xanthic acids (14)

Xanthic acid	Dissociation constant
C_2	1.0×10^{-5}
C_3	1.0×10^{-5}
C_4	7.9×10^{-6}
C_5	1.0×10^{-5}

Xanthate, dithiophosphate, and dithiocarbamate are capable of undergoing oxidation to the dimers: dixanthogen, dithiophosphatogen, and thiouram disulfide, respectively. The standard cell potentials for the oxidation of these thiols are as follows (2, 9):

$$X_{2(\ell)} + 2e^- \rightleftarrows 2X^- \qquad E^\circ = -0.06 \text{ v}$$

$$(DTP)_{2(\ell)} + 2e^- \rightleftarrows 2DTP^- \qquad E^\circ = 0.25 \text{ v}$$

$$(DTC)_{2(\ell)} + 2e^- \rightleftarrows 2DTC^- \qquad E^\circ = -0.068 \text{ v}$$

It can be seen from these potentials that diethyl dithiophosphate (DTP^-) is more difficult to oxidize than ethyl xanthate (X^-) or diethyl dithiocarbamate (DTC^-).

ADSORPTION UNDER OXYGEN-DEFICIENT CONDITIONS

Mechanisms involved in the adsorption of thiols on sulfides are dependent on oxygen tension. The adsorption of various xanthates on galena in a solution containing less than 5 ppb oxygen in contact with a nitrogen atmosphere containing less than 10^{-6} mole fraction oxygen is presented in figure 1. Two phenomena can be noted; namely, that adsorption is independent of pH and, secondly, that adsorption density is somewhat less for longer chain xanthates. The adsorption density of 2×10^{-6} mole EX^-/g galena represents monolayer coverage, assuming that one xanthate ion adsorbs on one surface lead ion site. These results are similar to those reported by Hagihara (19), Greenler (18), and Leja and Poling (26), in which one-to-one coordination of xanthate to surface lead ion was observed. The fact that adsorption occurs at high pH values indicates that xanthate ion rather than xanthic acid is the active species in this system.

Chemisorption of xanthate under these conditions can be noted from the data in figure 2, in which the zeta potential of galena in the virtual absence of oxygen is presented as a function of pH. It can be noted that galena has a PZC at pH 2.6 and that the zeta potential is negative above this pH. In the presence of 1×10^{-3} mole/liter ethyl xanthate, the zeta potential becomes more negative over this pH range. Similarly to the adsorption data presented in figure 1, the zeta potential is constant and independent of pH. An increase in the zeta potential is indicative of the formation of a new phase on the mineral surface. Further, adsorption of a negatively charged, short-chain collector ion on a negatively charged surface could only occur by chemical reaction between the collector and surface metal ion.

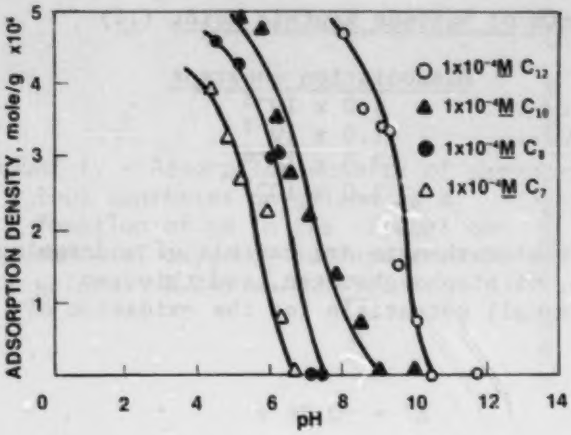

FIGURE 4. - Adsorption density of various xanthates on sphalerite as a function of pH in the virtual absence of oxygen. Surface area of sphalerite: 1.302 m^2/g (15).

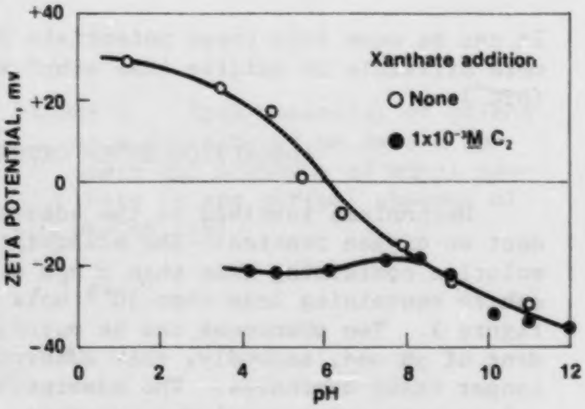

FIGURE 5. - Zeta potential of sphalerite as a function of pH in the absence and presence of ethyl xanthate in the virtual absence of oxygen (15).

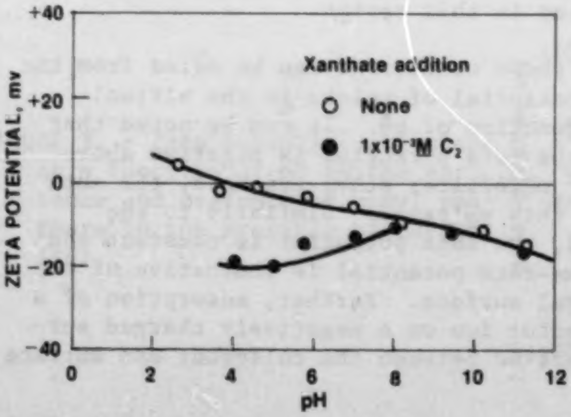

FIGURE 6. - Zeta potential of pyrite as a function of pH in the absence and presence of ethyl xanthate in the virtual absence of oxygen (15).

The difference in surface properties of galena in the absence and presence of oxygen can be seen by comparing the electrokinetic data given in figures 2 and 3. The data in figure 3 were established in the presence of air, and a PZC can be noted for galena at pH 7.9. Chemisorption of xanthate can also be inferred from these data.

Adsorption of various xanthates on sphalerite in the virtual absence of oxygen has also been established as a function of pH. (See fig. 4.) As shown, adsorption is not possible above pH 6.6 with heptyl xanthate and above pH 7.4 with octyl xanthate. In this system monolayer coverage occurs at 1.6×10^{-5} mole xanthate/g sphalerite.

With the titration technique used in this work (15), it was not possible to establish whether xanthates whose hydrocarbon chains are shorter than seven carbon atoms are adsorbed. As a result, electrokinetic experiments were made for this determination. Chemisorption of ethyl xanthate on sphalerite can be noted in figure 5.

Adsorption of octyl xanthate on sphalerite has also been studied as a function of concentration (15). When the xanthate concentration is increased by one order of magnitude, the maximum pH of adsorption is increased by one unit, that is, from pH 6.4 to 7.4. Since the pK's of xanthic acids are about 5, with an addition of 1×10^{-4} mole/liter octyl xanthate, the concentration of octyl xanthic acid at pH 6.4 is 3.8×10^{-6} mole/liter. With an addition of 1×10^{-3} mole/liter ethyl xanthate, the concentration of ethyl xanthic acid at pH 7.4 is 3.8×10^{-6} mole/liter. These data indicate that xanthic acid is probably the xanthate species adsorbed in this system. With this species, xanthate could chemisorb, while water is formed by combination of the hydrogen ion from xanthic acid and adsorbed hydroxide (4, 6). Zinc xanthates are not particularly insoluble compounds, and the necessity for xanthic acid rather than xanthate ion for adsorption to occur may be related to the additional free energy decrease that the system experiences when water is formed and split out under these conditions.

In the case of pyrite, adsorption of short-chain xanthates does not occur above about pH 8 in the virtual absence of oxygen, and adsorption is below monolayer coverage (15). Similarly to sphalerite, ethyl xanthate chemisorbs on pyrite under these conditions. (See fig. 6.) Just as with sphalerite, then, xanthic acid appears to be the species actively adsorbed on pyrite in the virtual absence of oxygen.

ADSORPTION IN THE PRESENCE OF OXYGEN

The role of oxygen in xanthate adsorption has been the subject of considerable controversy over the years. Some investigators (16, 29, 35) have stated that the presence of oxygen is absolutely necessary for xanthate adsorption on sulfides, while others (14, 26) have found the presence of quantities of oxygen at monolayer coverage to be deleterious to xanthate adsorption.

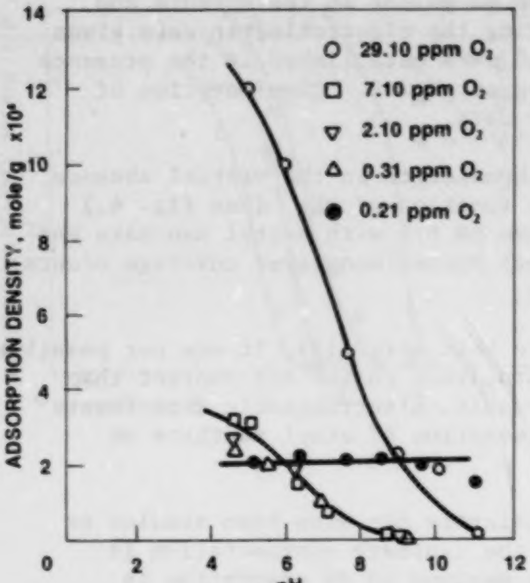

FIGURE 7. - Adsorption density of ethyl xanthate on galena as a function of pH and oxygen concentration. Xanthate concentration: 1 x 10^{-4} M. Surface area of galena: 0.243 m^2/g (14).

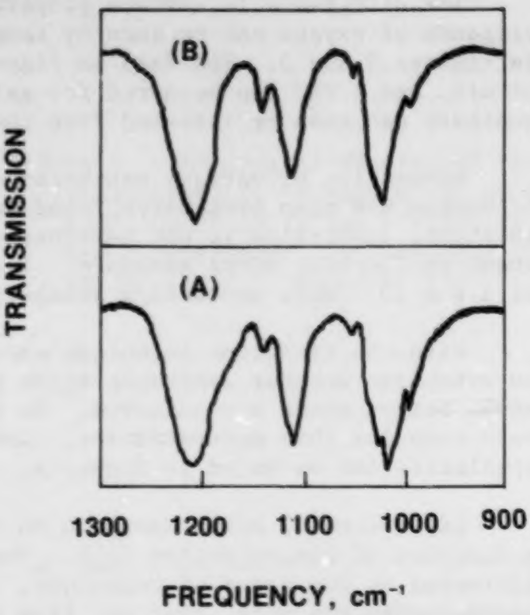

FIGURE 9. - Infrared spectra of lead ethyl xanthate (A) and of galena after contact with ethyl xanthate (B) (26). (*Courtesy, American Chemical Society.*)

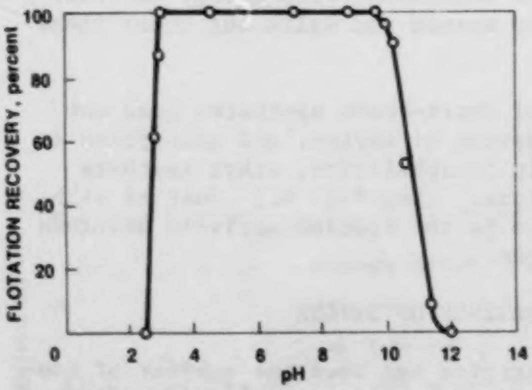

FIGURE 8. - Flotation recovery of galena as a function of pH with 1 x 10^{-5} M ethyl xanthate in the presence of air (13). (*Courtesy, AIME.*)

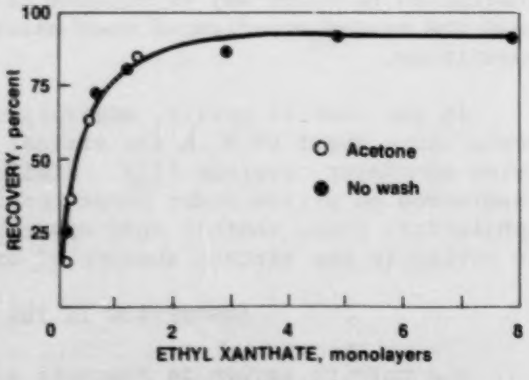

FIGURE 10. - Variation in flotation of galena with concentration of ethyl xanthate at the surface (8). (*Courtesy, American Institute of Chemical Engineers.*)

Xanthate adsorption on galena is presented as a function of pH and oxygen concentration in figure 7. As can be seen, small quantities of oxygen have no effect on xanthate adsorption. When the concentration of oxygen is such that monolayer coverage would result if all of the oxygen present would have adsorbed, in this case 0.31 ppm, adsorption of xanthate is inhibited. With higher concentrations of oxygen, though, xanthate adsorption is enhanced.

The inhibition of xanthate adsorption in the presence of small quantities of oxygen is kinetics controlled. The data contained in figure 7 were established with a 5-minute conditioning period. With a 10-minute conditioning period, xanthate adsorption is enhanced in the presence of oxygen (14). In fact, multilayer coverage of xanthate is obtained under these conditions. In the cases of pyrite and sphalerite, any amount of oxygen present in the system enhances xanthate adsorption even with relatively short conditioning periods.

ELECTROCHEMICAL PHENOMENA

In addition to chemisorption of collectors, certain thiol collectors undergo electrochemical oxidation to dimers, such as dixanthogen, at the surface of certain sulfide minerals.

When a sulfide mineral is placed in an aqueous solution, the mineral develops a potential termed the rest potential. Rest potentials of various sulfide minerals in a solution containing 6.25×10^{-4} mole/liter ethyl xanthate at pH 7 are presented in table 3. Comparison of these values should be made with the reversible potential for xanthate oxidation in this system which is 0.13 volt (IUPAC). When the rest potential is larger than the reversible or Nernst potential, oxidation of xanthate to dixanthogen occurs. With reference to table 3, dixanthogen is the reaction product found on the various mineral surfaces with rest potentials greater than +0.13 volt. Covellite appears to be an exception, but these anomalous results are apparently due to dissolution of the covellite followed by oxidation of xanthate with Cu^{+2} and adsorption of dixanthogen from solution.

TABLE 3. - Products of the interaction of sulfide minerals with ethyl xanthate (6.25×10^{-4} M at pH 7). Reversible potential for oxidation to dixanthogen is 0.13 v (2).

Mineral	Rest potential (v)	Product
Pyrite	0.22	Dixanthogen.
Arsenopyrite	.22	Do.
Pyrrhotite	.21	Do.
Chalcopyrite	.14	Do.
Covellite	.05	Do.
Bornite	.06	Metal xanthate.
Galena	.06	Do.

When the rest potential is cathodic or less than the reversible xanthate/dixanthogen potential, oxidation of metal xanthate cannot occur, and metal xanthates are adsorbed on the sulfide surface.

CONDITIONS OF THE SULFIDE SURFACE UNDER FLOTATION CONDITIONS

Sulfide mineral systems fall essentially into one of two categories: those in which thiol collectors are adsorbed chemically and those in which dimer formation results from electrochemical oxidation of collector on the mineral surface. Galena, chalcocite, and sphalerite fall into the first category, while pyrite falls into the second. Chalcopyrite, on the other hand, exhibits both chemisorption and dimer formation.

Galena

The flotation response of galena with 1×10^{-5} mole/liter ethyl xanthate in the presence of air is presented in figure 8. As can be noted, complete flotation is effected from pH 2 to pH 10.

Xanthate is present in two forms on a galena surface under conditions in which flotation occurs: xanthate chemisorbed at monolayer coverage and bulk-precipitated lead xanthate adsorbed at multilayer coverage (22). Dixanthogen does not form under these conditions and is not observed (2, 35). (See table 3.) Confirmation of the presence of bulk lead ethyl xanthate on the galena surface is provided by the infrared spectra in figure 9. Presented are the spectra of lead ethyl xanthate and galena after contact with ethyl xanthate. The absorption bands of lead ethyl xanthate occur at 1014, 1110, and 1212 cm^{-1}. After contact with ethyl xanthate, absorption bands at 1020, 1112, and 1210 cm^{-1} are noted.

The multilayers of lead ethyl xanthate are held together by van der Waal's bonding of the hydrocarbon chains of the xanthate, and these layers can be dissolved with organic reagents such as acetone. However, the xanthate chemisorbed at monolayer coverage cannot be leached from the surface. These facts can be noted from the data presented in figure 10 and from the data of Leja, Little, and Poling (22).

Also shown in figure 10 is the floatability of galena as a function of multilayer coverage of lead ethyl xanthate. For flotation to be effected in the presence of multilayer coverage, the precipitate of lead ethyl xanthate must be hydrophobic, and this has been shown to be the case (8).

In the chemisorption of xanthate at monolayer coverage, one xanthate ion adsorbs on each surface lead ion to form an unleachable phase of lead xanthate. Some investigators (7, 31-32, 35) have suggested that surface sulfide ions are oxidized electrochemically to elemental sulfur by oxygen in this adsorption process, but no elemental sulfur has ever been detected on the surface (8).

For a charged species, namely xanthate ion, to chemisorb with no transfer of charge, an ion of similar charge must be replaced on the surface. Hydroxyl ion will be adsorbed under these conditions and could be replaced readily by xanthate ion in moderately basic medium.

In oxygen-deficient systems, only monolayer coverage of xanthate occurs on galena (fig. 1). In systems open to air, multilayer coverage occurs, and these phenomena are postulated to result from the following sequence of events:

1. Oxidation of surface sulfide to thiosulfate and sulfate. In the presence of oxygen, galena is oxidized to lead sulfate according to equation 1,

$$PbS_{(s)} + 2O_{2(g)} \rightleftarrows PbSO_{4(s)}, \qquad K = 10^{126} \qquad (1)$$

With the following equilibrium expression,

$$\frac{(\cancelto{1}{a_{PbSO_4}})}{(\cancelto{1}{a_{PbS}})\,(P_{O_2})^2} = 10^{126}$$

At equilibrium, $P_{O_2} = 10^{-63}$ atm.

Since the oxygen tension in air is 0.2 atm, oxidation of sulfide to thiosulfate and sulfate occurs.

2. Metathetic replacement of surface thiosulfate and sulfate by carbonate. With systems open to the air, carbonate will be present, and the galena surface will carbonate at the expense of thiosulfate and sulfate. That is,

$$PbSO_{4(s)} + CO_3^{-2} \rightleftarrows PbCO_{3(s)} + SO_4^{-2} \qquad (2)$$

3. Metathetic replacement of surface lead carbonate, sulfate, and thiosulfate by xanthate. At the usual flotation pH of 8 to 9, xanthates are more stable than lead carbonate, sulfate, or thiosulfate, and lead xanthate will form by metathetic replacement of these lead salts.

The stoichiometric exchange between xanthate ion abstracted and reduced sulfur-oxygen, sulfate, and carbonate ions released to solution is shown in table 4. As can be noted, a considerable portion of the ions replaced are carbonate. Mellgren (24) has verified these reactions using calorimetric measurements.

Adsorption of xanthate on galena, then, apparently occurs in two stages: the first stage comprises chemisorption of one xanthate ion on each surface lead ion, during which exchange of xanthate ion for hydroxyl ion probably takes place; the second stage comprises the formation and adsorption of bulk-precipitated lead ethyl xanthate formed by metathetic replacement of sulfur-oxygen species and carbonate on the surface.

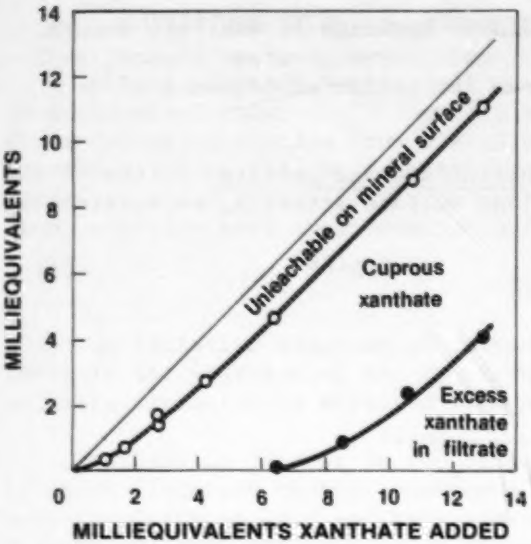

FIGURE 11. - Distribution of amyl xanthate species after adsorption of amyl xanthate on chalcocite (17).

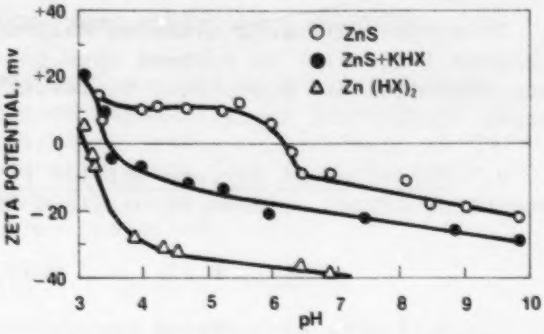

FIGURE 12. - Zeta potential of zinc hexyl xanthate and sphalerites in the absence and presence of 1.25 x 10^{-4} M hexyl xanthate as a function of pH (10). (*Courtesy, Elsevier Scientific Publishing Co.*)

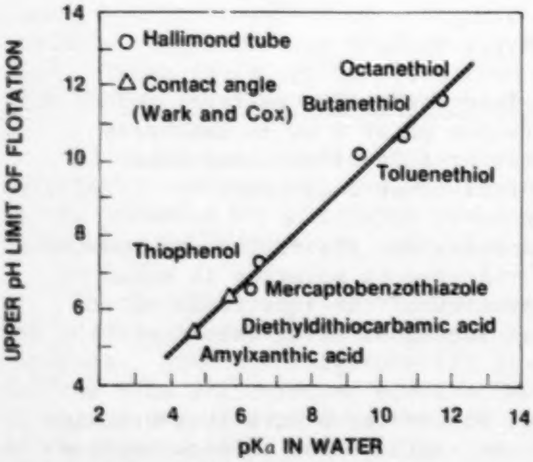

FIGURE 13. - Relation between collector acidity and upper pH limit of sphalerite flotation; 1.25 x 10^{-4} M collector concentration (28). (*Courtesy*, AIME.)

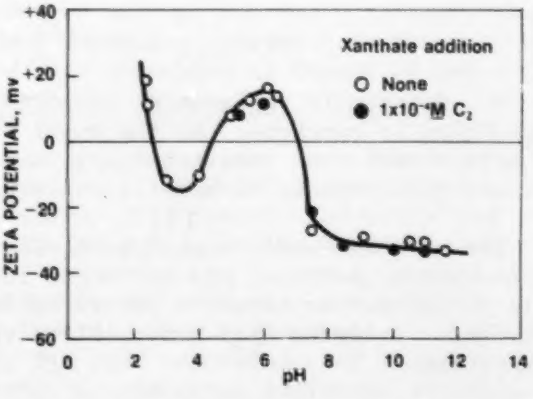

FIGURE 14. - Zeta potential of pyrite as a function of pH in the absence and presence of ethyl xanthate in the presence of air (14).

TABLE 4. - Ion exchange between galena and xanthate[1] (30)

(Courtesy, AIME)

Original xanthate solution[2]	Xanthate ion abstracted	Ions emitted			
		Reduced sulfur-oxygen	Sulfate ions	Carbonate ions	Total ions emitted
200.0	[3]39.0	8.0	5.8	26.0	39.9
200.0	[4]52.3	12.7	12.8	--	--
200.0	[5]58.3	13.8	16.1	27.2	57.1
200.0	[6]64.8	14.1	18.7	25.8	57.6

[1] Added as potassium ethyl xanthate; all ions in this table expressed as milligrams potassium ethyl xanthate per liter, or the stoichiometric equivalent.

[2] 300 ml solution added for each 30 g galena.

[3] Without exposure after grinding and before xanthating.

[4] Exposure 1 week.

[5] Exposure 2 weeks.

[6] Exposure 3 weeks.

Chalcocite

Similarly to galena, xanthate adsorption on chalcocite is also a two-stage process. The presence of an unleachable xanthate species on the chalcocite surface following xanthate adsorption has been demonstrated by Gaudin and Schuhmann (17). These authors also demonstrated that, following the formation of an unleachable chemisorbed layer, multilayers of cuprous xanthate form and adsorb on the surface. The relative distribution between unleachable amyl xanthate, cuprous amyl xanthate, and xanthate remaining in solution is presented as a function of xanthate addition in figure 11. With relatively high levels of addition of xanthate, e.g., 6 meq, approximately 25 percent of the xanthate added is unleachable, while the remaining 75 percent is present as cuprous xanthate on the chalcocite surface.

Ion exchange experiments similar to those in the galena-amyl xanthate system were also conducted by Dewey (5) in the chalcocite-amyl xanthate system. These results, presented in table 5, show that approximately half the ions exchanged upon xanthate adsorption are hydroxyl, and the balance are principally carbonate and some sulfate. The equivalence between xanthate abstracted and anions released does not appear to be as close as that obtained in the galena-xanthate system. However, when the relatively large amount of unleachable xanthate is taken into account, the amount of xanthate adsorbed is close to the amount of anions emitted to solution.

Similar adsorption phenomena have been observed in the dithiophosphate-chalcocite system. Chander and Fuerstenau (3) observed chemisorption of dithiophosphate as well as the formation of cuprous and cupric diethyl dithiophosphate on the surface of chalcocite.

TABLE 5. - Effect of time of grinding on products from chalcocite (50 g) treated with 10 millimoles (2.02 g) potassium n-amyl xanthate (5)

Substance[1]	Time of grinding (hr)		
	1.25	2.5	5
	Products leached from surface (mg)		
Cuprous xanthate	1,670	1,524	1,224
Compounds A, A', and B ..	0	171	246
Compound C	0	0	177
	Products in filtrate (millimoles)		
OH^-	5.30	3.43	3.48
CO_3^{-2}	2.39	3.86	3.95
SO_4^{-2}	.51	.65	.93
Reducing ions	.00	.18	.16
Residual X^-	1.77	.30	.00
Total anions	9.97	8.41	8.52
Potassium cation	9.73	8.49	6.63
pH	11.8	12.0	12.0

[1] Cuprous xanthate = $Cu_2[SC(S)OC_5H_{11}]_2$;
Compound A = $Cu_2S \cdot Cu_2[SC(S)OC_5H_{11}]_2$;
Compound A' = $Cu_2S \cdot Cu_2[SC(O)OC_5H_{11}]_2$;
Compound B = $2Cu_2S \cdot Cu_2[SC(S)OC_5H_{11}]_2$;
Compound C = $3Cu_2S \cdot Cu_2[SC(S)OC_5H_{11}]_2$.

Sphalerite

After exposure to xanthate, the collector species on the surface of sphalerite readily identifiable with infrared analysis is bulk-precipitated zinc xanthate (10, 36). The major absorption bands of zinc hexyl xanthate occur at 1375, 1227, 1112, and 1047 cm^{-1}. After contact with hexyl xanthate at pH 5.5, absorption bands are measured at 1380, 1227, 1112, and 1047 cm^{-1} on sphalerite. These results are similar to those presented by Yamasaki and Usui (36) with sphalerite after contact with dodecyl xanthate. Dixanthogen is not present on the surface.

Additional evidence for the presence of a separate phase on the sphalerite surface after contact with xanthate is provided by the electrokinetic data shown in figure 12. The values of the zeta potential of sphalerite contacted with hexyl xanthate are between those of sphalerite and zinc hexyl xanthate. Further, the precipitate of zinc hexyl xanthate is noted to reverse in electrical sign at approximately the pH value at which zeta reversal of sphalerite in contact with xanthate occurs.

These observations are in agreement with those of other investigators. Plaksin and Anfimova (25) concluded that two forms of adsorption occur in this system. Weakly attached xanthate is removed by water washing, while firmly attached xanthate is dissolved with pyridine. Shvedov and Andreeva (27) have shown that under flotation conditions, four to five times monolayer coverage is adsorbed.

Just as in the case of the oxygen-deficient sphalerite-xanthate system, Steininger's (28) data indicate that the weak acid species of sulfhydryl collectors are chemisorbed on sphalerite in the presence of oxygen. As shown in figure 13, there is a linear relationship between the upper pH limit for flotation of sphalerite and the pK_a of the collector. Steininger has also shown that a linear correlation exists between extent of flotation per unit of time and pK_a of collector.

Pyrite

In the case of pyrite, the species of xanthate responsible for flotation in the presence of short-chain xanthates is dixanthogen. This conclusion has been drawn from spectroscopic (12), electrokinetic (12), electrochemical (23, 33, 35), and flotation (12) data.

The presence of only dixanthogen on the pyrite surface after contact with xanthate has been shown clearly with infrared spectroscopy (12). The principal absorption bands of diamyl dixanthogen occur at 1021 and 1258 cm^{-1}, After contact with amyl xanthate, the principal absorption bands of pyrite occur at 1028 and 1258 cm^{-1}, which correspond closely with those of dixanthogen.

The adsorption of an electrically neutral species on the surface is also apparent from the data presented in figure 14. That is, the zeta potential of pyrite is the same in the absence and presence of ethyl xanthate. This should be contrasted with the electrokinetic behavior of galena conditioned with xanthate (fig. 3).

Dixanthogen forms by anodic oxidation of xanthate ion on the surface of pyrite coupled with cathodic reduction of adsorbed oxygen (23, 33, 35). That is,

$$2X^- \rightleftarrows X_2 + 2e \qquad \text{Anodic} \qquad (3)$$

$$\tfrac{1}{2}O_{2(ads)} + H_2O + 2e \rightleftarrows 2OH^- \qquad \text{Cathodic} \qquad (4)$$

where X^- represents xanthate ion and X_2 represents dixanthogen. Since sulfides are electronic conductors, electron transfer occurs through the solid. The overall reaction is

$$2X^- + \tfrac{1}{2}O_{2(ads)} + H_2O \rightleftarrows X_2 + 2OH^- \qquad (5)$$

This reaction can occur thermodynamically up to about pH 11; above this pH xanthate ion is the stable species of xanthate.

Flotation of pyrite, then, is possible below pH 11 with short-chain xanthates but is depressed above about pH 11. These phenomena are shown clearly in figure 15. With low levels of addition of ethyl xanthate, two regions of flotation are obtained from about pH 3 to pH 9. The intermediate region of depression is not related to a lack of dixanthogen, however.

Another collector has been shown to function similarly in the pyrite system, and this is dithiophosphate. Diethyl dithiophosphatogen has been found to form at pH 4 and below in the presence of pyrite but not at pH 6 and above. (See table 6.)

TABLE 6. - Diethyl dithiophosphate oxidation in the absence and presence of 100 x 200-mesh pyrite; reaction time, 10 min (11)

(Courtesy, AIME)

pH	Pyrite (g)	DTP^-(M)	Fe^{+3}(M)	$(DTP)_2$ Formed(M)
2.0	0	5×10^{-4}	2.5×10^{-4}	7×10^{-6}
3.0	0	5×10^{-4}	2.5×10^{-4}	nil
2.0	2	5×10^{-4}	0	4.3×10^{-5}
3.0	2	5×10^{-4}	0	3.3×10^{-5}
3.0	2	5×10^{-4}	0	$< 7 \times 10^{-6}$
4.0	2	5×10^{-4}	0	$< 7 \times 10^{-6}$
6.0	2	5×10^{-4}	0	nil
8.0	2	5×10^{-4}	0	nil

This phenomenon is illustrated well with the contact angle data presented in figure 16. The lack of bubble contact above pH 6 in the presence of high concentrations of dithiophosphate is due to the instability and lack of formation of dithiophosphatogen under these conditions. Pyrite rejection in basic medium when dithiophosphate is used as the collector is well known.

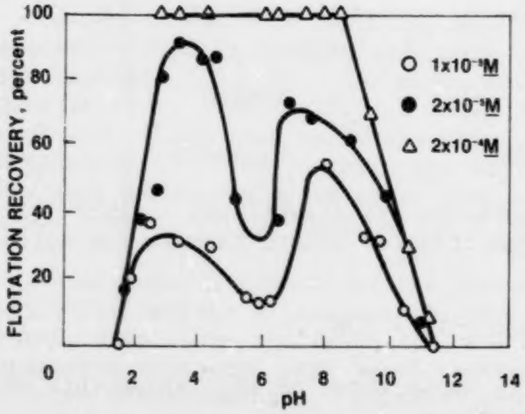

FIGURE 15. - Flotation recovery of pyrite as a function of pH with various additions of potassium ethyl xanthate (12). (*Courtesy*, AIME).

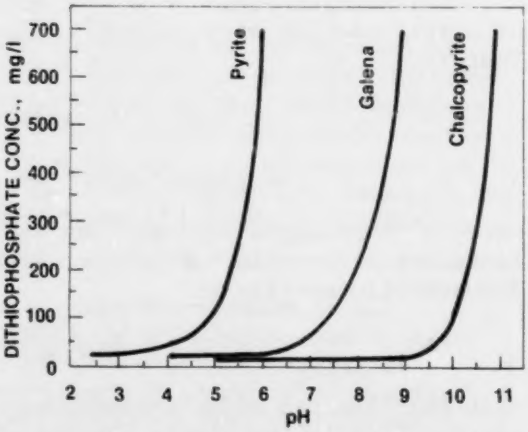

FIGURE 16. - Contact curves for several sulfide minerals as a function of diethyl dithiophosphate concentration and pH (34). (*Courtesy*, AIME.)

Chalcopyrite

Chalcopyrite responds exceptionally well to flotation with xanthate as collector. In the presence of 1 x 10^{-5} mole/liter ethyl xanthate, complete flotation is possible from about pH 3 to pH 12 (13). From this response, it is assumed that both electrochemical oxidation of xanthate to dixanthogen as well as chemisorption of xanthate on chalcopyrite are responsible for flotation. That is, since dixanthogen is not stable above about pH 11 (12), depression of chalcopyrite would occur above pH 11, as it does for pyrite, if only dixanthogen were responsible for flotation. As further evidence, Kuhn (21) in a detailed infrared spectroscopic study noted the presence of both dixanthogen and cuprous xanthate on chalcopyrite after contact with dixanthogen.

In an electrochemical investigation, Allison and coworkers (2) found dixanthogen on chalcopyrite after contact with ethyl xanthate (table 3). Abramov (1) has observed both dixanthogen and chemisorbed xanthate on chalcopyrite after contact with xanthate. According to Abramov, flotation is apparently reduced significantly under conditions in which dixanthogen does not form on the chalcopyrite surface. However, good flotation can be achieved in the presence of chemisorbed xanthate only, but collector coatings corresponding to 4 to 5 monolayers are required.

REFERENCES

1. Abramov, A. A. Character of the Adsorption of Butyl Xanthate and Dixanthogen and the Flotation of Chalcopyrite. Obogashch. Rud, v. 11, No. 4, 1966, p. 6.

2. Allison, S. A., L. A. Goold, M. J. Nicol, and A. Granville. The Products of Reaction Between Sulfide Minerals and Aqueous Xanthate Solutions and a Correlation of the Products with Electrode Rest Potential. Met. Trans., v. 3, 1972, p. 2613.

3. Chander, S., and D. W. Fuerstenau. Effect of Potassium Diethyldithiophosphate. Trans. Inst. Min. Metall, Sec. C, v. 84, No. 814, September 1974, pp. C180-C185.

4. Cook, M. A., and J. C. Nixon. Theory of Water-Repellant Films on Solids Formed by Adsorption from Aqueous Solutions of Heteropolar Compounds. J. Phys. & Coll. Chem., v. 54, 1950, p. 445.

5. Dewey, F. Reactions of Some Sulfur-Bearing Collecting Agents With Certain Copper Minerals. M.S. Thesis, Montana School of Mines, Butte, Montana, 1933, 106 pp. Available from Montana College of Mineral Sciences, Interlibrary Loan Dept., Butte, Montana 59701.

6. Eyring, E. M., and M. E. Wadsworth. Differential Infrared Spectra of Adsorbed Monolayers -n- Hexathiol on Zinc Minerals. Min. Eng., v. 8, 1956, p. 531.

7. Finkelstein, N. P. Quantitative Aspects of the Role of Oxygen in the Interaction Between Xanthate and Galena. Separation Sci., v. 5, 1970, p. 227.

8. Finkelstein, N. P., S. A. Allison, V. M. Lovell, and B. V. Steward. Advances in Interfacial Phenomena, ed. by P. Somasundaran and R. B. Grieves. AIChE Symposium Series, No. 150, v. 71, p. 165.

9. Finkelstein, N. P., and L. A. Goold. The Reaction of Sulphide Minerals With Thiol Compounds. National Institute of Metallurgy, South Africa, Rep. No. 1439, 1972, 125 pp.

10. Fuerstenau, M. C., K. L. Clifford, and M. C. Kuhn. The Role of Zinc-Xanthate Precipitation in Sphalerite Flotation. Internat. J. Miner. Proc., v. 1, 1974, p. 307.

11. Fuerstenau, M. C., J. Huiatt, and M. C. Kuhn. Dithiophosphates vs. Xanthate Flotation of Chalcocite and Pyrite. Trans. AIME, v. 250, 1971, p. 227.

12. Fuerstenau, M. C., M. C. Kuhn, and D. A. Elgillani. The Role of Dixanthogen in Xanthate Flotation of Pyrite. Trans. AIME, v. 241, 1968, p. 148.

13. Fuerstenau, M. C., J. D. Miller, and M. C. Kuhn. Chemistry of Froth Flotation. Handbook of Mineral Processing, AIME, New York, 1980.

14. Fuerstenau, M. C., M. Misra, and B. R. Palmer. Xanthate Adsorption on Selected Sulfides in the Presence of Oxygen. Submitted for publication to the Internat. J. Miner. Proc.

15. Fuerstenau, M. C., C. A. Natalie, and R. M. Rowe. Xanthate Adsorption on Selected Sulfides in Oxygen-Deficient Systems. Submitted for publication to the Internat. J. Miner. Proc.

16. Gaudin, A. M. Flotation. McGraw-Hill, New York, 2d ed., 1957.

17. Gaudin, A. M., and R. Schuhmann. The Action of Potassium n-Amyl Xanthate on Chalcocite. J. Phys. Chem., v. 40, 1936, p. 257.

18. Greenler, R. G., An Infrared Investigation of Xanthate Adsorption by Lead Sulfide. J. Phys. Chem., v. 66, 1962, p. 379.

19. Hagihara, H. Mono- and Multilayer Adsorption of Aqueous Xanthate on Galena Surfaces. J. Phys. Chem., v. 56, 1952, p. 616.

20. Kakovsky, I. A. Physicochemical Properties of Some Flotation Reagents. Proc. 2d Internat. Cong. of Surface Activity, London, 1957.

21. Kuhn, M. C. A Mechanism of Dixanthogen Adsorption on Sulfide Minerals. Doctor of Science Thesis, Colorado School of Mines, Golden, Colorado, 1968, 171 pp. Available from Colorado School of Mines, Arthur Lakes Library, Interlibrary Loan Dept, Golden, Colorado 80401.

22. Leja, J., L. H. Little, and G. W. Poling. Xanthate Adsorption Studies Using Infrared Spectroscopy, Part II. Evaporated Lead Sulfide, Galena, and Metallic Lead Substrates. Trans. IMM, v. 72, 1963, p. 414.

23. Majima, H., and M. Takeda. Electrochemical Studies of the Xanthate-Dixanthogen System on Pyrite. Trans. AIME, v. 241, 1968, p. 431.

24. Mellgren, O. Heat of Adsorption and Surface Reactions of Potassium Ethyl Xanthate on Galena. Trans. AIME, v. 235, 1966, p. 46.

25. Plaksin, I. N., and E. A. Anfimova. The Study of Several Problems in the Interaction of Xanthates With the Surface of Copper and Zinc Ores During Flotation. Izvest. Akad. Nauk. S.S.S.R., Otdel. Tekh. Nauk., 1954, No. 5, pp. 95-104.

26. Poling, G. W., and J. Leja. Infrared Studies of Xanthate Adsorption on Vacuum Deposited Films of Lead Sulfide and Metallic Copper Under Conditions of Controlled Oxydation. J. Phys. Chem., v. 67, 1963, p. 2121.

27. Shvedov, D. A., and A. O. Andreeva. Scientific Investigatory Work on the Theory and Practice of Flotation (Papers). Ob"edinenie Nauchno-Teknicheskikh Izdatel'stv, No. 4, 1938, p. 130.

28. Steininger, J. Collector Ionization in Sphalerite Flotation with Sulfhydryl Compounds. Trans. Aime., v. 238, 1967, p. 251.

29. Taggart, A. F., G. R. M. del Giudice, and O. A. Ziehl. Case for the Chemical Theory of Flotation. Trans. AIME, v. 112, 1934, p. 348.

30. Taylor, T., and A. F. Knoll. Action of Alkali Xanthates on Galena. Trans. AIME, v. 112, 1934, p. 382.

31. Tolun, R., and J. A. Kitchener. Electrochemical Study of the Galena-Xanthate Flotation System. Trans. IMM, v. 73, 1964, p. 313.

32. Toperi, D., and R. Tolun. Electrochemical Study and Thermodynamic Equilibria of the Galena-Oxygen-Xanthate Flotation System. Trans. IMM, v. 78, 1969, p. C191.

33. Usul, A. H., and R. Tolun. Electrochemical Study of the Pyrite-Oxygen-Xanthate System. Internat. J. Miner. Proc., v. 1, 1974, p. 135.

34. Wark, I. W., and A. B. Cox. Principles of Flotation. III. An Experimental Study of the Influence of Cyanide, Alkalies, and Copper Sulfate on Effect of Sulfur-bearing Collectors at Mineral Surfaces. Trans. AIME, v. 112, 1934, p. 267.

35. Woods, R. Flotation, A. M. Gaudin Memorial Volume, ed. by M. C. Fuerstenau. AIME, New York, 1976, p. 298.

36. Yamasaki, T., and S. Usui. Infrared Spectroscopic Studies of Xanthate Adsorbed on Zinc Sulfide. Trans. AIME, v. 232, 1965, p. 36.

EFFECTS OF POINT DEFECTS ON FLOTATION[1]

by

F. F. Aplan[2], G. Simkovich[3], E. Y. Spearin[4], and K. C. Thompson[5]

It is well known that the behavior of minerals from seemingly similar deposits, or even from within a single deposit, may not only differ from one another in chemical and physical properties but also differ in their response to such mineral beneficiation processes as flotation, electrostatic separation, and chemical dissolution. When gross chemical and physical differences are apparent, a difference in response to beneficiation is anticipated; however, sometimes very slight changes in composition, often imperceptible in the usual mineralogical examination, may cause a significant change in the response of that mineral to a beneficiation process. An ore containing even a small proportion of the desired mineral in some form that is more difficult to concentrate will then show either an overall decrease in recovery or a decrease in concentrate grade.

In many solids, including a wide variety of minerals, impurities or defects in the natural crystalline solid, called point defects, are known to have a profound effect on the nature of the solid. Changes in electrical and surface properties due to natural or artificially induced point defects at a concentration of 1 mole-percent, and often very much less, have been well documented in the literature (7). One such example has been in the development of semiconductor devices that have revolutionized the electronics industry. The economic impact of these solid-state devices has been massive. More recently, attention has focused on the application of these principles to ore beneficiation studies. As applied to flotation, the pioneering and independent studies by Plaksin and Shafeev (11) and by Simkovich (16) showed that point defects in solids may act as active sites for adsorption, for flotation collectors, or for potential determining ions.

---

[1] This work was done in the Mineral Processing Laboratories of The Pennsylvania State University.

[2] Mineral Processing Section, The Pennsylvania State University, University Park, Pa.

[3] Metallurgy Section, The Pennsylvania State University, University Park, Pa.

[4] Research Laboratories, Inland Steel Corp., East Chicago, Ind.

[5] Utah International, Sunnyvale, Calif.

A number of investigators (5, 9, 11-16) working with such solids as AgCl, Al_2O_3, CaF_2, PbS, ZnO, and ZnS showed that their surface properties in solution, ability to adsorb collectors, and floatability can be altered by introduction of point defects, as, for instance, by controlled doping. Simkovich (16), for example, demonstrated that the ionic solid, horn silver (AgCl), and the amphoteric semiconductor, galena (PbS), exhibit marked differences in their flotation behavior depending upon the type and concentration of the point defects present in the solid. Other studies (17) have demonstrated the marked effect point defects may have on the response of particles to electrostatic separation. Simkovich and Wagner (18) have shown that the rate of chemical dissolution of a solid may also be influenced in a major way by the presence of these point defects.

In spite of these indications that point defects may have a substantial effect on the nature of the solid and hence on beneficiation processes, the main thrust of flotation research in the past few decades has been largely concentrated on a study of the liquid phase and interactions at the solid-liquid interface. Typically, only the gross nature of the solid is considered, and such differences in the nature of the solid as those caused by point defects, resulting from a rather subtle change in the composition, have generally been ignored. In an effort to rectify this oversight, the senior authors have been engaged in a major research effort concerning the effect of these solid-state defects on flotation, electrostatic separation, and chemical dissolution processes. This report represents a portion of the flotation results obtained in that study.

FLOTATION AND SURFACE PROPERTIES OF THE P-TYPE SEMICONDUCTOR, NiO

NiO is an excellent example of a solid whose electrical properties may be affected profoundly by small amounts of impurities.

Theoretical Background

The point defect structure of NiO illustrates well this effect. It is rather well accepted that the majority of point defects in NiO are doubly charged cation vacancies, V(Ni)" (the symbol ' denotes a single negative charge and the symbol " a double negative charge in comparison to the defect-free, undisturbed site) and holes, ⊕, which are formed in accord with the reaction

$$\tfrac{1}{2}O_2 = V(Ni)'' + 2\oplus + NiO \qquad (1)$$

with the equilibrium condition

$$K_1 = [V(Ni)''][\oplus]^2 P_{O_2}^{-1/2} \qquad (2)$$

where P indicates partial pressure, [ ]'s indicate concentration terms, and K_1 is a constant for a particular temperatute and total pressure. (Holes may be formed, for example by substituting Ni^{+3} for Ni^{+2} in the cation sublattice.) In a pure crystal of NiO, electrical neutrality requires

$$2[V(Ni)'']^{\circ} = [\oplus]^{\circ} \tag{3}$$

where the superscript ° indicates intrinsic defect concentrations. Utilizing equation 3 in equation 2 gives either

$$[\oplus]^{\circ} = \left(2K_1P_{O_2}^{1/2}\right)^{1/3} = \text{const } P_{O_2}^{1/6} \tag{4}$$

or

$$[V(Ni)'']^{\circ} = [K_1P_{O_2}^{1/2}/2]^{1/3} = \text{const } P_{O_2}^{1/6} \tag{5}$$

The electrical conductivity, σ, of NiO is primarily dependent upon the concentration of holes in NiO, because the mobility of the holes is considerably higher than that of the cationic vacancies. Hence, at a particular temperature one has the relationship:

$$\sigma \propto [\oplus] \tag{6}$$

Hence, for pure nickel:

$$\sigma = \text{const } P_{O_2}^{1/6} \tag{7}$$

and, of course, at a constant oxygen pressure the conductivity of pure NiO should be a constant.

Consider now the effect of small amounts of impurities dissolved in NiO. Two cases will be taken into account, that of an impurity based upon a higher valent cation, say Al_2O_3, and that of an impurity based upon a lower valent cation, say Li_2O.

The dissolution of Al_2O_3 into NiO may be given as

$$Al_2O_3 = 2Al(Ni)^{\bullet} + V(Ni)'' + 3NiO \tag{8}$$

where $Al(Ni)^{\bullet}$ indicates a trivalent aluminum ion substituted for a divalent nickel ion, the site bearing an excess positive charge (the symbol $^{\bullet}$ denotes a single positive charge on the center).

In accord with equation 8 the dissolution of a higher valent cation into the nickel ion sublattice results in an increase in cation vacancies. Hence, in accord with equations 2 and 6 the number of electron holes and, hence, the electrical conductivity of the NiO doped with the higher valent cation, should decrease.

Conversely, the dissolution of a lower valent cation, say Li_2O, increases the concentration of holes in accord with the reaction

$$Li_2O + \frac{1}{2}O_2 = 2Li(Ni)' + 2\oplus + 2NiO. \qquad (9)$$

Therefore, the conductivity of Li_2O doped NiO should be higher than that of pure NiO and should increase as the content of the dopant, Li_2O, is increased.

Advantage has been taken of this fact to effect a high-tension (often improperly called "electrostatic") separation (17). As will be demonstrated, these changes in the nature of the solid also manifest themselves in flotation separations.

Electrophoretic Mobility Studies

Samples of NiO were prepared from reagent-grade NiO and sintered at 1,275°C. Doped NiO was produced in a similar manner after first adding 1 mole-percent of Li_2O or Al_2O_3.

The samples were finely ground and their electrophoretic mobilities measured with a Zeta Meter. These tests, summarized in table 1, indicate that the point of zero charge (PZC) can be substantially altered by doping. The PZC of the "pure" NiO occurs at pH 7.5; doping with 1 mole-percent of the monovalent ion (Li^+) lowers it to pH 6.4; while doping with 1 mole-percent of a trivalent ion (Al^{+3} or Cr^{+3}) raises it to pH 9.4. Since pH 9.4 is also the PZC of alumina (8), the sample doped with Cr^{+3} was also tested to insure that the shift in PZC was due to the doping and not to the Al^{+3} per se. The data show this to be exactly the case.

TABLE 1. - Shift in PZC of NiO due to doping

	PZC (pH)
NiO - 1% Li_2O	6.4
NiO - "pure"	7.5
NiO - 1% Al_2O_3	9.4
NiO - 1% Cr_2O_3	9.4

Flotation Testing

Flotation tests using 1×10^{-4} mole/liter sodium dodecyl sulfate and 5×10^{-5} mole/liter dodecyl ammonium hydrochloride were made in the Hallimond tube using 48 x 65-mesh particles and a 60-second flotation time. Flotation results for the Li^+ doped, the undoped or "pure," and the Al^{+3} doped NiO are given in figure 1. The data are shown to be in complete accord with the electrostatic theory of flotation (1, 6, 8). Below the PZC, the surface is positively charged and the solid is best floated with the anionic dodecyl sulfate. Above the PZC, where the surface is negative, flotation is best achieved with the cationic dodecyl amine. Doping with Li^+, which shifts the PZC to a lower value, is also seen to shift the floatability of the NiO to lower pH values, as may be seen by comparing figures 1(A) and 1(B). Figure 1(C) shows that doping with Al^{+3} shifts the PZC and hence the floatability

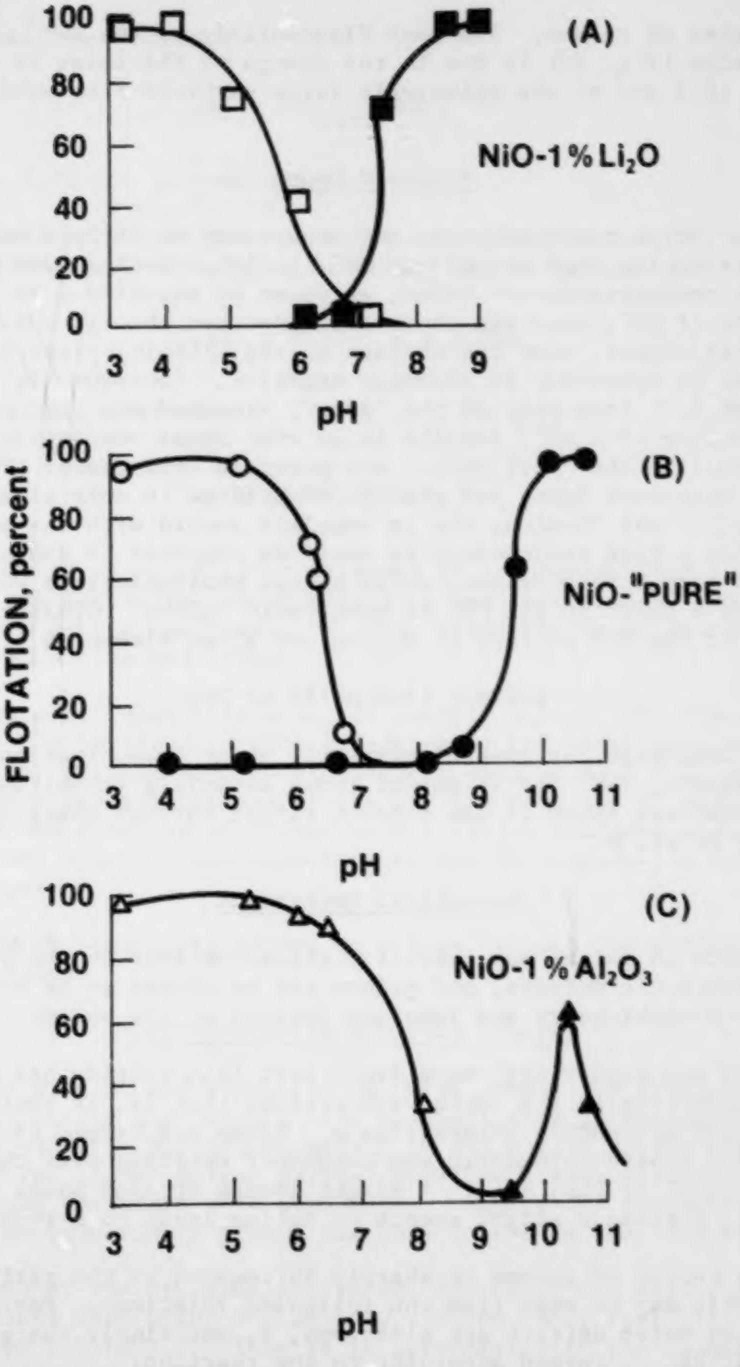

FIGURE 1. - Flotation recovery of lithium-doped nickel oxide (A), "pure" nickel oxide (B), and aluminum-doped nickel oxide (C). Collectors: solid points, cationic dodecyl amine; open points, anionic dodecyl sulfate.

of NiO to higher pH values. The poor floatability of the Al^{+3} doped nickel oxide with amine (fig. 1C) is due to the change of the amine to the RNH_2° form near pH 10.5 and to the relatively large particle size used in these experiments.

Proposed Model

NiO is a p-type semiconductor, and conduction is through holes ($\oplus$). The potential determining ions are H^+ and OH^- (1, 10). Doping with Li^+ greatly increases the concentration of holes, as shown by equation 9 and so enhances the adsorption of OH^-, over and above that adsorbed through specific adsorption from other causes, that the surface at the slipping plane (where the zeta potential is measured) is strongly negative. Consequently, the PZC is lowered (to pH 6.4) from that of the "pure", sintered NiO (PZC at pH 7.5). Conversely, doping with Al^{+3} results in an even lower concentration of holes than are present in the "pure" NiO. Any possible enhancement of OH^- adsorption is thus very much less, and the PZC is shifted to more alkaline values (PZC at pH 9.4). Our findings are in complete accord with the prediction by Parks (10) that p-type semiconductors would be expected to exhibit a shift in the PZC to more acidic values, while n-type semiconductors would be expected to show a shift of the PZC to more basic values. Greater details of the response of the NiO surface to doping are given elsewhere (2).

SURFACE PROPERTIES OF PbS

Another semiconductor mineral currently under investigation in our laboratories is galena, PbS. It is one of those materials exhibiting amphoteric electronic behavior, since it can conduct either through quasi-free electrons, $\ominus$, or through holes, $\oplus$.

Theoretical Background

The defects in galena may consist of either defects in the ionic crystal lattice or electronic defects, and galena may be either p- or n-type depending on the stoichiometry and impurity content of the solid.

Simkovich and Wagner (19) have found that lead sulfide has a Frenkel type defect structure in the cation sublattice; that is, it contains both cation vacancies and cation interstitials. Bloem and Kröger (3) found lead sulfide to be a nonstoichiometric semiconductor existing over the narrow range of $Pb_{1.0008}S$ to $PbS_{1.0003}$. A slight excess of lead makes it an n-type semiconductor, whereas a slight excess of sulfur leads to p-type conduction.

Thus the nature of galena is sharply influenced by the partial pressure of sulfur. This may be seen from the following relations. For the case of n-type PbS, the major defects are electrons, $\ominus$, and singly charged cation interstitials, $Pb_{int}^{\cdot}$, formed according to the reaction:

$$PbS = Pb_{int}^{\cdot} + \ominus + \frac{1}{2}S_2(g) \qquad (10)$$

with the equilibrium condition:

$$K_2 = [\mathrm{Pb}^{\cdot}_{\mathrm{int}}][\theta]P_{S_2}^{1/2} \tag{11}$$

where brackets indicate concentrations.

For the case of p-type PbS the major defects are holes, $\oplus$, and singly charged lead vacancies. Here, the formation may be written as:

$$\frac{1}{2}S_2(g) = V(Pb)' + \oplus + PbS \tag{12}$$

with the equilibrium condition:

$$K_4 = [V(Pb)'][\oplus]P_{S_2}^{-1/2} . \tag{13}$$

In accord with equation 11 an increase in the equilibrium sulfur pressure will decrease the concentration of electrons and interstitial lead until the galena becomes a p-type conductor. At this point the major point defects become cation vacancies and holes.

The presence of impurities also, of course, affects the concentration of point defects. In particular, with reference to the electronic defects it may be noted that soluble monovalent sulfides such as Ag_2S will always increase the p-type characteristics of the PbS (in both the p- and n-type ranges), while the presence of higher valent cation sulfides such as Bi_2S_3 will increase the n-type characteristics of the PbS (again, in both the p- and n-type ranges).

Most naturally occurring galena is n-type, though the p-type is occasionally also found.

Electrophoretic Mobility Studies

Samples of natural and synthetic PbS were used. The synthetic galena was prepared by mixing high-purity lead and sulfur in an enclosed Pyrex tube and heating to 400° C. Nonstoichiometric n- and p-type galena were prepared by careful control of the sulfur partial pressure during reaction. Silver- and bismuth-doped materials were also made. Samples for the electrophoretic mobility studies were finely ground and then tested in the Zeta Meter.

All but one of the PbS samples tested, including the synthetic galena and natural galena from Coeur d'Alene, Id.; Bixby, Mo.; Park City, Utah, gave PZC values at pH 2.0 to 2.1. This is in agreement with the values reported by Healy and Moignard (4). The PZC of the natural sample from Baxter Springs, Kans., however, was found to be at pH 6.7. These surprising results prompted a more thorough study of the electrokinetic properties of PbS. This study led to the discovery that if, after grinding, the synthetic samples were washed with distilled water and the supernatant liquid removed, not only were the PZC values of the synthetic PbS samples shifted to higher pH values, but a significant differentiation between the various samples could then be seen. The data are summarized in table 2.

TABLE 2. - Points of zero charge of synthetic PbS

PbS sample	PZC (pH)		
	Unwashed	Washed	In 5 x 10^{-7} M $NaSH \cdot \chi H_2O$
Nonstoichiometric p-type ..	2.1	5.8	2.1
Nonstoichiometric n-type ..	2.1	6.7	2.1

This prompted a more detailed study of the differences between the washed and unwashed samples. It was suspected that the differences were due to some potential determining ion such as HS^-, and so the electrophoretic mobilities of the washed samples were determined in the presence of various concentrations of hydrated NaSH. NaSH concentrations of 5 x 10^{-7} mole/liter or greater were found to be sufficient to revert the PZC to 2.1 (see table 2). It was therefore concluded that HS^- and/or S^{-2} are potential determining ions. Alternatively, one could conjecture that $S°$, formed by reduction at the PbS surface, may be responsible for the PZC values at pH 2.1.

A more detailed report of our findings for the electrophoretic mobility of PbS as influenced by point defects and by OH^- and SH^-, together with flotation results with xanthate, dixanthogen, dodecyl amine, and dodecyl sulfate collectors, is being readied for publication elsewhere.

Proposed Model

It would appear that for p-type PbS (see equation 13), the holes tend to fix OH^- onto the surface or, alternatively, repel H^+. The net effect of this p-type semiconductivity is to shift the PZC to a more acidic value, as indicated by the PZC of 5.8 noted for the washed nonstoichiometric p-type material. For the n-type material, the highly mobile electrons move the PZC to more alkaline values (pH 6.7). The mechanism is not unlike that proposed for NiO upon doping (2).

These studies are a part of a much larger program to evaluate the effect of point defects on the surface properties of solids and their response to such beneficiation processes as flotation, high-tension ("electrostatic") separation, and leaching.

ACKNOWLEDGMENTS

The authors wish to acknowledge the National Science Foundation for financial support in the conduct of this research under Grant ENG 78-18834. Acknowledgment is also made to Ms. K. Ridge and Mr. R. A. Fensterer for help in some of the electrophoretic mobility and flotation experiments.

REFERENCES

1. Aplan, F. F., and D. W. Fuerstenau. Principles of Nonmetallic Mineral Flotation. Froth Flotation, 50th Anniversary Volume, ed. by D. W. Fuerstenau, New York, AIME, 1962, p. 170.

2. Aplan, F. F., G. Simkovich, and E. Y Spearin. Flotation and Surface Properties of the p-Type Semiconductor NiO as a Function of Point Defects. Submitted to J. Colloid and Interface Sci. Presented at 53d Colloid and Surface Science Symposium, Rolla, Mo., June 11-13, 1979.

3. Bloem, J., and F. A. Kröger. The P-T-X Phase Diagram of the Lead Sulfur System. Z. Physik. Chem., v. 7, ch. 1, 1956.

4. Healy, T. W., and M. S. Moignard. A Review of Electrokinetic Studies of Metal Sulfides. Flotation, A. M. Gaudin Memorial Volume, ed. by M. C. Fuerstenau, New York, AIME, 1976, p. 275.

5. Honig, E. P., and J. H. Th. Hengst. The Point of Zero Charge and Solid State Properties of Silver Bromide. J. Colloid and Interface Sci., v. 31, 1969, p. 545.

6. Iwasaki, I., S. R. B. Cooke, and A. F. Colombo. Flotation Characteristics of Geothite. BuMines RI 5593, 1960, 25 pp.

7. Kröger, F. A. The Chemistry of Imperfect Crystals. John Wiley & Sons, Inc., New York, 1964, 1039 pp.

8. Modi, H. J., and D. W. Fuerstenau. Flotation of Corundum: An Electrochemical Interpretation. Trans. AIME, v. 217, 1960, p. 381.

9. Mular, A. L. Effects of Impurities on the Flotation Behavior of Zinc Oxide. Trans. AIME, v. 232, 1965, p. 204.

10. Parks, G. A. The Isoelectric Points of Solid Oxides, Solid Hydroxides, and Aqueous Hydroxo Complex Systems. Chem. Rev., v. 65, 1965, p. 177.

11. Plaksin, I. N., and R. S. Shafeev. Influence of Surface Properties of Sulfide Minerals on Adsorption of Flotation Reagents. Trans. IMM, v. 72, 1962-63, p. 715.

12. _____. Relation Between Energy Structure of Mineral Crystals and Their Flotation Properties. Proc. 8th Internat. Miner. Proc. Cong., Leningrad, paper S-3, 1968, p. 1-8.

13. Rao, B. U., H. H. Lovell, and G. Simkovich. The Flotation of Fluorite as a Function of Ionic Point Imperfections. Trans. AIME, v. 241, 1968, p. 328.

14. Richardson, P. E., and E. E. Maust. Surface Stoichiometry of Galena in Aqueous Electrolytes and Its Effect on Xanthate Interactions. Flotation, A. M. Gaudin Memorial Volume, ed. by M. C. Fuerstenau, New York, AIME, 1976, p. 364.

15. Roy, P., and D. W. Fuerstenau. The Effect of Doping on the Point of Zero Charge of Alumina. Surface Sci., v. 30, 1972, p. 487.

16. Simkovich, G. The Influence of Solid State Point Defects Upon Flotation Processes. Trans. AIME, v. 227, 1963, p. 306.

17. Simkovich, G., F. F. Aplan, and R. A. Fensterer. Point Defects in the Electrostatic Separation of Nickel Oxide. IEC Fundamentals, v. 11, 1972, p. 275.

18. Simkovich, G., and J. B. Wagner. The Influence of Point Defects on the Kinetics of Dissolution of Semiconductors. J. Electrochem. Soc., v. 110, 1963, p. 513.

19. _____. Self-Diffusion of Lead 210 in Sample Crystals of Lead Sulfide as a Function of Stoichiometry and Doping Additions. J. Chem. Phys., v. 38, 1963, p. 1368.

THERMODYNAMICS OF SULFIDE MINERAL FLOTATION SYSTEMS

by

Douglas W. Fuerstenau[1]

ABSTRACT

This paper discusses thermodynamic relationships involved in the wetting behavior and flotation of sulfide minerals and reviews the thermodynamics of collector adsorption in several different sulfide mineral systems. Both physical and chemical adsorption systems are included and interpreted in light of thermodynamic and model considerations.

INTRODUCTION

Flotation is a physiochemical process in which mineral beneficiation is achieved through establishing contact between mineral particles and air bubbles dispersed in an aqueous phase. Thermodynamics predicts whether or not a change will tend to occur but says nothing about the rate at which the change takes place. Because of the dynamic conditions prevailing in a flotation cell, it is not possible thermodynamically to predict the recovery and grade of the mineral product produced in flotation under a given set of operating conditions. It is possible, however, to predict how the flotation response may change with various variables such as temperature, pH, and collector concentration. Although complete equilibrium conditions do not exist in a flotation cell, in some stages of the flotation process equilibrium or quasi-equilibrium conditions do exist. The following kinds of information can be obtained from thermodynamic considerations:

1. Surface energies of liquids and solids can be calculated, and from thermodynamic relationships surface free energies can then be evaluated.

2. The energies of wetting, spreading, and adhesion of phases are determined by the interfacial tensions of the respective interfaces. Thermodynamics permits prediction of these phenomena.

3. Changes in surface or interfacial tensions can be evaluated as a function of adsorption densities using thermodynamic relationships. Knowledge of such changes in interfacial tensions is essential to predict bubble-particle contact in flotation.

---

[1] Department of Materials Science and Mineral Engineering, University of California, Berkeley, Calif.

4. The stability of the thin aqueous film between a mineral surface and an approaching bubble depends upon the thermodynamics of thin films.

5. Surface thermodynamics with ionic or polarized systems permits evaluation of the properties of the electrical double layer, including surface tension, surface charge, and surface potential phenomena.

6. The free energy of adsorption, a measure of the strength of the bond between a reagent (such as a collector) and the mineral surface, can be evaluated from adsorption or thermodynamic measurements. If thermodynamic data are available at different temperatures, the heat and entropy of adsorption can be calculated. Direct measurements of heat of adsorption can be used to establish the nature of reagent-mineral interactions and the distribution of reactive sites at the surface. The effect of temperature on flotation can be predicted if thermodynamic data are available.

7. In the case of somewhat reactive solids, such as sulfide minerals, it is possible to predict from thermodynamic data the conditions in which a metal-reagent complex (or a disulfide of the collector in the case of thiol reagents) will form. It is now generally believed that formation of such compounds is essential for good floatability.

8. Conditions for the formation of reagent-metal-hydrolysis complexes in solution can be predicted from thermodynamic data.

9. The stability of colloidal suspensions can be interpreted in terms of thermodynamic considerations, including slime coating phenomena.

THERMODYNAMICS OF WETTING

Bubble-particle contact is one of the key factors controlling the process of froth flotation. The general thermodynamic condition for three-phase contact is defined by Young's equation for the system depicted schematically in figure 1:

$$\gamma_{SG} - \gamma_{SL} = \gamma_{LG} \cos \theta \tag{1}$$

where γ_{SG}, γ_{SL}, and γ_{LG} are the tensions of the solid/gas, solid/liquid, and liquid/gas interfaces, respectively, and θ is the contact angle. The change in the free energy accompanying the replacement of a unit area of the solid/liquid interface by solid/gas interface is given by Dupre's equation:

$$\Delta G = \gamma_{SG} - (\gamma_{SL} + \gamma_{LG}). \tag{2}$$

Combination of Dupre's equation with Young's equation yields the following expression for the free energy change accompanying dewetting:

$$\Delta G = \gamma_{LG} (\cos \theta - 1). \tag{3}$$

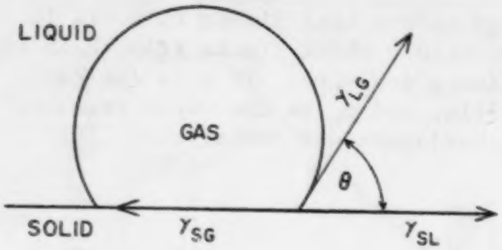

FIGURE 1. - Schematic representation of the three-phase equilibrium contact between an air bubble and a solid immersed in a liquid. The contact angle θ is the angle between the liquid/gas and the liquid/solid interfaces, measured through the liquid.

Thus, for any finite value of the contact angle, there will be a free energy decrease upon attachment of a mineral particle to an air bubble. The theoretical relationship of Dupre's equation expresses the maximum possible decrease in the free energy of the system resulting from the bubble-particle contact, which can be realized only when there are no other energy-consuming effects, such as deformation of the bubble. Often considerable hysteresis exists in measured contact angles because of surface roughness, contamination, nonequilibrium adsorption effects, etc. (1). If there is hysteresis, that is, if a liquid-advancing contact has a different value than a liquid-receding angle, equilibrium is not attained in the system; under these conditions the use of Young's equation is not valid. The relation given by equation 2 assumes that there is no liquid layer between the bubble and the particle after contact. In some cases there may be a thin liquid layer between the bubble and the solid, even after attachment. The thinning of this layer is believed to control flotation, and particularly flotation kinetics. Laskowski (28) has attempted to modify this equation for the presence of a liquid layer by making the following substitutions:

1. $G_s(h)$ for γ_{SG} where G_s is the free energy of a column of liquid layer (of height h) and solid of unit cross section and

2. $G_s(h) = \gamma_{SL} + \gamma_{LG}(h)$. $\gamma_{LG}(h)$ is the surface tension of the liquid/gas interface expressed as a function of the thickness of a liquid layer h.

These substitutions lead to

$$\Delta G(h) = \gamma_{LG}(h) - \gamma_{LG} \qquad (4)$$

where $\Delta G(h)$ expresses the energy barrier in the transition from no contact to bubble contact that must be overcome for attachment to occur (28).

Derjaguin (9) suggested that the thermodynamic properties of thin films are different from those of the bulk phase and introduced the concept of a "disjoining pressure," Π, as a measure of the corresponding change in the thermodynamic properties. In effect, it is the change of free energy with thickness and is given by the expression:

$$\gamma = \gamma_o + \int_h^{\infty} \Pi \, dh \qquad (5)$$

where γ is the specific surface free energy of the thin liquid film, γ_o is the specific surface free energy of an infinitely thick liquid film, h is the thickness of the film, and Π is the disjoining pressure. If p is the vapor pressure in equilibrium with a flat thin film, and p_o is the vapor pressure in equilibrium with the bulk liquid, then Derjaguin and Shcherbakov (10) showed

$$RT \ln \frac{p}{p_o} = V_m \left(\frac{\partial G}{\partial h}\right)_{A,T} \tag{6}$$

where V_m is the molar volume of the liquid and the term $\partial G/\partial H$ is the disjoining pressure, Π. If Π is positive, the thin film is stable.

The disjoining pressure can be due to many effects. It is usual to consider that these effects are additive (33) and that the disjoining pressure can be broken down into a number of components:

$$\Pi = \Pi_{LL} + \Pi_{SL} + \Pi_{el} + \Pi_h + \Pi_p + \Pi_i \tag{7}$$

where

Π_{LL} is the disjoining pressure of the liquid film in the absence of a solid,

Π_{SL} is the disjoining pressure due to the effect of the solid on the liquid film,

Π_{el} is an electrostatic term to account for double layer effects,

Π_h is the contribution from hydrogen bonding,

Π_p is the contribution from polar interactions, and

Π_i is the change in free energy due to any other specific interactions between the liquid layer and the surface.

Chander and Fuerstenau (5) have made an attempt to explain the natural floatability of molybdenite using this approach. Figure 2 clearly shows that the flotation of molybdenite is affected by the electrical potential at surface (a topic covered in more detail later); the change in zeta potential manifests itself in the Π_{el} term of equation 7.

For most minerals, however, polar interactions at the interface give rise to positive disjoining pressures and, hence, to nonflotation. Organic surface-active agents, called collectors, are added to the system to adsorb at the mineral surface and reduce the polar interactions between the mineral and water.

Control of the wettability of minerals is achieved through the adsorption of collectors, which change the interfacial tensions such that the contact angle becomes finite. Changes in surface tension at an interface

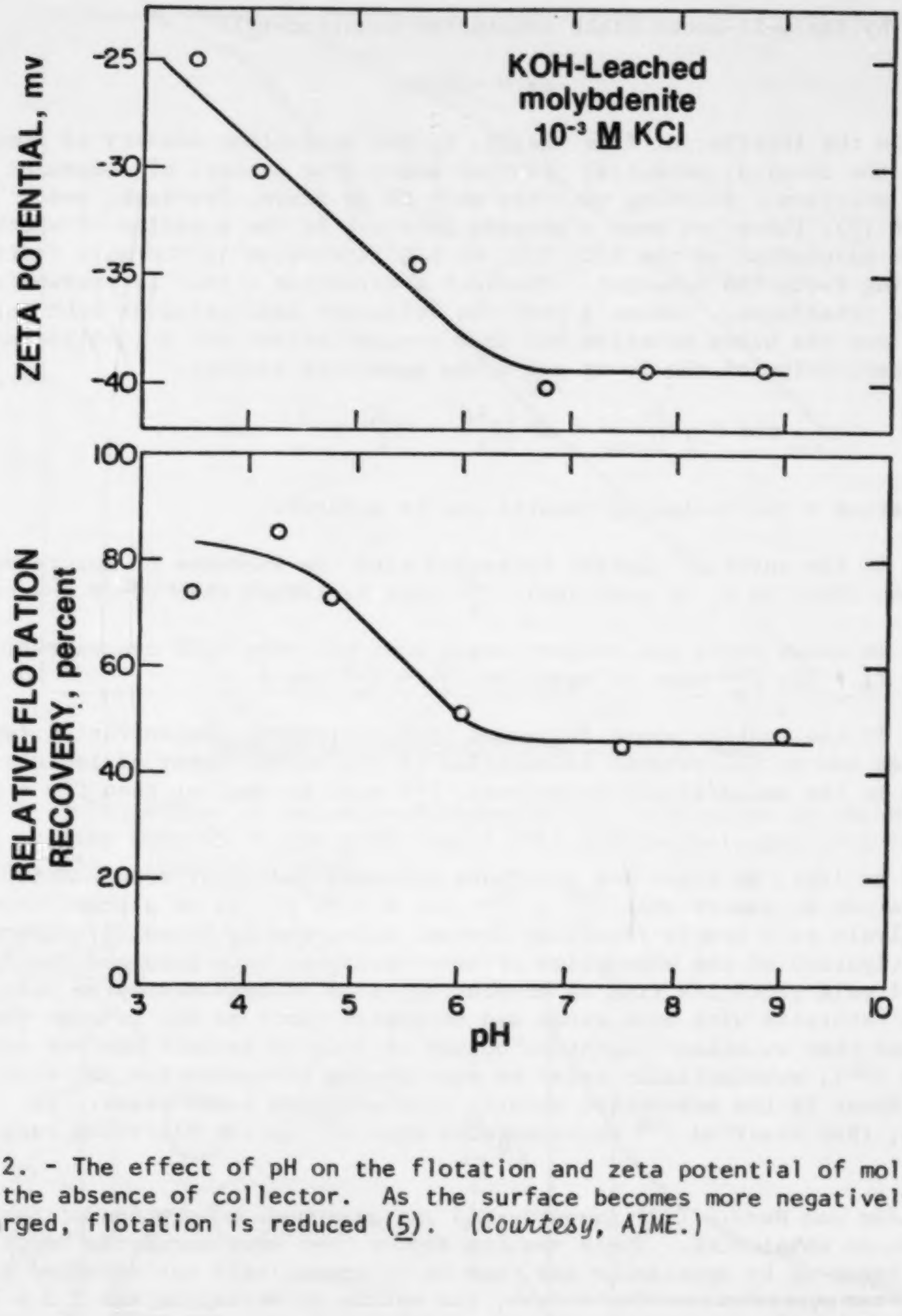

FIGURE 2. - The effect of pH on the flotation and zeta potential of molybdenite in the absence of collector. As the surface becomes more negatively charged, flotation is reduced (5). (*Courtesy, AIME.*)

is given by the well-known Gibbs adsorption equation (1):

$$d\gamma = -\Sigma\Gamma_i d\mu_i \tag{8}$$

where γ is the interfacial free energy, Γ_i the adsorption density of component i and μ_i the chemical potential (partial molar free energy) of component i in the bulk solution. Starting with the work of de Bruyn, Overbeek, and Schuhmann (8), there has been a growing interest in the question of whether collector adsorption at the S/L, S/G, or L/G interfaces is the main factor controlling flotation behavior. Consider a collector x that is present at all three interfaces. Assuming that the collector adsorption at each interface follows the Gibbs equation and that concentrations and activities are equal, combination of the Young and Gibbs equations yields:

$$\gamma_{LG} \sin\theta \frac{d\theta}{d \ln C_x} = RT \left[\Gamma_x^{SG} - (\Gamma_x^{SL} + \Gamma_x^{LG} \cos\theta)\right]. \tag{9}$$

From equation 9 the following results can be deduced:

1. If the angle of contact increases with the increase of solute concentration ($d\theta/d \ln C_x$ is positive), Γ_x^{SG} must be larger than $\Gamma_x^{SL} + \Gamma_x^{LG} \cos\theta$.

2. In cases where the contact angle does not vary with concentration ($d\theta/d \ln C_x = 0$), Γ_x^{SG} must be equal to $\Gamma_x^{SL} + \Gamma_x^{LG} \cos\theta$.

3. If the contact angle decreases with increasing concentration (which may happen due to the reverse orientation of the second layer of ionic surfactants at the solid/liquid interface), Γ_x^{SG} must be smaller than $\Gamma_x^{SL} + \Gamma_x^{LG} \cos\theta$.

As early as 1954, de Bruyn and coworkers stressed the first result obtained from equation 9, namely that $\Gamma_x^{SG} > \Gamma_x^{SL}$ (for $\theta < 90°$). In an attempt to apply that analysis to a simple flotation system, Aplan and de Bruyn (2) undertook an investigation of the adsorption of hexylmercaptan onto gold and the flotation of gold particles from an aqueous solution of hexylmercaptan using nitrogen saturated with both water and mercaptan vapor as the gaseous phase. They found that excellent flotation occurs at 3 to 30 percent surface coverage (low Γ^{SL}), substantially below an equilibrium concentration where an abrupt change in the adsorption density from solution takes place. In addition, they observed Γ^{SG} to be greater than Γ^{SL} in the flotation range (fig. 3).

Gaudin and Harris (17) investigated the gas-phase adsorption of hexylmercaptan on sphalerite. Their results showed that hexylmercaptan vapor is readily taken up by sphalerite and that it is essentially not desorbed by water. After equilibration for 4 days, the uptake of mercaptan was 2.2×10^{-9} mole/cm^2, and after 7 days it was 2.7×10^{-9} mole/cm^2. Subsequent evacuation for 7.5 hours reduced the 7-day uptake only to 2.4×10^{-9} mole/cm^2, indicating its strong adherence to the mineral. Gaudin and Harris calculated the monolayer coverage to be 7.4×10^{-10} mole/cm^2, but a Langmuir-type calculation indicates the monolayer to be 1.6×10^{-9} mole/cm^2, using their measured surface area. By means of infrared spectroscopy, Wadsworth and Eyring (11)

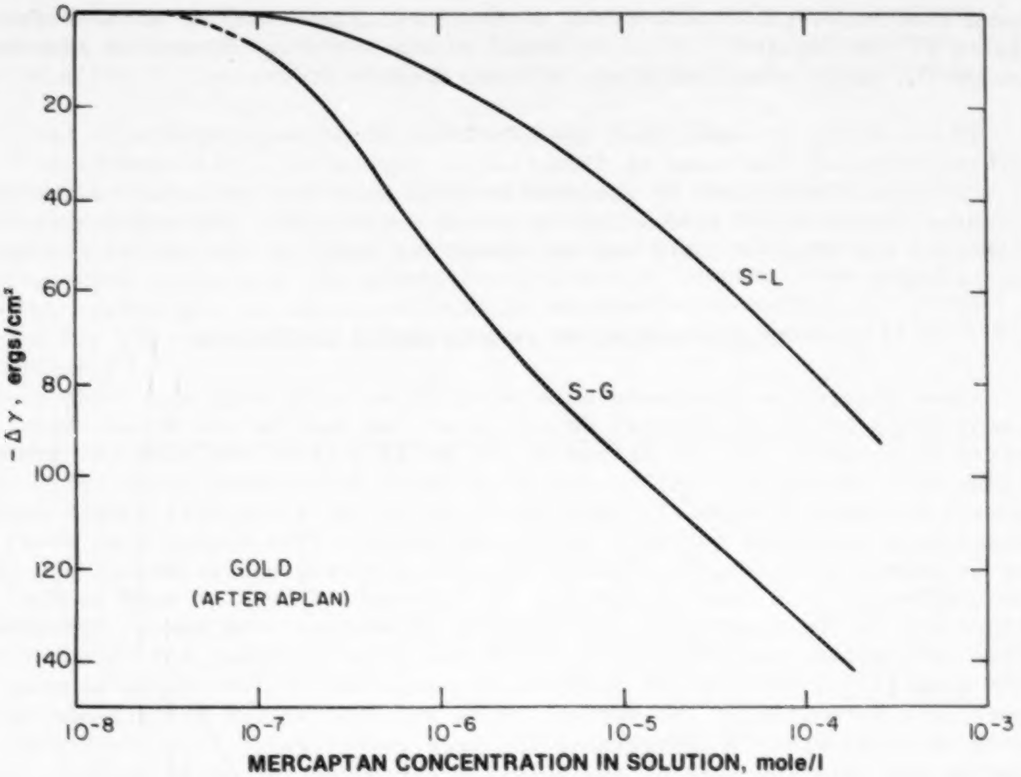

FIGURE 3. - The effect of mercaptan concentration in solution on the decrease in surface tension on the gold-liquid (SL) and the gold-gas (SG) interfaces (2). (*Courtesy*, AIME.)

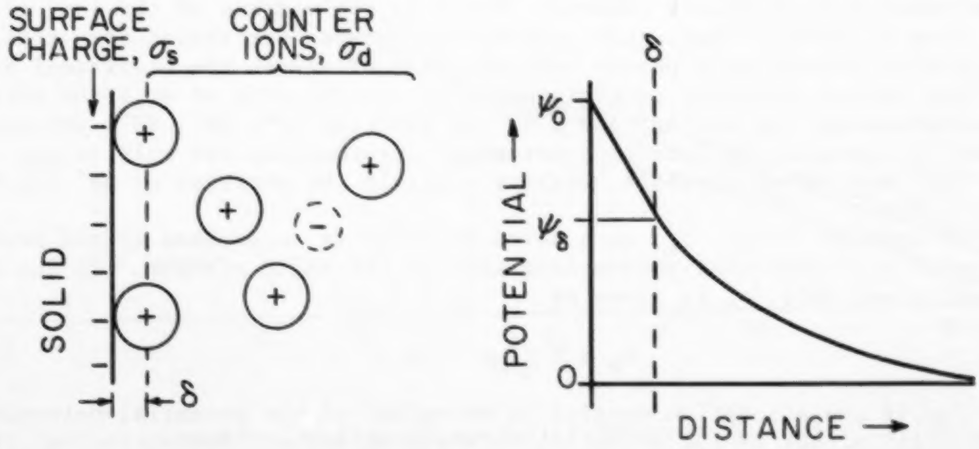
SURFACE CHARGE, σ_s
COUNTER IONS, σ_d
SOLID
δ
δ
ψ_0
ψ_δ
POTENTIAL →
0
DISTANCE →

FIGURE 4. - Schematic representation of the electrical double layer and the potential drop across the double layer at the solid/water interface. The ghost anion represents a negatively adsorbed anion.

showed that vapor-phase adsorption of hexylmercaptan (RSH) on sphalerite results in the formation of Zn-SR bonds at the surface. Mercaptan adsorbed through the vapor phase makes the mineral readily floatable.

It should be stressed that the interface of primary importance to collector/mineral reactions in flotation is the solid/liquid interface. The collector simply must be adsorbed at this interface in order to reduce molecular attractions between the solid and the liquid. Secondly, most collectors are water-soluble and are therefore added to the system in the aqueous phase.

THERMODYNAMICS OF SULFIDE/WATER INTERFACES

Since adsorption phenomena at mineral/water interfaces are controlled in most cases by the electrical double layer, we must be concerned with factors responsible for the charge on the solid surface and with the behavior of ions that adsorb as counter ions to maintain electroneutrality (27). Figure 4 presents a schematic representation of the electrical double layer counter ions extending out into the liquid phase. This figure also shows the drop in potential across the double layer, neglecting the potential due to dipole effects. The closest distance of approach of counter ions to the surface (δ) is the Stern plane. Depending on whether ions remain hydrated or are dehydrated upon adsorption, there can exist an inner and an outer Stern plane (20), but for our purposes we shall not differentiate between these. The potential at the surface is Ψ_o and that at the Stern plane is ψ_δ (which is considered to approximate the zeta potential). From the Stern plane on out into the bulk of the solution the potential drops to zero.

In the case of solids such as $BaSO_4$, AgI, and Ag_2S, the surface charge arises from a preference of one of the lattice ions for sites at the solid surface as compared with the aqueous phase. Equilibrium is attained when the electrochemical potential $\bar{\mu}$ ($\bar{\mu} = \mu + vF\phi$, where ϕ is the Galvani potential in the phase, F is Faraday's constant, and v is the valence of the ion) of these ions is constant throughout the system. Those particular ions that are free to pass between both phases and therefore establish the electrical double layer are called potential-determining ions. In the case of Ag_2S the potential-determining ions are Ag^+ and S^{-2}. In addition, H^+, OH^-, HS^-, and such complexing agents as CN^- are also potential-determining, but only in the sense that any change in their activity controls the activity of Ag^+ and S^{-2}.

The surface charge, σ_s, on a solid in water is determined by the adsorption density of potential-determining ions on the solid surface. In the case of a univalent salt, σ_s is given by

$$\sigma_s = F\ (\Gamma_{M^+} - \Gamma_{A^-}) \qquad (10)$$

where Γ_{M^+} is the adsorption density in moles/cm^2 of the potential-determining cation, Γ_{A^-} is that of the potential-determining anion. Hence, for AgI, M^+ and A^- are simply Ag^+ and I^-, and for silver sulfide they are Ag^+ and S^{-2}. For silver sulfide, the surface charge is then given by:

$$\sigma_s = F\ (\Gamma_{Ag^+} - 2\Gamma_{S^{-2}}). \qquad (11)$$

From a model of the double layer, the surface charge per unit area (and the charge in the diffuse part of the double layer), σ_d, is given by the Gouy-Chapman relation (27) as modified by Stern (for a symmetrical electrolyte):

$$\sigma_s = -\sigma_d = [(2\varepsilon RT/\pi)C]^{1/2} \sinh (vF\psi_\delta/RT) \qquad (12)$$

where ε is the dielectric constant of the liquid, C is the electrolyte concentration in moles/cm^3, and v is the valence of the ions for a symmetrical electrolyte. Further, if ψ_δ does not change appreciably, this equation shows that the surface charge and the adsorption density of counter ions should vary as the square root of the concentration of added electrolyte, as Morrow (18) found for the adsorption of dodecylammonium acetate on sphalerite at low concentrations.

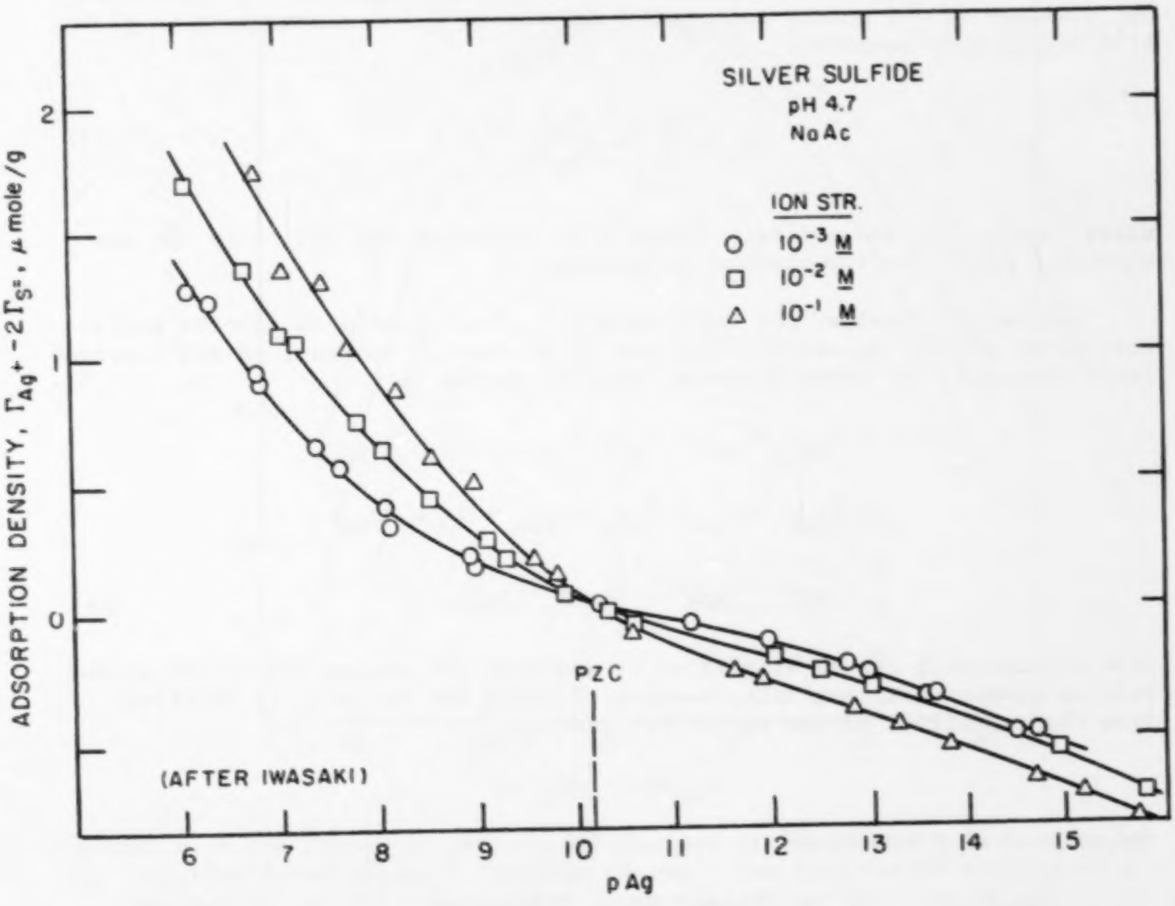

FIGURE 5. - The adsorption density of potential-determining ions of silver sulfide as a function of pAg and ionic strength, using sodium acetate as the indifferent electrolyte. At the intersection of all the curves, the surface is uncharged, the double layer is absent (4). (*Courtesy, American Chemical Society.*)

Using a simple titration procedure (12), the magnitude of the surface charge can be determined if the surface area of the solid/liquid interface is known. Figure 5 presents typical adsorption isotherms of Ag^+/S^{-2} on Ag_2S. Note that the charge on the surface increases with ionic strength and that all of the curves cross at a point (pAg 10.2). At this point, the surface charge, σ_s, is zero; that is, $\Gamma_{Ag^+} - 2\Gamma_{S^{-2}} = 0$. The activity of potential-determining ions at which this occurs is called the point-of-zero charge, the PZC. The importance of the PZC is that the sign of the surface charge has a major effect on the adsorption of all other ions and particularly those ions charged oppositely to the surface, because such ions function as the counter ions to maintain electroneutrality.

Assuming that potential differences due to dipoles, etc., remain constant, the total double layer potential (that is, the surface potential, ψ_o) is considered to be zero at the PZC. The value of the surface potential at any activity of 1-1 valent potential-determining (P.D.) electrolyte is given by a Nernst-type equation:

$$\psi_o = \frac{RT}{F} \ln \frac{a_{M^+}}{(a_{M^+})_{PZC}} \tag{13}$$

where $(a_{M^+})_{PZC}$ is the activity of the P.D. cation at the PZC, R is the gas constant, and T the temperature in Kelvins.

Let us now consider the Gibbs equation for a mineral in aqueous media. For silver sulfide in contact with sodium nitrate at constant pH and constant ionic strength, the Gibbs equation for this system is

$$\begin{aligned} d\gamma = &- \Gamma_{Ag^+}\, d\mu_{Ag^+} - \Gamma_{S^{-2}}\, d\mu_{S^{-2}} - \Gamma_{HS^-}\, d\mu_{HS^-} \\ &- \Gamma_{H_2S}\, d\mu_{H_2S} - \Gamma_{NO_3}\, d\mu_{NO_3} - \Gamma_{Na^+}\, d\mu_{Na^+} \\ &- \Gamma_{AgS^-}\, d\mu_{AgS^-} - \Gamma_{AgHS}\, d\mu_{AgHS}. \end{aligned} \tag{14}$$

This relationship can be simplified by assuming the adsorption of the silver sulfide complexes is neglible, because of their low activity in solution. From the definition of the solubility product,

$$d\mu_{Ag^+} = -\frac{1}{2} d\mu_{S^{-2}}$$

and because at constant pH,

$$d\mu_{HS^-} = d\mu_{H_2S} = d\mu_{S^{-2}},$$

the Gibbs equation simplifies to

$$d\gamma = - \left(\Gamma_{Ag^+} - 2\Gamma_{S^{-2}} + \underset{0}{\Gamma_{HS^-}} + \underset{0}{\Gamma_{H_2S}}\right) d\mu_{Ag^+}. \tag{15}$$

Equations 14 and 15 can be rewritten in terms of the surface charge and the EMF of the reversible Ag/Ag_2S electrochemical cell, E (12):

$$d\gamma = -\sigma_S dE. \tag{16}$$

Integration of the Gibbs equations permits evaluation of the change in interfacial free energy at the solid/water interface:

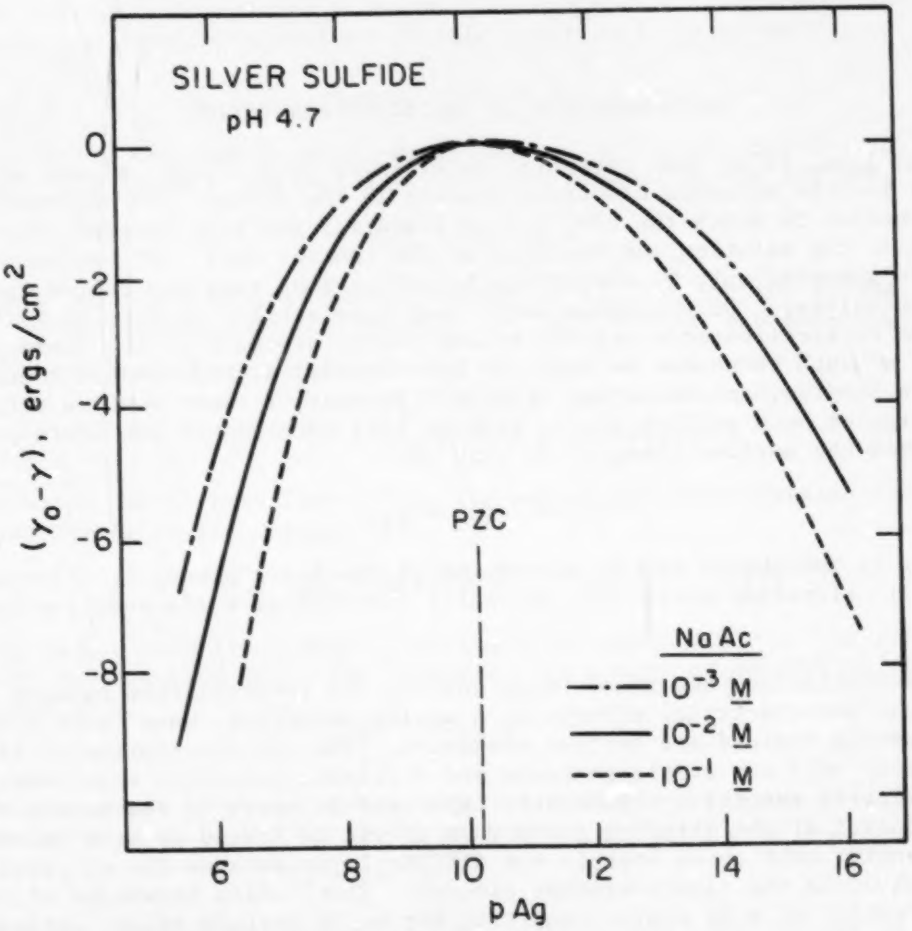

FIGURE 6. - The change in interfacial tension at the silver sulfide/aqueous solution interface as a function of pAg. The interfacial tension is a maximum at the PZC, where there is no adsorption (4). (*Courtesy, American Chemical Society.*)

$$\gamma - \gamma_o = - \int_{\mu_{Ag^+(PZC)}}^{\mu_{Ag^+}} \left(\Gamma_{Ag^+} - 2\Gamma_{S^{-2}} \right) d\mu_{Ag^+} \tag{17}$$

where γ_o is the interfacial free energy at the PZC. Figure 6 illustrates the change in interfacial tension of the solid/water interface for silver sulfide at different ionic strengths. The surface tension is a maximum at the PZC and decreases with any change in pAg from that condition.

THERMODYNAMICS OF COLLECTOR ADSORPTION

All ions, other than potential-determining (P.D.) ions, adsorb as counter ions to maintain electroneutrality in the system. In contrast to the situation in which the P.D. ions are special for each mineral, any ions present in the solution can function as the counter ions. If the counter ions are adsorbed only by electrostatic attraction, they are called indifferent electrolytes. On the other hand, some ions exhibit surface activity in addition to electrostatic attraction and adsorb strongly in the Stern plane because of such phenomena as covalent bond formation, hydrophobic bonding, hydrogen bonding, and solvation effects. Because of their surface activity, the charge of such surface-active counter ions adsorbed in the Stern plane can exceed the surface charge. In this case

$$\sigma_s = - (\sigma_\delta + \sigma_d) \tag{18}$$

where σ_δ is the charge due to adsorption in the Stern plane, δ. (See equation 12.) Flotation collectors generally function as surface-active counter ions.

Electrokinetic phenomena, which involve the interrelation between mechanical and electrical effects at a moving interface, have found widespread use in colloid and surface chemistry. The two electrokinetic effects most widely used are electrophoresis and streaming potential measurements. Electrokinetic results are generally expressed in terms of the zeta potential, the potential at the slipping plane when liquid is forced to move relative to the solid; only those ions in the diffuse layer outside the slipping plane are involved in the electrokinetic process. Thus, while knowledge of the zeta potential at some single condition may be of certain value, determination of the change in zeta potentials with varying solution conditions is extremely useful. From these changes, modes of adsorption of various kinds of ions can be ascertained if one makes the useful assumption that the slipping plane and the Stern plane coincide. This approximation seems permissible because the potential differences between the plane δ and the slipping plane are small compared with the total potential differences across the double layer. It should be pointed out that the case in which there is no ambiguity is when $\psi_\delta = 0$, for then the zeta potential must be zero.

Information on the thermodynamic aspects of collector adsorption can be obtained from experimentally measured adsorption isotherms. Analysis of adsorption isotherms to obtain thermodynamic data for collector adsorption has been made by various approaches. Fuerstenau and coworkers (13) have successfully used the Stern-Grahame model of the electrical double layer to explain the adsorption of alkylammonium ions at the quartz/water interface and alkyl sulfonates at the alumina/water interface. These collector ions are considered to be adsorbed as counter ions in the double layer.

First of all, equilibrium in heterogeneous systems is attained when the chemical potential of species i is equal in all phases. For collector species i, its chemical potential in bulk solution is given by

$$\mu_i = \mu_i^o + RT \ln a_i \tag{19}$$

where μ_i^o is its standard chemical potential and a_i is its activity in solution. The chemical potential of the same species at the surface, μ_i^s, is

$$\mu_i^s = (\mu_i^o)^s + RT \ln a_i^s \tag{20}$$

where $(\mu_i^o)^s$ is the standard chemical potential of this species at the surface and a_i^s is its activity in the surface. At equilibrium, since $\mu_i = \mu_i^s$,

$$\frac{a_i^s}{a_i} = \exp \frac{\mu_i^o - (\mu_i^o)^s}{RT} . \tag{21}$$

This relation can be transformed into the well-known Stern-Grahame equation by making the following assumptions:

$$a_i = C \text{ (the bulk concentration) and } a_i^s = \Gamma_\delta/2r \tag{22}$$

where Γ_δ is the adsorption density in the Stern plane and r is the effective radius of the adsorbed ion. The standard free energy of adsorption, ΔG^o_{ads}, is defined as

$$\Delta G^o_{ads} = (\mu_i^o)^s - \mu_i^o . \tag{23}$$

Substituting these three relations into equation 21 yields the Stern-Grahame equation (13):

$$\Gamma_\delta = 2rC \exp(-\Delta G^o_{ads}/RT) . \tag{24}$$

Another approach to developing the Stern-Grahame equation can be made by applying the Law of Mass Action to a binary mixture of similarly sized molecules showing ideal behavior in both the liquid phase and in the adsorbed layer. This leads to

$$\frac{x_1^s \, x_2}{x_2^s \, x_1} = K \tag{25}$$

where x_1 and x_2 refer to the mole fraction of solute and solvent, respectively, in the liquid phase, and x_1^s and x_2^s are mole fractions in the adsorbed state. Since $x_2^s = 1 - x_1^s$, equation 25 can be rewritten as

$$\frac{x_1^s}{1 - x_1^s} = K \frac{x_1}{x_2} = \frac{x_1}{x_2} \exp \left(\frac{-\Delta G^o_{ads}}{RT}\right). \tag{26}$$

At small values of x_1, equation 26 becomes essentially identical to the usual form of the Stern-Grahame equation (and to the Langmuir equation).

The Stern-Grahame approach is useful in that it allows one to take electrical effects into account when dealing with ionic collectors. If ions adsorb only through electrostatic interactions, then the standard free energy of adsorption is given by

$$\Delta G^o_{ads} = \Delta G^o_{elec} = vF\psi_\delta \tag{27}$$

where v is the valence of the adsorbed ion including sign. On oxide minerals, alkali cations appear to be surface-inactive; that is, only electrostatic interactions appear to be operative. Nitrate, chloride, and perchlorate anions are surface-inactive on oxides (15). Acetate, borate, and nitrate anions do not exhibit surface activity on silver sulfide (13).

When an ion exhibits surface affinity, it is considered to be specifically adsorbed, and the free energy of adsorption has additional terms:

$$\Delta G^o_{ads} = vF\psi_\delta + \Delta G^o_{spec} \tag{28}$$

where ΔG^o_{spec} represents specific interaction terms. Certain inorganic ions exhibit surface activity: Ba^{+2} on quartz, Ba^{+2} and SO_4^{-2} on alumina, Ca^{+2} and SO_4^{-2} on rutile, and hydrolyzed metal cations on a wide variety of solids (13). Equation 28 shows that if ΔG^o_{spec} is finite, then the ion will be positively adsorbed even if ψ_δ is zero or has the same sign as the adsorbing ion. An estimation of ΔG^o_{spec} can be made for conditions when ψ_δ is zero (that is, when the electrophoretic mobility of the particles is zero).

For the adsorption of organic collectors of interest to flotation scientists, various attempts have been made to split ΔG^o_{ads} as follows (13):

$$\Delta G^o_{ads} = \Delta G^o_{elec} + \Delta G^o_{chem} + \Delta G^o_{CH_2} + \Delta G^*_{CH_2} + \Delta G^o_{solv} + \ldots \tag{29}$$

where

ΔG^o_{elec} is the electrostatic contribution to the total free energy,

$\Delta G^o_{CH_2}$ represents the interaction due to association of the hydrocarbon chains of adsorbed collector ions at the interface (sometimes called hydrophobic bonding),

$\Delta G^*_{CH_2}$ represents the interaction of the hydrocarbon chain with a hydrophobic surface,

ΔG^o_{chem} represents the free energy due to the formation of covalent bonds with the surface, and

ΔG^o_{solv} is the contribution of solvation effects on the polar head of the adsorbate (collector) and adsorbent (mineral) to adsorption.

It is often customary to lump the ΔG^o terms other than ΔG^o_{elec} together and call it ΔG^o_{spec} (i.e., $\Delta G^o_{spec} = \Delta G^o_{chem} + \Delta G^o_{CH_2} + \Delta G^o_{solv}$). To date, only hydrophobic bonding and chemical bonding in specific adsorption have been quantified. Hydrocarbon chain association does not actually result from any significant attraction between chains but results mainly from the entropy increase due to the freeing of water molecules that have been immobilized by the hydrocarbon chains (7).

Specific adsorption can be either physical or chemical in nature. If the ions are adsorbed only through such forces as electrostatic attraction and through hydrophobic bonding (van der Waals interaction between hydrocarbon chains), the process should be termed physical adsorption or physisorption. If the collector forms covalent bonds with metal ions in the surface of the mineral, then the process should be termed chemisorption. Much of the work with collector adsorption at interfaces has been concerned with physisorption, such as in the quartz alkylammonium and the alumina alkyl sulfonate systems (14). Adsorption isotherms and electrokinetic measurements strongly suggest that at low concentrations, these collector ions are adsorbed as individual ions in the Stern plane, but that at higher concentrations they associate at the interface into two-dimensional aggregates, termed hemimicelles (16).

By means of the Stern-Grahame model of the double layer, the contribution of the cohesive energy per mole of CH_2 groups to the adsorption potential can be quantitatively evaluated. If the standard free energy for removing 1 mole of CH_2 groups from water through association is ϕ, then the total contribution is $n\phi$ if n is the number of CH_2 groups in the chain. Thus, the contribution from hydrocarbon chain association to the adsorption process is

$$\Delta G^o_{CH_2} = n\phi. \tag{30}$$

The adsorption density, Γ_δ, of collector ions in the Stern plane in the absence of chemisorption will be given by

$$\Gamma_\delta = 2rC \exp\,(-\Delta G^o_{ads}/RT) = 2rC \exp\,(-\nu F\psi_\delta - n\phi)/RT. \tag{31}$$

For the sulfonate/alumina system, ϕ has been evaluated to be about -1.0 RT (about 2.5 kj/mole of CH_2 groups), in agreement with values obtained from solubility data and micelle formation (34-35). Due to the role that CH_2 groups have in controlling the adsorption-free energy in these systems, collector chain length will significantly affect flotation behavior.

Most of the detailed research on sulfide mineral/collector interactions has been concerned with sulfhydryl-type (xanthate, dithiophosphate) reagents. However, some work has been reported on the adsorption of cationic collectors on sulfide minerals.

Figure 7 presents Gaudin and Morrow's isotherm for the adsorption of dodecylammonium acetate on sphalerite at pH 6, under which conditions sphalerite is negatively charged (15). This isotherm shows that the amount of dodecylammonium ions adsorbed on sphalerite at constant pH varies as the square root of the bulk concentration of collector, in accordance with the predictions of equation 12. At about 2 x 10^{-4} M, the adsorption isotherm increases sharply due to hemimicelle formation at the interface. By means of the Stern-Grahame equation and the results given in figure 7, the standard free energy for the adsorption of dodecylammonium acetate (DAA) on sphalerite has been evaluated. The results, given in figure 8, clearly show the marked increase in the absolute magnitude of the adsorption-free energy upon hydrocarbon chain association of the adsorbed collector.

Iwasaki and de Bruyn (24) have conducted a detailed investigation of the adsorption of DAA on silver sulfide. Their results, summarized in figure 9, indicate that collector/sulfide mineral interactions not only are coulombic but also include other specific interactions. As can be seen in figure 9, the adsorption of the cationic collector increases sharply as the mineral surface becomes more negatively charged at constant collector concentration. Considering the negatively charged condition first, collector adsorption increases as the bulk solution concentration is increased. Interestingly, at a given surface charge and collector concentration, the amount of collector adsorbed also increases with increased ionic strength, indicating that sodium ions are not competing with dodecylammonium ions for sites at the surface. When the surface is negatively charged, there is a simple linear relation between surface charge and dodecylammonium adsorption.

$$\left(\frac{\partial \sigma_{DA^+}}{\partial \sigma_s}\right)_{\mu_{DAA}} = \text{constant} = 0.8. \qquad (32)$$

However, in this system, there still is appreciable adsorption when the surface is positively charged. The specific adsorption is probably due to a combination of electrostatic and hydrophobic bonding effects. Sulfide minerals tend to be naturally hydrophobic, and the specific adsorption of the dodecylammonium ions on silver sulfide may result from squeezing the hydrocarbon chain from the solution by displacing water molecules at the silver sulfide surface. This would be quantified by the $\Delta G^o_{CH_2}$ in equation 29, with the adsorbed ions tending to lie flat on the surface.

Chemisorption occurs in many mineral-collector systems. Chemisorption is often arbitrarily referred to as an adsorption process in which the adsorbate attaches to the surface of the adsorbent with a molar free energy of approximately 40 kj or greater. In terms of the concepts of equation 28, chemisorption occurs when ΔG^o_{chem} has some finite value. In flotation systems chemisorption is of primary interest since selectivity may be obtained if

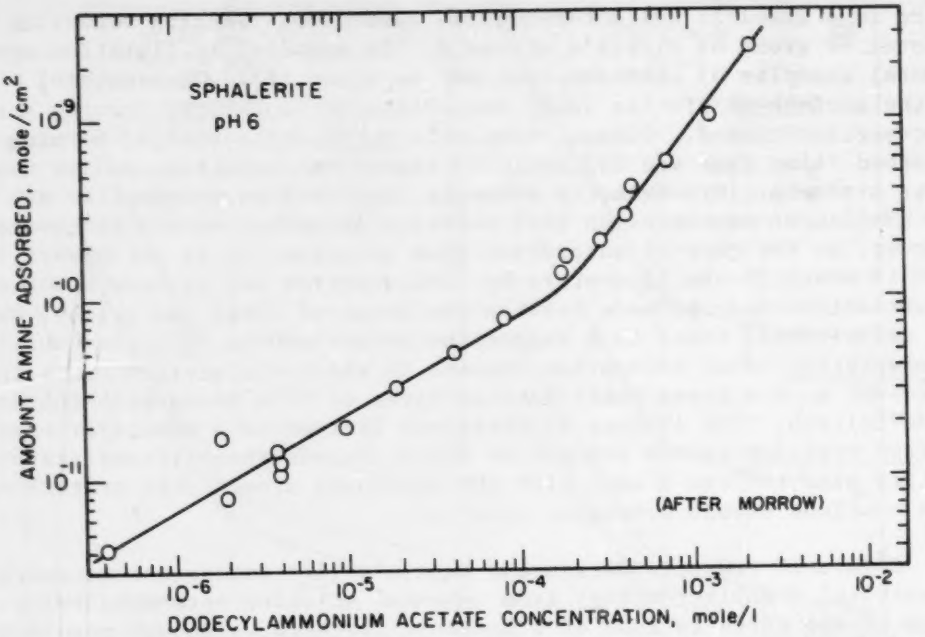

FIGURE 7. - The adsorption density of dodecylammonium acetate on sphalerite as a function of collector concentration at pH 6. At low concentrations the adsorption density is proportional to the square root of the bulk concentration and the change in slope reflects hemimicelle formation at the interface (18, 31). (*Courtesy, AIME.*)

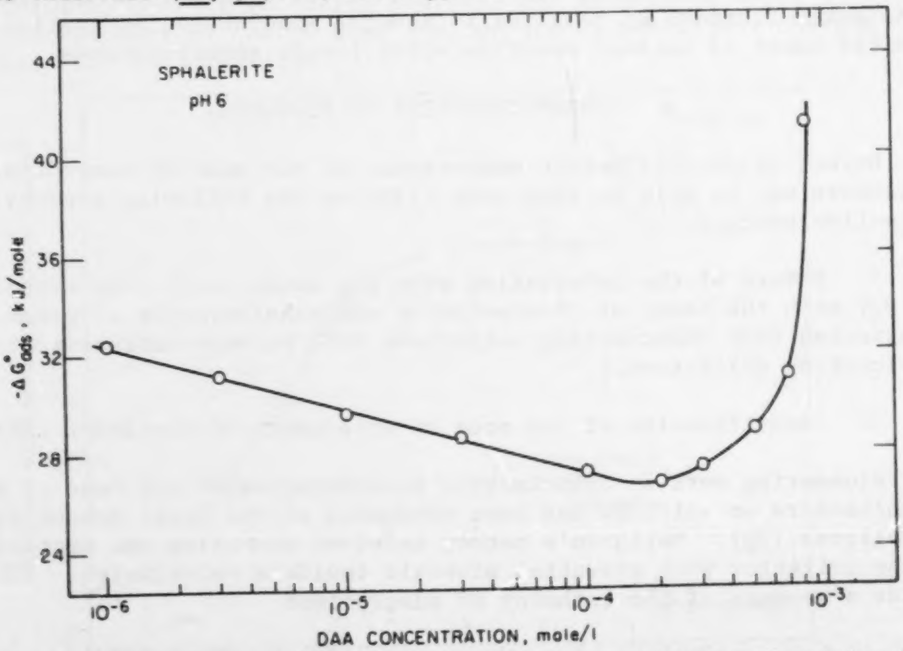

FIGURE 8. - The standard free energy of adsorption of dodecylammonium ions on sphalerite for the isotherm given in figure 7.

there is a specific collector-mineral adsorption reaction rendering a single mineral or group of minerals air-avid. In nonmetallic flotation systems several examples of chemisorption may be cited (13). Hexanethiol chemisorbs on the surface of zincite (ZnO) and willemite (Zn_2SiO_4), forming a strong zinc-mercaptan bond. Oleate chemisorbs on fluorite (CaF_2), forming strongly adsorbed films that are difficult to remove; on hematite; and on numerous other minerals. Hydroxamates strongly chemisorb on chrysocolla and hematite. The bonding of xanthates on such sulfides as galena occurs by chemisorption. However, in the case of adsorption from solution, it is not always clear what is meant in the literature by chemisorption and surface reaction, and a distinction must be made between the usage of these two terms. The following definitions, based on a suggestion by Damjanovic (6), are useful: *Chemisorption* is an adsorption process in which the surface atoms in the adsorbent do not leave their lattice sites to form bonds with the adsorbate. By definition, this process is therefore limited to a monolayer coverage. *Surface reaction* is the process in which the adsorbent leaves its regular lattice site to form a bond with the adsorbate atom. This process may therefore continue beyond monolayer coverage.

Figure 10 presents Harris and Gaudin's (17) adsorption isotherm of hexanethiol (hexylmercaptan) from aqueous solution onto sphalerite. The shape of the curve is that of a Langmuir isotherm, although monolayer coverage should occur at about 8×10^{-10} mole/cm^2 coverage. Calculations in terms of the Langmuir model indicate that the standard free energy of adsorption of the mercaptan on sphalerite is -48 kj/mole. However, since the adsorption process appears to be quite irreversible (17), such a calculation is not strictly valid. Figure 10 also shows that the uptake of mercaptan by sphalerite after 20 hours of reaction is several monolayers, indicating the possible onset of surface reaction after longer reaction times.

THERMOCHEMISTRY OF FLOTATION

Direct microcalorimetric measurement of the heat of adsorption of collectors may be able to shed some light on the following aspects of the collection process:

1. Nature of the interaction with the substrate. (For example, by analogy with the heats of chemisorption and physisorption of gases, it may be expected that chemisorbing collectors will be more exothermic than physisorbing collectors.)

2. Identification of the mode of attachment of flotation collectors.

Pioneering work on calorimetric determination of the heat of adsorption of collectors on sulfides has been conducted at the Royal School of Mines by Mellgren (30). Mellgren's method involved measuring the heat of reaction of the collector with prewetted minerals inside a calorimeter. This process yields a measure of the enthalpy of adsorption:

$$\left\{\begin{matrix}\text{Collector}\\ \text{in water}\end{matrix}\right\} + \left\{\begin{matrix}\text{Mineral}\\ \text{in water}\end{matrix}\right\} \xrightarrow{\Delta H_{ads}} \left\{\begin{matrix}\text{Adsorbed}\\ \text{collector}\end{matrix}\right\}$$

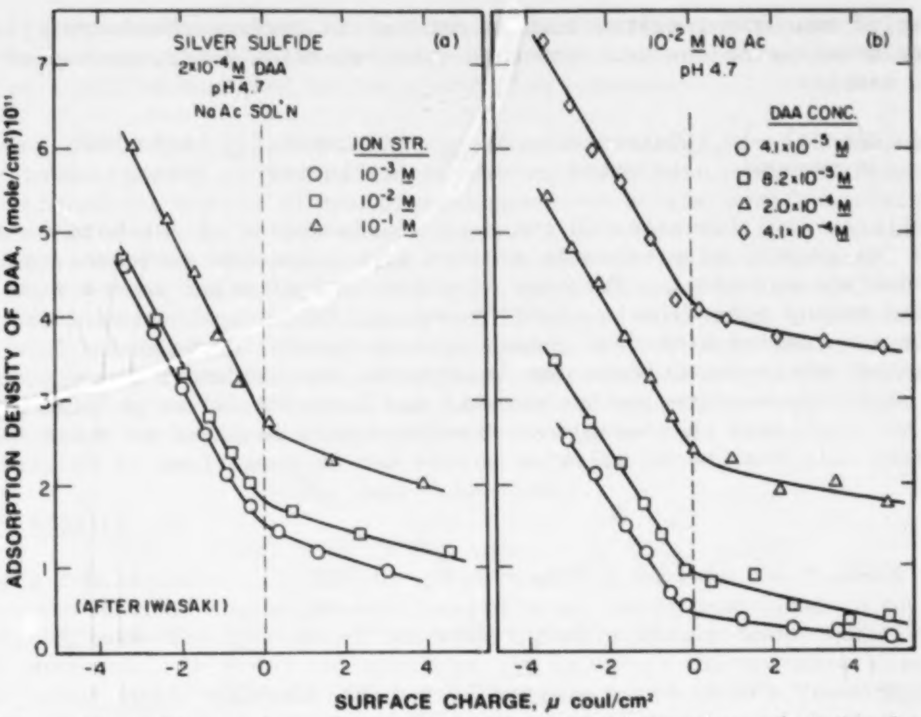

FIGURE 9. - The effect of surface charge on the adsorption of dodecylammonium acetate on silver sulfide. As the surface becomes negatively charged, the adsorption density increases sharply, but adsorption appears to be almost independent of charge when the surface is positively charged (3). (*Courtesy, Dr. I. Iwasaki.*)

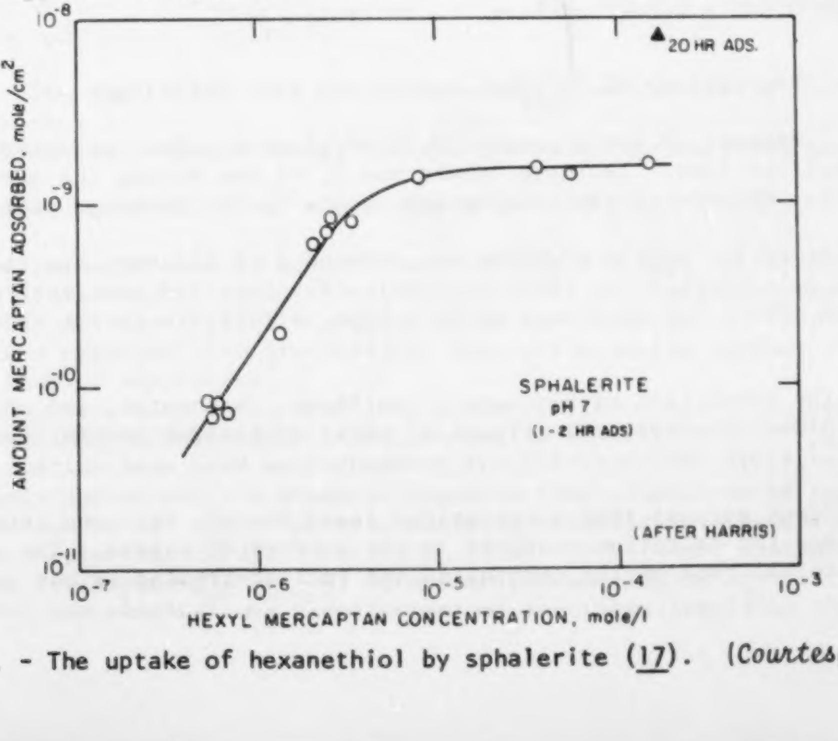

FIGURE 10. - The uptake of hexanethiol by sphalerite (17). (*Courtesy, AIME.*)

The heat of immersion, quite commonly studied in surface chemistry (1), involves determining the heat involved upon immersing a dry, evacuated mineral sample:

$$\left\{\begin{matrix}\text{Mineral}\\ \text{in vacuum}\end{matrix}\right\} + \left\{\begin{matrix}\text{Collector}\\ \text{in water}\end{matrix}\right\} \xrightarrow{\Delta H_{\text{imm}}} \left\{\begin{matrix}\text{Adsorbed}\\ \text{collector}\end{matrix}\right\} + \left\{\begin{matrix}\text{Adsorbed}\\ \text{water}\end{matrix}\right\}$$

Mellgren (30) investigated the heat of adsorption of xanthate on galena samples "as ground" or previously treated with potassium carbonate, sulfate, or thiosulfate solutions. The heat of adsorption of ethyl xanthate on untreated galena (-83 kj/mole of Pb^{+2}) was equivalent to that obtained when xanthate was reacted with lead thiosulfate at neutral pH values. This was as expected, since thiosulfate was found to be the oxidation product on the galena used. He measured rather erratic and large ΔH values at high pH values and concluded that secondary reactions were involved at these high pH values. His results on sulfated galena can be summarized as follows:

ΔH, kj/mole Pb^{+2}

$$PbSO_4 + 2KX\ (0.124) \rightarrow PbX_2 + K_2SO_4\ (0.012) \qquad -92.0 \pm 0.8$$

$$Pb(OH)_2 + 2KX\ (0.05) \rightarrow PbX_2 + 2KOH \qquad -49.3 \pm 4.2$$

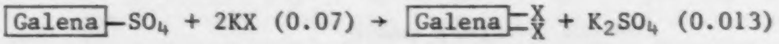

$$\boxed{\text{Galena}}\!-SO_4 + 2KX\ (0.07) \rightarrow \boxed{\text{Galena}}\!\substack{-X\\ -X} + K_2SO_4\ (0.013) \qquad -94.5$$

(in 0.01 M K_2SO_4 solution, pH 7.2 initially)

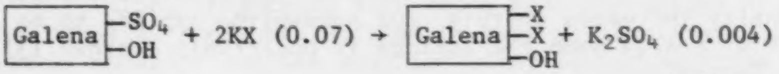

$$\boxed{\text{Galena}}\!\substack{-SO_4\\ -OH} + 2KX\ (0.07) \rightarrow \boxed{\text{Galena}}\!\substack{-X\\ -X\\ -OH} + K_2SO_4\ (0.004) \qquad -93.6$$

(in 0.001 M K_2SO_4 solution, pH 10 initially)

Some observations of Mellgren's work are the following:

1. Treatment of 100 g galena (3.92 m^2/g) with K_2SO_4 extracted 0.388 meq thiosulfate ions. Xanthate uptake was 0.344 meq during the adsorption experiment. Therefore, xanthate uptake occurs by ion exchange with sulfate.

2. At pH 10, xanthate uptake was reduced to 0.293 meq, but the heat value per mole of Pb^{+2} was the same, indicating that hydroxyl ions have a depressant effect but that only sulfate ions participate in the xanthate reaction.

3. The adsorption of xanthate on sulfated, carbonated, and untreated galena (thiosulfate-covered) at neutral pH is equivalent to the heat of reaction of ethyl xanthate with the corresponding bulk lead salts.

These findings suggest that metathetical reactions are involved between the xanthate and the oxidation products on the surface of galena. The quantities of xanthate adsorbed on the carbonate- and sulfate-treated galena surfaces are equivalent to the quantities of thiosulfate released into the solution after the treatment, which leads one to the conclusion that an ion exchange mechanism might be involved in the adsorption process.

Haung and Miller (21) recently conducted a detailed kinetic and thermodynamic investigation of adsorption in the amyl xanthate/pyrite system. To help determine the nature of the dixanthogen bond at the pyrite surface, they measured the heat of immersion of pyrite in water as 5,370 erg/cm^2, rather high compared with the heats of immersion for oxides in water. The reason may involve the oxidation and hydrolysis of soluble iron-sulfur salts. They also measured the heat of immersion of pyrite in liquid diamyldixanthogen as only 240 erg/cm^2. This value is typical of physical adsorption. Their work showed that xanthate adsorption by pyrite involves the formation of dixanthogen by an electrochemical reaction at the solid surface, in agreement with the conclusions of other investigators:

$$\tfrac{1}{2}O_2\ (aq) = \tfrac{1}{2}O_2\ (ads) \tag{33}$$

and

$$2X^- + 2H^+ + \tfrac{1}{2}O_2\ (ads) = X_2\ (ads) + H_2O. \tag{34}$$

The measured heat of the adsorption reaction at low pH was found to be between -262 and -234 kj/mole of adsorbed dixanthogen and independent of surface coverage. In order to interpret the results, the enthalpy change for the anodic half cell reaction was calculated to be 39.0 kj/mole X_2 from thermochemical measurements of I_2 titration, which agrees with the value reported by Mellgren (37.7 kj/mole X_2) (30):

$$2X^- = X_2\ (\ell) + 2e;\ \Delta H_{anod} = 39.0\ \text{kj/mole}\ X_2. \tag{35}$$

The enthalpy change for the cathodic half cell reaction for the formation of water was calculated (24) to be

$$\tfrac{1}{2}O_2\ (aq) + 2H^+ + 2e \rightarrow H_2O\ (aq);\ \Delta H_{cath} = -278\ \text{kj}. \tag{36}$$

Thus, the predicted enthalpy change for the overall reaction would be

$$\tfrac{1}{2}O_2\ (aq) + 2H^+ + 2X^- \rightarrow H_2O\ (aq) + X_2\ (\ell);\ \Delta H = -239\ \text{kj}. \tag{37}$$

Based on the measured heat of adsorption, the very low heat of immersion of pyrite into liquid dixanthogen, the predicted enthalpy change for equation 37, the uptake of xanthate by pyrite appears to be the formation of dixanthogen at the surface together with its physical adsorption at the surface (with a very small heat of adsorption).

THERMODYNAMIC EQUILIBRIA IN SULFIDE FLOTATION

The flotation of sulfide minerals requires that conditions be such that collector compounds are stable at the interface. Sufficient thermodynamic data for the copper/sulfur/diethyldithiophosphate (DTP)/water system now exist in the literature (25-26, 29) to enable calculation of equilibrium constants for the chemical and electrochemical reactions involving the various species. Such calculations have been made (3-4) using equilibrium constants for 40 different reactions. Similar calculations have also been recently published for the copper/ethyl xanthate/water system (22). These equilibria are represented in the form of conventional potential-pH (or Eh-pH) diagrams and will be discussed in the following paragraphs, using the Cu_2S/DTP/water system. These diagrams, however, cannot adequately represent the influence of DTP^- concentration. Eh-pH diagrams are, therefore, usefully supplemented with analogous Eh-p(DTP) diagrams (where $p(DTP) = -\log DTP^-$).

As for the choice of concentrations of dissolved species, standard states, and sign conventions, the activity of all pure solids and liquids is taken as unity, and the free energy of formation of all elements and H^+ ions is taken as zero. The standard half-cell electrode potentials, E^o's, are standard reduction potentials measured with respect to a standard hydrogen electrode. Consider the reaction in which a species in its oxidized state O is being reduced to state R, then $O + ne = R$, with

$$E = E^o - 2.303 \frac{RT}{nF} \log \frac{[R]}{[O]} \tag{38}$$

and

$$\Delta G = \Delta G^o + 2.303 \frac{RT}{nF} \log \frac{[R]}{[O]} \tag{39}$$

where $\Delta G = -nFE$; $\Delta G^o = -nFE^o$; and quantities in square brackets, [ ], refer to activities of the respective species. This reaction proceeds from left to right if E is positive.

The activity (or concentration) of DTP^- is treated as an independent variable. The copper ion activity is not externally controlled and is determined by the system itself. The thermodynamic calculations discussed subsequently show that $[Cu^{+2}]$ and $[DTP^-]$ cannot be fixed independently, because of the low solubility product of CuDTP for the reaction

$$Cu^{+2} + DTP^- + e = CuDTP$$

$$[Cu^{+2}]\,[DTP^-] = 6.3 \times 10^{-19}. \tag{40}$$

The value of $[Cu^{+2}]$ would be so small, in the range of concentrations of DTP^- used in this investigation, that its value would be governed by kinetic rather than equilibrium considerations. Therefore, unless otherwise stated, the value of $[Cu^{+2}]$ in solutions containing DTP has been taken to be equal to 10^{-8}, which appears to be consistent with experimental observations.

The concentration of each dissolved sulfur species, [S], in equilibrium with copper sulfides would be determined by the extent of oxidation of the sulfide. The Eh-pH diagrams are drawn using $[S] = 10^{-6}$. Slight changes in [S] in solution do not significantly alter the nature of these diagrams.

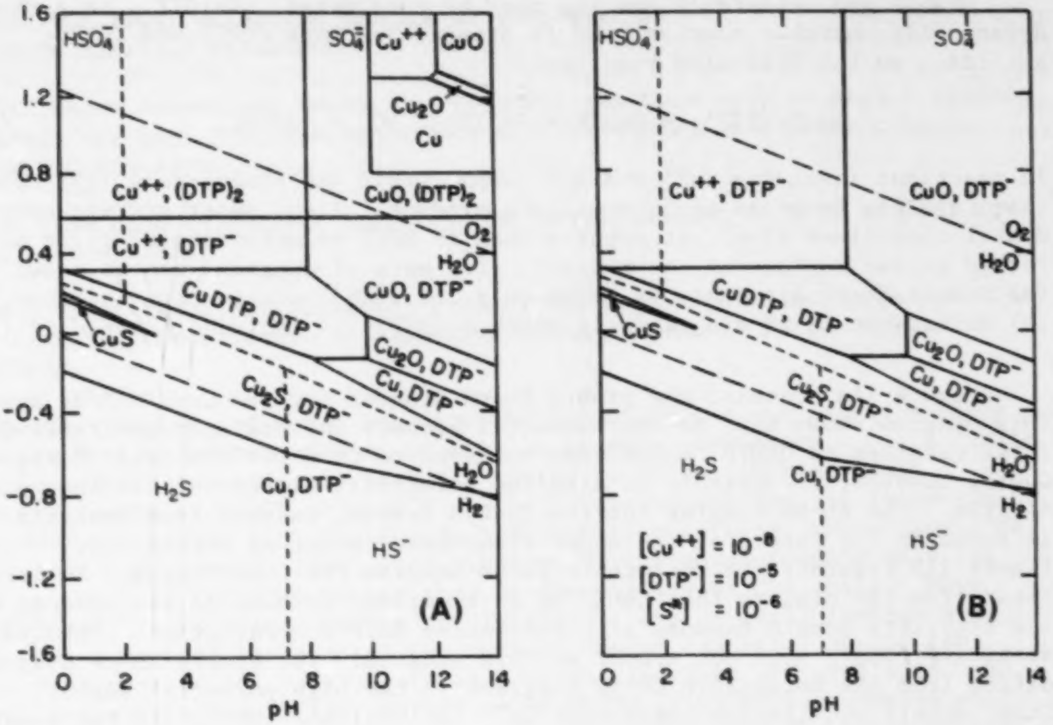

FIGURE 11. - Stable (A) and metastable (B) Eh-pH diagrams for the $Cu_2S/DTP/H_2O$ system at 25° C. The insert shows the Eh-pH diagram for the Cu/H_2O system (3). (*Courtesy, Instituto di Arte Mineraria e Preparazione.*)

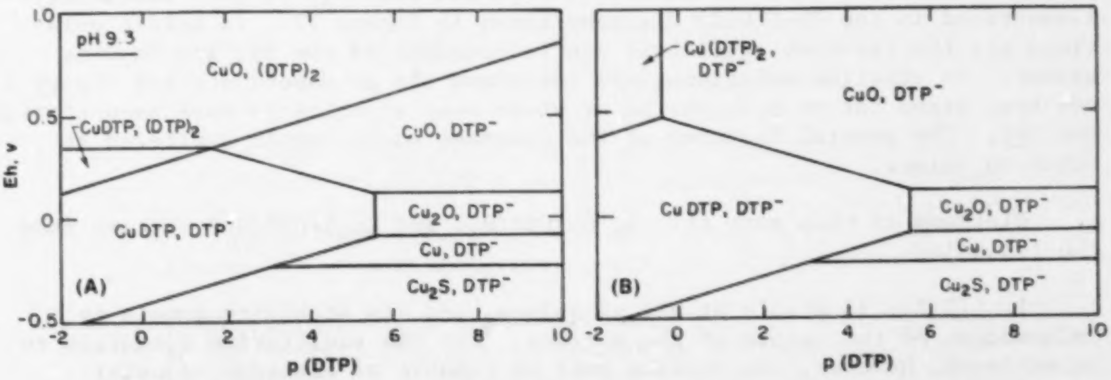

FIGURE 12. - Stable (A) and metastable (B) Eh-p(DTP) diagrams for the $Cu_2S/DTP/H_2O$ system at pH 9.3 (3). (*Courtesy, Instituto di Arte Mineraria e Preparazione.*)

Stable and metastable species must be considered. $Cu(DTP)_2$ is a thermodynamically unstable species, and it dissociates into CuDTP and $(DTP)_2$ according to the following reaction:

$$Cu(DTP)_2 = CuDTP + \frac{1}{2}(DTP)_2, \ \Delta G^o = -36 \text{ kj}. \qquad (41)$$

In reactions involving Cu^{+2} and DTP^- ions, Goold and Finkelstein (19) observed that $Cu(DTP)_2$ forms as an intermediate product. Also, under certain experimental conditions (3-4), it appears that in KDTP solutions $Cu(DTP)_2$ is also formed at the surface of the mineral. Two sets of diagrams can be drawn (3): (a) stable Eh-pH diagrams, in which only the stable species are included, and (b) metastable Eh-pH diagrams, in which $Cu(DTP)_2$ is included instead of $(DTP)_2$.

Figure 11A presents the stable Eh-pH diagram for the $Cu_2S/DTP/H_2$ system. This diagram shows that as the potential becomes increasingly positive, Cu_2S first oxidizes to CuDTP, which then oxidizes to Cu^{+2} (or CuO) and $(DTP)_2$. CuDTP, however, is unstable in alkaline solutions, as represented in the diagram. The Eh-pH diagram for the $Cu-H_2O$ system, redrawn from Pourbaix (32), is shown in the insert at the upper right-hand corner of figure 11A. Figure 11B presents the metastable Eh-pH diagram for this system. It is clear from the diagram that CuDTP is an important species in the system, and its stability domain expands with increasing KDTP concentration. The $Cu(DTP)_2$ stability domain does not appear on this diagram. The stable Eh-pH diagrams differ from the metastable Eh-pH diagrams in the high potential region. Under stable equilibrium conditions Cu^{+2} (or CuO) and $(DTP)_2$ are the products of oxidation, whereas under metastable equilibrium conditions, Cu^{+2}, CuO, or $Cu(DTP)_2$ is the product of oxidation and $Cu(DTP)_2$ can exist only at large DTP^- concentration. If the Cu^{+2} ion concentration can be increased, for example, by polarizing a Cu_2S electrode in DTP^- solution, the stability domain of $Cu(DTP)_2$ as well as that of CuDTP expands (4).

The influence of DTP^- ion concentration and copper ion concentration on the stability domains of CuDTP, $(DTP)_2$, and $Cu(DTP)_2$ is more adequately illustrated in the Eh-p(DTP) diagrams shown in figure 12. In acidic solutions all the reaction equilibria are independent of the pH, and Cu_2O is absent. In alkaline solutions, the reactions are pH dependent; and figure 12 has been drawn for pH 9.3, the pH at which many experiments have been carried out (4). The general features of the diagrams would remain unaltered at other pH values.

Diagrams of this sort for the $Cu/DTP/H_2O$ and $Cu_2S/DTP/H_2O$ systems show the following:

1. $(DTP)_2$ is stable at all pH values, and its stability domain is independent of the nature of the surface. For the equilibrium situation to be achieved, however, the surface must be capable of electron transfer, since it is recognized that $(DTP)_2$ does not form in bulk solutions.

2. The maximum pH value below which CuDTP is stable, pH_s, is given by:

$$pH_s = 14.8 - p(DTP).$$

3. The final oxidation product of the solid is Cu^{+2} in acidic solutions and CuO in alkaline solutions.

4. Under metastable conditions $Cu(DTP)_2$ can form only at high electrode potentials and high DTP^- concentrations. Under these conditions, neither Cu^{+2} or CuO can form.

5. The high potential region of the Eh-pH diagrams is very similar for Cu and Cu_2S systems.

6. Under incipient flotation conditions, both copper and copper sulfides would oxidize, the products of oxidation being determined by the solution conditions.

Contact angles and hence the floatability of copper and copper sulfide are determined by thermodynamics as well as kinetic parameters. For a finite contact angle it is necessary that the system be in the thermodynamic stability domain of CuDTP or $Cu(DTP)_2$, the metal-reagent species responsible for hydrophobicity of both the solids. In acidic solutions, where dissolved copper ions can normally form, precipitation of the metal-reagent salt can occur in the bulk solution rather than at the surface of the solid. When this happens, the surface remains nonfloatable (zero or small contact angle) and at the same time large metal and reagent losses can occur due to continued formation of the precipitate as long as reactants are available. In neutral and alkaline solution, formation of CuDTP or $Cu(DTP)_2$ competes with the simultaneous formation of Cu_2O or CuO. Depending upon the rates of the reactions involving these species, the surface can be predominantly CuDTP and/or $Cu(DTP)_2$ (floatable) or Cu_2O and/or CuO (nonfloatable).

ACKNOWLEDGMENT

The support of the National Science Foundation for the preparation of this paper is acknowledged.

REFERENCES

1. Adamson, A. W. Physical Chemistry of Surfaces. Interscience, New York, 2d ed., 1967, 747 pp.

2. Aplan, F. F., and P. L. de Bruyn. Adsorption of Hexyl Mercaptan on Gold. Trans. AIME, v. 226, 1963, p. 235.

3. Chander, S., and D. W. Fuerstenau. On the Flotability of Sulfide Minerals with Thiol Collectors: The Chalcocite Diethydithiophosphate System. Proc. 11th Internat. Miner. Proc. Cong., Cagliari, Italy, 1975, p. 583.

4. Chander, S., and D. W. Fuerstenau. Electrochemical Reaction Control of Contact Angles on Copper and Synthetic Chalcocite in Aqueous Potassium Diethyldithiophosphate Solutions. Internat. J. Miner. Proc., v. 2, 1975, p. 333.

5. Chander, S., and D. W. Fuerstenau. On the Natural Flotability of Molybdenite. Trans. AIME, v. 252, 1972, p. 62.

6. Damjanovic, A. Modern Aspects of Electrochemistry, ed. by J. O'M. Brockris and B. E. Conway. Plenum, New York, v. 5, ch. 5, 1969, 344 pp.

7. Davis, J. T., and E. K. Rideal. Interfacial Phenomena, Academic Press, New York, 1963, p. 159.

8. de Bruyn, P. L., J. T. G. Overbeek, and R. Schuhmann. Flotation and the Gibbs Adsorption Equation. Trans. AIME, v. 199, 1954, p. 519.

9. Deryagin, B. V. The Rigidity of Thin Layers of Water. J. Phys. Chem. (USSR), v. 3, 1932, pp. 29-42.

10. Deryagin, B. V., and L. M. Shcherbakov. Effect of Surface Forces on Phase Equilibria of Polymolecular Layers and on Contact Angle. Colloid J. USSR, v. 23, 1961, p. 33.

11. Eyring, E. M., and M. E. Wadsworth. Differential Infrared Spectra of Adsorbed Monolayers-n-Hexanethiol on Zinc Mineral. Trans. AIME, v. 205, 1956, p. 531.

12. Freyberger, W. L., and P. L. de Bruyn. The Electrochemical Double Layer on Silver Sulfide. J Phys. Chem., v. 61, 1957, p. 586.

13. Fuerstenau, D. W. Interfacial Processes in Mineral/Water Systems. Pure and Appl. Chem., v. 24, 1970, p. 135.

14. Fuerstenau, D. W., and T. W. Healy. Principles of Mineral Flotation Adsorptive Bubble Separation Techniques, ed. by R. Lemlich. Academic Press, Inc., New York, 1972, pp. 91-131.

15. Fuerstenau, D. W., and S. Raghavan. Some Aspects of the Thermodynamics of Flotation. Ch. 3 in Flotation, A. M. Gaudin Memorial Volume, ed. by M. C. Fuerstenau. AIME, New York, 1975, p. 21.

16. Gaudin, A. M., and D. W. Fuerstenau. Quartz Flotation with Anionic or Cationic Collectors. Trans. AIME, v. 202, 1955, p. 668.

17. Gaudin, A. M., and D. L. Harris. Adsorption of a Mercaptan on Zn Minerals. Trans. AIME, v. 199, 1954, p. 925.

18. Gaudin, A. M., and J. G. Morrow. Adsorption of Dodecylammonium Acetate on Hematite and its Flotation Effect. Trans. AIME, c. 199, 1954, p. 1196.

19. Goold, L. A., and N. P. Finkelstein. The Reaction of Sulfide Minerals with Thiol Compounds. Nat. Inst. Met., Johannesburg, South Africa, Rept. No. 1439, June 1972, 125 pp.

20. Grahame, D. C. The Electrical Double Layer and the Theory of Electrocapillarity. Chem. Rev., v. 41, 1947, p. 441.

21. Haung, H. H., and J. D. Miller. Kinetics and Thermochemistry of Amyl Xanthate Adsorption by Pyrite and Marcasite. Internat. J. Miner. Proc., v. 5, 1978, p. 241.

22. Hepel, T., and A. Pomianowski. Diagrams of Electrochemical Equilibria of the System Copper-Potassium Ethylxanthate-Water at 25° C. Internat. J. Miner. Proc., v. 4, 1977, 345 p.

23. Iwasaki, I. Electrochemical Study of Adsorption on Silver Sulfide Surfaces. Sc.D. dissertation, Massachusetts Institute of Technology, 1957, 125 pp. Available from Microreproduction Laboratory, Bldg. 14, Room 0551, Massachusetts Institute of Technology, Cambridge, Mass. 02139.

24. Iwasaki, I., and P. O. de Bruyn. The Electrochemical Double Layer on Silver Sulfide at pH 4.7. I. In the Absence of Specific Adsorption, J. Phys. Chem., v. 62, 1958, p. 594.

25. Kakovskii, I. A., B. A. Stepanov, O. F. Ryazantseva, and N. V. Serebryakova. Redox Potentials of Dithiophosphates. Russ. J. Phys. Chem., v. 33, 1959, p. 178.

26. Kalman, A. B., P. M. Etelka, V. N. Hedvig, and K. Laszlo. Nehez Donoratumu Komplexek Kemiaja. IV. Mag. Kem. Foly., v. 76, 1970, p. 138.

27. Kruyt, H. R. Colloid Science. Elsevier, Amsterdam, v. 1, 1952, p. 389.

28. Laskovski, J. Particle-Bubble Attachment in Flotation. Miner. Sci. Eng., v. 6, No. 4, 1974, p. 223.

29. Latimer, W. M. Oxidation Potentials. Prentice-Hall, Englewood Cliffs, N.J., 1952, p. 39.

30. Mellgren, O. Heat of Adsorption and Surface Reactions of Potassium Ethyl Xanthates on Galena. Trans. AIME, v. 235, 1966, p. 46.

31. Morrow, J. G. Adsorption of Dodecylammonium Acetate on Hematite and Sphalerite, Ph.D. Thesis, MIT, 1952. Available from Microreproduction Laboratory, Bldg. 14, Room 0551, MIT, Cambridge, Mass. 02139.

32. Pourbaix, M. Atlas of Electrochemical Equilibria in Aqueous Solutions. Eh-pH diagram for Cu-H_2O System. Pergamon, New York, 1966, p. 384.

33. Sheludko, A. Thin Liquid Films. Advances in Colloid Interface Sci., v. 1, No. 4, 1967, p. 391.

34. Somasundaran, P., and D. W. Fuerstenau. Mechanism of Alkyl Sulfonate Adsorption at the Alumina-Water Interface, J. Phys. Chem., v. 70, 1966, p. 90.

35. Wakamatsu, T., and D. W. Fuerstenau. Effect of Hydrocarbon Chain Length on the Adsorption of Sulfonates at the Solid/Water Interface. Advan. Chem. Ser., v. 79, American Chemical Society, Washington, D.C., 1968, p. 161.

FLOTATION RESEARCH AT THE AVONDALE RESEARCH CENTER: AN INTRODUCTION

by

Garrett R. Hyde[1]

ABSTRACT

This paper reviews some of the research studies carried out at the Bureau of Mines Avondale Research Center to develop viable technology for recovering mineral and metal values from low grade and complex sulfide ores.

INTRODUCTION

At the 1978 AIME annual meeting in Denver, former Bureau of Mines Chief Scientist, Dr. Earl Hayes, said that by the year 2000 new technology must reduce energy consumption in obtaining minerals by 25 percent. Reduction of energy consumption is only one of the problems faced by the minerals industry. Other problems include the environmental effects of effluents, the changing composition of ore bodies, concentrating very low grade ores, and separating complex mixtures of minerals.

Several years ago it became clear to Bureau scientists that research at a more fundamental level would be required to solve these problems effectively. It seemed logical for the Bureau to undertake research having, in addition to short-range objectives, the long-term, broad objectives necessary to develop fundamental data from which new technology could be developed.

The Flotation Fundamentals project at Avondale has a broad objective to improve efficiency and reduce losses in existing mineral processing operations and to develop the technology for separating very low grade and complex ores.

For practical reasons our efforts have been confined primarily to sulfides. Present work is directed toward improving selectivity of copper-nickel separation in Duluth gabbro and other domestic copper-nickel ores and toward improving sphalerite-pyrrhotite separation in a milling operation that is losing recoverable zinc due to inefficient separation. These studies, along with others on specific minerals such as galena, are carried out from a fundamental viewpoint to assist in the development of new technology.

---

[1] Research physicist, Avondale Research Center, Bureau of Mines, Avondale, Md.

This is not to say that we do not do any laboratory-scale flotation studies. In fact, the experimental work is about equally divided between practical flotation studies and those designed to obtain more fundamental flotation parameters. Consider for example our work on the Duluth gabbro ores.

The Duluth gabbro ores contain approximately 0.3 percent copper as chalcopyrite and cubanite and approximately 0.1 percent nickel as pentlandite and pyrrhotite. Figure 1 shows a "nickel's" worth. The Treasury Department claims that today's nickel coin has about 25 percent nickel--about the same proportions of nickel and copper as the gabbro ore. Based on pilot-plant studies, the Bureau of Mines Twin Cities Research Center has determined parameters for a bulk sulfide flotation plant to recover the sulfide minerals (3). Dr. Iwasaki at the University of Minnesota has developed a flowsheet, based on bench-scale flotation studies, to differentially separate the copper and nickel ores (1). Our efforts were confined to determining the physiochemical factors governing the initial differential separation stage of his flowsheet.

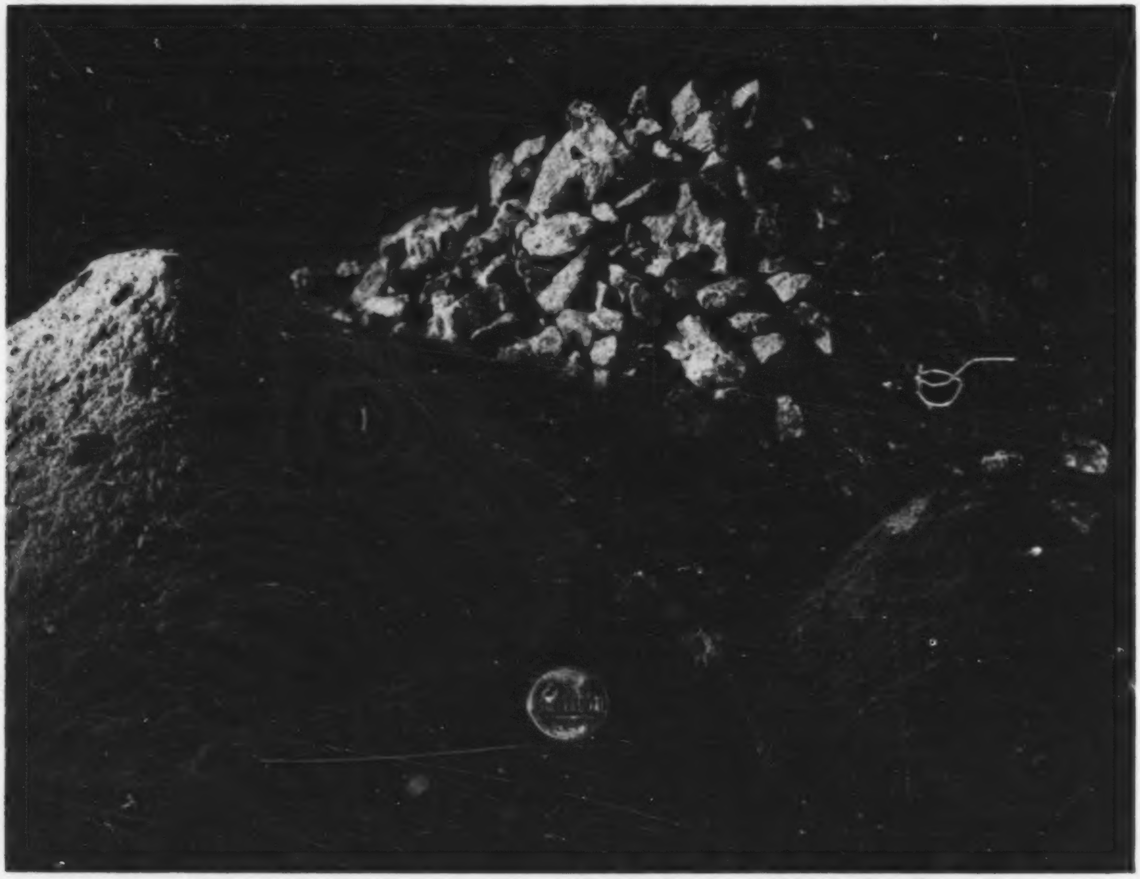

FIGURE 1. - The quantity of crude Duluth gabbro ore (background) required to obtain nickel and copper for the nickel coin. Waste tailings are shown on the left and bulk sulfide concentrate on the right. Concentrates of nickel sulfide and copper sulfide are in the foreground.

The initial approach to this problem was to look at the flotation behavior following the guidelines established by previous workers and attempt to isolate the factors having the largest effect on the quality of the separation.

Laboratory-scale flotation studies were carried out in a pneumatic cell to obtain both rate and recovery data under steady-state conditions (fig. 2). Pulp is introduced continuously along with ethylxanthate collector at the near end of the cell. Particles remain in each froth chamber on the average of 4 to 5 minutes. The distance along the cell at which the pulp is recovered is proportional to the sum of the conditioning and flotation times. Figure 2 was taken about 15 minutes after the pulp flow was started. Under steady-state conditions, more than 90 percent of the bulk sulfides are recovered within the first 5 minutes.

Differential studies were also carried out in the pneumatic cell, but the bulk sulfide pulp was reground to 95 percent minus 400 mesh and preconditioned with lime at pH 12.4 for 30 minutes prior to flotation to help depress the nickel-iron minerals. Dextrin, the depressor, was added to the cell with the conditioned pulp, and ethyl xanthate was added after 10 minutes. That is, the xanthate is added to the third froth chamber. Typical grade and recovery profiles obtained in the cell are shown in figure 3A. The best separation achieved under these conditions occurred after 15 minutes with the following results:

Copper concentrate (froth)	
40% recovery, 19% grade	14% Ni
Nickel concentrate (tail)	
84% recovery, 2% grade	51% Cu

Two factors were immediately apparent: about half the copper was depressing along with the nickel, and about 14 percent of the nickel floated with the copper. Optical microscopic examination of the nickel concentrate showed that most of the copper was liberated and should have floated. However, particle-size distribution studies showed median sulfide particle diameters of 6 µm, based on volume-percent. Based on the total number of particles counted, 95 percent were less than 6 µm and 50 percent less than 2.5 µm in diameter. The sulfides were being selectively overground, producing very sluggish flotation response. Eliminating a regrind before the differential float gave a median particle diameter of 17 µm, or about 3 times larger particles. The change in flotation response is shown in figure 3B. Copper recovery increased to 60 percent but maintained the same 19 percent grade. Approximately 16 percent of the nickel floated with this copper concentrate (froth). Nickel recovery remained approximately the same at 89 percent and at a 3-percent grade. The copper remaining with the nickel concentrate (tail) decreased to 32 percent, however. The coarser grind of 98 percent minus 100 mesh has improved the copper recovery without sacrificing nickel recovery. Optical microscopic studies showed the coarse grind was sufficient for liberation. The fine-particle fraction was also greatly reduced. Presently the modal analysis is being examined to determine the minimum grinding required for liberation. To improve the nickel depression, the effects of lime treatment on collector and starch uptake will be examined.

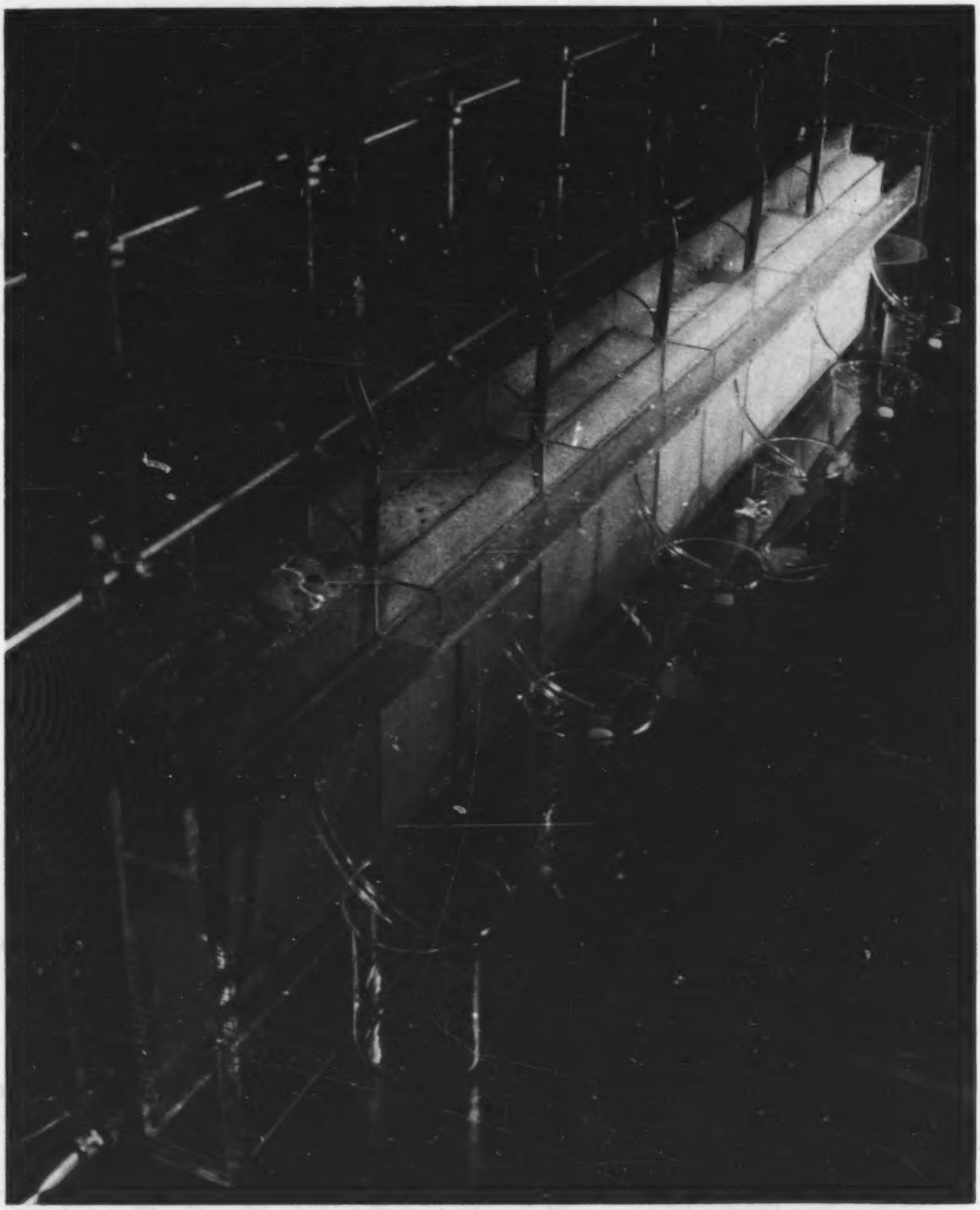

FIGURE 2. - Pneumatic flotation cell used to obtain both rate and recovery data under steady-state conditions.

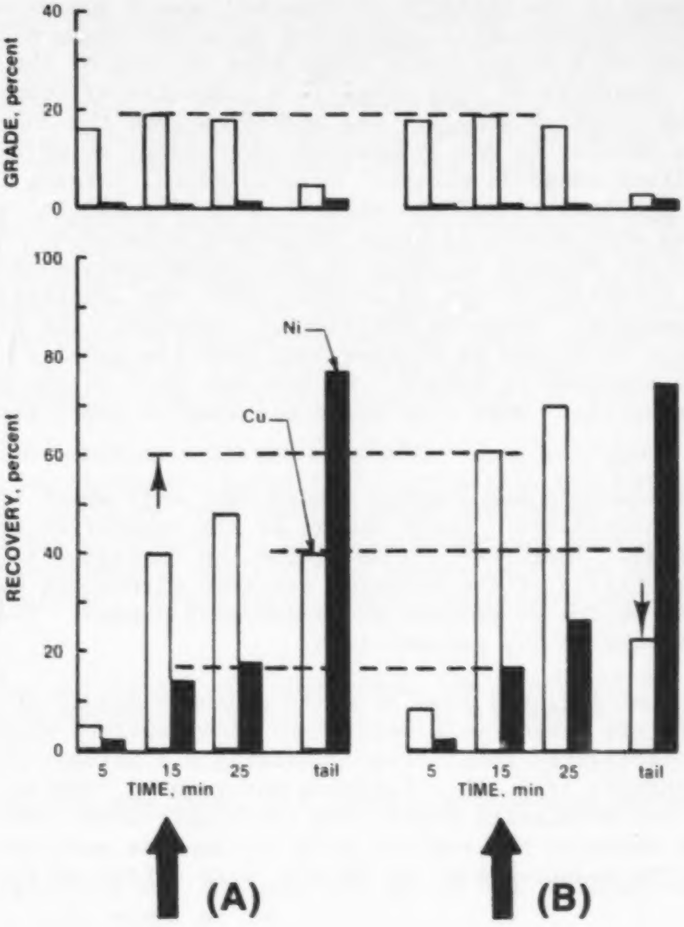

FIGURE 3. - Grade and recovery of copper and nickel obtained from tests using the pneumatic cell. A, including regrind of bulk sulfide pulp; B, with no regrind. Copper recovery was much higher using the coarser-ground material without any sacrifice in nickel recovery.

Another phase of the research is directed toward improving the efficiency of sphalerite-pyrrhotite separation in an operating mill. The poor separation occurs in a zinc-cleaner stage near the end of the mill flowsheet. Therefore, the chemistry in this stage is a composite of reagent additions and reactions of previous stages. The underflow from the copper roughers, about 1 percent sphalerite and 99 percent pyrrhotite, at pH 8.9 is activated with copper sulfate added in excess. Lime is added, raising the pH to 12.4 to depress the pyrrhotite, and the sphalerite is floated in the zinc rougher. The zinc rougher concentrate is about 55 percent sphalerite and 45 percent pyrrhotite. Sulfur dioxide is added to this concentrate until the pH drops to 4.5. After conditioning for 40 minutes, both the sphalerite and pyrrhotite become depressed. With the addition of collector, the pyrrhotite becomes floatable first and is floated away from the sphalerite. At least that is what is supposed to happen. In reality, most of the sphalerite comes up with the pyrrhotite. When this stage was sampled there was no apparent upgrading.

Optical microscopic examination showed that only about 10 percent of the sphalerite was unliberated. Large chunks of the sphalerite could not be obtained for study. Therefore, to determine the contained iron the X-ray fluorescence capability of the scanning electron microscope was used, particle by particle, on the 85-percent-minus-200-mesh powder. The sphalerite contained an average of 5.2 percent iron.

The effects of included iron on ethyl xanthate uptake at pH 4.5, the operating pH of this stage, were determined from separate adsorption measurements on copper-activated sphalerite containing 0.1 percent Fe and 3.0 percent Fe, respectively (fig. 4). Xanthate was removed from solution at a faster rate by the sphalerite containing the higher iron. After 60 minutes, the higher iron material had removed about 4 times as much xanthate from the solution. The measurements, at pH 4.5, were corrected for xanthate decomposition.

Subsequently, the effects of sulfur dioxide on xanthate uptake were measured in separate experiments (fig. 5). Following the mill procedures of reducing the pH from 12.4 to 4.5 with sulfur dioxide and then adding xanthate,

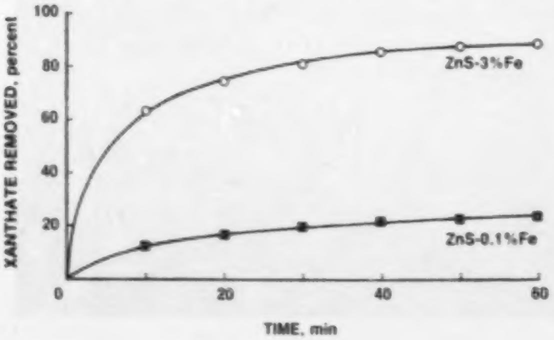

FIGURE 4. - The effect of iron in the sphalerite lattice on ethyl xanthate uptake.

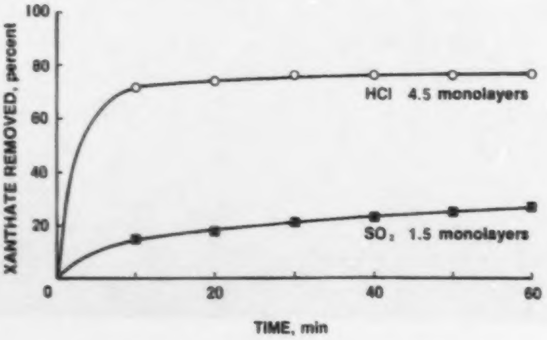

FIGURE 5. - The effect of SO_2 on xanthate uptake.

the xanthate lost from solution, after correcting for decomposition, was about one-third of that when the measurement was repeated using HCl to lower the pH. Calculating the collector surface coverage from the measured surface area and assuming that all of the xanthate removed from solution went on the surface, about 1.5 monolayers of collector were adsorbed when sulfur dioxide was used and about 4.5 monolayers when HCl was used.

From other flotation experiments, it was determined that a monolayer of ethyl xanthate was sufficient to float sphalerite. Therefore, the depressing action of sulfur dioxide on sphalerite does not appear to be totally through control of xanthate uptake. There are, however, possible homogeneous reactions in equilibrium with the adsorption that could consume xanthate and would have been measured as a xanthate loss from solution, such as the formation of zinc xanthate. The data of figure 5 have not been corrected for this.

A series of laboratory flotation studies were subsequently carried out on sphalerite containing 0.1 percent Fe, sphalerite containing 3 percent Fe, and pyrrhotite. Solution from the flotation cell shown in figure 6 was continuously circulated through the UV spectrometer and back into the cell, allowing determinations of collector concentrations from spectral scans after each reagent addition. Using the treatment procedures employed in the mill, it was found:

1. With no additional zinc ion added, the 3 percent Fe sphalerite and the pyrrhotite depressed at pH 6.3 to 7. The 0.1 percent Fe sphalerite was not depressed.

2. If zinc ion was added, all three minerals were depressed between pH 6.3 and 7.

3. No depression was obtained for any of the minerals at pH 4.5, the operating pH of this stage at the mill.

4. The depression was accompanied by a precipitate formed in the flotation cell.

More recent experiments have shown that the lime required to reach pH 12.4, preceding SO_2 conditioning, varies from sample to sample. If a larger quantity of lime is added, then more SO_2 is needed to lower the pH to 4.5. Under this condition, depression of the low-iron sphalerite has been observed at pH 4.5, provided zinc ion is present. Depression occurs if the product of the SO_3^{-2} and Zn^{+2} concentrations is greater than the solubility product of $ZnSO_3$, suggesting that $ZnSO_3$ must precipitate in order to have depression.

Other researchers (2) have suggested that the mechanism of depression of sphalerite by sulfur dioxide is by the formation and deposition of a zinc sulfite precipitate on the surface, which renders the surface hydrophilic. Presently, experiments are being carried out to identify and determine the chemical form of the precipitate produced in the flotation experiments. This is a difficult problem because other metal ions, including calcium and copper, are present in addition to zinc. From solubility considerations, zinc sulfate can probably be ruled out, but zinc sulfite, calcium sulfate, calcium

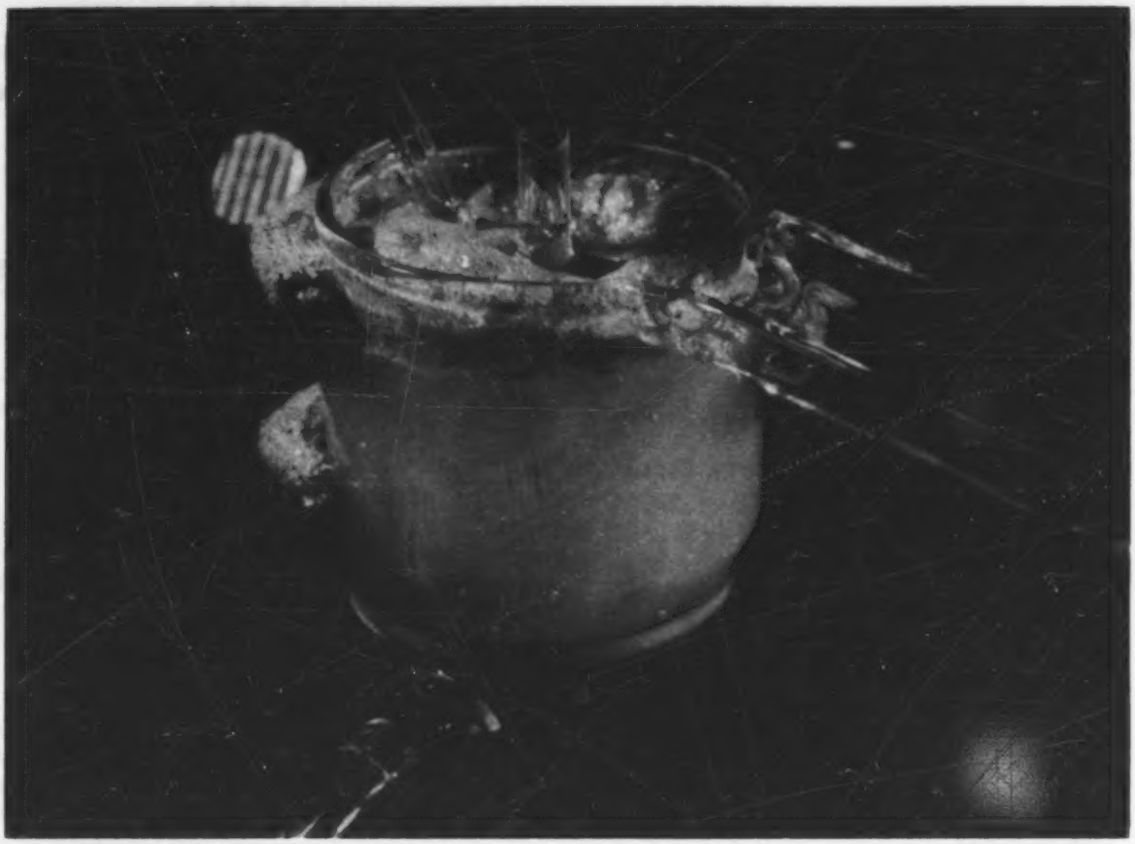

FIGURE 6. - Laboratory cell used for flotation and depression studies on sphalerite.

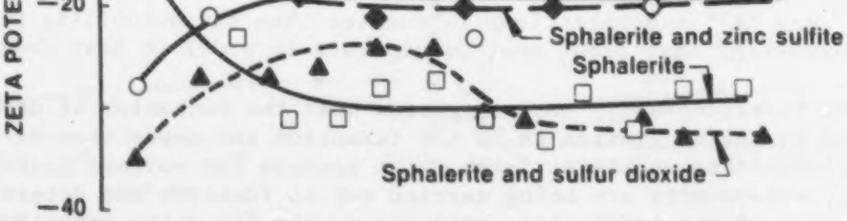

FIGURE 7. - The effects of sulfite on the zeta potential of activated low iron sphalerite in the presence of ethyl xanthate.

sulfite, and other calcium and zinc oxides and hydroxides are distinct possibilities to coprecipitate over this pH range. Both $[SO_4]^{-2}$ and $[SO_3]^{-2}$ have infrared active bands. However, other compounds in the flotation pulp also contribute to bands in these regions. To resolve the problem, a series of laboratory flotation studies are currently being carried out with reagents carefully chosen to avoid external introduction of sulfite, sulfate, and unwanted metal ions. For example, Zn^{+2} is being added as the chloride rather than as the sulfate. These precipitates are less complex and facilitate subsequent analysis, yet they still can be correlated closely with flotation response.

Zeta potential measurements as a function of pH (fig. 7) made on zinc sulfite, activated and xanthated sphalerite, and activated and xanthated sphalerite treated with zinc sulfite tend to support the zinc sulfite precipitate mechanism. The zeta potential of activated sphalerite with 0.1 percent Fe treated with zinc sulfite is closer to that of the zinc sulfite than to that of the untreated activated sphalerite. When the activated sphalerite was treated with SO_2, the zeta potential shows a tendency toward that of zinc sulfite near pH 5. The quantity of sulfur dioxide used to treat these samples was less than required for depression or zinc sulfite precipitation.

This talk was intended to give an overview of the research carried out at the Avondale Research Center, as an introduction to fundamental research. Earlier work in xanthate adsorption on galena under oxidizing and nonoxidizing conditions or on a conceptual model for the role of oxygen in xanthate adsorption on galena has not been discussed because these studies have been, or are being published at this time. What I have attempted to do is to outline the current problems we are investigating, the approach to the solutions, and to give a progress report on what we have learned to date.

THE EFFECT OF THE SPACE CHARGE LAYER OF GALENA ON THE KINETICS OF THE OXYGEN REDUCTION REACTION

by

Paul E. Richardson[1], and Daniel L. Edelstein[2]

ABSTRACT

This paper describes some of the more fundamental flotation research carried out by the Bureau of Mines in order to improve the technology for processing low-grade and complex sulfide ores. Specifically combined electrochemical, interfacial capacitance, and surface photovoltage (SPV) techniques have been used to study the oxygen reduction reaction on natural and synthetic lead sulfide crystals. It is shown that under moderate cathodic polarization, changes in the electrode potential occur predominantly across the space charge layer of the lead sulfide electrodes. Although order-of-magnitude changes occur during polarization in the equilibrium surface density of electrons and holes, the equilibrium surface densities have no direct effect on the reaction kinetics because with moderate cathodic polarization, the rate of oxygen reduction is much less than the saturation current for minority carriers (maximum rate at which the minority carriers can diffuse to the surface). However, the finite space charge potential strongly affects the apparent kinetics, giving rise to anomalously large Tafel slopes.

INTRODUCTION

This paper discusses recent studies carried out at the Bureau of Mines Avondale (Maryland) Research Center to determine the relationship between the semiconducting properties of galena and the kinetics of the oxygen reduction reaction. This work, as part of a larger Bureau research program to improve or develop new minerals processing technology, thus addresses two topics in sulfide flotation that have already been the subject of 20 years of experimentation and debate and still remain controversial: First, the mechanism by which oxygen acts as a necessary (and nearly universal) flotation reagent for many sulfide ores, and, second, whether or not the semiconducting properties of sulfides influence their reaction with oxygen and other flotation reagents. The oxygen reduction reaction on sulfides is also of fundamental as well as practical importance as a component reaction in leaching and dissolution processes and in the weathering of ores.

---

[1] Supervisory research physicist.

[2] Geologist.

A great deal of work has been published on reactions in the galena-oxygen-xanthate system, and a number of theories has been proposed to explain the action of oxygen. Most of this work has been discussed critically in recent review papers (7, 11-12, 17, 27)[3]. The proposals on how oxygen influences the xanthate-galena interaction that are particularly relevant to the present work are the semiconducting model first proposed by Plaksin and co-workers (19) in 1957 and the mixed potential electrochemical model proposed by Salamy and Nixon (23). Both assume that the hydrophobic species formed on the surface is an oxidized form of the xanthate ion. In the semiconducting model, the adsorption of oxygen is assumed to localize electrons at oxygen chemisorption sites, thereby decreasing the free electron concentration at the surface and simultaneously increasing the free hole concentration. This increase in free hole concentration energetically favors the oxidation of the negative xanthate ion, which may occur via either a conduction or a valence band mechanism according to the reactions:

$$O_2 + e^- = (O_2^-)_{ads} \tag{1}$$

$$ROCS_2^- = (ROCS_2)_{ads} + e^-, \text{ conduction band} \tag{2}$$

$$ROCS_2^- + e^+ = (ROCS_2)_{ads}, \text{ valence band} \tag{3}$$

where R represents the hydrocarbon part of the xanthate species, the subscript ads denotes an adsorbed species, and e^- and e^+ denote a conduction band electron and valence band hole, respectively.

More recently, Woods (27-28) has proposed the following mixed potential reactions for the ethylxanthate-oxygen-galena system:

$$C_2H_5OCS_2^- \rightleftarrows (C_2H_5OCS_2)_{ads} + e^- \tag{4}$$

$$(C_2H_5OCS_2)_{ads} + C_2H_5OCS_2^- \rightleftarrows (C_2H_5OCS_2)_2 + e^- \tag{5}$$

$$2(C_2H_5OCS_2)_{ads} \rightleftarrows (C_2H_5OCS_2)_2 \tag{6}$$

and

$$\tfrac{1}{2}O_2 + H_2O + 2e^- \rightleftarrows 2OH^- \tag{7}$$

in which the xanthate ion is oxidized first to an adsorbed radical and then to dixanthogen while oxygen is simultaneously reduced to provide a charge compensating cathodic process. Step 4 involves a chemisorbed radical which, according to Woods, renders the surface only slightly hydrophobic, whereas step 6 leads to physically adsorbed dixanthogen, which renders it strongly hydrophobic.

Both of these models involve oxygen reduction. The essential difference between them is the emphasis on oxygen adsorption and its effect on the carrier densities in the semiconducting model as opposed to the treatment of galena as a metal in the mixed potential electrochemical model. Essentially, the semiconducting model is a special case of the mixed potential model. In the former, the adsorption densities as well as the rate of oxygen reduction and xanthate oxidation may be expected to be dependent on the electron and hole densities at the surface of galena or on the rate of diffusion of minority carriers to the surface.

---

[3] Underlined numbers in parentheses refer to items in the list of references at the end of this report.

Several investigators, however, have concluded that galena behaves like a metal electrode (9, 11, 28). This implies that changes in the interfacial potential occur solely across the solution side of the interface and that the surface concentrations of carriers are independent of electrode potential. This implication was largely inferred from electrochemical data or from xanthate adsorption and flotation behavior of n- and p-type samples, but none of these investigators attempted to measure directly the potential drop across the space charge layer of galena, the most important parameter characterizing the interface. Such behavior would also be contrary to that expected at a semiconductor-electrolyte interface and to previously published studies (21-22) carried out at Avondale.

In the Avondale studies the surface photovoltage (SPV) was used to show that relatively large changes in the space charge potential of galena can be brought about by relatively moderate polarization. It was also shown that the flat band potential of galena is dependent on the bulk carrier densities and occurs at electrode potentials more cathodic than the normal rest potential. Hence, at the rest potential, a net negative charge exists at the interface proper, and to maintain electrical neutrality the space charge layer is depleted of electrons or enriched in holes relative to their concentration in the bulk. These studies were carried out under dynamic polarization conditions (cyclic voltammetry and step current polarization) in a borate solution containing little oxygen. Over the potential range of -0.7 to ≈ 0.2v (S.C.E.) the dominant faradaic currents arose from the anodic dissolution and cathodic reduction of galena (or surface reaction products), and no information was obtained on the oxygen reduction reaction.

In the work described in this paper, we have studied the oxygen reduction reaction on galena using steady-state polarization measurements at several different oxygen partial pressures. At the same time the SPV and the interfacial capacitance of the electrodes were measured to obtain information on the partitioning of the total interfacial potential between the space charge layer of the solid and the Helmholtz layer in the solution.

EXPERIMENTAL

General

The electrochemical cell (cell 1), associated gas train, water source, and cleaning procedures used for most of the work reported in this paper have been described in detail elsewhere (21-22). The electrolyte was 0.1M sodium tetraborate. The cell was purged with ultra-high-purity nitrogen or sparged with nitrogen containing known oxygen partial pressures ($PO_2 = 10^{-3}$ and 10^{-2}atm) for experiments where measurements are reported as a function of oxygen concentration. Separate measurements on a platinum electrode in this cell have shown that the diffusion current due to residual oxygen when sparging with nitrogen is 10^{-6} amp/cm^2, which corresponds to a $PO_2 \approx 10^{-4}$ atm (25).

For one set of experiments a different electrochemical cell (cell 11) was constructed. This cell contained a flat quartz optical window that allowed more uniform illumination of the sample for the surface photovoltage measurements. The sample, mounted on a glass tube, was inserted in the cell through a sliding O-ring seal so that it could be positioned with respect to the light source or the reference electrode. The seals in this cell were not as leaktight as those of cell 1, with the residual oxygen partial pressure, although not measured, probably being closer to 10^{-3} atm than the 10^{-4} atm measured in cell 1. For this reason, measurements using the gas mixtures were not attempted, and the results presented are for the unknown residual level.

Measurements on one natural and two synthetic galena samples are reported in this paper. The source of the natural sample was near Galena, Kans. Conductivity and Hall effect measurements carried out on numerous samples from this source showed these samples are almost always n-type, probably degenerate, with typical carrier densities of 2×10^{18} cm^{-3} and an electron mobility of 590 cm^2/v-sec. The results reported in this paper for one sample are typical of numerous samples from this source. The synthetic samples were obtained from the Naval Surface Weapons Center. Hall effect and conductivity measurements on a specimen from the same crystal growth run showed this crystal to be slightly p-type, with a hole density of 6×10^{16} cm^{-3} and a mobility of 324 cm^2/v-sec. However, our photovoltage and capacitance data indicate that the two synthetic samples mounted as electrodes are probably very close to intrinsic, perhaps very slightly n-type. This discrepancy may be due to actual differences in the crystals or to surface trapping characteristics that are different under anodic and cathodic polarization.

For all the work reported in this paper, the samples were cleaved in situ in the electrochemical cells. Figure 1 shows a sample prior to and after cleavage and illustrates the mounting technique. A platinum wire spot welded to the back surface provided an excellent ohmic contact. A sharp blow on a glass rod resting on the projecting portion of the samples resulted in (100) cleavage. Typically more than 95 percent of the electrode surface after cleavage was that of the freshly cleaved surface. The cleavage procedure was selected because in previous measurements (21) it was found that the SPV on cleaved samples is about an order of magnitude larger than that of polished samples for equivalent light intensities, showing that polishing introduces recombination centers at or just beneath the galena surface.[4]

Figure 2 is a schematic of the cells and measuring equipment. A calomel electrode connected via a thin capillary to the cell was used as the reference electrode. The constant current for the polarization studies was obtained from Keithley model 261 picoampere source.[5]

---

[4] Defect states at the surface or in the space charge region would also increase the capacitance as long as the charge transfer between these states and the valence or conduction band is fast compared to the measurement time. Highly reactive centers produced by polishing could also affect the hydrophobicity by acting as sites for hydroxide adsorption.

[5] Reference to specific equipment is for identification only and does not imply endorsement by the Bureau of Mines.

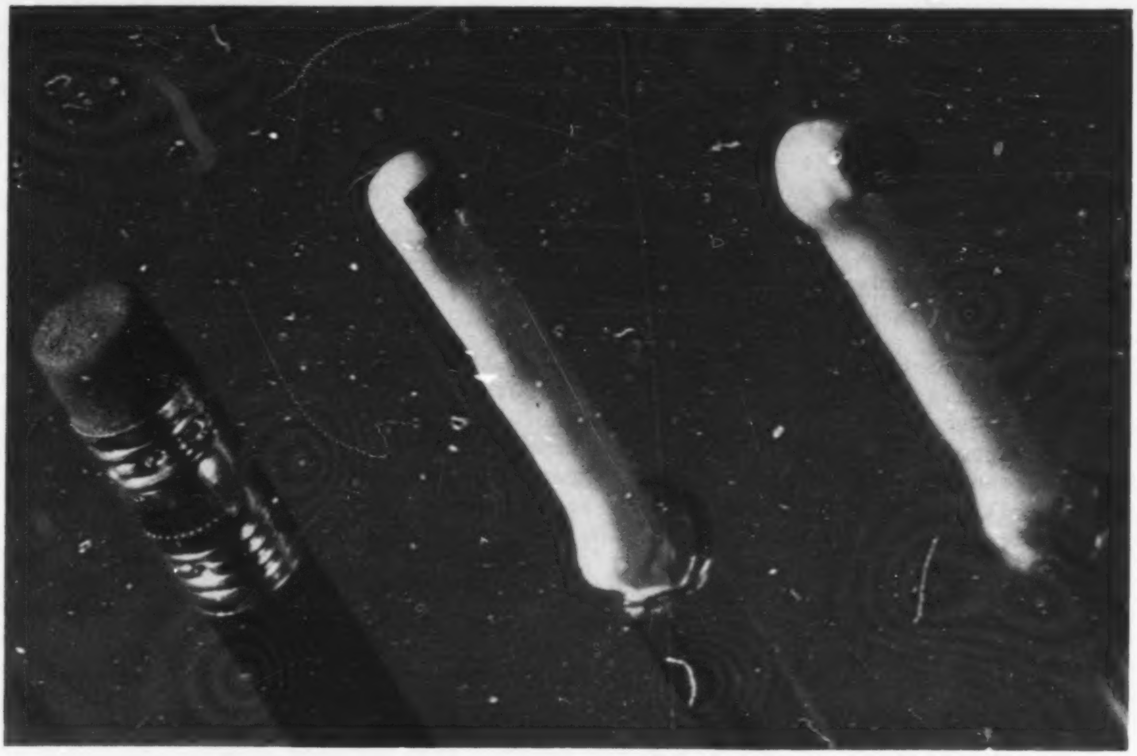

FIGURE 1. - Mounted samples prior to and after cleavage.

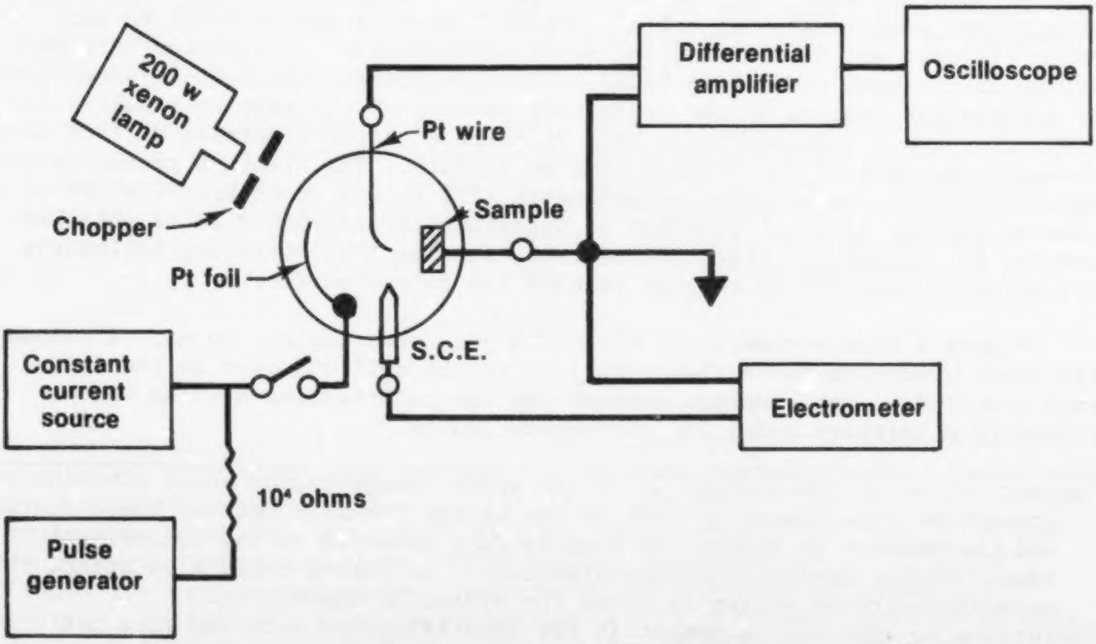
200 w xenon lamp
Chopper
Pt foil
Pt wire
Sample
S.C.E.
Differential amplifier
Oscilloscope
Electrometer
Constant current source
10^4 ohms
Pulse generator

FIGURE 2. - Schematic of cell and circuitry.

The constant current charging pulse used for the capacitance studies was obtained from an EH model 123A pulse generator in series with a 10^4 or 10^5 ohm resistor. The pulse amplitude was 0.1 to 1 ma/cm^2, and the pulse width was 15 to 20 μsec. The interfacial capacitance was determined by analyzing the electrode response to the current pulse, using either a Tektronix model 7633 storage oscilloscope or a Biomation model 805 transient digitizer to record the signal. A typical oscilloscope trace of the current pulse and the resulting electrode response, the latter measured with respect to the platinum wire probe, are shown in figure 3. The electrode response of galena is characterized by a nearly vertical rise and fall in potential when the pulse is applied and terminated, a linear increase in potential from ≈ 4 μsec to the end of the pulse, and an exponential (nearly linear in the time span of fig. 3) decrease in potential starting ≈ 4 μsec after the pulse is terminated. A slight oscillation in the current pulse and in the electrode response occurs during the first 3 μsec after the pulse is applied and after it is terminated. This results from the pulse generator being terminated with the cell impedance, rather than a 50-ohm matched load. The first 3 μsec of the response curve can be neglected, with negligible errors in the result, since the important quantities are the slope, $\Delta V/\Delta t$, of the linear rise and the decay constant τ for the relaxation process.

Although the response shown in figure 3 does not define a unique equivalent circuit, it is consistent with the simple combination of resistances and capacitances (shown in fig. 4) that has previously been proposed (6) to represent the impedance of the germanium-electrolyte interface. In the present case, C is taken to represent the series combination of the Helmholtz double layer capacitance in solution and the space charge layer capacitance of

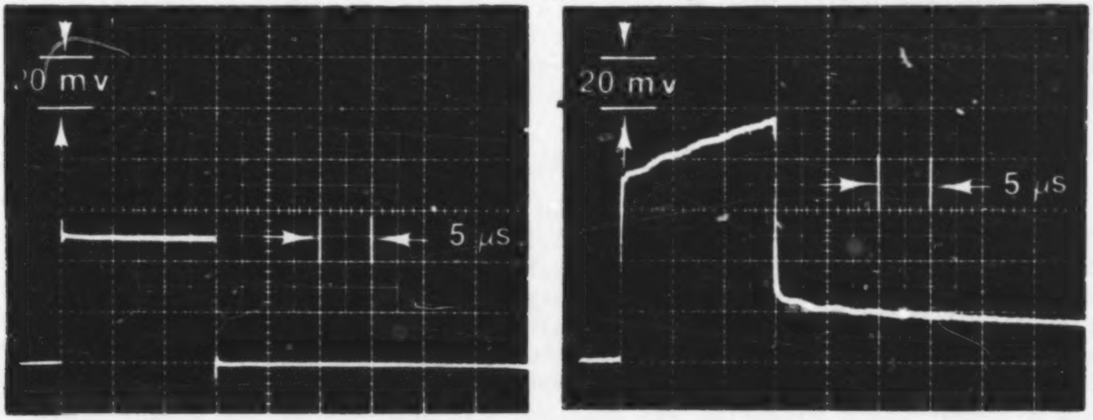

FIGURE 3. - Typical current pulse (left) and electrode response curves (right).

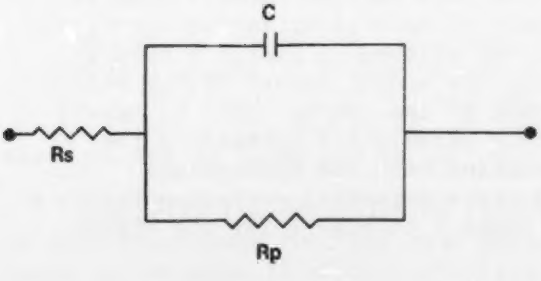

FIGURE 4. Equivalent circuit for analysis of the electrode response to a constant current pulse.

galena just beneath the surface. The parallel resistance, R_p, has been associated with the resistive impedance of faradaic reactions at the interface, and the series resistance, R_s, with the resistance of the electrolyte, the sample, and the electrical contacts (6). The voltage response V(t) of this equivalent circuit, using the linear approximation for the exponentials, is

$$V(t) = IR_s + It/C. \tag{8}$$

The capacitance was calculated using

$$C = I\Delta t/\Delta V \tag{9}$$

where I is the amplitude of the current pulse and $\Delta t/\Delta V$ is determined from the slope of the charging curve over the linear region.

The SPV measurement technique is described in detail elsewhere (21). The transient SPV signals were picked up by the platinum wire probe and recorded with the oscilloscope or the transient digitizer.

The time dependence of the electrode potential at cleavage was measured with respect to both the platinum wire probe and the calomel reference electrode. The platinum-galena signal was coupled to the transient digitizer with a unity gain, high impedance Keithley 604 differential amplifier. The nearly instantaneous negative change in electrode potential at cleavage was used to trigger the transient digitizer. The electrode potential was recorded with respect to platinum over the range of 10^{-2} to ≈ 4 sec after cleavage. The calomel-galena signal was coupled to a strip chart recorder through a Keithley 616 electrometer. The slow response of the recorder limited measurements of this signal to times > 2 sec. The platinum-galena potential was referenced to the calomel-galena potential using the overlapping time ranges of the two measurements.

Measurement Sequence

A typical experimental run consisted of (1) cleaning thoroughly with acid and water-rinsing the cell, (2) filling the solution and reference electrode compartments with 0.1M sodium tetraborate prepared from recrystallized reagent-grade sodium tetraborate, and purging the cell with an ultra-high-purity inert gas, (3) inserting the sample through a side port, and recording the rest potential and SPV of the uncleaved sample, (4) cleaving the sample while continuously recording the electrode potential and measuring the SPV until a steady-state potential was reached, (5) determining the steady-state cathodic polarization behavior of the sample in nitrogen-purged borate and measuring the capacitance and photovoltage at each current density used in the polarization study (at the cathodic limit of each polarization curve, the current was disconnected and the potential was allowed to increase back to the steady-state potential), (6) determining the anodic branch of the polarization curve (again disconnecting the current at the anodic limit to permit the potential to decrease to the open circuit value), (7) increasing the oxygen partial pressure by sparging the solution with the appropriate nitrogen-oxygen mixture until a new steady-state potential corresponding to a higher PO_2 was reached, and (8) repeating steps 5 through 7 for the higher oxygen containing solution.

RESULTS

Figures 5, 6, and 7 show the results of the combined polarization, differential capacitance, and SPV measurements for the synthetic sample S-1, the natural crystal N-1, and the synthetic sample S-2, respectively. The results for S-1 and N-1 were obtained in cell 1 with the known residual oxygen partial pressures, whereas the data for S-2 were obtained in cell 2 with the unknown residual oxygen level.

Polarization Measurements

The top curves in each figure show the constant current polarization behavior at three oxygen partial pressures for samples S-1 and N-1, and at the unknown oxygen concentration for sample S-2. In obtaining these data, the time required to reach a steady-state potential after each change in current density ranged from 15 minutes to ≈ 1 hour, with the shorter times being obtained at the higher oxygen concentrations. In some cases, true steady-state potentials were not reached even after an hour, and slight extrapolations were used to estimate the steady-state potential.

The polarization curves are independent of changes in agitation produced by the sparging gas, except for a slight shift in potentials to more positive values at the highest cathodic current densities. Thus, for potential $\gtrsim$ -0.4 v(S.C.E.), the reaction kinetics are not mass transport controlled.

The general dependence of the open-circuit potential of S-1 and N-1 on oxygen partial pressure as well as the voltage-current behavior of the three samples at potentials around the open-circuit potential are as expected for an open-circuit dissolution reaction in which galena is oxidized to a soluble solution species, while oxygen is simultaneously reduced to maintain overall charge neutrality.

It can be seen from figures 5 and 6 that the oxygen reduction reaction is first order with respect to PO_2 for both of these samples, with a 10-fold increase in PO_2 producing a corresponding 10-fold increase in current. The Tafel regions are not well defined for the cathodic branches, with the slopes ranging from ≈ 0.160 to 0.220 for S-1, ≈ 0.345 for S-2, and ≈ 0.210 for N-1. These slopes are anomalously large and fit no known kinetic model for reactions at metal or semiconductor electrodes. The anodic branches, on the other hand, have well-defined Tafel regions with slopes of approximately 0.085 for S-1 and 0.060 for S-2 and N-1. At the higher anodic potentials, the curves tend to merge, showing that the anodic dissolution process is zero order with respect to PO_2.

Extrapolation of the Tafel region of the cathodic polarization curves to the rest potential yields values for the open circuit dissolution current of $\approx 5 \times 10^{-9}$ amp/cm^2 for S-1 and N-1 for the $PO_2 \approx 10^{-4}$ atm curves. The dissolution current for these two samples increases to $\approx 4 \times 10^{-8}$ amp/cm^2 when the PO_2 is increased to 10^{-2} atm.

Comparing the polarization curves of figures 5 and 6, it is seen that, at each equivalent PO_2, the rest potential of the degenerate n-type sample (fig. 6) is about 15 mv more positive than the rest potential of the nearly

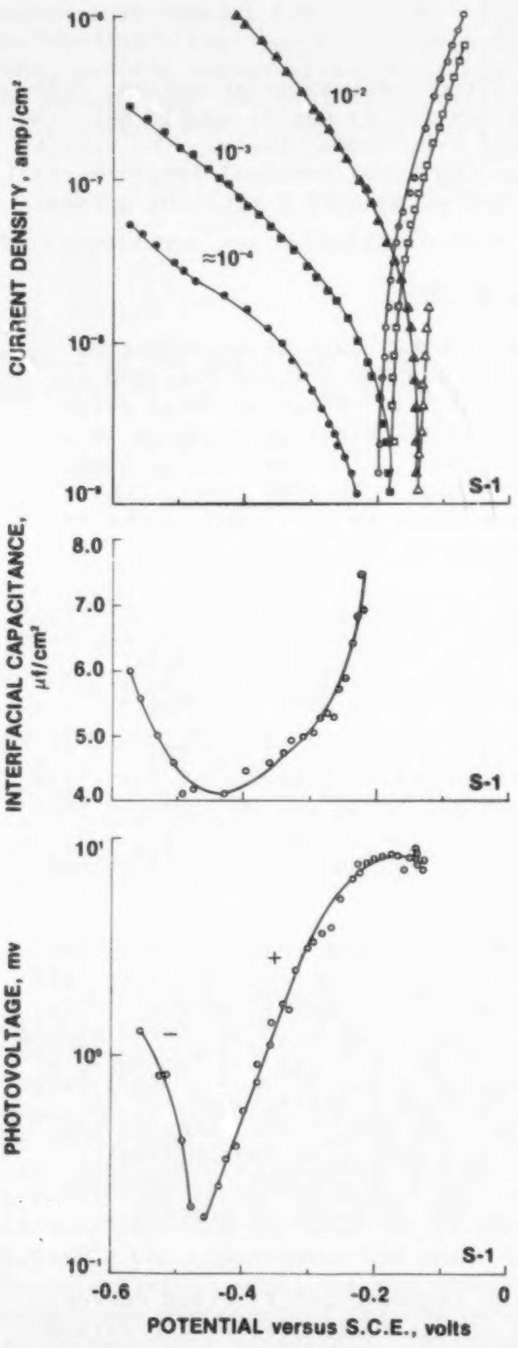

FIGURE 5. - Current, capacitance, and SPV versus potential for sample S-1 at 10^{-2}, 10^{-3}, and $\approx 10^{-4}$ atm of oxygen. ▲,■ , ● - cathodic. △,□ , 0 - anodic.

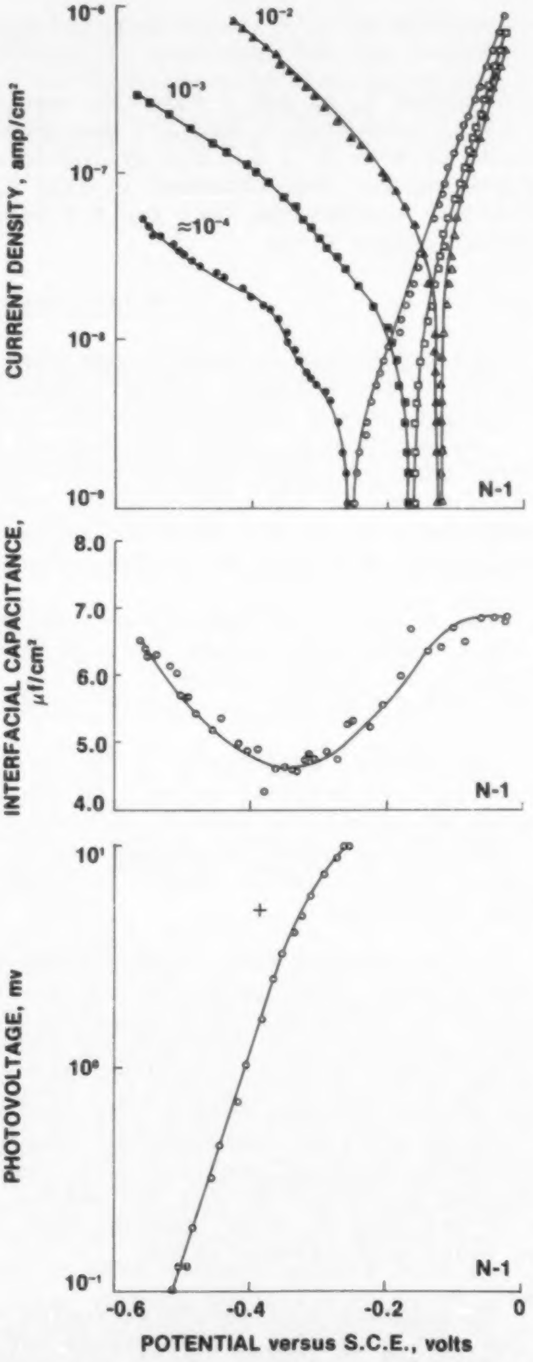

FIGURE 6. - Current, capacitance, and SPV versus potential for sample N-1 at 10^{-2}, 10^{-3}, and $\approx 10^{-4}$ atm of oxygen. ▲,■ , ● - cathodic. △,□, 0 - anodic.

intrinsic synthetic sample (fig. 5). This shift to positive potentials with increasing electron density is opposite to that recently reported by Gutierrez and Lopez (13). However, with the low open-circuit dissolution currents observed in the present work, it is felt that the differences in the rest potential of S-1 and N-1 are not due to differences in the carrier densities. Trace impurity differences in the sample or adsorbed on the surface, especially those that are good catalysts for oxygen reduction, could readily shift the dissolution potential.

A further comment concerns the magnitude of the current density of both the anodic and cathodic branches of the polarization curves. Although the electron concentration of S-1 is several orders of magnitude less than that of N-1, the current density for the same PO_2 at equivalent potentials is nearly the same for both samples. This comparison may also be made with S-2, assuming a residual PO_2 of $\approx 10^{-3}$ atm.

Interfacial Capacitance

The middle set of curves in figures 5, 6, and 7 shows the differential capacitance of the three electrodes measured during the polarization experiments in the nitrogen-purged solution. In these figures, the capacitance has been normalized to the geometrical area of the electrodes, neglecting the

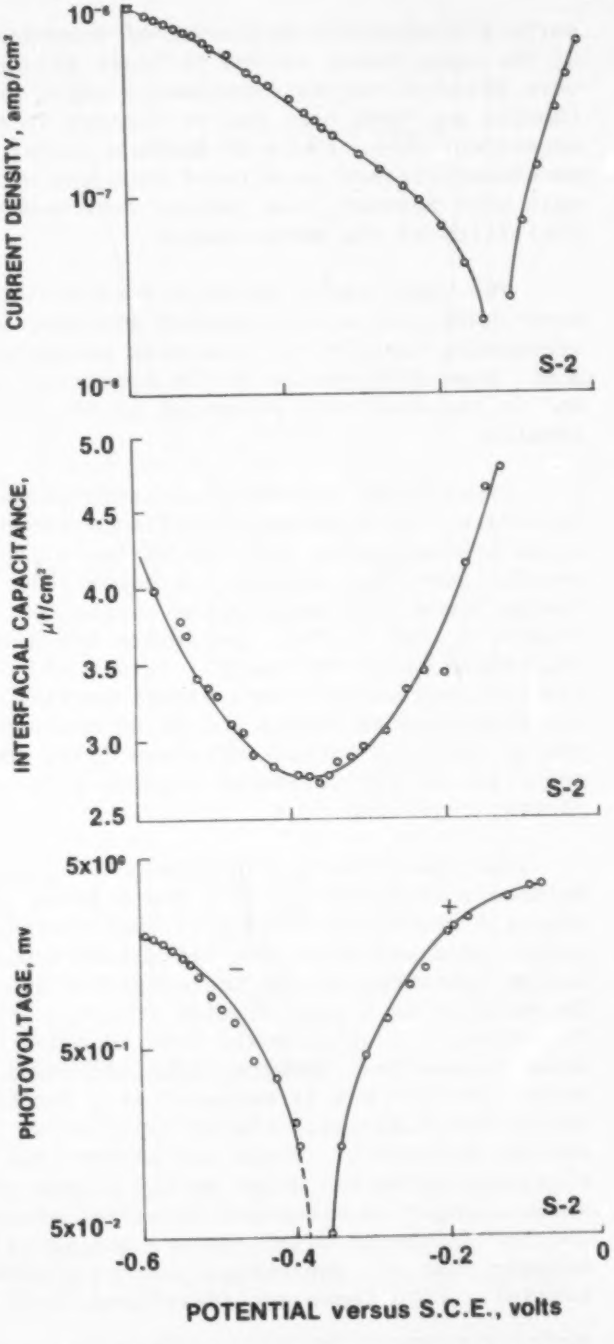

FIGURE 7. - Current, capacitance, and SPV versus potential for sample S-2.

surface roughness. Inclusion of a surface roughness factor would shift each of the capacitance curves to lower values. Some changes in the capacitance were observed during experiments using the nitrogen-oxygen mixtures. These changes may have been due to changes in the surface roughness factor from one experiment to another; to surface states associated with oxygen; or to a pseudocapacitance associated with the oxygen-reduction reaction. For the most part however, the changes were small and within the experimental reproducibility of the measurements.

The capacitance curves for each electrode are similar in general shape, each exhibiting a well-defined minimum, with the magnitude of the capacitance increasing rapidly for electrode potentials cathodic and anodic to the minimum. Some differences in the magnitude of the capacitance at the minimum, and in the electrode potential of the minimum, occur for the different samples.

Considering currently accepted models for the semiconductor-electrolyte interface, the measured capacitance shown in these figures is expected to arise predominantly from two series capacitances, that of the Helmholtz double layer just outside the surface in solution, and that of the space charge layer just beneath the surface of galena.[6] The Helmholtz layer capacitance, C_h, at sulfide electrodes has never been measured. However, at metal electrodes it is typically $\geq 16\ \mu f/cm^2$ in 0.1M electrolytes (5). It is generally found to be a more slowly varying function of electrode potential than the experimental curves and to be nonsymmetrical. Assuming $C_h = 16\ \mu f/cm^2$ at the galena-0.1M borate interface (18), one can expect that it makes some contribution to the curves of figures 5, 6, and 7 and therefore cannot be completely neglected.

The space charge capacitance of galena can be calculated by solving Poisson's equation (16) for the diffuse charge in the space charge region. Figure 8 shows the results of such calculations for highly n-type and slightly p-type lead sulfide. The calculated and experimental curves cannot be directly compared because the experimentally measured interfacial capacitance, in addition to a contribution from C_{sc}, is expected to contain a series contribution, C_h, which would tend to shift the measured curves to slightly lower values than would be obtained for $C_h >> C_{sc}$. Furthermore, the experimental capacitance is measured as a function of electrode potential, whereas the theoretical space charge capacitance is plotted as a function of the surface potential. These scales are equivalent only when changes in the electrode potential occur solely across the space charge layer. In the case where changes in electrode potential occur across both the space charge layer and the Helmholtz double layer, the experimental capacitance curves should be broader than the theoretical curves plotted as a function of the surface potential. With these considerations, both the overall shape as well as

---

[6] Other possible components to the total interfacial capacitance include those of any surface states and pseudocapacities due to faradaic reactions. However, it is unlikely that these would give smooth, nearly symmetrical curves over a wide potential range.

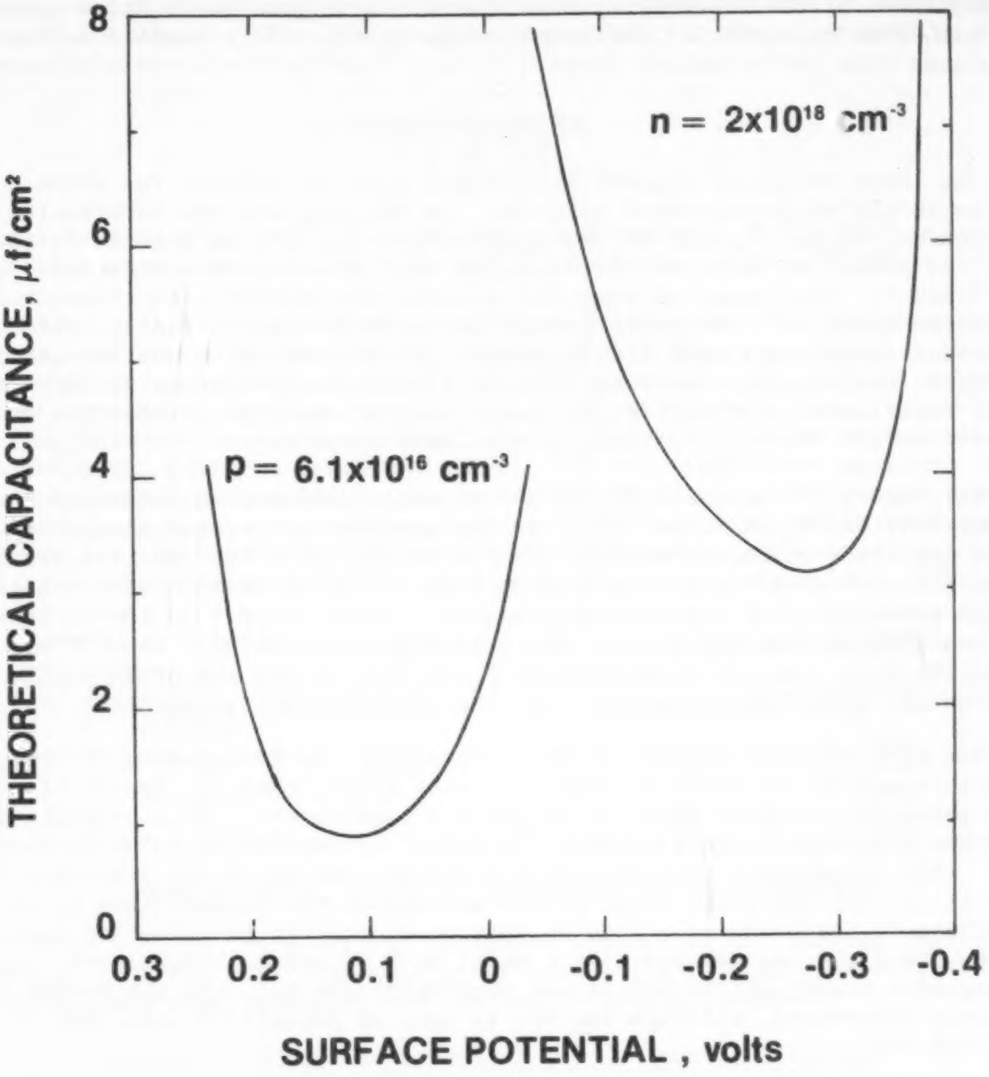

FIGURE 8. - Theoretical capacitance of the space charge layer of galena calculated using an intrinsic carrier density = 2.1 x 10^{15} cm^{-3}, a band gap = 0.42 ev, and a relative dielectric constant = 160. Left curve for bulk carrier density of 6 x 10^{16} cm^{-3}; right curve for a bulk carrier density of 2 x 10^{18} cm^{-3}.

the magnitude of the interfacial capacitance are in good qualitative agreement with that expected for the space charge layer, with a smaller series contributions from the Helmholtz layer.

SPV Measurements

The lower curves of figures 5, 6, and 7 show the SPV for the three samples in the nitrogen-purged solution. As observed for the interfacial capacitance, slight changes in the magnitude of the SPV, as well as in the electrode potential where the SPV reverses sign (cusp in the curves of fig. 5 and 7), were observed when the solution was sparged with the nitrogen-oxygen gas mixtures. These differences may reflect changes in the surface recombination velocity from one experiment to the next or to surface states associated with oxygen. However, for the most part the changes in the different experiments were within the normal scatter observed in the data and may have arisen from fluctuations in the light intensity.

The theory of the small-signal SPV at semiconducting surfaces has been presented by Frankl and Ulmer (8), and its application to the galena-0.1M borate interface discussed in previous papers (21-22). The positive branches of the SPV in figures 5, 6, and 7 correspond to the relaxation of a negative surface potential, the negative branches of figures 5 and 7 to the relaxation of a positive surface potential. Only the positive branch of the SPV was observed for N-1. This is consistent with the Hall effect and conductivity measurements that showed samples from this source to be degenerate n-type.

The zero cusps in figures 5 and 7 correspond, in the absence of trapping in surface states, to the flat band potential (fbp), that is, to the electrode potential at which there is no space charge layer.[7] This provides a reference electrode potential where the surface potential is known to be zero. This occurs at ≈ -0.465 v(S.C.E.) for S-1 and at -0.375 v(S.C.E.) for S-2. At the fbp the Fermi level at the surface of N-1 already lies at or very close to the conduction band so that with cathodic polarization beyond the fbp the electrode behaves like a metal with no space charge layer. Since the negative branch of the SPV is not observable for N-1, the fbp cannot be precisely determined, although the SPV is zero at potentials less than -0.52 v(S.C.E.).

Theoretically, the SPV should saturate under strong anodic and cathodic bias, with the ratio of the saturation SPV's given by (10)

$$\frac{\mathrm{SPV}(V_E \rightarrow -\infty)}{\mathrm{SPV}(V_E \rightarrow +\infty)} = \frac{n_b}{P_b} \tag{10}$$

---

[7] In the presence of surface states, additional structure can appear on the otherwise theoretically smooth SPV curves. In addition, surface states may also cause a shift in the zero of the SPV such that it no longer corresponds to the fbp.

where n_b and P_b denote, respectively, the bulk concentrations of electrons and holes in the sample. The SPV curves do not exhibit perfect saturation, but reasonable extrapolation yields

$$\begin{aligned} n_b/P_b &\approx 2 \text{ for S-1} \\ &\approx 4 \text{ for S-2} \\ &\approx 9 \times 10^5 \text{ for N-1.} \end{aligned}$$

The electron-hole ratio for N-1 was calculated using $n_b = 2 \times 10^{18}$ cm^3. This suggests that S-1 and S-2 are very nearly intrinsic, perhaps slightly n-type.

Table 1 lists the electrode potentials of the zero SPV, the capacitance minimum, and their separation, ΔV_E, on the electrode potential scale for the three samples. In this same table, calculations of the theoretical values for the capacitance minimum on the surface potential scale using the above electron/hole ratios are also shown. The quantity ΔV_s is the calculated surface potential difference between the fbp and the capacitance minimum. Within the experimental uncertainties in determining the fbp and the capacitance minimum, there is a good correlation between the values of ΔV_E determined experimentally and the theoretical values, if it is assumed that changes in the electrode potential occur across both the space charge and Helmholtz layers.

TABLE 1. - Relative potentials of fbp and capacitance minimum

Sample	Experimental			Theoretical		
	V_E(fbp)	$V_E(C_{min})$	ΔV_E	V_s(fbp)	$V_s(C_{min})$	ΔV_s
S-1	-0.465	-0.410	0.055	0	-0.036	0.036
N-1	<- .510	- .347	>.163	0	- .270	.270
S-2	.375	- .375	0	0	- .018	.018

Behavior of Electrode Potential and SPV at Cleavage

Table 2 lists the electrode potential and SPV of the samples before cleavage, 10^{-2} sec after cleavage (time resolution of measurements), and after a steady-state rest potential was reached following cleavage.

TABLE 2. - Electrode potential and SPV during cleavage

Sample	Rest potential before cleavage		Instantaneous potential at cleavage		Rest potential after cleavage	
	V_E(volts)	SPV(mv)	V_E(volts)	SPV(mv)	V_E(volts)	SPV(mv)
S-1	-0.232	+3.6	-0.465	0	-0.225	+6.5
N-1	- .237	+5.9	<- .540[1]	0	- .240	+7.8
S-2	- .137	+1.75	- .380	0	- .137	+4.0

[1] Estimate; actual potential not obtained on this sample (see text).

The "before cleavage" columns show the electrode potential and SPV of the samples with five faces exposed to the electrolyte. These samples had been exposed to the atmosphere for very long times (months to years). When these samples are inserted in the electrolyte a steady "before cleavage" potential is reached within ≈ 10 minutes, and the SPV is positive for each sample showing that the surface potential is negative.

When an electrode is cleaved, the electrode potential instantaneously decreases by several hundred millivolts and the corresponding SPV is zero. The instantaneous potential of N-1 at cleavage was not obtained because of an incorrect setting of the triggering level of the transient digitizer for this particular experiment. However, many natural crystals from the same source have been cleaved, and the potential at cleavage is typically in the range of -0.54 to -0.69 v(S.C.E.) (21). There appears to be a correlation between the instantaneous potential at cleavage and the electron density, with the more n-type samples reaching a more negative potential at cleavage. That the SPV vanishes at cleavage shows, at this point in time and at the corresponding instantaneous electrode potential reached at cleavage, there is no space charge layer just beneath the electrode surfaces. The potential reached at cleavage is the fbp and is nearly identical to the fbp determined during the subsequent polarization experiments. It is likely that the fbp also corresponds to the point of zero charge, referenced with respect to the electrode potential rather than with respect to pH. This supposition is inferred by considering that if there is any interfacial charge existing 10^{-2} sec after cleavage, it should be compensated, at least in part, by the space charge layer of galena. Since the SPV is zero, however, there is no compensating space charge layer, and hence the net charge at the interface is zero. Another possibility is that a large concentration of surface states exists at cleavage and effectively shields the space charge layer from the influence of a net charge just outside the surface. The net charge in the surface states would also have to be zero to give the fbp. This would be coincidental and not consistent with an easily polarized space charge layer.

At longer times following cleavage, the electrode potential of each sample slowly increases from the "at cleavage" value to the steady rest potential. Along with the increase in rest potential, the SPV continuously increases from zero to a relatively large positive value, showing the buildup of a space charge layer containing a net positive charge; that is, a layer that is electron deficient and hole rich relative to the respective bulk concentrations. This positive space charge clearly compensates a net negative charge at the interface proper, which is assumed to arise from either a dissolution or adsorption reaction.

It is also of interest that the rest potential is nearly the same before cleavage as after cleavage, showing that air oxidation has little influence on potentials measured after the electrodes have equilibrated with the electrolyte. Any oxidation products formed in air and affecting the interfacial charge may thus be considered the same as those formed in borate, or else to be soluble.

DISCUSSION

Distribution of the Interfacial Potential

Both the SPV and the capacitance results of figures 5, 6, and 7 can be satisfactorily accounted for by assuming that changes in the electrode potential are partitioned between the Helmholtz double layer in solution and the space charge layer just beneath the surface of galena according to

$$dV_h = \gamma(V_E)dV_E \tag{11}$$

$$dV_{sc} = [1-\gamma(V_E)]dV_E, \tag{12}$$

where dV_h and dV_{sc} are, respectively, the incremental changes in the Helmholtz layer and space charge layer potentials resulting from an incremental change, dV_E, in the electrode potential. The quantity $\gamma(V_E)$ satisfies the inequality $0 < \gamma(V_E) \leq 1$ and, in general, is expected to be a function of the electrode potential. For the case $\gamma(V_E) = 1$, the behavior would be that of a metal electrode, and for $\gamma(V_E) < 1$ the behavior would be that of a semiconductor electrode. If we assume the simplest model for the galena-0.1M borate interface, consisting of two perfectly polarizable double layers corresponding to the Helmholtz and space charge layers, it can be shown from the formulas for series capacitances that

$$\gamma(V_E) = (1 + C_h/C_{sc})^{-1} \tag{13}$$

and

$$1 - \gamma(V_E) = (1 + C_{sc}/C_h)^{-1}. \tag{14}$$

The capacitance data of figures 5, 6, and 7 then represent

$$C_I^{-1} = C_h^{-1} + C_{sc}^{-1}, \tag{15}$$

where C_I is the measured interfacial capacitance. Substituting equation 15 into 13 yields

$$\gamma(V_E) = C_I/C_h \tag{16}$$

from which $\gamma(V_E)$ can be calculated if C_h is known. Figure 9 shows the results of these calculations for the three samples using $C_h = 16$ μf/cm². Unfortunately, it is not possible to accurately determine the uncertainty in $\gamma(V_E)$ that arises either from assuming that $C_h = 16$ μf/cm² or from neglecting the surface roughness factor. However, the data in figure 9 probably represent an upper limit for $\gamma(V_E)$, with the actual value being lower than calculated because of the surface roughness factor.

The curves in figure 9 represent a graphical fit of the following parabolic equations to the calculated $\gamma(V_E)$ values:

$$\text{S-1, } \gamma(V_E) = 0.250 + 4.27(V_E + 0.410)^2 \tag{17}$$

$$\text{N-1, } \gamma(V_E) = 0.285 + 2.91(V_E + 0.347)^2 \tag{18}$$

$$\text{S-2, } \gamma(V_E) = 0.173 + 2.36(V_E + 0.375)^2 \tag{19}$$

Using these analytical expressions for $\gamma(V_E)$ it is possible to integrate equations 11 and 12 to obtain the distribution of potential between the space charge layer and the Helmholtz layer. The results of this integration are shown in figure 10 for the three samples. In carrying out the integration, ΔV_{sc} and ΔV_h were arbitrarily chosen equal to zero at the rest potential of the electrodes at the highest PO_2 studied. The integrations were carried

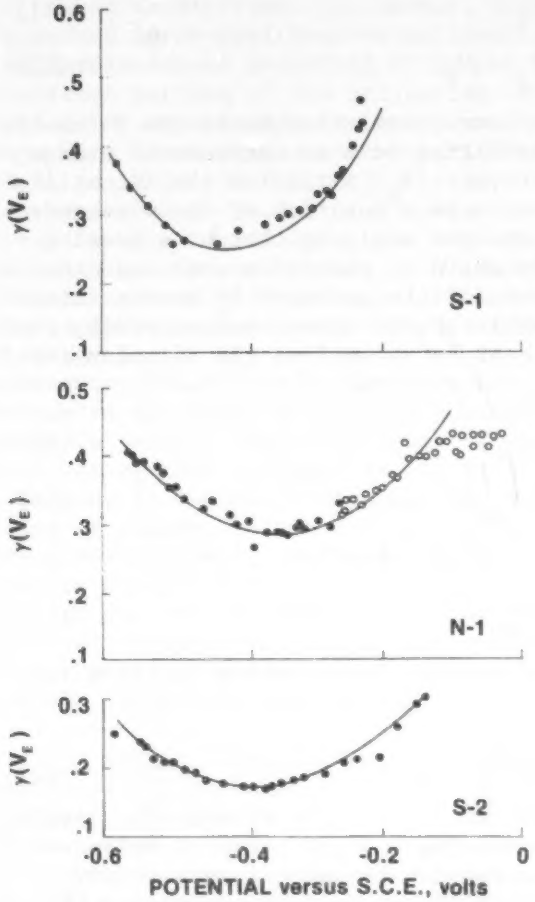

FIGURE 9. - Plots of $\gamma(V_E)$ versus electrode potential for S-1 (top), N-1 (middle), and S-2 (bottom).

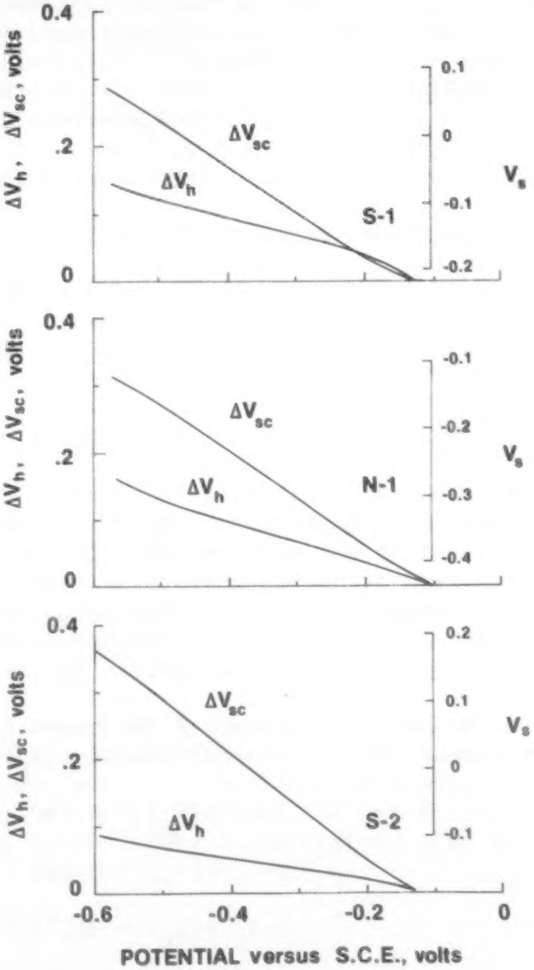

FIGURE 10. - Plots of ΔV_{sc} and ΔV_h for S-1 (top), N-1 (middle), and S-2 (bottom). The right axis shows the absolute surface potential obtained by using the fbp as a reference for $V_s = 0$.

out from this potential to the cathodic limit of the polarization curves. The inserted vertical axis in each figure shows the surface potential of the electrodes obtained by using the fbp as determined from the SPV measurements as a reference potential to fix $V_s = 0$ for S-1 and S-2. The capacitance minimum was used to fix $V_s = -0.270$ v for N-1, according to the calculation shown in figure 8.

Theoretically, the maximum change in the surface potential of galena, corresponding to the difference in V_s observed under strong anodic polarization and under strong cathodic polarization, should equal the band gap, ΔE_g, or

$$(\Delta V_{sc})_{max} = \Delta E_g = 0.42 \text{ v.}$$

This can be compared with the ΔV_{sc} values of 0.29 v for S-1, 0.36 v for S-2, and 0.32 v for N-1. Perfect saturation of the SPV does not occur at the anodic and cathodic limits; this is in agreement with these results, which show $\Delta V_{sc} < \Delta E_g$.

In a future experiment, the electrodes will be polarized beyond the ranges shown in figures 5, 6, and 7 in an attempt to saturate V_s at its maximum negative and positive values. This should provide a test of the results obtained using the above procedure to calculate ΔV_{sc}; that is, the calculated ΔV_{sc} should be 0.42 v. The measured interfacial capacitance at this point should also be predominantly that of C_h. The potential range was restricted in these experiments because in a previous paper (22) it was shown using cyclic voltammetry that polarization at potentials slightly outside the range used here gave rise to rapidly increasing dissolution currents on both the anodic and cathodic sides, and subsequently, to nonreproducible cyclic voltammagrams. Some explanation can now be given for this behavior. For the potential ranges used in those experiments, the interfacial potential drop during polarization occurs mainly across the space charge layer, with smaller changes in ΔV_h. However, as discussed subsequently, it is only ΔV_h, and not ΔV_{sc}, that determines the rate of reactions on galena. Once V_s saturates, at a positive or negative value, subsequent changes in the interfacial potential should occur solely across the Helmholtz layer, with a subsequent rapid increase in reaction rate.

Kinetics of the Oxygen Reduction Reaction

Based on the results shown in figure 10, or more simply on the behavior of the SPV and capacitance, it is clear that large changes occur in the surface potential of galena during the polarization experiments. There are several possible effects on the rate of the oxygen reduction reaction. The rate equations for a reduction at semiconducting electrodes can be written (18):

$$I_c = k\ [0] n_s e^{(\alpha nF/RT)(V_h^\circ - V_h)} \tag{20}$$

and

$$I_v = k^1 [0] e^{(\alpha nF/RT)(V_h^\circ - V_h)} \tag{21}$$

where I_c and I_v refer, respectively, to processes involving charge transfer to conduction and valence bands corresponding to the reactions

best copy available

best copy available

$$0 + ne^- \rightarrow R,\ e^- = \text{conduction band electron} \qquad (22)$$

$$0 \rightarrow R + ne^+,\ e^+ = \text{valence band hole.} \qquad (23)$$

The other symbols have their usual meaning; k, k^1 = rate constants; [0], [R] = concentrations of the oxidized and reduced form of the redox couple, respectively, at the Stern plane; n_s = surface concentrations of electrons; α = transfer coefficient; n = number of electrons; F = faradays; R = gas constant; T = temperature; and $V_h^\circ - V_h$ = the change in the Helmholtz voltage from a fixed reference value V_h°. In writing equations 20 and 21, we have assumed that $V_h^\circ - V_h = \Delta V_h$ is sufficiently large that the rate of the back reaction, or, in the case of galena, the rates of both the back reaction and the anodic dissolution process, are negligible compared to the rate of the forward reaction. Experimentally, this corresponds to the Tafel regions of the oxygen reduction curves.

Three characteristics of equations 20 and 21 cause the kinetic behavior of semiconductors to differ from that of metal electrodes. First, the quantity $V_h^\circ - V_h$ is not equal to the change in electrode potential, as is often assumed for metals in concentrated electrolytes. In fact, as we have shown for galena, large changes in ΔV_{sc} also occur, and the proper application of kinetic equations requires knowledge of the potential distribution. Second, there are two pathways for the charge transfer process, one involving electron transfer from the conduction band to the redox species in the electrolyte just outside the surface (reaction 22), the other involving hole injection from the redox species to the valence band (reaction 23). Third, the surface electron concentration, as a reactant in equation 20, has been explicitly included in the rate equation for the conduction band process. A similar term for the surface hole concentration is not required for hole injection into the valence band, since the available states for the injection process are large enough not to be rate determining.

The effect of n_s in equation 20 on the kinetic behavior is analogous to the factor [0] for the concentration of the oxidized form of the redox couple at the outer Helmholtz phase. In order to calculate n_s, it is usually necessary to solve the continuity equation for electrons and holes for the non-equilibrium situation that exists when a current flows across the interface (18). However, for the relatively small current densities used in these experiments, the surface concentrations of both electrons and holes are given, to a very good approximation, by the equilibrium Boltzmann distribution:

$$n_s = n_b e^{-(F/RT)V_s},\ p_s = p_b e^{(F/RT)V_s} \qquad (24)$$

where n_b and p_b are the bulk electron and hole densities, respectively. This can be shown by considering the effect of a current flow, I, across the interface on the surface potential, which can be written (18):

$$V_s = -(RT/F)\ln(n_s/n_b) + (RT/F)\ln(1 + I/I_n^{lim}). \qquad (25)$$

The first term corresponds to the Boltzmann distribution factor, and the second arises from concentration polarization of electrons at the surface due to the current flow. The quality I_n^{lim} is the limiting diffusion current of electrons to the surface (saturation current) and is given by (18)

$$I_n^{lim} = qD_n n_b/L_n \qquad (26)$$

where D_n is the diffusion rate constant for electrons, L_n is their average diffusion length, and q is the electron charge. For galena, $D_n \simeq 11$ cm^2/sec and $L_n \simeq 0.01$ cm (21). The lowest limiting current for electrons would occur for a degenerate p-type specimen with $n_b \simeq 10^{12}$ cm^{-3}, which gives $I_n^{lim} \simeq$ 350 μa/cm^2. For the samples used in this work, $n_b >> 2 \times 10^{12}$ cm^{-3}, and the corresponding limiting current densities are sufficiently large compared to the interfacial current that the concentration polarization term in equation 25 can be neglected.

This argument suggests that, although the equilibrium electron and hole densities at the surface change by many orders of magnitude (given by equation 24) over the cathodic polarization curves, their diffusion rate to the surface is sufficiently fast that they are not rate determining for the oxygen reduction reaction. This conclusion is also supported by comparing the experimental polarization curves in figures 5 and 6. Although the electron concentration is approximately 3 orders of magnitude larger for N-1 (fig. 6) than for S-1 (fig. 5), the magnitudes of the current density for equivalent oxygen partial pressures are nearly the same on the two samples. The quantity n_s in equation 20 can thus be incorporated into the rate constant k. Since equations 20 and 21 then have exactly the same form, it is not possible from the polarization experiments to distinguish between the electron trapping process represented by reaction 22 and the hole injection process represented by reaction 23. The oxygen reduction reaction may then be written:

$$I = kPO_2 e^{(\alpha nF/RT)\Delta V_h}. \qquad (27)$$

This rate equation differs from that of a metal, because ΔV_h is not equivalent to the change in electrode potential.

In figure 11 the cathodic branches of the polarization curves of figures 5, 6, and 7 have been replotted using the ΔV_h values shown in figure 10 for the three electrodes. The Tafel slope for the oxygen reduction reaction, when plotted versus the change in Helmholtz overvoltage, is ≃ 0.060 for each of the electrodes, suggesting a two-electron reduction process. However, it should be cautioned that the Tafel slope obtained by this procedure is sensitive to $\gamma(V_E)$. For example, an error in $\gamma(V_E)$ of a factor of 2 arising from the uncertainty in the Helmholtz capacitance, surface roughness, or measurement errors would change the slope of the Tafel curves by approximately the same factor. As mentioned previously, it is believed that the calculated $\gamma(V_E)$ values represent an upper limit, with the actual value lying below the values shown in the plots of figure 9. Thus, if the true $\gamma(V_E)$ values are one-half the calculated values, the corrected Tafel slopes would be ≃ 0.03, suggesting a four-electron reduction process. The important points are that (1) the reaction rate is not dependent on the bulk carrier densities or the equilibrium surface densities and (2) the potential is partitioned between the two double layers. The net result is to cause the experimentally measured Tafel slopes to increase, according to exactly how the potential is partitioned. Essentially, the potential drop across the space charge layer is nonfaradaic, and the anomalously large Tafel slopes are due to failure to correct the apparent electrode potential for this nonfaradaic component.

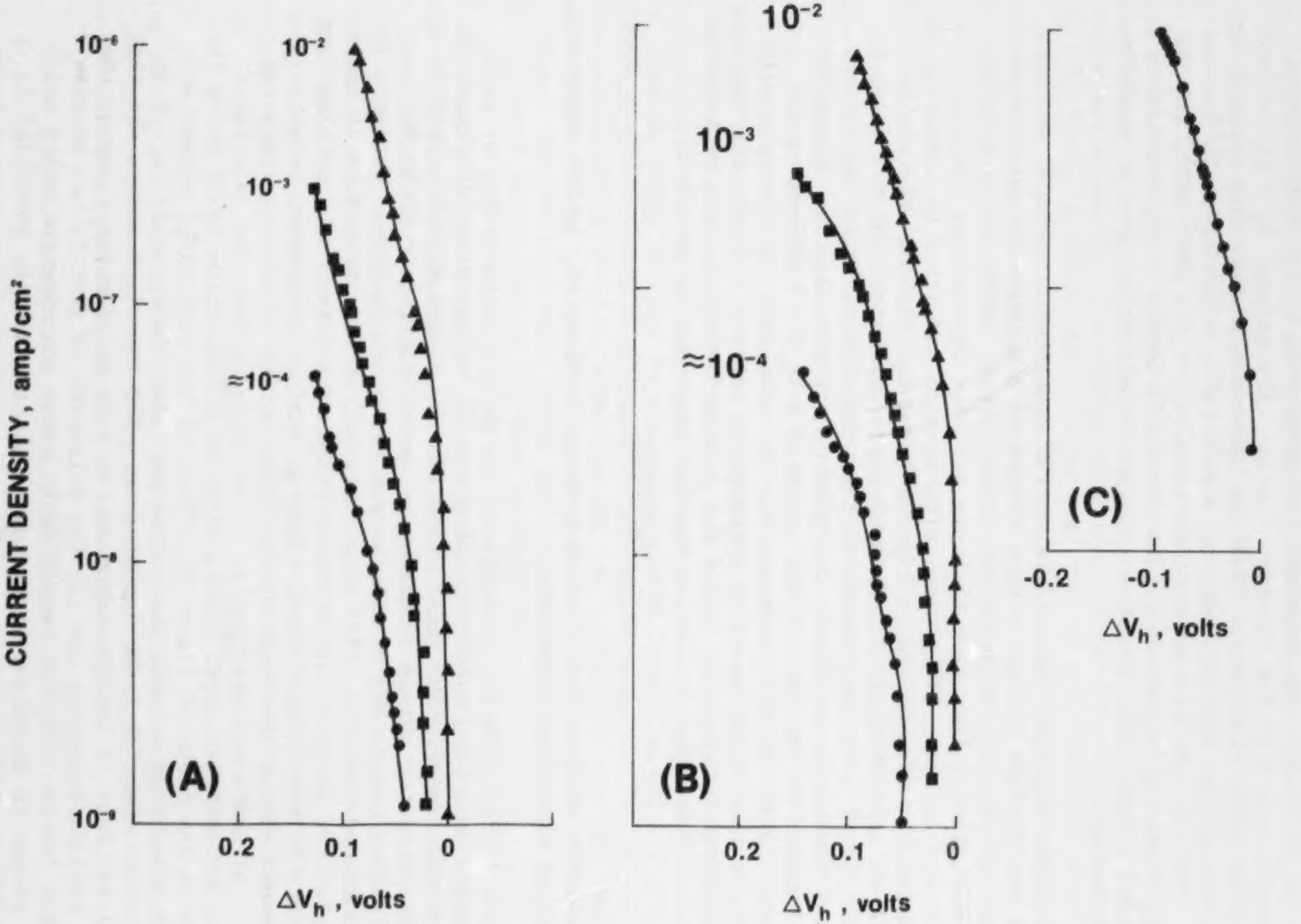

FIGURE 11. - Current-voltage curves for oxygen reduction versus ΔV_h. Curves are labeled with oxygen partial pressure. A - sample S-1, B - sample N-1, C- sample S-2.

Recently, Biegler and coworkers (3, 20) have studied the reaction of oxygen on galena and a number of other sulfides using linear sweep voltammetric techniques and found that the catalytic activity of galena for oxygen reduction is less than that of chalcopyrite, arsenopyrite, and pyrrhotite. Ahmed (1-2), using the same technique, also found that galena was a poor catalyst for this reaction compared to pyrite and cobalt sulfide. It is likely that the nonfaradaic component of the interfacial potential is the reason for the poor catalytic activity of galena. However, all these sulfides are semiconductors, and before reaching this conclusion a careful study of the effect of the semiconducting properties on the catalytic activity and the determination of the distribution of potential at the interface would have to be made for each of the sulfides. Biegler (4) has also carried out measurements on several pyrite samples that had been characterized electrically and shown to be n-type, n-type metallic, and p-type. Although differences in the Tafel slope for oxygen reduction were observed for the different samples, he concluded that there is no obvious correlation between the kinetic parameters for oxygen reduction and the semiconducting character. This conclusion may be premature, since no attempt was made to measure the space charge potential.

Origin of the Interfacial Charge

From our measurements of cyclic voltammetry and SPV on galena (21-22), and from the time dependence of the electrode potential and SPV after cleavage, we concluded that the interfacial charge was largely determined by the stoichiometry of the electrodes in a narrow spatial region near the surface relative to the underlying stoichiometry in the bulk. The results in this paper are also consistent with the model illustrated in figure 12.

At cleavage, the composition of the electrode is assumed to be perfectly homogeneous from the bulk to the surface proper, and there is no interfacial charge, as shown by the zero SPV. The electrode potential subsequently increases slowly with time to a steady-state rest potential, with the corresponding SPV becoming increasingly positive as the rest potential increases. This is attributed to a dissolution reaction in which lead is leached from the surface, leaving lead vacancies, V_b^{+2}. Lead vacancies in lead sulfide are known to act as acceptors, with very small ionization energies of 0.02 ev or less (24, 26). Because of the small ionization energies, the cation vacancy can readily localize an electron from a neighboring anion, leaving a net negative charge at the surface proper and increasing the free hole concentration just beneath the surface by reactions of the type given by

$$\begin{array}{ll|c|ll|l}
S^{--} & Pb^{++} & & S^{--} & Pb^{++} & \\
Pb^{++} & S^{--} & & Pb^{++} & S^{--} & \\
S^{--} & Pb^{++} & + O_2 + 2H^+ \rightarrow & S^{--} & V_{Pb}^{++} & + Pb^{++} + 2H_2O_2 \\
Pb^{++} & S^{--} & & Pb^{++} & S^{--} & \\
S^{--} & Pb^{++} & & S^{--} & Pb^{++} & \\
\multicolumn{2}{l}{V_E = fbp} & \multicolumn{1}{c}{} & \multicolumn{2}{l}{V_E > fbp} & \multicolumn{1}{l}{}
\end{array}$$

FIGURE 12. - Model illustrating mechanism for the formation of negative charge at the surface of galena.

$$V_{Pb}^{++} = V_{Pb}^{+} + e^{+} \tag{28}$$

This negative charge is largely compensated by the positive space charge of mobile carriers just beneath the surface, and to a lesser extent by changes in the Helmholtz layer just outside the surface. During subsequent cathodic polarization, it is assumed that the excess surface sulfur is reduced until the electrodes are again homogeneous at the particular electrode potential corresponding to the fbp. Cathodic polarization beyond the fbp is assumed to produce sulfur vacancies, that act as shallow donors; when ionized, these vacancies give rise to a net positive charge at the surface. This positive surface charge is compensated by a negative space charge beneath the surface and to a lesser extent by a change in the Helmholtz layer.

Another possible origin of the negative surface charge at potentials anodic to the fbp is oxygen or hydroxide ion chemisorption. In considering a model involving chemisorption, several different cases can be distinguished. For example, chemisorption may occur simultaneously with changes in stoichiometry, so that the net charge at the interface proper is composed of that associated with the chemisorbed species and that associated with cation or anion vacancies. Chemisorption may also give rise to soluble or insoluble reaction products. In the former case, the net result could probably be interpreted better in terms of stoichiometric changes at the surface; in the latter case, a chemisorption process would be an appropriate interpretation. However, as pointed out by Lee (15), the formation of insoluble surface compounds in which the lead/sulfur ratio differs from that of PbS must certainly change the stoichiometry. Examples of compounds in which the stoichiometry changes in the lead-deficient direction include $PbO{\cdot}PbSO_4$ and PbO, whereas $Pb_2S_2O_3$ should change the stoichiometry in the sulfur-deficient direction. On this basis, oxygen chemisorption and the formation of surface oxidation products may also be considered to change the stoichiometry in the surface region.

It is particularly interesting that both the interfacial charge and the chemical species on the surface appear to be unique functions of electrode potential. This follows from the reproducibility of the polarization curves such as those of figures 5, 6, and 7 and the interfacial capacitance and SPV. Earlier cyclic voltammetry studies also showed that the redox processes on galena could be reproduced over many cycles, suggesting that the oxidation products formed at anodic potentials are reduced at cathodic potentials, so that the surface is continuously renewed during each cycle. Although the hydrophobicity of galena in the absence of a collector has not yet been determined as a function of electrode potential, it is certain that the existence, or absence, of natural hydrophobicity will depend on the charge at the interface and on the exact chemical species present. Since these both are functions of electrode potential, the natural hydrophobicity should also be potential dependent, as found by Heyes and Trahar (14) for chalcopyrite.

The quantity of charge at the interface at the rest potential can be estimated from the interfacial capacitance data of figures 5, 6, and 7. The area under the curves essentially represents the integral capacitance from which the charge over a desired potential range can be calculated. Considering just the area underneath the curves from the fbp to the rest potential in the nitrogen-purged solutions yields interfacial charges of 1.1, 1.3, and 0.8 $\mu C/cm^2$ for S-1, N-2, and S-2, respectively. The density of lead sites on the (100) surface is 5.67×10^{14} cm^{-2} (17), so these values represent fractional surface compositional changes of only 1.2, 1.5, and 0.9 percent, respectively.

CONCLUSIONS

Specific

Measurements of the interfacial capacitance and the SPV at the galena-0.1M borate interface have independently demonstrated that large changes in the potential drop across the space charge layer of galena occur during moderate cathodic polarization of the electrodes. This potential drop is essentially "nonfaradaic" since the rate of oxygen reduction is much less than the saturation diffusion current of minority carriers to the surface. Thus, no concentration polarization of the current carriers occurs. The effect of this component of the interfacial potential on the apparent kinetics of the oxygen reduction is to give anomalously large Tafel slopes. A tentative estimate of the correct Tafel behavior for oxygen reduction, based on an assumed Helmholtz layer capacitance of 16 $\mu f/cm^2$ and a surface roughness of unity, gives a corrected Tafel slope of ≈ 0.060, suggesting that a two-electron reduction process is rate determining. The reaction has also been shown to be first order with respect to oxygen partial pressure.

The Tafel slope of the anodic dissolution reaction has been found to be in the range 0.060 to 0.085. In contrast to that of the oxygen reduction reaction, the Tafel slope for the anodic dissolution reaction is only slightly affected by the potential drop across the space charge layer. The reason for this is that, at the rest potential, a relatively large negative interfacial charge exists at the surface proper. Most of this charge is compensated by a positive space charge layer just beneath the surface, with the result that the Fermi level at the surface already lies at or very close to the valence band edge at the rest potential. With slight anodic polarization, little or no further change occurs in the space charge potential, and the electrodes behave like metal electrodes. For the small current densities encountered in the dissolution reactions, the rate of carrier diffusion to the surface is not rate determining.

Implications in Minerals Processing

Although the results obtained in this investigation provide a much better understanding of the relationship between the semiconducting properties of galena and the kinetics of the oxygen reduction, a great deal more work is required before these results can be related to interactions in the galena-oxygen-xanthate system, and to the flotation behavior of galena. However, several features of the data are expected to have an important bearing on mineral flotation.

It is unlikely (because of the large limiting current density for diffusion of electrons or holes to the surface) that the rate of supply of either electrons or holes to the surface is rate determining in the oxidation of xanthate ions to a hydrophobic species. Thus, the major semiconducting effect expected is one in which slight differences in the potential distribution at the interface occur between samples with different bulk carrier densities. In addition, illumination or adsorption may also cause a slight change in the distribution of potential, and a corresponding rearrangement of the charge at the interface. This semiconducting effect may have an influence on the quantity of xanthate absorbed, but not nearly as large an effect as would be expected for reactions that occur rapidly enough for the supply of either electrons or holes to the surface to be rate limiting.

Oxygen is believed to be instrumental in giving rise to the net negative charge observed on the surface of galena at the rest potential, and the resulting space charge layer that is depleted of electrons and enriched in holes. Although the exact mechanism for the formation of the negative charge is not known, it is consistent with either a chemisorption or a leaching process in which the effective sulfur-lead ratio at the surface is increased. Both the charge at the surface and the exact chemical composition should determine the natural hydrophobicity as well as affect subsequent reactions with xanthates.

ACKNOWLEDGMENT

The authors wish to thank Dr. Donald Ernst, Research Chemist, Naval Surface Weapons Center, Silver Spring, Md., for kindly supplying the synthetic lead sulfide crystals used in this study.

REFERENCES

1. Ahmed, S. M. Electrochemical Studies of Sulphides, I. The Electrocatalytic Activity of Galena, Pyrite, and Cobalt Sulphide for Oxygen Reduction in Relation to Xanthate Adsorption and Flotation. Internat. J. Miner. Process., v. 5, 1978, pp. 163-174.

2. _____. Electrochemical Studies of Sulphides, II. Measurement of the Galvanic Currents in Galena and the General Mechanism of Oxygen Reduction and Xanthate Adsorption on Sulphides in Relation to Flotation. Internat. J. Miner. Process., v. 5, 1978, pp. 175-182.

3. Biegler, T. Oxygen Reduction on Sulphide Minerals. Part II, Relation Between Activity and Semiconducting Properties of Pyrite Electrodes. J. Electroanal. Chem., v. 70, 1976, pp. 265-275.

4. Biegler, T., D. A. J. Rand, and R. Woods. Oxygen Reduction on Sulphide Minerals. Part I. Kinetics and Mechanism at Rotated Pyrite Electrodes. Electroanal. Chem. and Interfacial Electrochem., v. 60, 1975, pp. 151-162.

5. Delahay, P. Double Layer and Electrode Kinetics. Interscience Publishers, New York, March 1966, p. 39.

6. Engell, H. J., and K. Bohnenkamp. Electrode-Solution Interfaces. Ch. in The Surface Chemistry of Metals and Semiconductors, ed. by H. C. Gatos. John Wiley & Sons, Inc., New York, 1960, pp. 225-243.

7. Finkelstein, N. P., and G. W. Poling. The Role of Dithiolates in the Flotation of Sulphide Minerals. Miner. Sci. Eng., v. 9, No. 4, October 1977, pp. 177-197.

8. Frankl, D. R., and E. A. Ulmer. Theory of the Small-Signal Photovoltage at Semiconductor Surfaces. Surface Sci., v. 6, 1966, pp. 115-123.

9. Gamboa, J. M., C. Gutierrez, and J. Llopis. (Adsorption of Ethyl Xanthate on Galenas of Different Semiconductor Types.) Anales de Quimica, v. 64, 1968, pp. 679-686.

10. Garrett, C. G. B., and W. H. Brattain. Physical Theory of Semiconductor Surfaces. Phys. Rev., v. 99, No. 2, July 15, 1955, pp. 376-387.

11. Granville, A., N. P. Finkelstein, and S. A. Allison. Review of Reactions in the Flotation System Galena-Xanthate-Oxygen. Trans. Inst. Min. and Met. (Sec. C: Miner. Processing and Extractive Met.), v. 81, 1972, pp. C1-C30.

12. Gutierrez, C. The Mechanism of Flotation of Galena by Xanthates. Miner. Sci. Eng., v. 5, No. 2, April 1973, pp. 108-118.

13. Gutierrez, C., and M. C. Lopez. Increase of the Rest Potential of Nonstoichiometric Lead Sulfide in 0.1M Borax With Its p-Semiconducting Character. J. Electrochem. Soc., v. 125, No. 4, April 1978, pp. 678-679.

14. Heyes, G. W., and W. J. Trahar. The Natural Flotability of Chalcopyrite. Internat. J. Miner. Process., v. 4, 1977, pp. 317-344.

15. Lee, R. N. O on PbS: A New Surface Mechanism Affecting Semiconductor Electrical Properties. Japanese J. Appl. Phys., supp. 2, pt. 2, 1974, pp. 311-314.

16. Many, A., Y. Goldstein, and N. B. Grover. Semiconductor Surfaces. North-Holland Publishing Co., Amsterdam, 1965, ch. 3.

17. Maust, E. E., Jr., P. E. Richardson, and G. R. Hyde. A Conceptual Model for the Role of Oxygen in Xanthate Adsorption on Galena. BuMines RI 8143, 1976, 56 pp.

18. Myamlin, V. A., and Y. V. Pleskov. Electrochemistry of Semiconductors. Inst. Electrochem., Acad. Sci. USSR. Plenum Press, New York, 1967, pp. 68, 107, 163, 179.

19. Plaksin, I. N., and S. V. Bessonov. Role of Gases in Flotation Reactions. Proc. 2d Internat. Cong. on Surface Activity, Butterworths, London, v. 3, 1957, pp. 361-367.

20. Rand, D. A. J. Oxygen Reduction on Sulphide Minerals. Part III. Comparison of Activities of Various Copper, Iron, Lead, and Nickel Mineral Electrodes. J. Electroanal. Chem., v. 83, 1977, pp. 19-32.

21. Richardson, P. E., and E. E. Maust, Jr. Combined Electrochemical and Photovoltaic Studies of the Galena-Electrolyte Interface. Ch. in Trends in Electrochemistry (1977), ed. by J. O'M. Bockris, D. A. J. Rand, and B. J. Welch. Plenum Press, New York, pp. 317-322.

22. _____. Surface Stoichiometry of Galena in Aqueous Electrolytes and Its Effect on Xanthate Interactions. Ch. in Flotation, A. M. Gaudin Memorial Volume, v. 1, ed. by M. C. Fuerstenau. American Institute of Mining, Metallurgical, and Petroleum Engineers, Inc., New York, 1976, pp. 364-392.

23. Salamy, S. G., and J. C. Nixon. Application of Electrochemical Methods to Flotation Research. Recent Developments in Mineral Dressing. Inst. Min. and Met., London, 1953, p. 503.

24. Scanlon, W. W. Polar Semiconductors. Ch. in Solid State Physics. Academic Press, New York, 1959, pp. 83-137.

25. Schuldiner, S., T. B. Warner, and B. J. Piersma. Potentiostatic Current-Potential Measurements on a Platinum Electrode in a High-Purity Closed System. J. Electrochem. Soc., v. 114, No. 4, April 1967, pp. 343-349.

26. Thomas, D. G. The Chemistry of Some Compound Semiconductors. Ch. in Semiconductors, ed. by N. B. Hannay. Reinhold Pub. Corp., New York, 1959, pp. 269-312.

27. Woods, R. Electrochemistry of Sulfide Flotation. Ch. in Flotation, A. M. Gaudin Memorial Volume, v. 1, ed. by M. C. Fuerstenau. American Institute of Mining, Metallurgical, and Petroleum Engineers, Inc., New York, 1976, pp. 298-333.

28. Woods, R. The Oxidation of Ethyl Xanthate on Platinum, Gold, Copper, and Galena Electrodes. Relation to the Mechanism of Mineral Flotaion. J. Phys. Chem., v. 75, No. 3, 1971, pp. 354-362.

ACTIVATION AND DEACTIVATION IN THE FLOTATION OF SULFIDE MINERALS

by

Douglas W. Fuerstenau[1]

ABSTRACT

The principles of activation of sulfide minerals are reviewed. Particular attention is given to the activation of sphalerite with copper sulfate. Factors controlling the prevention or deactivation of sphalerite are also discussed.

INTRODUCTION

The classic example of a sulfide mineral that generally does not respond well to flotation with thiol collectors is that of sphalerite. For example, with short-chained xanthates, sphalerite does not float, and this phenomenon can be used to separate it from other sulfide minerals. However, by the addition of copper sulfate to the system, sphalerite then responds readily to flotation. Finkelstein and Allison (3) have recently published a thorough review of the activation of sphalerite.

This paper first discusses the flotation of minerals requiring activation and then presents some of the aspects of the chemistry of activation and deactivation.

THE FLOTATION OF SULFIDES WITHOUT ACTIVATION

Table 1, after Sutherland and Wark (15), shows the conditions under which various sulfide minerals respond to flotation at 1.56 x 10^{-4} M (equivalent to 25mg/l KEX).

---

[1] Department of Materials Science and Mineral Engineering, University of California, Berkeley, Calif.

TABLE 1. - Response of sulfide minerals[1] to sulfhydryl collectors [1.56 × 10^{-4}M]

Collector / Mineral	Methyl xanthate	Sodium aerofloat	Ethyl xanthate	Butyl xanthate	Amyl xanthate	Hexadecyl xanthate	Potassium di-amyl dithiocarbamate
Sphalerite	Response to collectors only in						
Pyrrhotite	the presence of activators						
Pyrite							
Galena							
Chalcopyrite			Response to collectors without activation				
Bornite							
Covellite							
Chalcocite							

[1] After Sutherland and Wark (15).

The solubility of sulfide minerals appears to play a role in their flotation with sulfhydryl collectors. There is considerable difference in various reported values of the solubility product of sulfides; values for this discussion, however, are listed in table 2. The most soluble sulfides, sphalerite and pyrrhotite, require activation under normal flotation conditions.

At higher concentrations of longer chained xanthates, sphalerite responds quite readily to flotation (fig. 1). In a detailed study of the flotation of sphalerite and marmatite without activation, M. C. Fuerstenau and coworkers demonstrated relationships between the solubility of zinc xanthates and flotation response (6). Figure 2, which presents the flotation response of sphalerite to xanthates of various alkyl chain lengths, shows the regular relation between the number of carbon atoms in the chain and flotation. The solubility products of the various zinc xanthates are given in table 3. The relationship between the carbon number, flotation response, and solubility product are illustrated graphically in figure 3. Infrared spectra with sphalerite and hexylxanthate indicate that the species at the interface is zinc hexylxanthate (fig. 4). As with other sulfides, pH has a marked effect on the flotation response of sphalerite. Figure 5 illustrates the regularity between collector concentration and pH in depressing sphalerite. M. C. Fuerstenau and coworkers (6) interpreted this phenomenon in terms of the competition between the formation of $Zn(AX)_2$ and $Zn(OH)_2$ at the surface:

$$\mathrm{Zn(AX)_2(s) = Zn^{+2} + 2AX^-;\ K = 1.55 \times 10^{-12}}$$

$$\mathrm{Zn(OH)_2(s) = Zn^{+2} + 2OH^-;\ K = 4.5 \times 10^{-17}}$$

$$\mathrm{Zn(AX)_2(s) + 2OH^- = Zn(OH)_2(s) + 2AX^-;\ K = 3.4 \times 10^{4}} \qquad (1)$$

They demonstrated that measured pH's for flotation depression agreed with those predicted by these relations.

THE ACTIVATION OF SPHALERITE

The general consensus has been that the process of activation of sphalerite with copper sulfate is controlled by the reaction:

$$\mathrm{ZnS(s) + Cu^{+2}(aq) = CuS(s) + Zn^{+2}(aq)} \qquad (2)$$

In a long-term (50 days), high-temperature (100° C) study of the activation of sphalerite with copper chloride, Cooke (2) observed a stoichiometric 1:1 Cu/Zn exchange, with the sphalerite surface becoming covered with covellite.

By contact angle and flotation experiments, Sutherland and Wark (15) have tested the activation behavior of sphalerite with various metal salts. Their results, summarized in table 4, indicate that successful activators are salts of metals that respond, or whose sulfides respond, readily to flotation with thiol collectors. In table 4, only those cations that proved to be activators are listed; all other metal cations did not function as activators for sphalerite. Detailed investigations of activation phenomena have been carried out with $\mathrm{Cu^{+2}}$, $\mathrm{Pb^{+2}}$ and $\mathrm{Ag^{+}}$, and some of these results are summarized in the following paragraphs.

After activation, flotation behavior is similar to that of the activator metal sulfide mineral. Since flotation response appears to be related to the solubility of metal xanthates, table 5 summarizes the solubility products of some metal xanthates (3).

Activation With Copper

Mao (7) conducted a detailed study of the uptake of $\mathrm{Cu^{+2}}$ by sphalerite, using $\mathrm{Cu^{64}}$ as a radioactive tracer. Mao's results showed that copper uptake follows the chemical exchange reaction:

$$\mathrm{ZnS(s) + Cu^{+2}(aq) = CuS(s) + Zn^{+2}(aq)} \qquad (3)$$

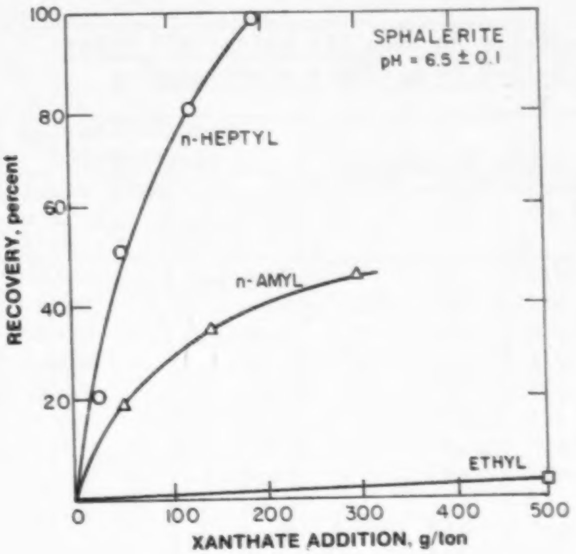

FIGURE 1. - Influence of selected xanthates on recovery of zinc blende (15). (Courtesy, *Australasian Institute of Mining and Metallurgy*.)

TABLE 2. - Solubility products of some metal sulfides (16)

Metal sulfide	Solubility product
FeS...........	2.5×10^{-19}
ZnS...........	2.6×10^{-26}
PbS...........	3.4×10^{-28}
CuS...........	4×10^{-36}
Ag_2S..........	6.3×10^{-52}
Cu_2S..........	8×10^{-49}

TABLE 3. - Solubility products of zinc alkyl xanthates (6)

Zinc xanthate	Solubility product
Ethyl..........	4.90×10^{-9}
Propyl.........	3.39×10^{-10}
Butyl..........	3.72×10^{-11}
Amyl...........	1.55×10^{-12}
Hexyl..........	1.26×10^{-13}

TABLE 4. - Activation of sphalerite by metallic salts; all other metal salts failed to activate sphalerite[1]

Metal	Salt used	Angle of contact			Direct flotation test method	
		Method I	Method II	Method III	Neutral solution	Acid solution, pH value, 4 to 5
Arsenic....	Trioxide............	Nil	Nil	60°	None....	Good.
Antimony...	Trichloride..........	Nil	[2]Nil	61°	None....	Good.
Nickel.....	Sulfate.............	Nil	Nil	Nil	None....	None.
Cobalt.....	Sulfate.............	Nil	Nil	61°	None....	Weak.
Thallium...	Nitrate.............	(3)	60°		Fair....	Fair.
Cerium.....	Sulfate.............	Nil	60°		Good....	
Lead.......	Nitrate.............	61°	62°		Good....	
Cadmium....	Sulfate.............	61°	59°		Good....	
Cupric.....	Sulfate.............	61°	60°		Good....	
Silver.....	Nitrate.............	62°	61°		Good....	
Mercuric...	Chloride............	63°	60°		Good....	
Mercurous..	Sulfate.............	[4]61°			Good....	
Bismuth....	Nitrate.............		[1]62°		Good....	
Gold.......	Acid chloride........		61°		Good....	
Platinum...	Chloroplatinic acid..		(3)	58°	Fair....	Good.

[1] After Sutherland and Wark (15).

[2] Less than 1 g/l because of hydrolysis.

[3] Irregular.

[4] Saturated solution.

TABLE 5. - Logarithm of the solubility products of some thiol collectors and hydroxides[1]

Ligand	Zinc (11)	Lead (11)	Copper (1)
Ethyl xanthate..........	- 8.31	-16.77	-19.28
Butyl xanthate..........	-10.43	(2)	-20.33
Hexyl xanthate..........	-12.90	(2)	(2)
Octyl xanthate..........	-15.82	(2)	-23.06
Ethyl dithiophosphate...	- 1.82	-11.12	-15.85
Hydroxide..............	-16.79	-16.09	-14.7

[1] After Finkelstein and Allison (3).

[2] Not determined.

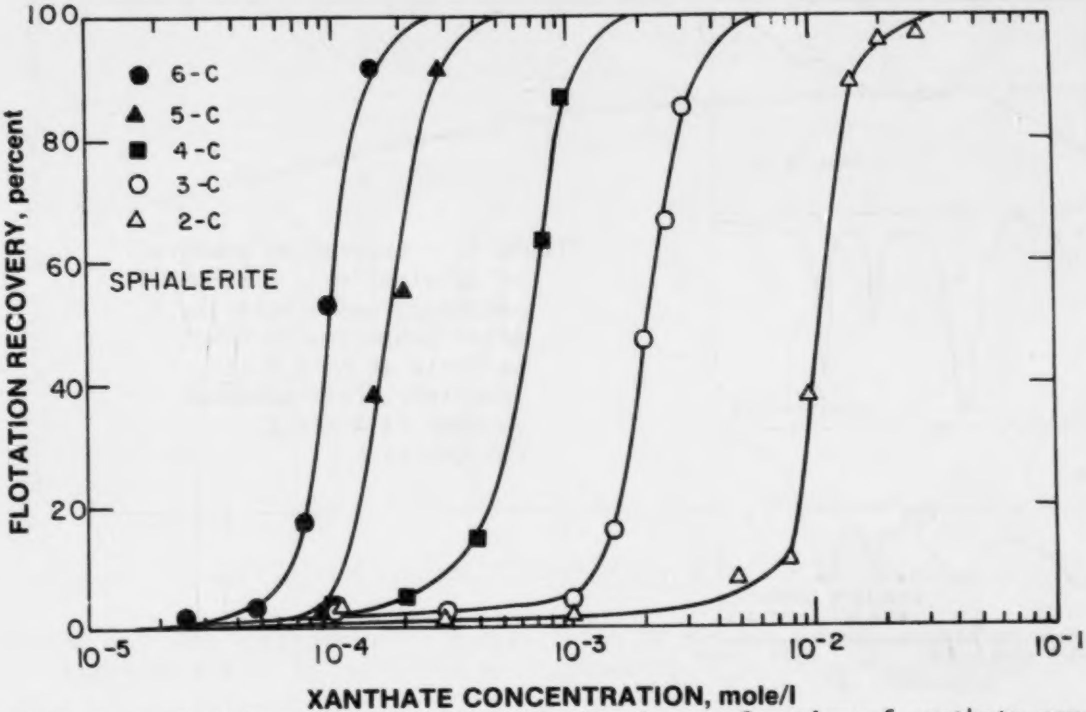

FIGURE 2. - Flotation recovery of sphalerite 1 as a function of xanthate concentration and hydrocarbaron chain length at pH 3.5 (6). (Courtesy, *International Journal of Mineral Processing.*)

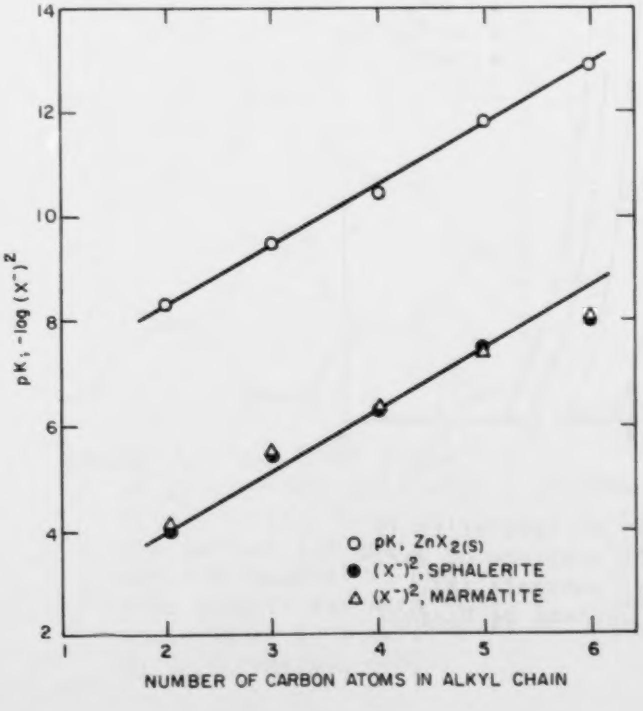

FIGURE 3. - Relationship between solubility products of various zinc xanthates and of the square of the concentration of xanthate necessary for 50-percent recovery of sphalerite 1 and marmatite at pH 3.5 and the number of carbon atoms in the alkyl chain (6). (Courtesy, *International Journal of Mineral Processing.*)

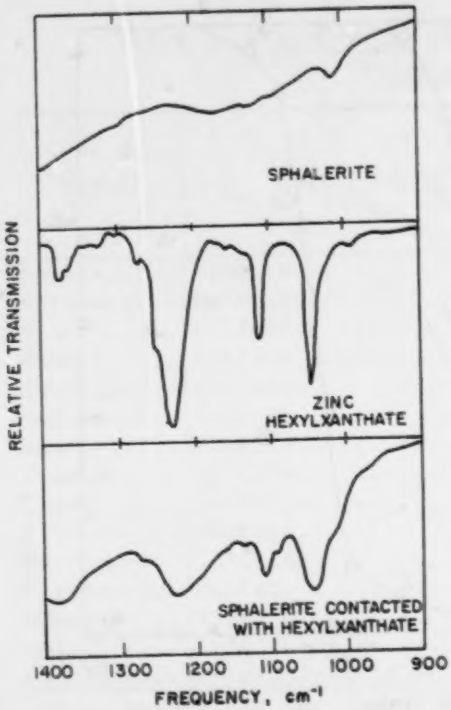

FIGURE 4. - Absorption spectra of sphalerite 1, zinc hexyl xanthate, and sphalerite 1 after contact with hexyl xanthate at pH 5.5 (6). (Courtesy, *International Journal of Mineral Processing*.)

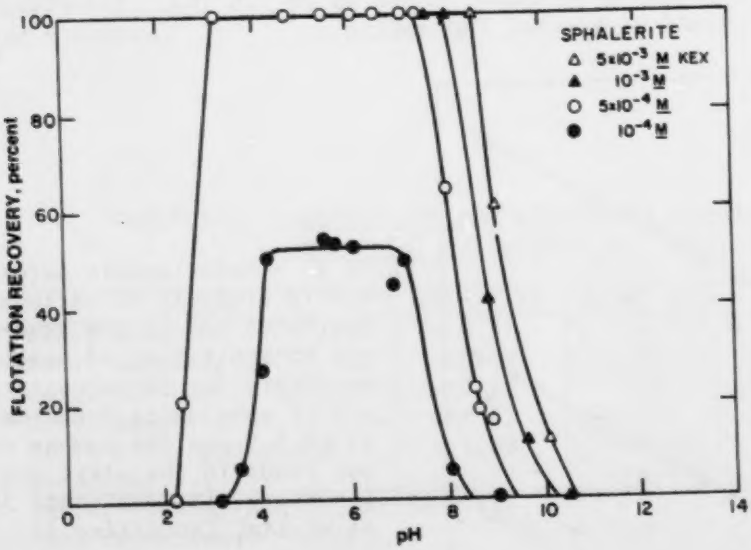

FIGURE 5. - Flotation recovery of sphalerite 11 as a function of pH in the presence of various concentrations of amyl xanthate (6). (Courtesy, *International Journal of Mineral Processing*.)

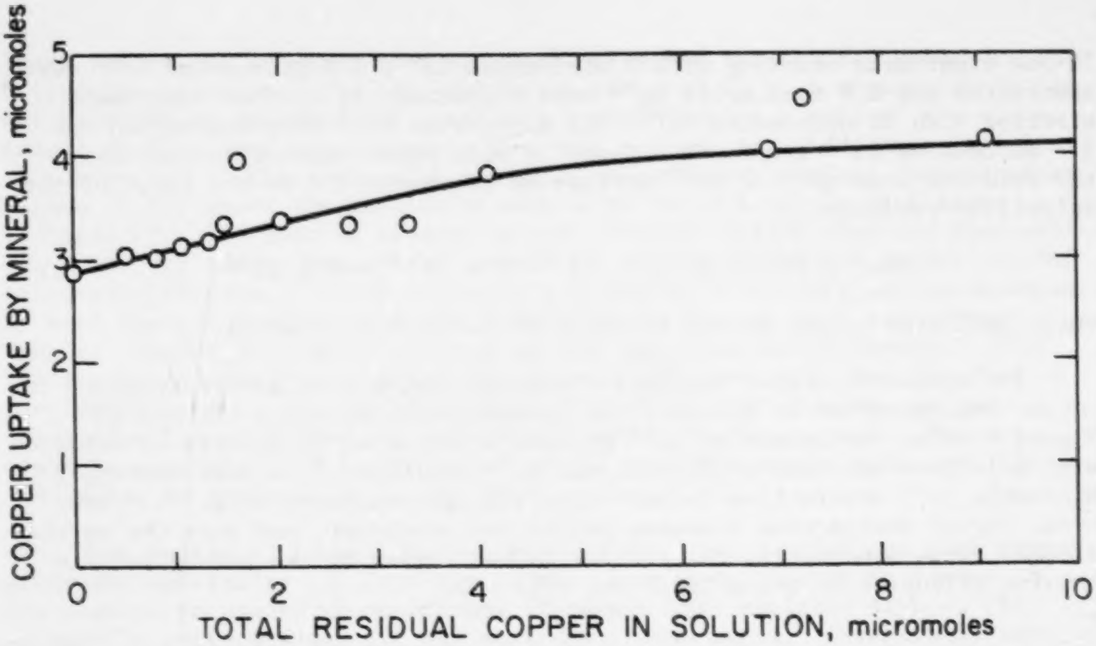

FIGURE 6. - The abstraction of copper (with 30 minutes agitation, 74 ml solution) by 5 g of 65 minus 100 mesh sphalerite (7). (Courtesy, AIME.)

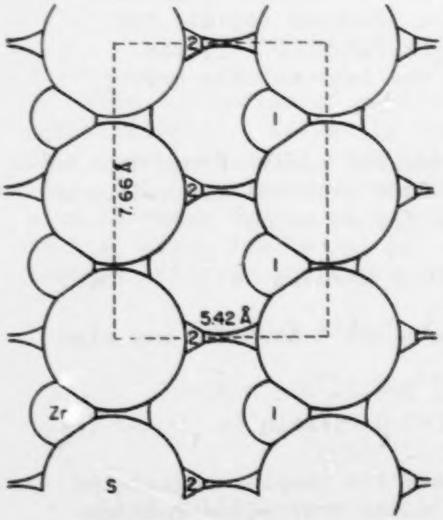

FIGURE 7. - The (110) plane of sphalerite. Unit area, 41.6 A^2. Zinc ions in the surface are designated by numeral 1, and zinc ions in the next lower layer by numeral 2 (7). (*Courtesy*, AIME.)

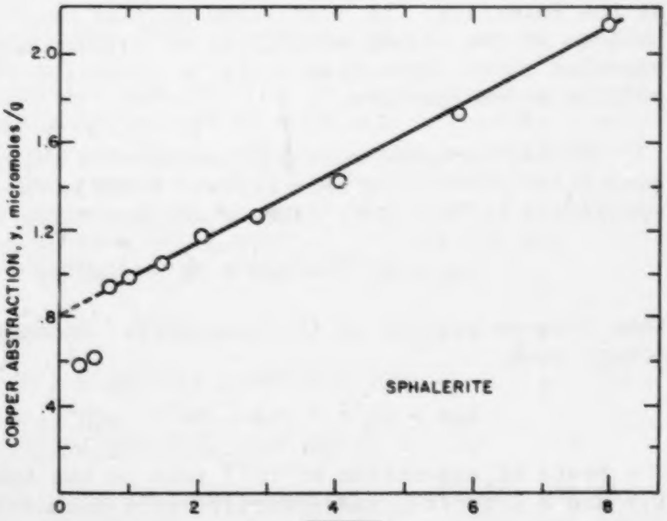

FIGURE 8. - The copper abstraction by sphalerite as a function of the square root of the contact time (5 g sphalerite 4.7×10^{-3} moles Cu^{+2}, and 74 ml water) (7). (*Courtesy*, AIME.)

In one experiment starting with 3 micromoles Cu^{+2}, 2.8 micromoles Cu^{+2} were abstracted and 2.9 micromoles Zn^{+2} were displaced; in another experiment starting with 10 micromoles Cu^{+2}, 4.5 micromoles Cu^{+2} were abstracted and 3.7 micromoles Zn^{+2} displaced. Thus, if bulk phase thermodynamics apply, the reaction constant for Cu^{+2} activation of sphalerite is the ratio of the solubility products:

$$[Zn^{+2}]/[Cu^{+2}] = 2.6 \times 10^{-26}/4 \times 10^{-36} = 6 \times 10^{10} \qquad (4)$$

which indicates a very strong affinity of Cu^{+2} for sphalerite.

The uptake of copper initially is rapid, being a slight function of the copper concentration in solution and controlled by solution diffusion. Figure 6 shows the uptake of Cu^{+2} by sphalerite after 30 minutes of reaction with solutions containing 14 different Cu^{+2} additions. In this system, 3 micromole Cu^{+2} abstraction is approximately one monolayer (fig. 7). However, copper abstraction proceeds beyond the monolayer, and once the uptake exceeds three monolayers, the process is controlled by the parabolic rate law for diffusion in the solid state (fig. 8).

$$\Gamma^2 = kt + b \qquad (5)$$

If copper salts are added in neutral or slightly alkaline conditions, copper hydrolysis products form, but these, too, can activate the system. Figure 9 presents some electrophoretic mobility results of Hukki and coworkers (11), which are typical for hydrolyzing metal systems (fig. 10). At the interface, the hydrolized species would be adsorbed rapidly but because of the higher solubility of $Cu(OH)_2$ [$K_{sp} = 1.6 \times 10^{-19}$], the adsorbed cupric hydroxide would be converted to the less-soluble copper sulfide at the surface.

Gochin and coworkers (13) conducted a calorimetric study of the heat of adsorption of Cu^{+2} on sphalerite. Their work showed that the activation of sphalerite by Cu^{+2} ions takes place according to the equation

$$ZnS + Cu^{+2} \rightarrow CuS + Zn^{+2} \quad :\Delta H^\circ_{25} = 62.8 \text{ kj/mole Cu} \qquad (6)$$

When iron is present in the sphalerite, exchange of Cu^{+2} for Fe^{+2} may also occur; thus,

$$FeS + Cu^{+2} \rightarrow CuS + Fe^{+2} \quad :\Delta H^\circ_{25} = 100.0 \text{ kj/mole Cu} \qquad (7)$$

The heats of adsorption of Cu^{+2} ions on two sphalerite samples containing 0.7 and 8.1 pct Fe, respectively, were measured under controlled deoxygenated conditions. Figure 11(a) shows the results obtained for the low-iron sample; the enthalpy change is presented as a function of adsorbed copper. The zinc and sulfate ion concentrations in solution after the reaction are also shown. These ions in solution were found to be proportional to the adsorbed copper, as expected. The heats of adsorption of Cu^{+2} increased from about 60.0 to 64.5 kj/mole Cu when the adsorbed copper increased from 0.10 to 0.24 millimole. Further increase in the adsorbed copper to 0.8 millimole led to a decrease in the heat of adsorption to 61.6 kj/mole Cu.

These values are in quite good agreement with the theoretical value for the activation reaction. The low heat value observed at high copper adsorption was ascribed to adsorbed but unreacted copper forming a part of the electrical double layer, a phenomenon that may account for differences in the stoichiometry of the activation reaction, observed by various investigators. Figure 11 (b) shows the results obtainted on the 8.1 pct Fe sphalerite (marmatite). The heat of adsorption was slightly larger than the theoretical value for copper adsorption quantities forming up to 1.8 layers on the sphalerite surface. Copper adsorption exceeding 1.8 layers was accompanied by heat changes smaller than the theoretical value, as with the former sample. Copper ions in solution after the reaction were detectable after two layers of copper were adsorbed, whereas all the copper was adsorbed on the low-Fe sample. It therefore appears that the iron present in the sphalerite has an inhibiting effect on the activation process. No iron could be detected in solution after any of the experiments with marmatite, indicating no exchange of Cu for Fe.

Some Hallimond tube flotation experiments were carried out with copper-activated sphalerite (5), and the results have been plotted in figure 12. The conditions where two monolayers of copper have replaced zinc at the sphalerite surface (fig. 12) are marked with the arrow. Essentially complete flotation is attained only with this extent of zinc replacement by the activating copper. However, it should be recalled that Hallimond tube flotation measures relative flotation kinetics. Note that an aeration rate of 1.0 cm^3/sec requires only about half the copper activation for 50 pct recovery as is required at an aeration rate of 0.5 cm^3/sec.

Sphalerite Activation With Silver Salts

The activation of sphalerite has been studied in detail using Ag^{110} as a tracer (8-9). Silver is rapidly abstracted by sphalerite, turning black in a short period of time (8). The uptake of silver continues indefinitely (fig. 13), following a logarithmic rate. After 2 months of reaction, a plus 325-mesh sample of sphalerite was found to assay 18 percent Ag (8), with an exact 2 moles of Ag^+ exchanging for 1 mole of Zn^{+2} during the process. Silver activation of sphalerite is controlled by

$$ZnS(s) + 2Ag^+ = Ag_2S(s) + Zn^{+2}$$

$$K = [Zn^{+2}]/[Ag^+]^2 = 3 \times 10^{-26}/6 \times 10^{-56} \approx 10^{26} \quad (8)$$

Sphalerite Activation With Lead Salts

Lead sulfide is only slightly less soluble than zinc sulfide. In this case, the reaction for activation would be

$$ZnS(s) + Pb^{+2} = PbS + Zn^{+2}$$

$$K = [Zn^{+2}]/[Pb^{+2}] = 3 \times 10^{-26}/3 \times 10^{-28} = 100 \quad (9)$$

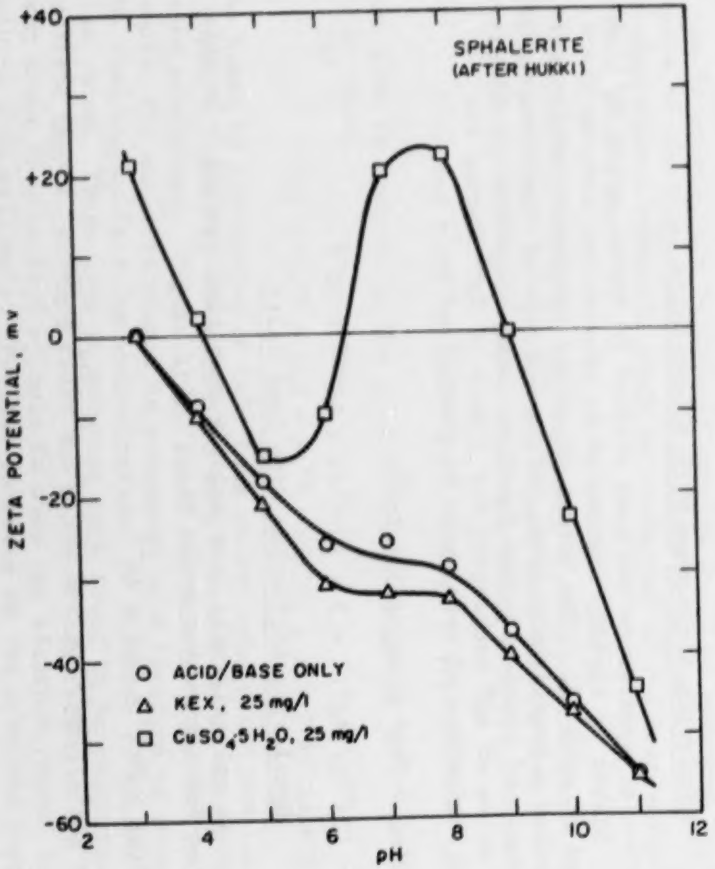

FIGURE 9. - Zeta potential of sphalerite versus pH with and without potassium ethyl xanthate (KEX) and copper sulfate.

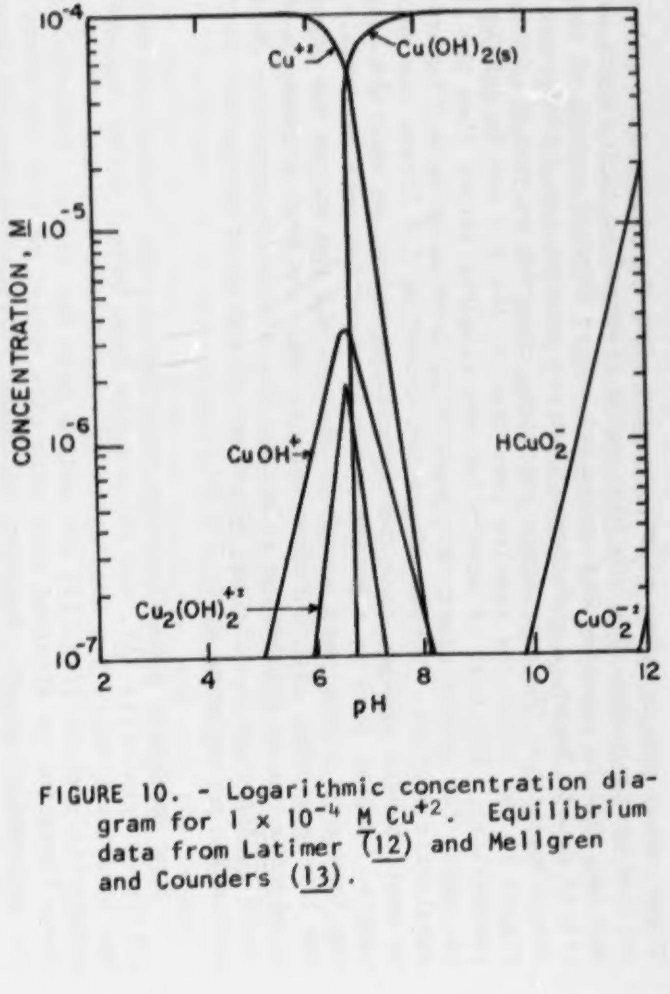

FIGURE 10. - Logarithmic concentration diagram for 1×10^{-4} M Cu^{+2}. Equilibrium data from Latimer (12) and Mellgren and Counders (13).

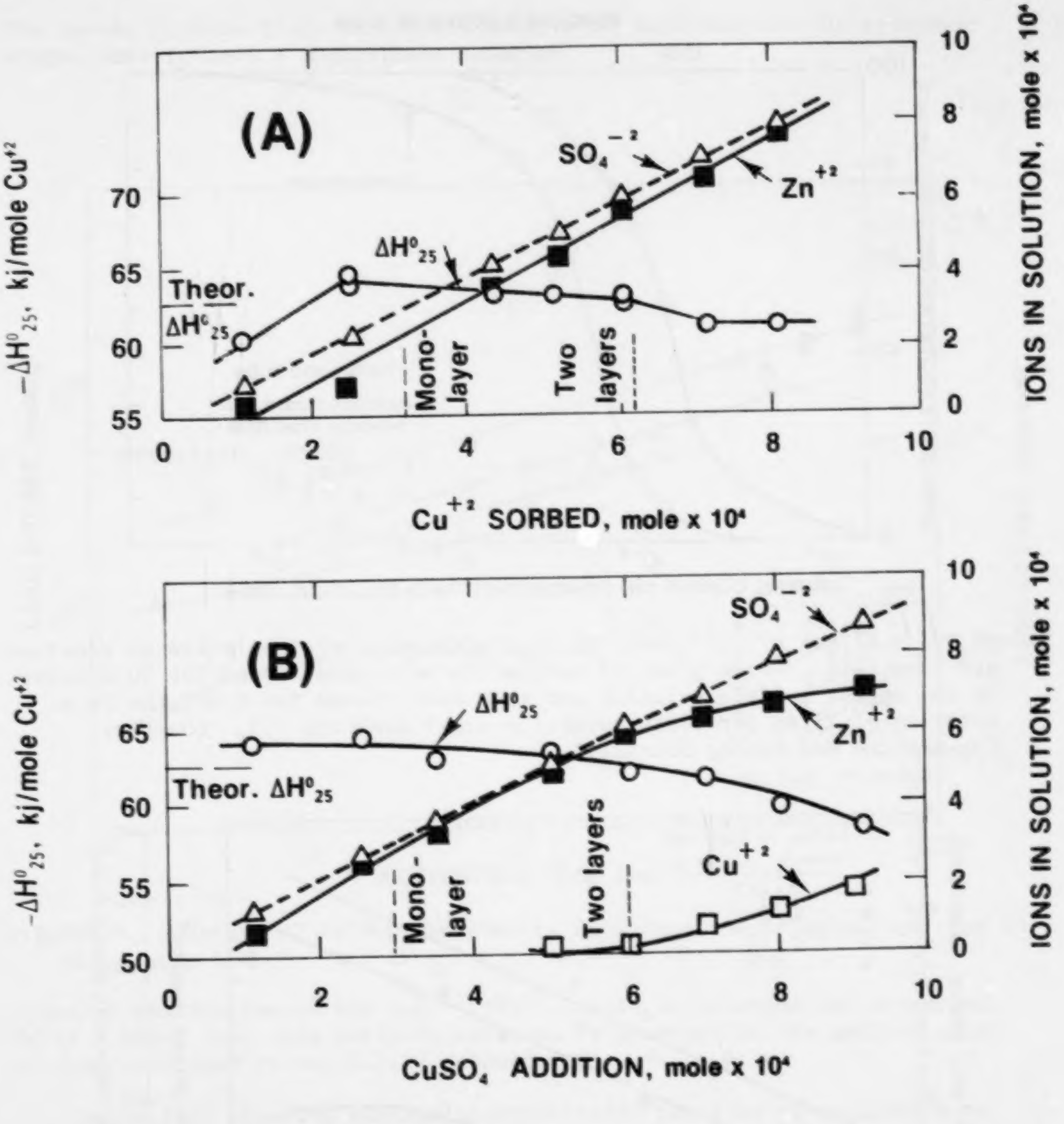

FIGURE 11. - Activation of two samples of sphalerite by Cu^{+2}. ΔH°, 25 heat of reaction; other lines show concentration of various ions left in solution: (a) sphalerite with 0.7 pct Fe; (b) sphalerite with 8.1 pct Fe (13). (Courtesy, *Institute of Mining and Metallurgy*.)

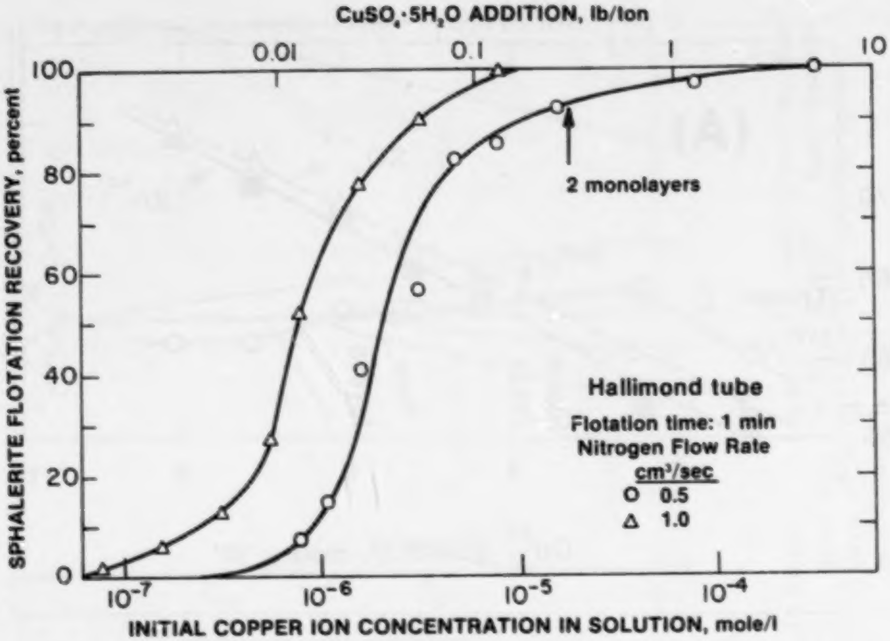

FIGURE 12. - Effect of Cu^{+2} addition on the recovery of sphalerite at constant gas flow rate. Three grams of sphalerite were conditioned for 30 minutes in the copper sulfate solution and then conditioned for 5 minutes in a solution of 25 mg per liter potassium ethyl xanthate (5). Courtesy, *Engineering and Mining Journal*.)

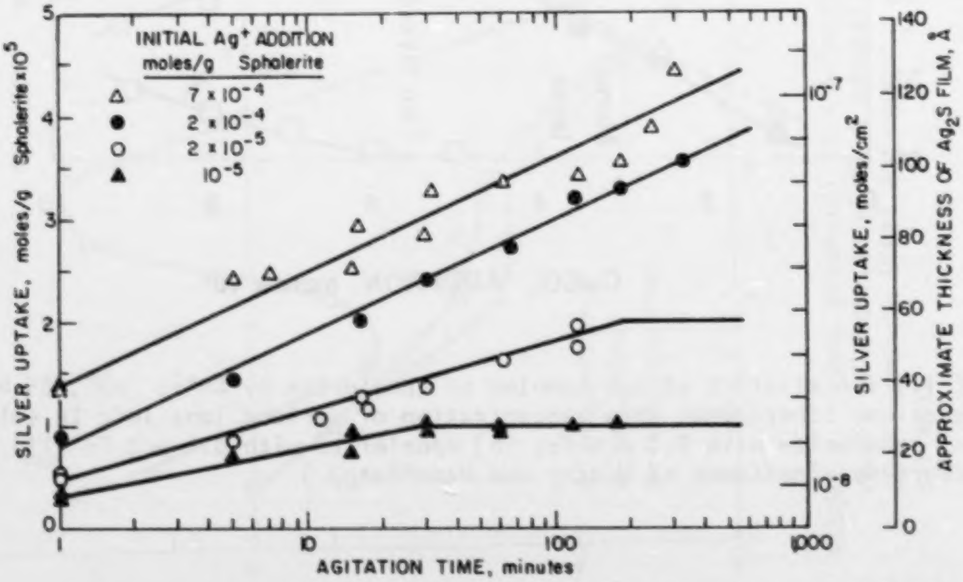

FIGURE 13. - Uptake of silver from solution by sphalerite as a function of time (8). (Courtesy, AIME.)

The uptake of lead (fig. 14), which is low and generally in the monolayer range, also follows a logarithmic relation

$$\Gamma = \frac{t^n}{k} \qquad (10)$$

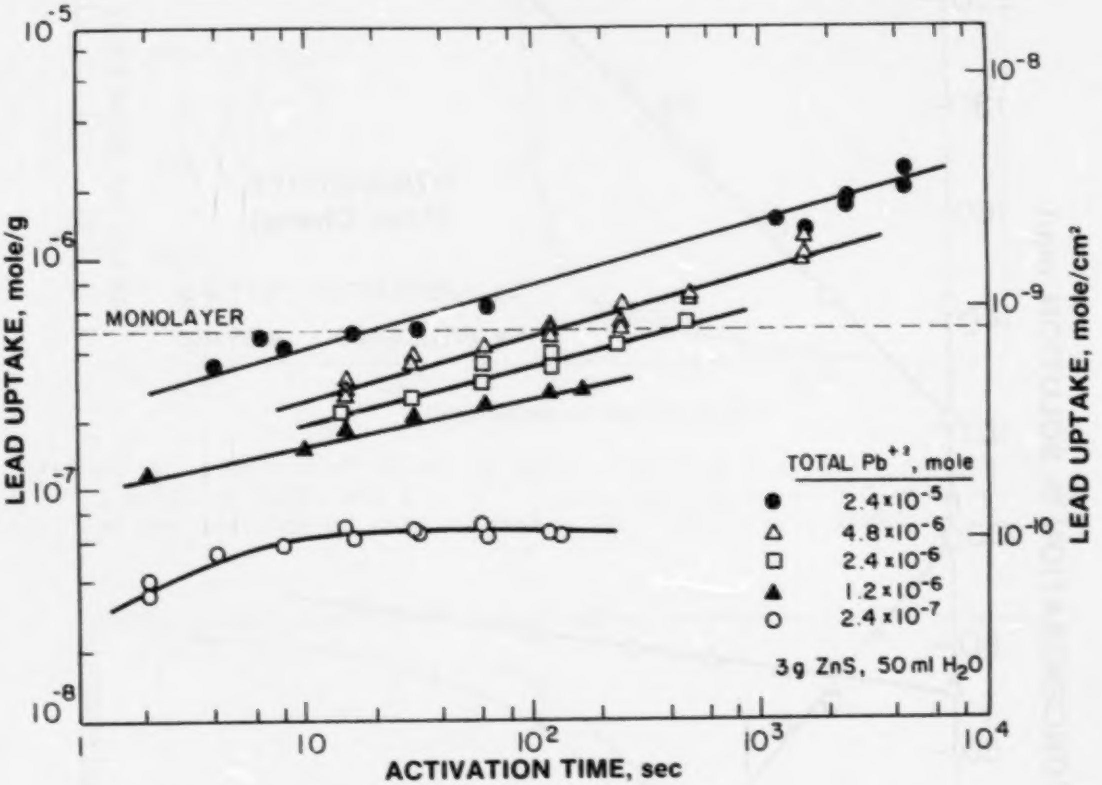

FIGURE 14. - Uptake of Pb^{+2} by sphalerite as a function of agitation time (4). (Courtesy, *AIME*.)

Detailed examination of the $(Zn^{+2})/(Pb^{+2})$ ratio in solution was conducted. Table 6 shows that this ratio in solution is somewhat in the general range of that predicted by solubility products.

Healy (10) observed similar electrokinetic behavior of sphalerite in the presence of lead nitrate as shown for copper in figure 9.

Natural Flotation of Activated Sphalerite

Finkelstein and coworkers (3) have reported that sphalerite samples from a number of different locations exhibit pronounced natural floatability after activation. The reasons for this are unclear, and further research in this area is required.

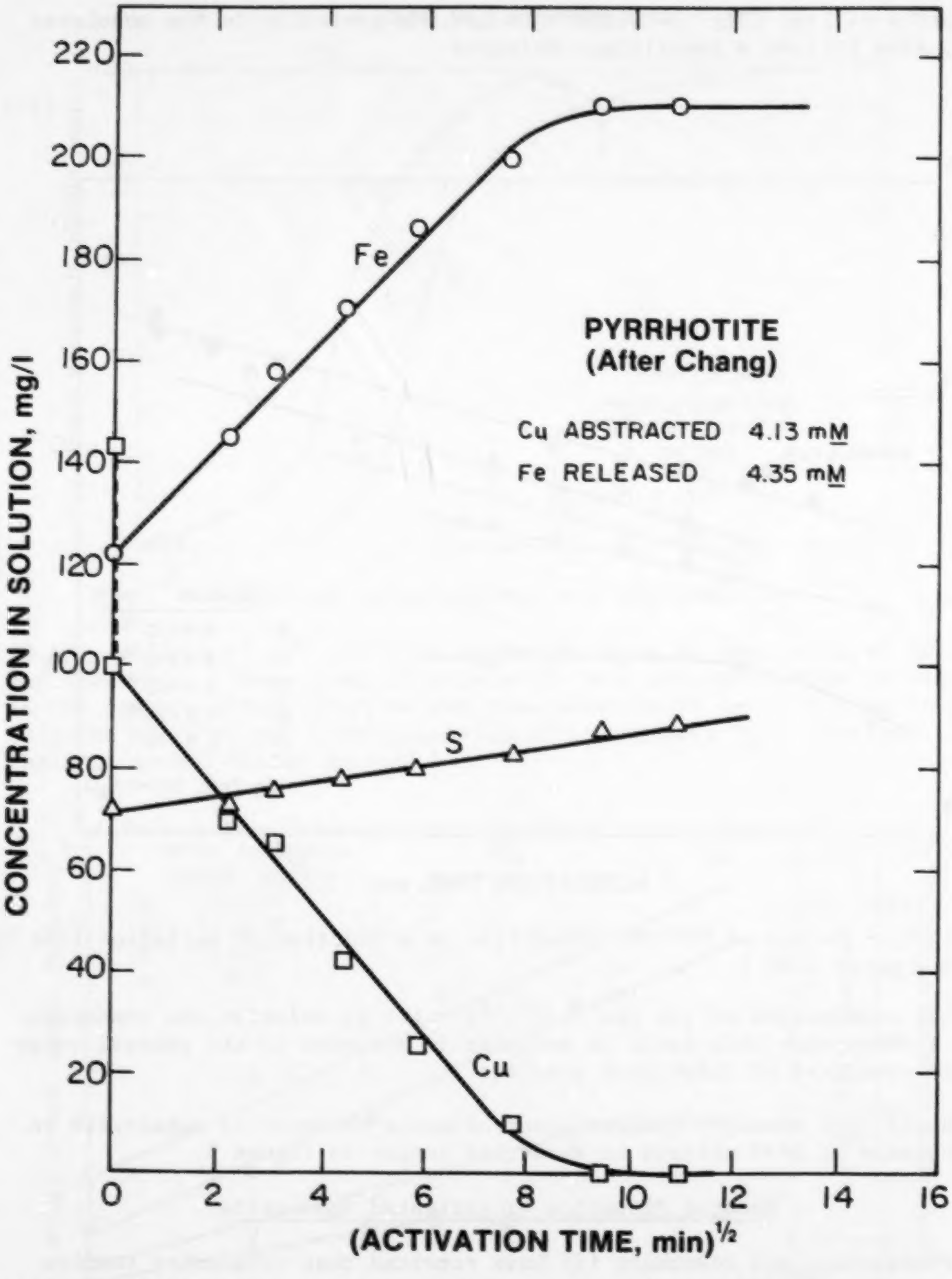

FIGURE 15. - Concentration of Fe, Cu, and S in the solution after the activation of pyrrhotite with copper sulfate (1). (Courtesy, AIME.)

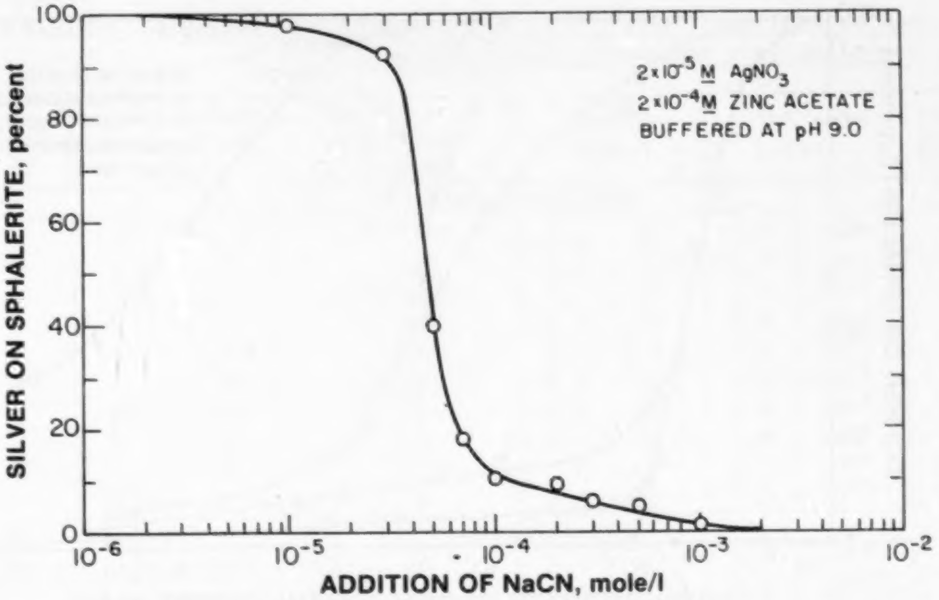

FIGURE 16. - Uptake of silver by sphalerite from a solution containing 2×10^{-5} M $AgNO_3$ and 2×10^{-4} M zinc acetate at pH 9.0 as a function of the addition of sodium cyanide (8). (Courtesy, *AIME*.)

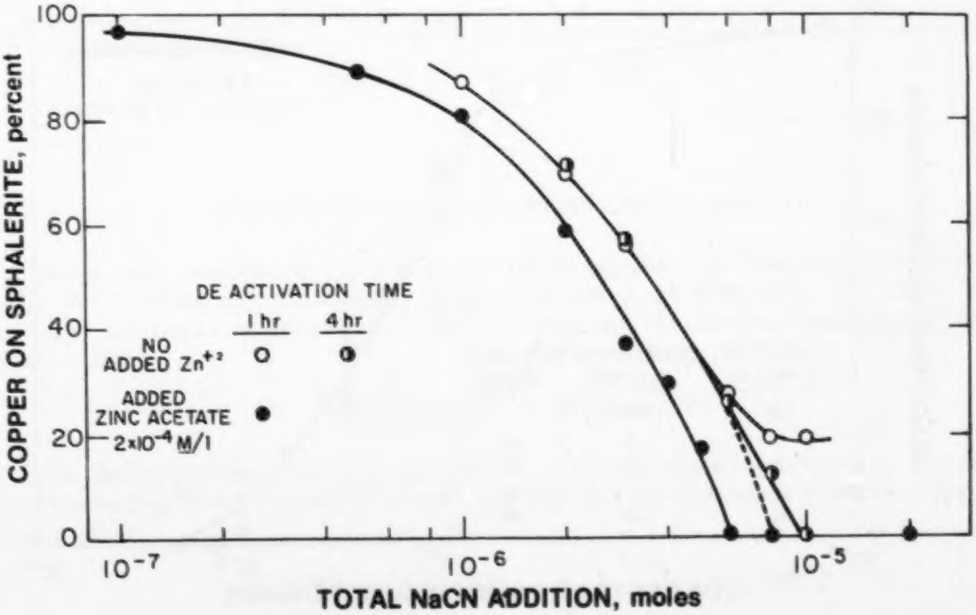

FIGURE 17. - Deactivation of Cu^{+2} -activated sphalerite with sodium cyanide at pH 9.0 (5 g ZnS, 2μmoles Cu^{+2}, 74 ml solution, preceded by 30 minutes activation. The dotted line represents the data for simultaneous agitation with $CuSO_4$ and NaCN for 1 hour and 4 hours (7). (Courtesy, *AIME*.)

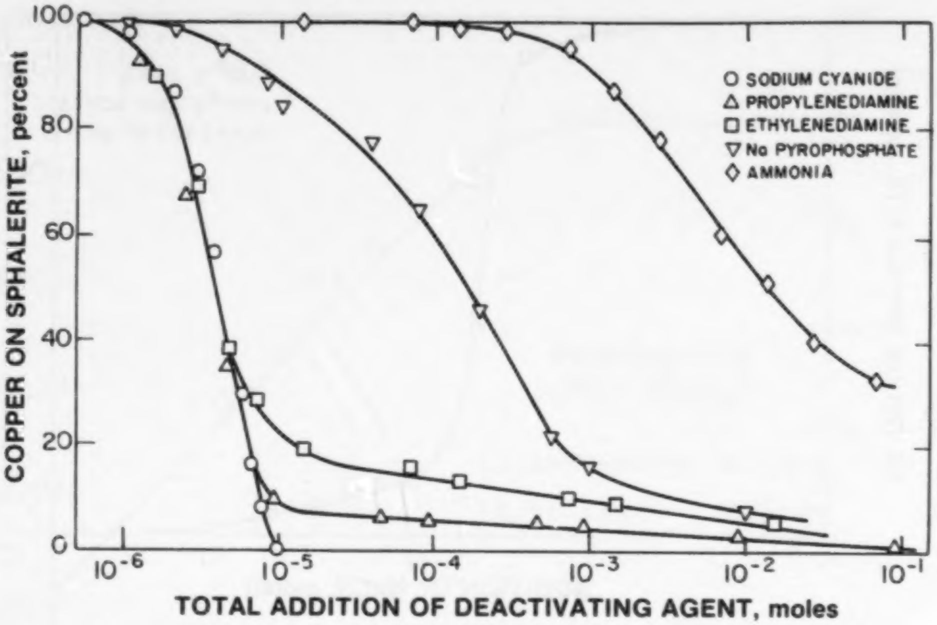

FIGURE 18. - Partition of copper between solution and sphalerite as a function of the addition of deactivating agent (7). (Courtesy, *AIME*.)

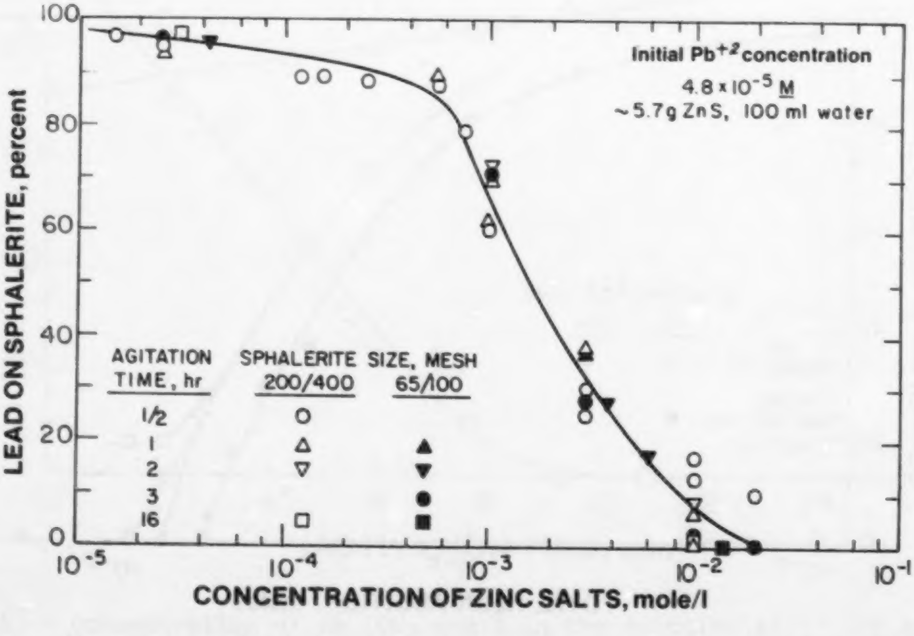

FIGURE 19. - The effect of Zn^{+2} on the distribution of Pb^{+2} between sphalerite and the aqueous phase (4). (Courtesy, *AIME*.)

TABLE 6. - Evaluation of the ratio $[Zn^{+2}]/[Pb^{+2}]$ for the uptake of Pb^{+2} from solutions containing zinc salts[1]

Agitation time, hr	Total zinc in solution, mole/1	Fraction of added lead on mineral, %	$[Zn^{+2}]$, mole/1	$[Pb^{+2}]$, mole/1	$\frac{[Zn^{+2}]}{[Pb^{+2}]}$
65 × 100-mesh sphalerite					
1	3×10^{-3}	37	2.5×10^{-3}	1.2×10^{-5}	210
2	4.2×10^{-5}	96	4.2×10^{-5}	1.9×10^{-6}	20
2	3.7×10^{-3}	28	3.0×10^{-3}	1.2×10^{-5}	250
2	6×10^{-3}	18	4.5×10^{-3}	1.0×10^{-5}	450
3	2.5×10^{-5}	97	2.5×10^{-5}	1.4×10^{-6}	20
3	1×10^{-3}	71	9.4×10^{-4}	9.1×10^{-6}	100
3	3×10^{-3}	28	2.5×10^{-3}	1.4×10^{-5}	180
3	1×10^{-2}	3	6.5×10^{-3}	8.8×10^{-6}	740
3	2×10^{-2}	0	1.0×10^{-2}	5.3×10^{-6}	1900
16	1.4×10^{-2}	0	8.2×10^{-3}	7.5×10^{-6}	1100
200 × 400-mesh sphalerite					
1	5.5×10^{-4}	90	5.5×10^{-4}	3.7×10^{-6}	150
1	1×10^{-3}	70	9.4×10^{-4}	9.3×10^{-6}	100
1	3×10^{-3}	38	2.5×10^{-3}	1.3×10^{-5}	190
1	1×10^{-2}	6	6.5×10^{-3}	8.4×10^{-6}	770
1	1×10^{-2}	0	6.5×10^{-3}	9.0×10^{-6}	720
2	1×10^{-3}	73	9.4×10^{-4}	8.5×10^{-6}	110
2	1×10^{-2}	9	6.5×10^{-3}	8.3×10^{-6}	790
16	3×10^{-5}	97.5	3.0×10^{-5}	1.2×10^{-6}	30
16	1×10^{-2}	1	6.5×10^{-3}	9.0×10^{-6}	720

ACTIVATION OF PYRRHOTITE BY COPPER SULFATE

Chang and coworkers (1) conducted a detailed experimental investigation of the activities and flotation characteristics of pyrrhotite. Their results (fig. 15) indicate a direct Zn^{+2}/Fe^{+2} exchange, following the parabolic kinetic law.

DEACTIVATION OF SPHALERITE

The deactivation, or prevention of activation, of sphalerite depends upon reversing the activation reaction involving a divalent activating cation, M^{+2}:

$$Zns + M^{+2} = MS + Zn^{+2}; \quad K_{act} = [Zn^{+2}]/[M^{+2}] \tag{11}$$

by making the ratio $(Zn^{+2})/(M^{+2}) > K_{act}$.

Because the solubility product of ZnS is generally so much larger than that of MS, the only way to control the $(Zn^{+2})/M^{+2})$ ratio is through complexing agents. For this, the M^{+2} complex must be more stable than the Zn^{+2} complex.

In the case of silver activation, the controlling reactions are

$$\begin{aligned} Ag(CN)_2^{-2} &= Ag^+ + 2CN^-; \quad K = 1.8 \times 10^{-19} \\ Zn(CN)_4^{-2} &= Zn^{+2} + 4CN^-; \quad K = 1.3 \times 10^{-17} \\ HCN(aq) &= H^+ + CN^-; \quad K = 4 \times 10^{-10} \end{aligned} \tag{12}$$

Figure 16 shows the uptake of Ag^+ by sphalerite in the presence of sodium cyanide. Calculation of the $(Zn^{+2})/(Ag^+)^2$ ration for all the data points showed the value to be about 10^{26}, as predicted by bulk thermodynamics (8).

Figure 17 presents similar data for the deactivaiton of Cu^{+2} -activated sphalerite. In this case, the situation is more complicated because cyanide reduced cupric to cuprous. The calculated ratios of $(Zn^{+2})/(Cu^{+2})$ and $(Zn^{+2})/(Cu^+)^2$ were 10^9 and 10^{22}, in approximate agreement with the expected values of 10^{11} and 10^{23}. Mao (7) also studied the deactivation of sphalerite with other complexing agents, and those results are presented in figure 18. Such chelating agents as ethylenediamine inhibit activation of sphalerite with copper, but only cyanide totally prevents the reaction from occurring (7).

In the case of lead activation, the addition of $ZnSO_4$ can indeed reverse the uptake of Pb^{+2} (fig. 19). In this case, the starting Pb^{+2} concentration was 5×10^{-5} M, and 10^{-2} M Zn acetate completely inhibits the uptake (7).

ACKNOWLEDGMENTS

The support of the National Science Foundation during the course of preparing this manuscript is gratefully acknowledged.

REFERENCES

1. Chang, C. S., S. R. B. Cooke, and I. Iwaski. Flotation Characteristics of Pyrrhotite with Xanthates. Trans. AIME, v. 199, 1954, p. 209.

2. Cooke, S. R. B. Flotation. Advances in Colloid Sci., v. 3, 1950, p. 357.

3. Finkelstein, N. P., and S. A. Allison. The Chemistry of Activation, Deactivation and Depression in the Flotation of Zinc Sulfide. Ch. 14 in Flotation, A. M. Gaudin Memorial Volume, ed. by M. C. Fuerstenau. AIME, New York, 1976.

4. Fuerstenau, D. W., and P. H. Metzger. Activation of Sphalerite with Lead Ions in the Presence of Zinc Salts. Trans. AIME, v. 217, 1960, p. 119.

5. Fuerstenau, D. W., P. H. Metzger, and G. D. Steele. How to Use This Modified Hallimond Tube...For Better Flotation Testing. Eng. and Min. J., v. 158, 1957, p. 93.

6. Fuerstenau, M. C., K. L. Clifford, and M. C. Kuhn. The Role of Zinc-Xanthate Precipitation in Sphalerite Flotation. Internat. J. Miner. Proc., v. 1, 1974, p. 307.

7. Gaudin, A. M., D. W. Fuerstenau, and G. W. Mao. Activation and Deactivation Studies with Copper and Sphalerite. Trans. AIME, v. 214, 1959, p. 430.

8. Gaudin, A. M., D. W. Fuerstenau, and M. M. Turkanis. Activation and Depression of Sphalerite with Silver and Zinc Ions. Mining Eng., v. 9, No. 1, 1957, pp. 65-69.

9. Gaudin, A. M., H. R. Spedden, and M. P. Corriveau. Adsorption of Silver Ion by Sphalerite. Trans. AIME, v. 190, 1951, p. 780.

10. Healy, T. W. Colloidal Precipitation as Activators and Depressants in Flotation. West Aust. Conf. Pap., Parkville, Victoria, May 1973, Parkville, Victoria, Aust. The Australasian I. M. M. Conf., Western Australia, 1973, (Conf. Ser. No. 2), 1973.

11. Hukki, R. T., and A. Palomaki, and E. Orivouri. Electrophoretic Investigation of the Activation of Sphalerite by Copper Sulfate in Flotation. Suomen Kemistilehti, v. B25, 1952, p. 42.

12. Latimer, W. M. Oxidation Potentials. Prentice-Hall, Englewood Cliffs, N. J., 1952, p. 187

13. Mellgren, O., R. J. Gochin, H. L. Shergold, and J. A. Kitchener. Thermochemical Measurements in Flotation Research. Proc. 10th Internat. Miner. Proc. Cong., London, 1973, p. 451.

14. Pedersen, J. J. Acid Dissociation of the Hydrated Cupric Ion. Danske Videnskaberne Selskab. Mat.-Fys. Medd., v. 20, 1943.

15. Sutherland, K. L., and I. Wark. Principles of Flotation. Australasian Inst. Min. Met., Melbourne, 1955, p. 95.

16. The Chemical Society. Stability Constants of Metal-Ion Complexes. Spec. Pub. No. 17, Burlington House, London, 1964, p. 215.

ENVIRONMENTAL CONSIDERATIONS IN TAILING DISPOSAL

by

G. W. Poling[1]

INTRODUCTION

Many who feel responsible for the maintenance and development of a viable mining industry view environmental protection legislation, recently enacted or soon to be enacted in both Canada and the United States, as unduly restrictive. In addition, there is some justification to contend that some of the effluent and water quality criteria presently used by both Federal regulatory agencies--the U.S. Environmental Protection Agency and the Canadian Environmental Protection Service--are unreasonable. For example, they do not normally relate directly to the specific needs of each environment. Regulations based on application of best practicable technology (BPT) and total metal contents for tailing effluents are two cases-in-point. Best practicable technology represents a moving baseline, whereas a criterion to protect the environment adequately should be almost fixed in time. Once adequate protection is achieved, a better "mouse trap" surely need not be installed just because it becomes available, even at an affordable price. Countrywide baseline criteria, based on BPT, also fail to take into account the sometimes wide variations in natural background levels. Mines should not be expected to remove naturally derived sediment and dissolved chemical loads from intake process waters in addition to "winning" minerals and metals from conventional ores.

Mill effluents typically contain both solid and liquid phases. In general, those elements within the solid-particulate phase remain unavailable to the aqueous or aquatic environment. Thus, effluent-quality criteria, based on assumed availability of all contained elements, are often unduly restrictive.

Mineral and metal products from our mining industries must compete on an international market, normally without benefit of any subsidization. Unreasonable environmental control costs constitute a local penalty and might cause a shift of mining operations and technical expertise to countries with less restrictive legislation. Our North American society will undoubtedly suffer from such shifts. Thus, we must endeavor to seek amendments to any

---

[1] Professor and Head, Department of Mining and Mineral Process Engineering, University of British Columbia, Vancouver, British Columbia.

unreasonable legislation in this field. As scientists and engineers our main responsibility lies in providing our legislators with reliable data and accurate interpretations on the environmental considerations of mine-mill waste disposal.

This paper presents the author's evaluation of current environmental protection legislation, guidelines, and criteria in use in Canada and the United States. Attention is focused primarily on the disposal of mill tailing on land and in water. Arguments and evidence favoring retention of the possibility of unconfined tailing discharges, particularly to marine waters, are presented. Marine disposal is relevant not only to mines situated along our coasts but also to future prospects for ocean mining and for safe disposal of dredged materials.

BRIEF REVIEW OF GOVERNMENT REGULATIONS

Amendments to the U.S. Federal Water Pollution Control Act in 1972 set July 1, 1977, as the date for application of best practicable control technology (BPT). BPT carries a proviso of economic feasibility as well. By July 1, 1983, the BPT economically achievable is to be in place. The U.S. Environmental Protection Agency (EPA) has also recently issued "Quality Criteria for Water" (30). These new criteria are claimed (22) in general to represent orders-of-magnitude reductions in critical levels of chemicals for various forms of aquatic life, as compared to State water quality standards typically in existence today. Because these new EPA criteria are based on total concentrations, at certain periods of the year many natural waters with no discernible degradation will fail to meet these new water quality standards (22).

While these new regulations and criteria are legally in place in the United States, they apparently are not being enforced in at least some jurisdictions, due to several cases of pending litigation about their rationale (that is, the inadequacy of their data base) (32).

The Canadian Government has recently enacted legislation pertaining to Metal Mining Liquid Effluent Regulations and Guidelines (16). These "Regulations," annexed to the Fisheries Act, place stringent restrictions on the amounts of selected deleterious substances allowed in effluents for new or expanded mines. Table 1 presents a summary of these regulations, which for the metals, are given as total values. These Federal regulations are at odds with those of certain Provincial Pollution Control Branches. British Columbia's objectives are based on dissolved metal contents as shown in table 2 (7). The new Canadian Federal regulations also virtually disallow any unconfined tailing discharges even to marine waters. Several existing (and proposed) mines along Canada's coasts currently employ (or would employ) this method of tailing disposal.

Existing mines in Canada are subject to the general prohibition of discharging deleterious substances under the existing Fisheries Act. The recently issued "guidelines" (16) allow negotiation of a compliance schedule for each existing mine to meet levels identical to those specified as regulations in table 1. The Federal Government estimates that as many as one-third of Canada's existing mines do not presently meet the new regulations and supplementary toxicity guidelines. The latter stipulate an objective of less than 50-percent fish mortality in a 96-hour, flow-through, acute lethality test (16).

TABLE 1. - Canadian Federally authorized levels of substances (16)

Item	Substance	Maximum authorized concentration, mg/l		
		Monthly arithmetic mean	In a composite sample	In a grab sample
1	Arsenic	0.5	0.75	1.0
2	Copper	.3	.45	.6
3	Lead	.2	.3	.4
4	Nickel	.5	.75	1.0
5	Zinc	.5	.75	1.0
6	Total suspended matter.	25.0	37.5	50.0
7	Radium 226	[1]10.0	[1]20.0	[1]30.0

[1]pCi/l.

Note: The concentrations are given as total values with the exception of radium 226, which is a dissolved value after filtration of the sample through a 3-micrometer filter. Minimum authorized monthly arithmetic mean value of pH, 6.0. Minimum authorized pH in a composite sample, 5.5. Minimum authorized pH in a grab sample, 5.0.

In rationalizing the use of total metal criteria for effluent regulations, the Canadian Environmental Protection Service (EPS) refers to compatability with EPA practice in the United States (15). In addition, EPS appears to have placed considerable emphasis on opinions given several years ago by G. Fred Lee, a well-known U.S. environmental scientist, in a review paper on "Chemical Aspects of Bioassay Techniques for Establishing Water Quality Criteria" (15, 21). In that paper Lee concluded "that the most reasonable approach for establishing meaningful water quality standards is one where the standards are based on the total of the chemical species" (21). This and other lengthy quotations from Lee's 1973 paper were used by Canadian EPS officers in their brief presented to a recent (January 1978) Public Enquiry into Pollution Control Objectives for Mining, Mine-milling and Smelting Industries of British Columbia (15). Their objective was to justify the proposal that "the total metal concentration approach reflects a more prudent measure to avoid undesirable conditions that might be encountered in the reasonably foreseeable future." It seems that Professor Lee was quoted out of context because his paper was concerned with the adoption of more meaningful bioassay procedures. Further, his more recent papers can leave no doubt that Lee does not support regulations based on total metal content. Extensive leaching and bioassay studies on mill tailing, and both natural and dredged sediments, have caused Lee to conclude that "bulk chemical criteria are not technically valid since the amounts of heavy metals available in sediments are not related to the total content of the metals in the sediments" (23). On the contrary, as a general rule, sediments were found to act as sinks for many contaminants. Evidence in support of these generalizations will be presented later.

TABLE 2. - British Columbian objectives for effluent discharges (7)

Characteristics	Description	Unit of measurement	Marine-water discharge			Fresh-water discharge		
			Level A	Level B	Level C	Level A	Level B	Level C
Total suspended solids (non-filterable residue)	That portion of the effluent, as discharged which is retained by an approved filter	mg/l	50[1]	150[1]	(2)	50[1]	150[1]	(2)
Total dissolved solids (filterable residue)	That portion of the effluent as discharged which passes through an approved 0.45-micron pore-sized filter	mg/l	-	-	-	<2,500	<3,500	<5,000
Colour[3]	Colour of the effluent, at the point of discharge	Approved units	-	-	-	-	-	-
pH[2]	The pH of the effluent at the point of discharge	pH units	6.5-8.5[4]	6.5-9.5	6.0-10	6.5-8.5[4]	6.5-9.5	6.0-10
Specific elements and compounds	Material contained in the effluent, at the point of discharge, which passes an approved 0.45-micron pore-sized filter (except where total values are required)	-	-	-	-	-	-	-
Aluminum (Al)	Dissolved in the effluent	mg/l	0.50	1.00	10.00	0.50	1.00	10.00
Ammonia (as N)	Dissolved in the effluent	mg/l	.50[4]	1.00	10.00	.50[4]	1.00	10.00
Antimony (Sb)	Dissolved in the effluent	mg/l	.05	.25	1.00	.05	.25	1.00
Arsenic (As)	Dissolved in the effluent	mg/l	.05	.25	1.00	.05	.25	1.00
Cadmium (Cd)[5]	Dissolved in the effluent	mg/l	.005	.01	.02	.005	.01	.02
Chromium (Cr)	Dissolved in the effluent	mg/l	.05	.30	.50	.05	.30	.50
Cobalt (Co)	Dissolved in the effluent	mg/l	.10	.50	1.00	.10	.50	1.00
Copper (Cu)	Dissolved in the effluent	mg/l	.05	.30	1.00	.05	.30	1.00
Cyanide (CN)	Total cyanide in the effluent	mg/l	.10	.50	2.00	.10	.50	2.00
Fluoride (F)	Dissolved in the effluent	mg/l	2.50	5.00	15.00	2.50	5.00	15.00
Iron (Fe)	Dissolved in the effluent	mg/l	.30	1.00	5.00	.30	1.00	5.00
Lead (Pb)	Dissolved in the effluent	mg/l	.05	.10	.50	.05	.10	.50
Manganese (Mn)	Dissolved in the effluent	mg/l	.05	.50	1.50	.05	.50	1.50
Magnesium (Mg)	Dissolved in the effluent	mg/l	-	-	-	150.	300.	500.
Mercury (Hg)	Total in the effluent	mg/l	.001[4]	.003	.01	.001[4]	.003	.01
Molybdenum (Mo)	Dissolved in the effluent	mg/l	.50[4]	1.00	10.0	.50[4]	1.00	10.00
Nickel (Ni)	Dissolved in the effluent	mg/l	.30	.50	1.00	.30	.50	1.00
Nitrates/Nitrites (as N)	Dissolved in the effluent	mg/l	10.00	25.00	50.00	10.00	25.00	50.00
Phosphate (as P)	Total in the effluent	mg/l	2.00	5.00	10.00	2.00	5.00	10.00
Selenium (Se)	Dissolved in the effluent	mg/l	.05	.10	1.00	.05	.10	1.00
Silver (Ag)	Dissolved in the effluent	mg/l	.10	.50	1.00	.10	.50	1.00
Sulphate (SO_4)	Dissolved in the effluent	mg/l	-	-	-	50.[4]	250.	1,000.
Uranyl (UO_2)	Dissolved in the effluent	mg/l	2.00	5.00	10.00	2.00	5.00	10.00
Zinc (Zn)	Dissolved in the effluent	mg/l	.50	5.00	10.00	.50	5.00	10.00
Oil and grease	Total in the effluent	mg/l	15.00	15.00	15.00	15.00	15.00	15.00

Note--Acceptable concentrations for characteristics not appearing in this list are to be determined as required. When all liquids are totally recycled, the applicability of the above objectives will be assessed.

[1] Initially, semiquarterly sampling on effluents and at control and test stations in receiving-waters; quarterly sampling on effluent discharged to closed systems.

[2] Daily sampling.

[3] To be reviewed.

[4] Tentative, subject to review.

[5] Subject to review where applied to smelters.

The three main problem areas in both EPA and EPS guidelines and regulations concerning effluents from mining and mineral processing plants seem to be:

1. These nationwide minimum objectives are too general and fail to take account of wide variations of natural background levels and wide variations in the nature of ore bodies.

2. Both systems of objectives are based on total metals or bulk chemical contents, whereas toxicity relates more directly to dissolved elements and compounds, and, most of the contents of solids remain unavailable to the environment.

3. Disallowance of any unconfined tailing disposal might eliminate environmentally acceptable and perhaps even preferable methods of disposal at specific sites--particularly at certain coastal sites.

The mineral industry in the United States has challenged certain of the EPA effluent limitations with 11 lawsuits filed in five U.S. Courts of Appeals (32). On May 24, 1976, EPA, as an apparent direct result, suspended its ore mining and dressing point source effluent regulations because of legitimate questions about the validity of their technical and economic bases. None of this controversy and suspension of EPA regulations has been acknowledged by the Canadian EPS. Instead, Canada-wide minimum regulations, based partly on the by-then suspended U.S. regulations, were proclaimed law on September 1, 1977 (16). As yet, these EPS regulations go unchallenged in the courts. Reviews of recent presentations regarding these new regulations by EPS authors have indicated full participation and cooperation by the Canadian mineral industry in their development (34). Similar to what apparently happened earlier in the United States, however (32), many industrial representatives maintain that their views were disregarded in the formulation of the eventual regulations and guidelines (25). Thus, claims of widespread industrial satisfaction with the present EPA and EPS regulations seem unjustified.

NEED FOR PERMITS BASED ON SITE-SPECIFIC ASSESSMENT

Each ore body is highly unique as is each environment in which the ore must be mined and processed. Because of the unique characteristics of each individual mine-mill site and surrounding environ, required levels of pollution abatement must be determined on a site specific basis. Regulatory agencies should acknowledge that heavy metal anomalies of natural origin must be expected in areas surrounding mines. These anomalies form the basis of geochemical and biogeochemical prospecting techniques. Figure 1 shows the range of abundancies of trace elements in soils (3). This figure should serve to quantify the need for site-specific assessments.

A recent survey of natural versus unnatural (or manmade) heavy metal concentrations in lake sediments in Canada provides evidence of many naturally contaminated regions (1). For example, it has been established that surface sediments in many lakes in the Sudbury area of Ontario have much high nickel concentrations than deeper sediments. This difference is due supposedly to man's activities in the area. One lake sediment in the Sudbury area exhibited a high concentration of 112 ppm nickel. Allan found, however, that these levels were exceeded in certain remote areas free from man's influence (1). For example, naturally contaminated surface lake sediment at the Muskox Intrusion in Canada's Northwest Territories exceeded 750 ppm nickel. Another location in northern Quebec, at Raglan, provided natural nickel concentrations in excess of 100 ppm.

Arsenic is another metal of environmental concern. Some lake sediments close to gold processing operations were found to contain concentrations as high as 556 ppm arsenic. Typical naturally contaminated lake sediments in the Canadian Shield assay 2 to 5 ppm arsenic. However, arsenic concentrations of up to 394 ppm in naturally occurring sediment have also been reported (1). Sediments of natural origin containing as much as 7,000 ppm copper are also reported (1).

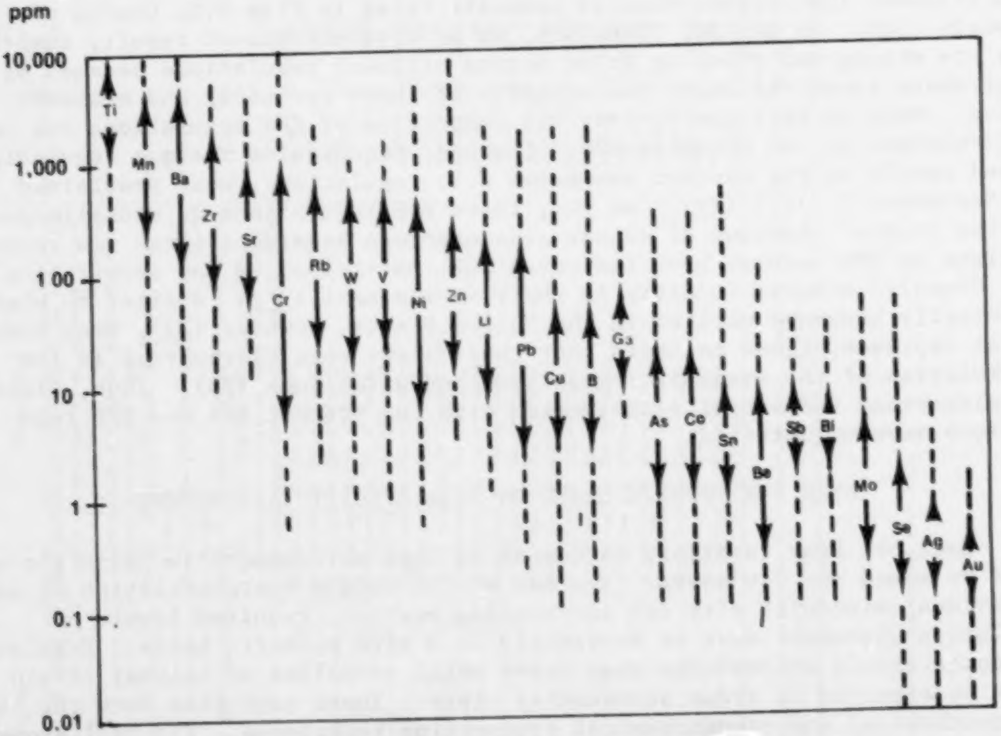

FIGURE 1. - Range of abundance of trace elements in soils (3). (*Courtesy, Australian Institute of Mining and Metallurgy.*)

Citing these data is not to argue that such levels of either natural or unnatural heavy metal contents are harmless to the environment or to man. However, hazardous bioaccumulation of heavy metals is, in fact, rare for most elements. Mercury is one important exception. High mercury contents (>0.5 ppm on a fresh weight basis) in fish muscle and fish livers have been traced to both natural and manmade contamination along the Pinchi fault in Central British Columbia (29). These data are cited to indicate that not all anomalies in heavy metals can be attributed to man's activities. Natural soils and sediments can exhibit major heavy metal anomalies, which emphasize the need for site-specific assessments. Natural levels of contamination of waters and sediments or suspended solids have been observed which on their own would exceed the effluent criteria listed in table 1.

Raw river waters also exhibit wide variations in dissolved trace elements. Table 3 presents a summary of 11 years of surveillance of 1,577 raw river waters and finished drinking waters in the United States (20). Close investigation of these data indicates that some of the maximum values would exceed current effluent regulations or objectives in either tables 1 or 2. Natural waters draining mineral-bearing regions have often been found to exceed the 0.5 ppm and 0.2 ppm maxima for zinc set by EPA for mine effluents and mill effluents, respectively. For example, in 93 analyses of such natural waters, only 10 met the EPA standards of 0.2 ppm zinc, and only 28 met the 0.5 ppm zinc standard (32).

Seasonal variations of chemical contents of natural streams can also be substantial. Table 4 shows ranges observed in fresh-water streams entering Rupert Inlet located toward the north end of Vancouver Island, B.C. (14).

Other factors that should be borne in mind in site-specific assessments relate to choosing the best system of tailing disposal. Everyone acknowledges that so-called "closed-circuit systems" employing onland tailing impoundment plus recycle of supernatant to the mineral processing plant can generally provide minimal environmental impact. In areas of high seismic activity, tailing impoundments might not be safe. In spite of recent improvements in their design, construction, and monitoring, tailing dams can fail. In areas of high precipitation, not all of the water entering the tailing pond can be recycled. The excess must be discharged to the environment. Sometimes the accumulation of large excess waters is seasonal. In periods of spring runoffs from melting of heavy snow loads, the excess pond water can contain significant suspended solids loads. These loads would be typical of natural conditions in surrounding streams and rivers at that time of year and far in excess of the 20 to 50 mg/l allowable according to Canadian Federal regulations.

Thus, in certain instances, onland tailing impoundments might not be the best method of tailing disposal. Even with onland impoundments, regulations and permits should allow sediment-laden discharge from tailing ponds at certain periods of a climatic cycle, if the extra sediment will not adversely affect the receiving environment.

TABLE 3. - Summary of dissolved trace elements in 1,577 surface waters[1] (Oct. 1, 1962, to Sept. 30, 1967)

Element	No. of positive occurrences	Frequency of detection, %	Observed values, µg/l		
			Min.	Max.	Mean
Aluminum[2]...	456	31.2	1.	2,760.	74.
Arsenic	87	5.5	5.	336.	64.
Barium	1,568	99.4	2.	340.	43.
Beryllium ..	85	5.4	.01	1.22	.19
Boron	1,546	98.0	1.	5,000.	101.
Cadmium	40	2.5	1.	120.	9.5
Chromium ...	386	24.5	1.	112.	9.7
Cobalt	44	2.8	1.	48.	17.
Copper	1,173	74.4	1.	280.	15.
Iron	1,192	75.6	1.	4,600.	52.
Lead	305	19.3	2.	140.	23.
Manganese ..	810	51.4	.3	3,230.	58.
Molybdenum .	516	32.7	2.	1,500.	68.
Nickel	256	16.2	1.	130.	19.
Phosphorus .	747	47.4	2.	5,040.	120.
Silver	104	6.6	.1	38.	2.6
Strontium ..	1,571	99.6	3.	5,000.	217.
Vanadium ...	54	3.4	2.	300.	40.
Zinc	1,207	76.5	2.	1,183.	64.

[1] After Kopp (20); courtesy, John F. Kopp.

[2] 1,464 aluminum analyses.

TABLE 4. - Range of variation in chemical content of natural streams (analysis unit - parts per billion) (14, 30)

Element	Permit limit	Fresh-water streams entering Rupert Inlet	Island Copper process-water intake
Copper	5	< 1 to 21.	< 1 to 6.6
Iron	200	< 20 to 6,740.	< 20 to 225.
Lead	5	< 1 to 23.	< 1 to 5.1
Manganese .	5	1 to 0.849	1 to 4.
Molybdenum	20	< 1 to 36.	< 1 to 7.2
Zinc	22	< 1 to 245.	< 1 to 245.

In Japan, land-use competition for agriculture mitigated against onland impoundment of tailing in certain areas (6). Tailings, instead, are pumped 45 miles to the seacoast where they are impounded in a diked-off area along a beach of the Japan Sea. This type of disposal should probably be considered as temporary onland disposal. Over a period of a few centuries, the disposal site might well become the equivalent of an unconfined submarine site.

Issuance of permits based on site-specific assessments does not obviate the usefulness of general objectives or minimum performance levels. This does, however, require intimate negotiations between mine-developers and regulatory agencies who ideally have close, first-hand knowledge of the site-specific conditions and environmental needs. National regulations imposed from afar do little to foster cooperation between industry and government.

Need for More Reasonable Effluent Criteria Than BPT and Total Metal Content

Effluent criteria based on application of best practicable technology arose from an early inability to define required levels of environmental protection. Thus, mines were expected, in effect, to do as well as they could. One problem with this criterion is that almost invariably, suppliers of equipment overestimate the capabilities and/or dependabilities of their products. These overestimates of available technology are sometimes written into regulations or permits. Alternatively, regulatory agencies have assumed a role of dictating to industry what equipment was "affordable." Neither alternative has pleased the mine operator or his shareholders. EPA estimated that for mines and mineral processing plants in the United States to comply with their current effluent guidelines would require a capital investment of less than \$100 x 10^6. Industrial estimates for this same figure are \$862 x 10^6 (26).

The most important criticism of basing pollution abatement policy solely on application of BPT is that it does not relate directly to the specific needs of each environment. In areas that are particularly sensitive to environmental contaminants, even application of BPT can be unacceptable. In areas where equipment in place produces effluents having no discernible impact on the environment, insisting on installation of additional new and better (or best) technology makes little sense. No improvement in the environment would be expected and money would be wasted.

Since the philosophy of BPT cannot be universally applied, it must be tempered with a site-specific policy keyed to achieving adequate environmental protection. The next major question, of course, is what is "adequate" protection? This critical question will be addressed in the following section of "Proposed Effluent Criteria."

Mill tailing effluent criteria based on bulk chemical contents are technically invalid, since not all elements will become biologically available in a toxic form. In fact, evidence abounds that there is no direct relationship between the bulk chemical contents of liquids or liquids plus particulate phases and toxicity (4, 8, 14, 17, 21-23). In some instances, aqueous habitats have been detoxified by adding mineral slimes (4, 8). Adsorption of contaminant onto the solid surfaces and eventual incorporation into buried sediments can effectively remove both organic and inorganic contaminants.

An example of detoxification might be informative. Dickson (8) showed that adding either natural red clay sediment or taconite tailing to aquaria, originally containing a dissolved copper concentration of 200 μg/l and holding trout fingerlings, detoxified the copper. All fingerlings died during a 96-hour exposure to the aquaria to which no solids had been added. A dissolved copper concentration of 125 μg/l persisted in the aquarium at the end of this test. No fingerlings died in the two aquaria that received the solid sediment. The taconite and clay adsorbed much of the copper. At the end of these latter tests, only 20 μg/l of soluble copper remained. There is also ample evidence that almost all dissolved elements being added to the sea naturally are constantly being removed either as solid precipitates or as adsorbed species on solids or even as seabed nodules (5). Thus, solid phases (sediments) normally act as effective "sinks" for dissolved contaminants.

Relatively rare situations exist where there is sufficient release of contaminants from sediments to cause deterioration in the overlying waters. Biological methylation of mercury in sediments is a well-known example, where toxins can be released. In some instances, ingestion of fine sediment by benthos can lead to bioaccumulation of heavy metals. Ingestion of fine sediments by mammals can also cause leaching of some contained heavy metals, since the solutions in a gut typically have a pH of about 2.0. Thus, the solid phase cannot be assumed to be inert; instead, evidence of the unavailability of its contents to the liquid phase should be required.

Proposed Effluent Criteria and Regulatory Mechanisms

Environmental control policies adopted by both EPA in the United States and EPS in Canada are concerned with regulation of effluents in an effort to reduce the level of contamination at its source. Most mining companies support this policy; certainly the Mining Association of British Columbia does (25). Alternate mechanisms aimed at retaining receiving water quality criteria or at economic incentives for pollution control are generally judged impractical for the present (30). The latter demands payment for use of assimilative capacity of a specific environment. Pay for use of the environment is supposed to motivate the discharger to reduce his discharges in order to pay less penalty. One difficulty is that money spent in penalties is thereby unavailable to effect pollution abatement!

Regulation of effluent to prevent pollution requires reasonable effluent quality criteria. The preceding arguments indicate that basing effluent criteria on application of BPT combined with "bulk chemical contents" leaves much to be desired. Instead, criteria to evaluate adequate environmental protection should be based on levels that will not impair the usefulness of the receiving water to man.

The toxicities of heavy metals and organic compounds (such as residual milling chemicals) are directly related to dissolved levels of these contaminants. Thus, guidelines and regulations should be based on these values supplemented by limitations on outflow rates and bioassays plus evidence of absence of risks of bioaccumulation. Additional evidence concerning the nonleachability of the solid phase in the receiving environment would also seem reasonable.

In Canada, both flow-through and static bioassay techniques are currently employed to assess acute toxicity (16). Levels risking chronic toxicity are usually taken in the range of 0.1 to 0.01 percent of the acutely toxic levels. In British Columbia a minimum dilution factor of 20:1 in the receiving water is required to provide protection against chronic toxicity from liquid effluents (7). An innovative method to determine toxicity has been developed recently in South Africa (27). This technique uses electronic measurement of disturbances in the opercular rhythm (gill breathing rhythm) of captive fish as a sensor of toxicity. This technique is capable of continuous monitoring of waters such as those destined for potable supplies.

Development of more meaningful bioassay and bioaccumulation techniques to determine both acute and chronic toxicity is a pressing research need. In two-phase, liquid-solid systems, these bioassays must adequately simulate natural water conditions in order to be meaningful. The previous example of sediments detoxifying copper in aquaria should underline this requirement. Additionally, organisms selected as sensors should nearly duplicate the sensitivity of organisms in the disposal area. Attention must also be focused on redox conditions and on time effects for adsorption, and ion exchange reactions are to be expected.

While these requirements might seem onerous, they are practical and should be preferred to accepting unreasonable criteria such as bulk chemical contents.

UNCONFINED TAILING DISPOSAL

Unconfined tailing disposal has recently been described by a United States EPA official as "one of the most blatant insults to the environment" (19). Why then would one propose retaining the possibility of unconfined tailings disposal methods? A rationale of out-of-sight, out-of-mind is obviously illegitimate! Instead, this proposal stems from evidence and a conviction that underwater disposal is sometimes an acceptable method offering perhaps the least overall environmental impact.

As mentioned earlier, onland, closed-circuit impoundment systems are either undesirable or even impossible to achieve in some areas. Underwater disposal, particularly to marine waters, might be an acceptable alternative disposal method. In some areas where tailings might be prone to generate acids, deep, underwater disposal in a lake, for example, has been an accepted, although rarely used, disposal technique (12). Should ocean mining become a reality, marine disposal would be the only feasible method.

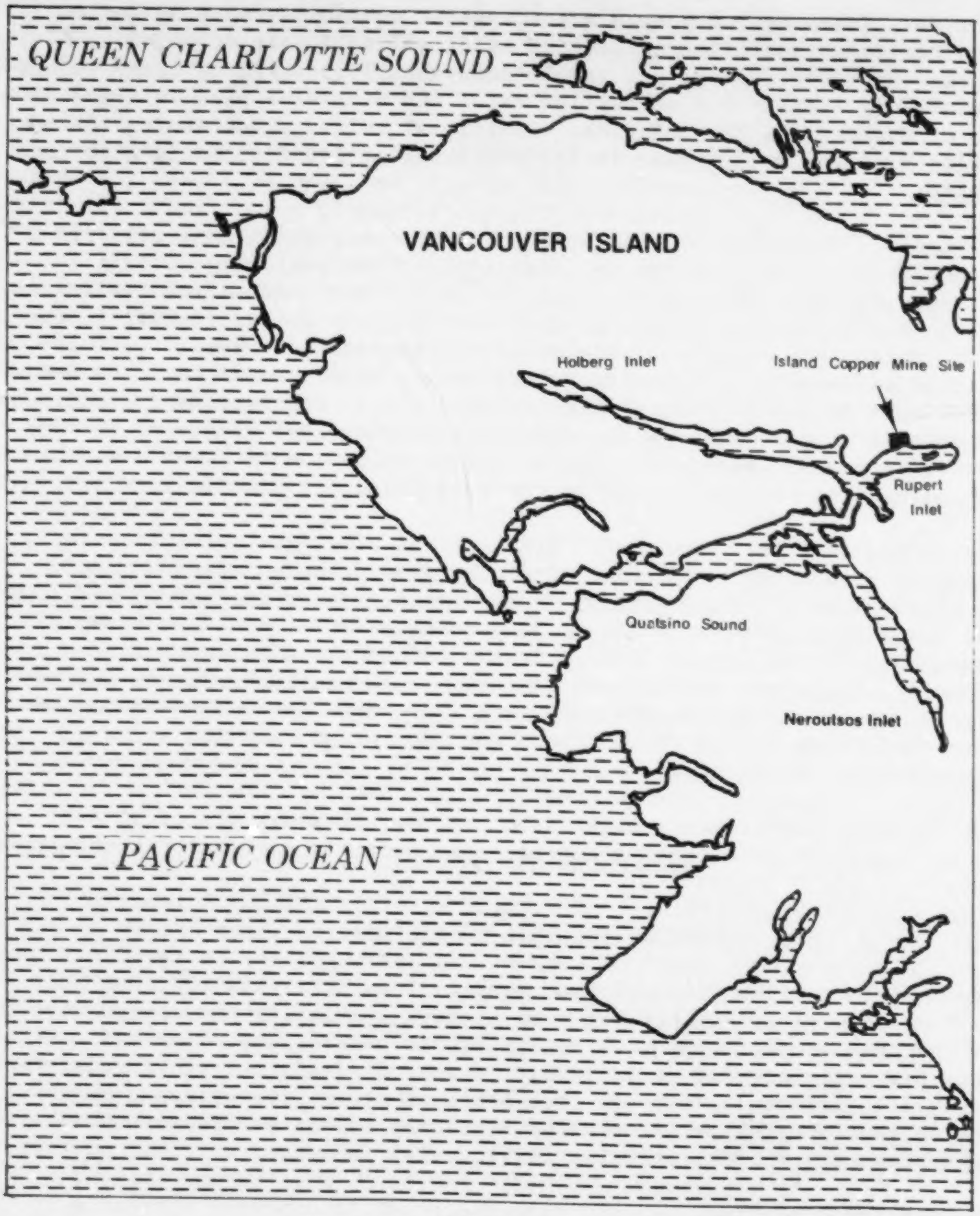
QUEEN CHARLOTTE SOUND
VANCOUVER ISLAND
Holberg Inlet
Island Copper Mine Site
Rupert Inlet
Quatsino Sound
Neroutsos Inlet
PACIFIC OCEAN

FIGURE 2. - Location of Island Copper Mine.

Many mines along Canada's coasts and around the world currently discharge tailing directly to the sea. Several of these have been operating for many years now with extensive environment monitoring programs in action (9-11, 14, 18, 24-25). Not all of the monitoring studies claim to have found negligible environmental impact, but most do. Of all the marine monitoring programs being conducted around the world, those at Rupert Inlet at the north end of Vancouver Island, B.C., where the Island Copper Mine discharges 30,000 to 50,000 tpd of mill tailing, are the most comprehensive. One monitoring agency has reported that 7 years of operation have resulted in minimal impact on the marine inlet ecosystem (10, 14, 25, 28). These findings have recently been contested by an EPS report (18)--but they are supported by the British Columbia Provincial Pollution Control Branch.

Submarine tailing disposal at the Island Copper Mine, Rupert Inlet, B.C., has been a contentious environmental issue from the initial planning stages of the mine project in 1968 (13). Figure 2 shows the geographical location of the Island Copper Mine. The thickened (35 to 45 pct solids) "siliceous" tailing (<4 pct total residual sulfide content) at a grind of 65 to 70 pct minus 200 mesh flows by gravity to a seawater premix tank and thence into Rupert Inlet via a polyurethane-lined 42-inch steel pipe to a depth of 150 feet. The tailing is prediluted with seawater (1:1 ratio) to prevent potential "upwelling" effects due to differences in compositions and temperatures of the liquid component. Pretreatment of tailing by coagulants ($Ca(OH)_2$) and flocculants (anionic polyacrylamides) in the thickeners, plus the effects of seawater-induced coagulation, are meant to assist sedimentation of the tailing solid components in the lower reaches of the inlet system trough. Figure 3 shows the tailing sediment distribution, as of December 1976, following discharge of more than 56 x 10^6 tons of solids into Rupert Inlet. Crab samplers, sediment coring, and continuous seismic profiling were used to monitor the actual tailing sediment distribution in the inlet system.

Upon discharge from the end of the submarine pipeline (just opposite the minesite in fig. 3), the tailing flows as a turbidity current or density current down the axial trough of the Rupert Inlet-Holberg Inlet system. The tailing turbidity current flows in a leveed channel formed by tailing sediment at the bottom of the inlet system, much like a conventional river on prairie sediments. The turbidity current presently appears to dissipate shortly after entering Holberg Inlet (see fig. 3).

Preventing suspended tailing sediments from significantly increasing turbidities in the near-surface, biologically productive zone is a prime requisite of this marine disposal scheme. Suspended sediment loads throughout the receiving water columns were monitored via nephelometry and gravimetric analysis on discrete water samples and in situ transmissometry using a towed, 1-meter path length optical cell. These studies indicate that the zone of increased turbidity due to tailing lies generally below 50 meters throughout the receiving water system. On occasional high tides, when deepwater exchange occurs, turbulent upwelling produces turbid "boils" off Hankin Point (see fig. 3). It is not yet clear whether this turbidity is caused by scouring of previously deposited tailing sediment or whether it emanates from upwelling from the turbidity current passing through the Rupert-Holberg gap at depth. The significance of this periodic updwelling seems a major point of contention between EPS monitoring data (25) and data from the Independent Monitoring Agency appointed by the British Columbia Provincial Pollution Control Branch. (See 11, 13-14, 28.)

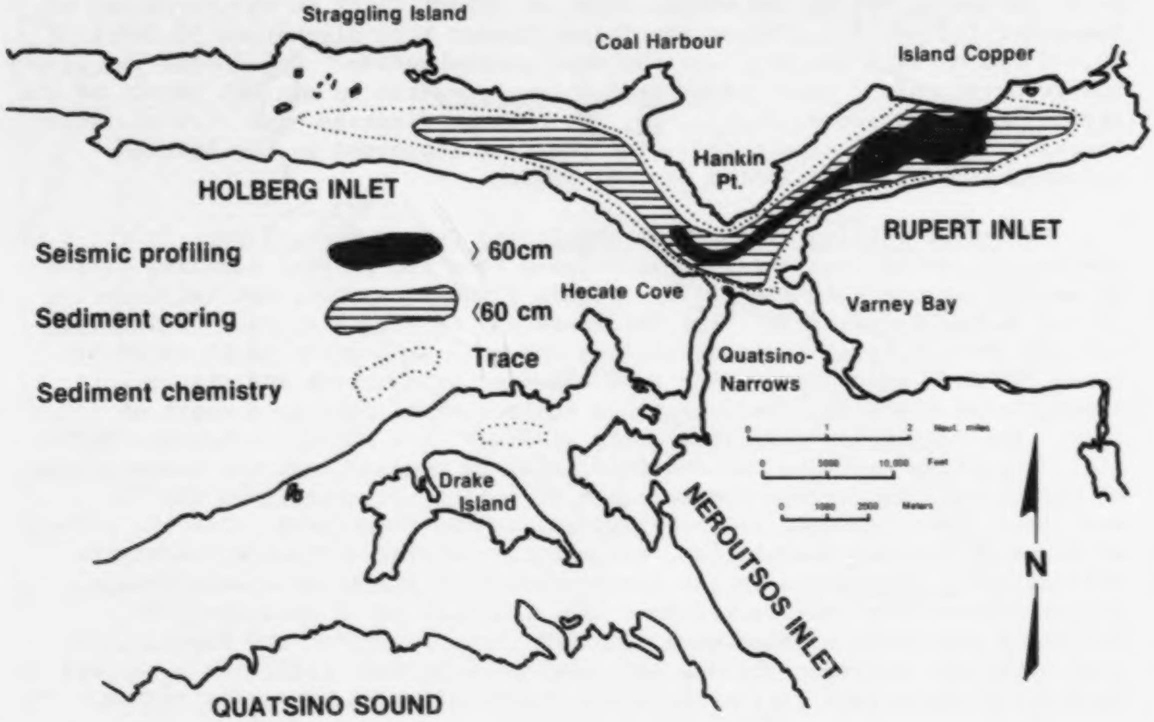
Straggling Island
Coal Harbour
Island Copper
Hankin Pt.
HOLBERG INLET
RUPERT INLET
Seismic profiling
⟩ 60cm
Sediment coring
⟨60 cm
Trace
Sediment chemistry
Hecate Cove
Varney Bay
Quatsino-Narrows
0 1 2 Naut. miles
0 5000 10,000 Feet
0 1000 2000 Meters
Drake Island
NEROUTSOS INLET
N
QUATSINO SOUND

FIGURE 3. - Tailings sediment distribution from Island Copper Mine in 1976.

Biological assessments of the effects of disposal of tailing into Rupert Inlet are extensive and cover a wide spectrum of both plant and animal kingdoms of the ecosystem. Phytoplankton are microscopic plants that photosynthesize new organic matter and form the basis of the marine food chain. Monitoring of these species consists of determining: the depth of the euphotic zone or lighted photosynthetic zone, the available nutrients, the standing crop, and the rate of assimilation throughout the receiving Inlet system and at outside control stations. The standing crop of phytoplankton is monitored by assessing the quantity of chlorophyll "a" pigment per unit volume. Figure 4 shows the results of these studies since the beginning of the preproduction monitoring program in 1970. If anything, there has been a slight increase in chlorophyll "a" levels at all stations over the 6 years of monitoring shown.

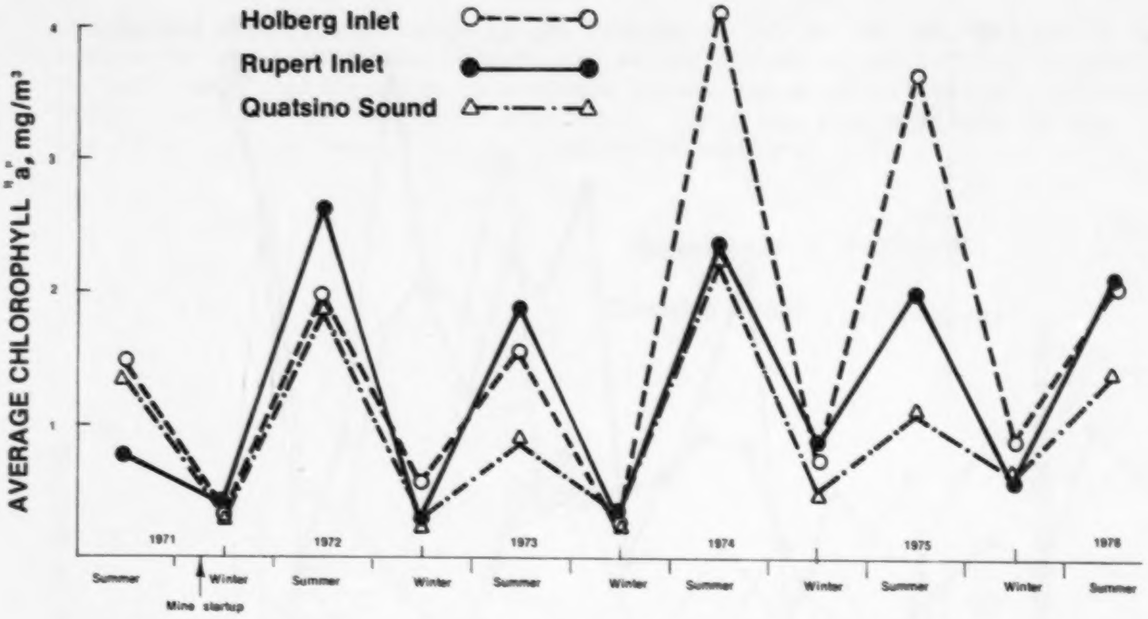

FIGURE 4. - Average chlorophyll "a" pigment per unit volume since 1970 (31). (*Courtesy- C. A. Pelletier.*)

Large plant species (macrophytes) have also been monitored at 10 sites in the Inlet system. Both diversity and abundance of these species appear normal. Intertidal plant growth is also being monitored routinely. Again, there is no evidence of a decrease in plant growth. Recently, a program was initiated to examine whether some plants might be accumulating potentially toxic heavy metals due to the tailing disposal. To date, our data indicate no increase in bioaccumulation of heavy metals.

Resident animal species, from zooplankton to large mud sharks, are monitored for population density, species diversity, and heavy metal contents. Zooplankton, at the base of the marine animal kingdom, are tiny swimming animals that feed upon the phytoplankton and in turn are fed upon by carnivores. Figure 5 shows their density appears to have increased slightly over the monitoring period. Figure 6 illustrates that zooplankton species diversity has not been adversely affected. Metal analyses of zooplankton show wide variability, due at least in part to wide differences among the various species present. Data in figure 7 illustrate this point for copper contents over the life of the mine. Zooplankton collected in September (9th month) of 1973 were predominantly ctenophores (small jellyfish type organisms) that contained very low copper contents. In contrast, the December 1974 samples were predominantly euphausids (shrimplike crustaceans) that apparently contained high copper contents. Thus, large variations in metal concentrations are due in part to variations in the types of organisms forming the bulk of the biomass. In addition, heavy metal contents within a single species appear to vary regularly through multiyear cycles. Thus, interpretation of data on heavy metal contents of zooplankton is extremely difficult. At the

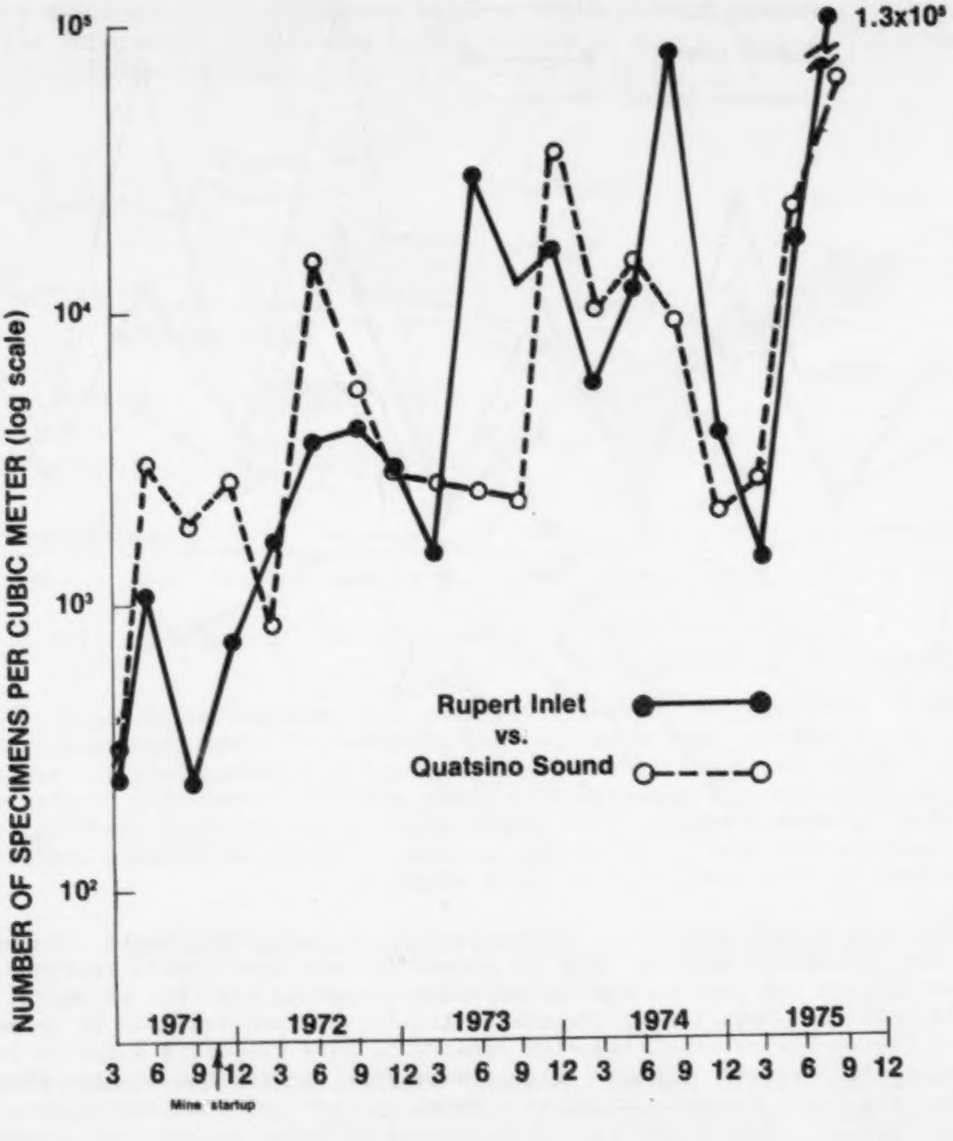

FIGURE 5. - Density of zooplankton at 100 feet since 1970 (31). (*Courtesy*, C. A. *Pelletier*.)

moment, no significant change in the content of Cu, Zn, Mo, Pb, Cd, As, or Hg within the zooplankton can be detected as attributed to the tailing disposal. It would seem that in order to evaluate trends, heavy metal contents of individual species will have to be monitored. (This has been suggested by the specialist on zooplankton in the independent agency.)

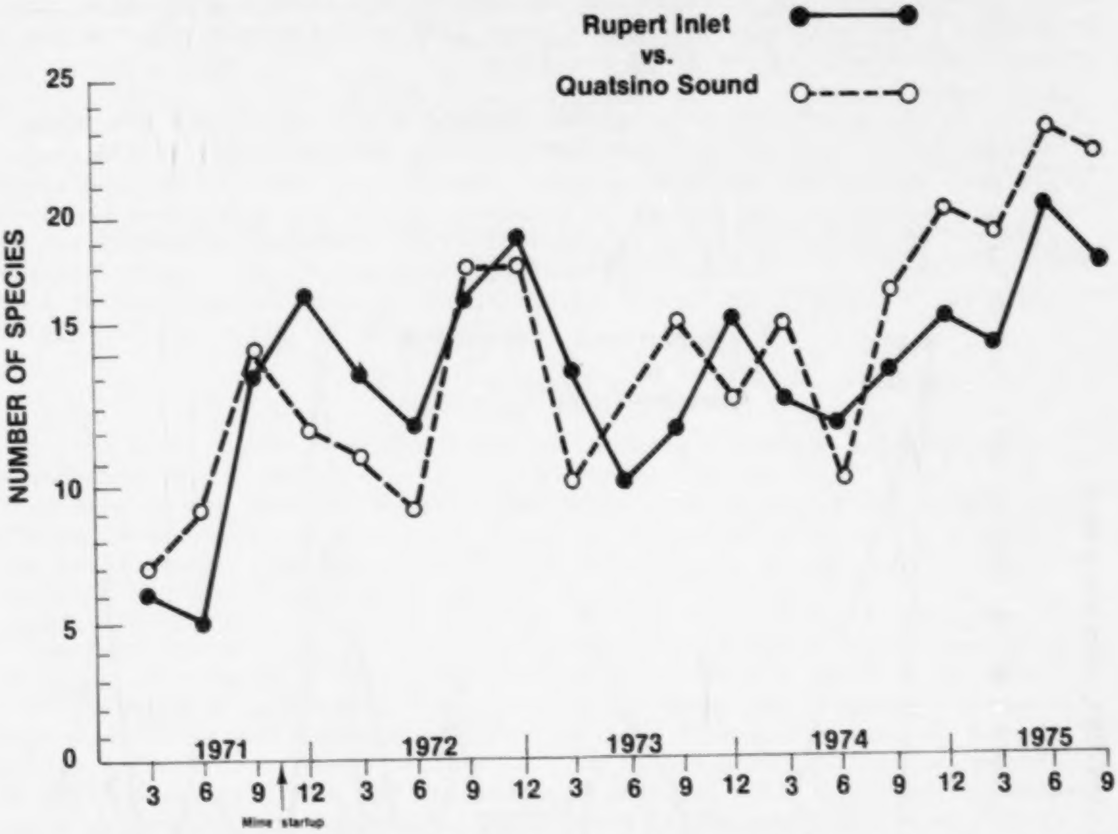

FIGURE 6. - Diversity of zooplankton species at 100 feet since 1970 (28). *(Courtesy, C. A. Pelletier.)*

Benthos such as polychaetes (worms) and mollusks have been obliterated over the bottom trough area of heavy deposition (see fig. 3), as was originally predicted. Benthic communities have recolonized tailing deposits during interruption in mining due to one 2-month labor strike. Also, communities are sustained in areas of light tailing deposition or where deposition is erratic. Crabs, shrimp, prawns, and both bottom-dwelling and pelagic fish have been monitored. No adverse effects on species populations and diversities due to tailing discharge have been observed. Metal levels in edible species remain low, and no point of metal entry to marine food chains has been identified to date.

General conclusions about the disposal of mill tailing into Rupert Inlet are that--

1. No detectable increase in dissolved metals have occurred in the water columns of the Rupert-Holberg Inlet system;

2. Tailing-derived turbidity remains in general below 50 meters depth, which is well below the euphotic--or photosynthetic--primary productive zone. Infrequent turbidity boils off Hankin Point have not adversely affected the primary productivity of the Inlet system;

3. There is evidence that benthic organisms will recolonize the areas currently obliterated by tailing sediments upon termination of tailing disposal into the Inlet system;

4. There is no evidence of significant heavy metals entering the marine food chain due to the tailing disposal.

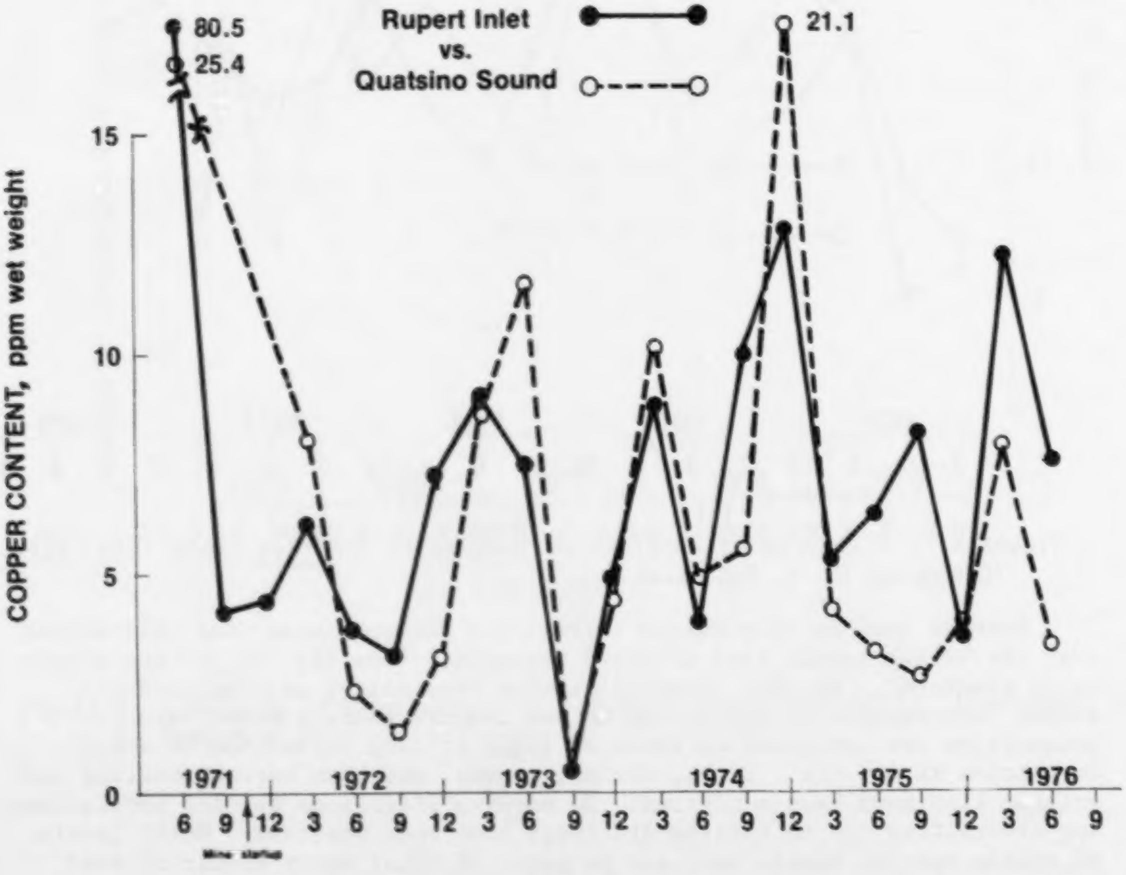

FIGURE 7. - Copper content of zooplankton since 1970 (28). (*Courtesy, C. A. Pelletier.*)

Monitoring of a marine tailing discharge at the Jordan River (copper) Mine on the west coast of Vancouver Island, B.C., has continued since mine shutdown in 1974 (10). Thus, this site offers an evaluation of natural rehabilitation of the marine disposal area. During operations at this mine, tailing sediments accumulated as mounds due to an apparent accidental breakage of the submarine tailing outfall. These mounds were eradicated and rehabilitated over a single season following mine closure. Very slight copper contamination of one species of little neck clam did not increase further. Ellis concluded that metal contamination had been effectively prevented at this site (10). His finding that this particular marine disposal site was almost completely rehabilitated within a single season lends credence to the proposal that marine disposal of mill tailing can offer an acceptable method. This is not to suggest that all tailing or all marine sites will be suitable (9). Indeed, tailing from massive sulfide ores might be found unsuitable due to the prospects of galvanically enhanced leaching of the less noble minerals. More research is necessary to define criteria for stability of tailing solids in marine environments. The contention is that marine disposal methods should not be disallowed by regulations without acceptable rationale for this action.

SUMMARY

The North American mining industry is being adversely affected by unreasonable and/or unduly restrictive pollution control legislation. This statement is not meant to suggest that either EPA in the United States or EPS in Canada have any objectives short of trying valiantly to help protect our environment. Instead, criticism is leveled only at the methods employed. Emphasis on Federal environmental control legislation is a current or relatively recent happening in both countries. Early lack of knowledge about criteria to evaluate environmental quality prompted legislators to opt in favor of reducing levels of contamination by forcing industry to apply best practicable technology. We should acknowledge that sometimes dramatic improvements in environmental quality resulted from application of this policy. Today there would probably seldom be any great difference between criteria based solely on BPT and criteria tempered with site-specific assessments as proposed in this paper. Of concern is the prediction that these differences might widen greatly in the foreseeable future. Continuing pursuit of BPT (or worse yet, best available technology) will result in gross wastage of materials, time, money, and energy, with perhaps little or no improvement of environmental quality (26).

Today our knowledge of the interactions of tailing with the environment is sufficiently advanced that we no longer need rely only on BPT. We have many years of experience with both chemical and biological monitoring criteria. Adequate tests have been developed to determine acute toxicities in systems simulating a particular natural disposal site. Both chemical leaching and biological assaying for toxicities and risks of bioaccumulation are practical. These and other arguments have been presented against basing regulations for tailing effluents on bulk chemical criteria. If metals or adsorbed species in or on particulate phases can be shown to remain unavailable to the water and biota, then bulk criteria have no bearing on toxicity.

Under these "typical" situations, concern with particulates should relate instead to their physical effects. Potential burial of benthos and generation of turbidity in the upper-euphotic zones of waters are two important "physical" concerns.

No attention has been directed in this paper to the potential toxic effects of large residual concentrations of milling chemicals in tailing effluents. Several good reviews of this subject can be found elsewhere (19, 33).

Direct discharges of tailing to underwater disposal sites, particularly marine sites, should be retained as one alternative for coastal mines (and obviously for ocean mining operations). Evidence has been presented in this paper that the main environmental impact of discharging tailing from the processing of a porphyry copper-molybdenite ore has been minimal (2, 11, 13, 28, 30). Anticipated physical burial of benthos (mainly bottom-dwelling worms) at the bottom of the marine inlet was the main impact. Evidence has also been presented that one marine disposal site was rapidly rehabilitated following closure of the Jordan River Mine (10). There is a real research need to improve criteria that make a tailing and a specific marine site either suitable or unsuitable for use of marine tailing disposal.

Now is a good time to reassess regulations governing discharges of tailing effluents to ensure that they are based on the best available rationale or "BAR," to coin a new acronym. The alternative is a potential loss of domestic production and greater reliance on foreign sources.

ACKNOWLEDGMENTS

The author has appreciated helpful discussions with several members of the Island Copper Mine Independent Agency Monitoring Team, particularly Professors J. B. Evans and J. Leja, of the University of British Columbia. Also, I have appreciated the information supplied by C. A. Pelletier, Chief of Environmental Quality of the Island Copper Mine.

REFERENCES

1. Allan, R. J. Natural Versus Unnatural Heavy Metal Concentrations in Lake Sediments in Canada. Proc. Internat. Conf. on Heavy Metals in the Environment, Toronto, 1975 (pub. 1977), pp. 785-808.

2. Andrews, R. D. Tailings: Environmental Consequences and a Review of Control Strategies. Proc. Internat. Conf. on Heavy Metals in the Environment, Toronto, 1975 (pub. 1977), pp. 645-675.

3. Berkman, D. A. Field Geologists' Manual. Australasian Inst. Min. and Met., Parkville, Victoria, Australia, 1976, p. 45.

4. Broman, P. G. Purification of Industrial and Municipal Waste Water by Means of Mineral Slime. Internat. Miner. Proc. Cong., Cagliari, Italy, p. 1371.

5. Chave, K. E. Chemical Reactions and the Composition of Sea Water. J. Chem. Ed., v. 48, 1951, pp. 148-151.

6. Couratin, P. Tailing Disposal - If You Can't Store It, Pump It. World Min., v. 5, May 1969, pp. 22-27.

7. Department of Lands, Forests, and Water Resources, British Columbia, Canada. Pollution Control Objectives for the Mining, Mine-Milling and Smelting Industries of British Columbia. Victoria, November 1973.

8. Dickson, F. The Effect of Copper on Rainbow Trout in the Presence of Taconite Tailing and Natural Sediments. Reserve Mining Co., Silver Bay, Minn., 1973.

9. Down, L. G., and J. Stocks. Environmental Problems of Tailings Disposal. Min. Mag., July 1977, pp. 25-33.

10. Ellis, D. V. Effectiveness of Exiting Pollution Controls as Shown by Four Case Histories; and Recommendations for Future Control. Brief presented to Pollution Inquiry, Victoria, B.C., January 1978. Available from British Columbia Pollution Control Branch, Victoria, B.C.

11. _____. Pollution Controls on Mine Discharges to the Sea. Proc. Internat. Conf. on Heavy Metals in the Environment, Toronto, 1975, (pub. 1977), pp. 677-685.

12. Environmental Canada. Mine and Mill Wastewater. Report EPS-3-WP-75-5, December 1975. Available from Environmental Canada, Ottawa

13. Evans, J. B., D. V. Ellis, and C. A. Pelletier. The Establishment and Implementation of a Monitoring Programme for Underwater Tailing Disposal in Rupert Inlet, Vancouver Island, B.C. Tailing Disposal Today, published by Miller Freeman, San Francisco, Calif., 1972, pp. 477-511.

14. Evans, J. B., and G. W. Poling. Discharging Flotation Mill Tailing Into a Coastal Inlet. Pres. at 77th Annual General Meeting of CIMM, Toronto, 1974.

15. Fisheries and Environment of Canada. Brief presented to the Pollution Inquiry Into the Mining, Mine-Milling and Smelting Industries of B.C., August 1977. Available from Environmental Canada, Ottawa.

16. Fisheries and Environment of Canada. Metal Mining Liquid Effluent Regulations and Guidelines. Rept. EPS-1-WP-77-1, April 1977 (in effect Sept. 1, 1977).

17. Glass, G. E. Identification and Distribution of Inorganic Components in Water; What to Measure. Ann. N.Y. Acad. Sci., v. 298, 1977, pp. 31-46.

18. Goyette, D., and H. Nelson. Marine Environmental Assessment of Mine Waste Disposed into Rupert Inlet, B.C. Fisheries and Environment of Canada, Rept. EPS PR-77-11, December 1977.

19. Hawley, D. Use, Characteristics and Toxicity of Mine-Mill Reagents in Ontario. Ministry of Environment Pub., Toronto, 1972.

20. Kopp, J. F. The Occurrence of Trace Elements in Water. Proc. 3d Conf. on Trace Substances in Environmental Health, Univ. Missouri, Kansas City, June 1969. Copies may be obtained from Interlibrary Loan Dept., Univ. Missouri Library, Kansas City, Mo.

21. Lee, G. F. Chemical Aspects of Bioassay Techniques for Establishing Water Quality Criteria. Water Res., v. 7, 1973, pp. 1525-1546.

22. Lee, G. F., and G. R. Lanza. Significance of Sediment Associated Contaminants in Water Quality Evaluation. Center for Envir. Studies, Univ. Texas at Dallas, Occasional Paper No. 11, 1978.

23. Lee, G. F., J. M. Lopez, and G. Mariani. Leaching and Bioassay Studies on the Significance of Heavy Metals in Dredged Sediments. Proc. Internat. Conf. on Heavy Metals in the Environment, Toronto, 1975 (pub. 1977), pp. 731-764.

24. Lesaca, R. M. Monitoring of Heavy Metals in Philippine Rivers, Bay Waters and Lakes. Proc. Internat. Conf. on Heavy Metals in the Environment, Toronto, 1975 (pub. 1977), pp. 285-307.

25. Mining Association of British Columbia. Brief presented to the Pollution Inquiry Into the Mining, Mine-Milling and Smelting Industries of British Columbia. Victoria, B.C., January 1978. Available from Pollution Control Branch, Victoria, B.C.

26. Mining Congress Journal. Costs of Complying with the Federal Water Pollution Control Act. V. 62, No. 10, October 1976, pp. 75-78.

27. Morgan, W. S. G. The Use of Fish as a Biological Sensor for Toxic Compounds in Potable Water. Prog. Water Technol., v. 10, No. 1-2, 1978, pp. 395-398.

28. Pelletier, C. A. Marine Tailings Disposal at Island Copper Mine, Rupert Inlet, B.C. Pres. at 74th Canadian Inst. Min. Annual Meeting, Ottawa, April 1977.

29. Peterson, C. R., H. V. Warren, R. E. Delavault, and K. Fletcher. Heavy Metal Content of Some Fresh Water Fishes in British Columbia. Fisheries Tech. Circ. No. 2, B.C. Fish and Wildlife Branch 1-34, 1970.

30. U.S. Environmental Protection Agency. Quality Criteria for Water. Rept. EPA-440/4-76-033, Washington, D.C., July 1976, p. 501.

31. University of British Columbia Press. The Practical Application of Economic Incentives to the Control of Pollution: The Case of British Columbia. Vancouver, 1977.

32. Walpole, J. R. Ore Mining and Dressing Effluent Guidelines - To BPT or Not to BPT. Min. Cong. J., v. 64, No. 2, February 1978, pp. 81-91.

33. Webb, M., H. Ruber, and G. Leduc. The Toxicity of Various Mining Flotation Reagents to Rainbow Trout. Water Res., v. 10, 1976, pp. 303-306.

34. World Mining. Tailing - Canadian Regulations and Practice, Marine Disposal Systems. V. 31, No. 5, May 1978, pp. 58-62.

INDUSTRIAL FLOTATION RESEARCH AND ITS INTERFACE WITH ACADEMICS

by

Nathaniel Arbiter[1]

The concept of an interface between industrial sulfide flotation research and practice and its academic counterpart presupposes a contact between the entities and, more important, a transfer of ideas across the boundary. My thesis will be that the contacts between the two disciplines have so far been inadequate and that the transfer of ideas has so far been a rare event.

Before coming to grips with the main problem, it is appropriate to review briefly the situation in each camp. Flotation practice is now 70 years old. It was born out of chance observations and empiricism, and its growth and development have continued along the same path. The principal areas of improvement have been in the proliferation of reagents both as to functions and effectiveness; in some improvements in flotation machinery, mainly toward increased simplicity of design and maintenance, and increasing size of units; and more recently, in increased availability of equipment for, and understanding of, control of the process.

With specific respect to flotation chemistry, there has been progress from the original "oily collectors," with their chance surface-active contaminants, through less selective chemical individuals, such as fatty acids and reconstructed acids, to xanthates and then dithiophosphates. More recently, a greater diversity of sulfide collectors has become available, the latest being the long-chain mercaptans.

Recent developments of new auxiliary reagents apart from frothers have been insignificant. It is safe to say that there has been nothing new in activation or depression of sulfides by inorganic cations, anions, or by pH control in decades. The use of organic depressants, even though many are available, is uncommon.

The major recent change in chemistry has been the shift from the natural frothers, pine oil and cresylic acid, toward the synthetic alcohols and the polypropylene glycols, with the gains primarily in selectivity.

---

[1] Professor emeritus, Krumb School of Mines, Columbia University; and group consulting metallurgist (retired), the Anaconda Co.

It is difficult to refrain from the old truism that each sulfide ore presents its own problems, mainly because of unique and variable physical associations of sulfide minerals, degrees of oxidation of sulfides, and variations in gangue minerals. Prolonged testing is usually necessary to bring out differences due to reagents, and the realizable improvements from this source become marginal because the easy gains are soon made.

Trends for the future are inevitably toward lower grade feeds and toward more complex intergrowths of sulfides, with more dilution by pyrite and pyrrhotite, and with finer grinding necessary because of finer dissemination. It is well established that peak flotation rates are in the 50 μm to 100 μm particle-size range, with an abrupt decrease above 150 to 200 μm and a gradual decrease below 50 μm. These effects are for physical reasons, and while they can be counteracted in part by increasing the intensity of the chemical environment, there will be a compensating loss in selectivity. Recoveries in the minus 10 μm fractions are invariably lower than in coarser sizes due to a combination of oxidation and physical effects. With the expected trends for the future, losses in fines can become a more serious problem.

For the long range viewpoint, industrial needs can be summarized as: optimizing sulfide mineral/collector response to obtain optimum particle-bubble adhesion with minimum solution levels of collector. This requires integrated knowledge of effects of collector structure, collector adsorption, and surface oxidation, among other variables. At the same time, there is needed a better understanding of fine-particle flotation dynamics, particularly with respect to whether conventional flotation equipment has inherent limitations for fine particle recovery; whether selective flocculation by collectors overcomes this wholly or partly; or whether selective flocculation by polymers with or without collectors, and by separation technology other than flotation, may be more effective. I will not consider here the area of control and automation except to mention that although U.S. industry is beginning to adopt the technology, most of the developments in hardware and control principles are coming from Australia, Finland, Canada, and South Africa.

The important question is who is doing what to improve industrial performance. There are three potential sources of activity: the mining companies; their suppliers, particularly chemical companies who develop and manufacture reagents; and the "third force," which includes universities, government laboratories, and the miscellany of private testing and developmental organizations who seek industry or government funds for short- or long-range projects. As a sample of recent activities, the Gaudin Memorial volumes provide interesting information.

Of the 22 papers in volume one on Fundamentals, only three are from industrial research laboratories; the remainder are from university or government laboratories. And there is room to question whether the industrial papers should be considered fundamental. Each concerns an already developed flotation process, and each seeks an explanation based on surface chemistry, but each is of limited fundamental significance. In volume two with 26 papers, 10 are from mining companies, all dealing with plant descriptions. The remaining 16, dealing with process dynamics, plant control, and nonmetallic plants, are from university or governmental laboratories or from equipment manufacturers.

If we look abroad, the same distributions are evident. In Western Europe, fundamental research comes from universities; less fundamental and to a lesser extent from government establishments. Mining companies, through patents and publications, are contributing to process development and flotation machinery. In the communist countries, while there is no distinction between government and industry, and although most research is carried out in government research institutes as opposed to universities, there is still a clear distinction between the research function and operations.

In Australia and South Africa, major research and development activities are centered in the governmental establishments, CSIRO and NIM, from which significant basic and applied work is coming. In both countries, in more theoretical areas such as surface chemistry and in kinetics, as well as in process modeling and control philosophy, the universities are active, with industry participating through financial support. A notable example of this is the Julius Kruttschmitt Metallurgical Centre at the University of Queensland with NIM Holdings Ltd., a major supporter, and with additional support through projects by 10 or more mining companies.

We see worldwide then a clear differentiation in function: the metallurgical industry helps to design and construct and then operates its plants; its research departments, mainly in the largest companies, are concerned with short-range problems in existing operations; with process development for new operations, usually involving modifications of existing technology; and very rarely with developing entirely new technology. As to fundamental research, it is safe to say that none is carried out anywhere by industry, and it is only occasionally supported by industry, with the universities and a few government laboratories carrying the burden.

What are the implications of this clearcut separation between functions--that is, between process development as industry's main and exclusive concern and research into fundamentals is restricted to the university and government laboratory? To answer this question we need to consider both motivation and methodology. The goal of industry is to produce at a profit in capitalist countries and to fulfill national needs in a communist country. The motivation for pure research is first to understand, and hopefully thereafter to put such understanding to use. As already noted, industrial research applies known technology or develops new technology and, most important, works almost exclusively within the unit operation and process framework. Flotation, as with any unit operation, is studied in laboratory or pilot plant models, or in the full-scale industrial setting. Rarely or never are the process elements isolated for study.

By contrast, in the pure research area, where flotation is concerned, extreme simplification is the rule: miniaturized systems, using single, pure minerals, and often single particles and bubbles. And often, the systems studied do not involve flotation at all but are isolates; properties of minerals; mineral/electrolyte potentials; flow potentials; adsorption equilibria; and wettability in the abstract.

We can now describe the interface I was asked to consider. I have struggled with this question for about 40 years and have arrived at different answers at different times, as have others. Permit me to give the evolution of my answers in order to illustrate how I arrived at my present position. When I first started teaching after about 8 or 9 years in industrial research, and in reaction to the constraints of the industrial environment, I felt there was no need to justify fundamental academic research. I felt with Whitehead that the function of the university need only be the "imaginative consideration of knowledge." And if one needed justification as to relevance in preparing students for an industrial career, it was that the discipline required in planning, carrying out, and analyzing rigorous fundamental research was justification enough. Men so trained were better prepared for less abstract work in the industrial arena than they would be without such training.

But then I developed misgivings in that I felt that engineers, even as part of a university faculty, still had obligations to the industry they represented; and that their research directions ought to be more closely related to current industrial problems. I therefore moved toward studies of process kinetics and analysis of process machinery, with some indications in the late 1950's and early 1960's that these studies could be valuable in improving machinery and aiding in process automation. On returning to industry in the late 1960's, I found that this experience was of value, ironically, not so much in flotation but in developing new leaching technology. But still more recently, the engineering science approach is being used by some of the flotation machine manufacturers in designing the largest cells.

In the past few years, I see new directions in sulfide mineral physics and chemistry which give me a sense of optimism and of confidence that an active interface is now in the making between the research sector and industry in this area as well. In particular, work on the electrochemistry of the sulfide/electrolyte interface, on the subtle role of oxygen in the natural flotability of the sulfides, and on the semiconductor properties of the sulfides is leading both to a more penetrating understanding of problems in hydrometallurgy and flotation, and, I am convinced, can lead to major advances in both fields.

To illustrate and to bring my discussion to a close, let me give you an example drawn from my own experiences. Until recently, in attempting to solve flotation problems, we have often been able to draw on our general physical chemistry background but have rarely if ever found use for specific theoretical research. In reading the proceedings of the recent Fourth Australian Electrochemistry Conference (2), I was pleased to find a clear theoretical explanation for a phenomenon that had puzzled me for 20 years.

The problem involved the exceptionally low lead recovery obtained by flotation of a fine-grained massive sulfide ore from New Brunswick. Pilot plant operations for over a year were able to obtain only a 40-percent lead recovery. Very fine grinding was required to obtain even a partial liberation of the galena from pyrite, but this alone could not account for the low recoveries.

Although oxidation is usually not a problem with lead ores, this possibility was eventually considered. Comparison by ammonium acetate leaching of ore freshly broken from mine faces with pilot plant feed ore which was stockpiled for 2 months showed that 20 to 30 percent of the galena had been oxidized in the coarsely broken rock. With ground flotation feed, all of the galena could be oxidized by alternate cycles of wetting with ammonium acetate solution and aeration on a filter. With such rapid oxidation indicated, the solution was clear; elimination of stockpiling and collector addition to the grind raised lead extractions to 80 percent.

But why such rapid oxidation? The papers by Peters (3) and Biegler, Rand, and Woods (1) indicate that pyrite will act as an oxygen electrode with a half-cell potential of 0.340 volt. Galena of all the common sulfides is most anodic with respect to pyrite: galvanic coupling of the two minerals results in oxygen reduction on pyrite, and oxidation of the sulfide in galena. For the same reason, the intimate physical contact of galena encased in pyrite should give the same effect by direct electron transfer between the two minerals.

Although this electrochemical explanation was very much post facto, such advances are for the first time placing theoretical studies in sulfide chemistry in a position to predict, instead of, as they have in the past, always being in a position of attempting to explain what industry knew very well how to do without explanation. Once we are in a position to propose new processing technology based on physicochemical fundamentals, we will have a true interface with permeability in both directions. And based on the developments in sulfide mineral physics and chemistry within the past few years, I am confident that we will be in just such a position within a very short time.

REFERENCES

1. Biegler, T., D. A. J. Rand, and R. Woods. Oxygen Reduction on Sulfide Minerals. Ch. in Trends in Electrochemistry, ed. by J. O'M. Bockris, D. A. J. Rand, and B. J. Welch. Plenum Press, New York, 1977, pp. 291-302.

2. Bockris, J. O'M., D. A. J. Rand, and B. J. Welch, eds. Trends in Electrochemistry. Plenum Press, New York, 1977.

3. Peters, E. Electrochemistry of Sulfide Minerals. Ch. in Trends in Electrochemistry, ed. by J. O'M. Bockris, D. A. J. Rand, and B. J. Welch. Plenum Press, New York, 1977, pp. 267-290.

SELECTIVE FLOCCULATION OF FINES

by

P. Somasundaran[1]

ABSTRACT

Selective flocculation, followed by a conventional mineral processing technique such as flotation, elutriation, or sedimentation, is a promising technique for the beneficiation of mineral slimes. In this paper, a review of basic chemical and hydrodynamical aspects of dispersion, flocculation, and selective flocculation is presented along with a discussion of mechanism of adsorption of polymers with functional groups. Selective flocculation achieved in the past with sulfide minerals and the problems involved are also discussed.

INTRODUCTION

In spite of the ever-increasing demand for mineral products, large amounts of fines and ultrafines generated during mining and milling are discarded today, mainly because of the inadequate technology for fines beneficiation. We are familiar with the incredible loss of mineral values as slimes in the nonmetallic minerals area. In the metallic minerals area also, there is considerable loss of mineral values as fines even though in a number of cases fines have been claimed to be treated successfully. The Climax mine of Amax is reported, for example, to have achieved a recovery of 90 pct in their flotation of 85 pct minus 44 µm feed of molybdenite ore, but it is to be noted that the loss is mostly in the minus 5 µm size fraction (5, 9). In the case of Pentlandite/pyrrhotite flotation, on the other hand, G. E. Agar in a personal communication has indicated that there is hardly any beneficiation obtained in the minus 20 µm size range. Data collected by Trahar and Warren (38) on the dependence of flotation of sphalerite particles on particle size, in both operating mills and the laboratory (fig. 1), clearly show that the recovery becomes poor where the particles are smaller than about 10 µm.

---

[1] Henry Krumb School of Mines, Columbia University.

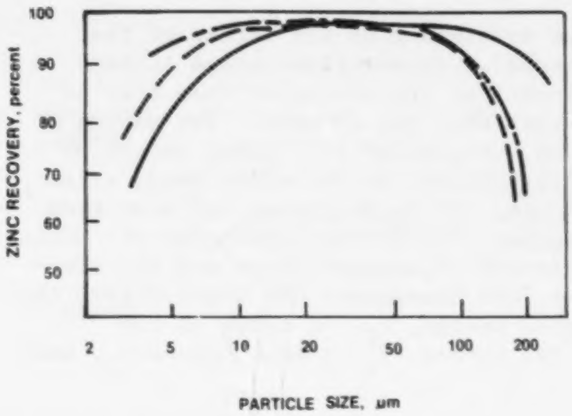

FIGURE 1. - Comparison of the batch flotation of sphalerite with data from operating mills. Batch flotation (— · — ·), Anthony et al., zinc circuit at Broken Hill South (—), (Cameraon, et al., 1979); zinc circuit at Morning Mill (---), (Gaudin, et al., 1931). (After Traher and Warren (38). *Courtesy, Elsevier Scientific Publication Co.*)

A similar effect has been observed also for lead and copper recoveries. In general, recovery of sulfide ores in the minus 20 µm size range is lower than that in the 100 by 20 µm range; this is due partly to lower floatability of fines, generally observed in all flotation systems. N. Arbiter, in a private communication, has also suggested that the lower floatability of fines is partly due to the higher oxidation of such fines.

The optimum size range for flotation does depend to a great extent on the nature of the mineral. Trahar and Warren (38) report that for sulfides the size range of maximum recovery increases in the order, galena (6-70 µm), sphalerite (8-90 µm), pyrrhotite (9-40 µm), chalcopyrite (15-60 µm, arsenopyrite (15-120 µm), and pyrite (20-150 µm). Specific gravities of these minerals (7.4-7.7, 3.9-4.1, 4.6, 4.1-4.3, 5.9-6.2, and 4.95-5.1, respectively) do not show any significant correlation with the minimum or maximum limit of the optimum size range for flotation. Evidently the fines, due either to their smaller size or to changes in their surface composition and properties, respond poorly to flotation, resulting in loss of mineral values that we can ill afford. If the reason for the decreased efficiency of fines flotation is the smaller size and the resultant lower collision and adhesion rates, the obvious solution is to aggregate the fines into coarser particles. Even if surface chemical changes such as oxidation are responsible, aggregation of the fines before such preflotation treatments as sulfidization might still be beneficial.

BACKGROUND

Fundamentals of Selective Aggregation

For selective aggregation, first of all it is necessary that at least one component is in complete dispersion. It is also necessary that there is a maximum possibility for aggregation among the particles of the other component, with very little aggregation between the particles of the components themselves. Conditions for this become evident when one examines the properties that govern interactions between the particles.

Colloidal particles in a system collide due either to Brownian motion or to external forces introduced by agitation, magnetic field, etc. Probability of adhesion during such collision will be determined by the nature of the total interactions between them. The repulsive interactions arise either from the overlap of similarly charged electrical interfaces or from that of adsorbed layers that prefer to be in contact with the solvent. The nature of repulsive interactions is, for this reason, determined to a great extent by the nature of the medium. Attractive interactions, on the other hand, arise from London dispersion forces, Keesom forces, and Debye forces and also from the steric compatibility between the adsorbed layers; the London-Van der Waals forces are not so much dependent on the nature of the medium as are the electrostatic forces. In accordance with the DLVO theory and HHF theory (14), the following expression is given for the total energy, V_T, in terms of the London-Van der Waals forces, V_V, electrical forces, V_E, steric forces V_S, and bridging forces, V_B:

$$
\begin{aligned}
V_T &= V_V + V_E + V_S + V_B \\
&= \frac{-A r_1 r_2 \alpha}{6(r_1 + r_2)H_o} + \frac{r_1 r_2 \varepsilon}{4(r_1 + r_2)}\left[2\psi_1\psi_2 \ln\frac{1 + \exp(-\kappa H_o)}{1 - \exp(-\kappa H_o)}\right. \\
&\qquad \left. + (\psi_1^2 + \psi_2^2)\ln\{1 - \exp(-2\kappa H_o)\}\right] + V_S + V_B \qquad (1)
\end{aligned}
$$

where r_1 and r_2 are radii of the two particles, ψ_1 and ψ_2 are surface potentials, and H_o is distance between their surfaces. A, the Hamaker constant, is the average for particles 1 and 2 in medium 3 and is given by $A = A_{12} + A_{33} - A_{13} - A_{23}$. ε is the dielectric constant, and $1/\kappa$ is the double layer thickness. α is a factor that takes into account the retardation of London forces under conditions of aggregation in secondary minimum (41). V_S can be positive or negative, depending on the solvent power of the medium for the adsorbed layer, and V_B can be considered to be always negative. Excluding V_S and V_B, it can be seen from equation 1 that V_T will be attractive at large and small distances, since the exponential of $-\kappa H_o$ will be smaller than the inverse power of H_o for large and small H_o. Typical variation of V_T as a function of distance between particles is illustrated in figure 2. The bottom curve is for particles with negligible electrical repulsion between them and the upper curves for conditions with increasing amounts of repulsion between the particles. On the basis of these considerations of total energy, we can derive the following conditions for selective aggregation:

1. Both type of particles should carry the same charge so that there will be no heterocoagulation between them. Repulsive energy should be larger in magnitude than the attractive energy.

2. Charge on the particles to be aggregated should be such that repulsive energy between them should be less than that of the attractive energy.

Conditions 1 and 2 can be met if the potential of the component to be aggregated is in the range of ± 10 to 20 mv and the potential of the other

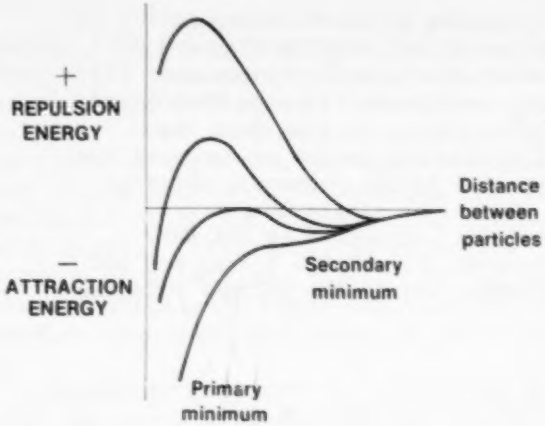

FIGURE 2. - Sum of repulsive and attractive interactions between particles as a function of distance of separation between them under various conditions.

component is about 40 or 50 mv with the same sign for the potential as that of the first component. This can be achieved by appropriate control of the ionic composition of the medium. Aggregation achieved in this manner is called selective coagulation as opposed to selective flocculation that is achieved normally with the help of polymers.

3. Polymers when adsorbed on the particles can essentially shift the surface of contact between them so that the electrical nature of the interfaces, which might not have been originally conducive for selective aggregation, assumes a secondary role. Evidently success of the use of polymers will depend upon selective adsorption on the mineral particles to be flocculated.

A major factor that affects the selectivity of the aggregation is the interference by the dissolved chemical species of one particle on account of either its adsorption or precipitation on the others. The significance of this effect was clearly shown recently by the authors for the calcite/apatite/oleate system (1). Smearing of one component on the other during grinding will also certainly reduce selectivity.

Adsorption of Polymers and Flocculation

The fundamentals of adsorption of polymers and its role in flocculation have been recently reviewed by Sresty and co-workers (35), and salient aspects of their review are presented here. Adsorption of polymers on minerals and the rate involved are dependent to a large extent on the polymer properties such as the molecular weight, the nature and concentration of the functional groups and configuration, the mineral properties such as surface charge and oxidization state, and the solution properties such as ionic strength and solvent power for the polymer. This dependence of adsorption on properties of polymer, particles, and solution can be exploited in the beneficiation of slimes using selective flocculation.

Forces responsible for polymer adsorption arise mainly from electrostatic, hydrogen, and covalent bonding. In the case of a polymer with a large number of charged units, electrostatic bonding is the predominant mechanism. The role of electrostatic forces are illustrated in figure 3, which shows the results obtained in our study of flocculation response of negatively charged synthetic silica (Biosil-A) to anionic (Separan AP-30) and cationic (Nalcolyte-610) polyacrylamides[2] (35). As can be seen from the figure, silica particles undergo excellent flocculation in the presence of the cationic polymer. The stability of the suspension is not, however, affected by the anionic polymer. A polymer can also flocculate similarly charged particles provided the magnitude of the interfacial potential is not very high (34). Under such conditions, the electrostatic repulsive forces are not strong enough to prevent the particles from coming within the polymer bridging range of each other.

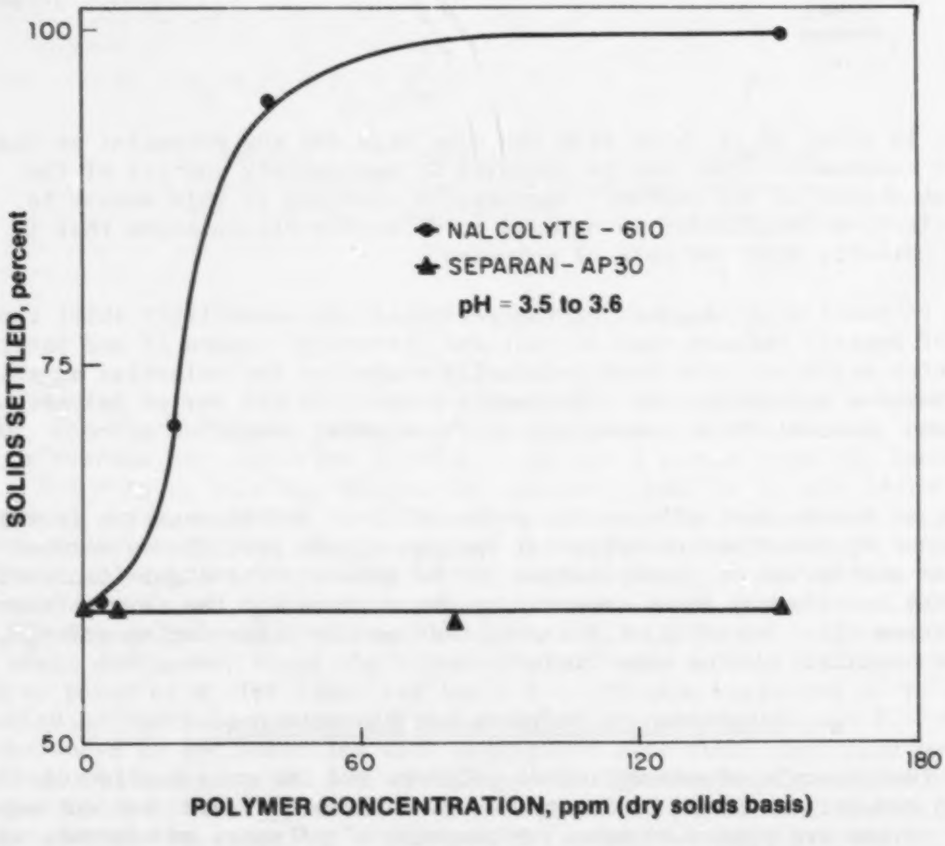

FIGURE 3. - Percentage of synthetic silica settled as a function of concentration of Nalcolyte-610 and Separan AP-30; reagentizing time, 30 seconds; settling time, 45 seconds (35). (*Courtesy, CRC Press.*)

---

[2] The suspension was conditioned with polymer for 30 seconds and allowed to stand for 45 seconds. The weight-percent of solids that settled into the bottom one-third volume fraction of the original suspension is taken as a measure of the flocculation. Additional experimental details are given by Gaudin and Malozemoff (11).

The role of electrostatic adsorption in the selective flocculation of galena from some other minerals has been discussed by Yarar and Kitchener (42). They noted that galena flocculation using an anionic polyacrylamide can be promoted by the addition of lead nitrate and inhibited by addition of sodium sulfide. Most interestingly, it was also observed that galena dried in contact with air did not undergo selective flocculation from quartz, presumably due to the fact that in a medium containing oxidized lead salts, the zeta potential of galena will be zero and hence it can also undergo coagulation with quartz. Similarly, no selective flocculation could be obtained with a mixture of galena and calcite in the absence of other additives, since the zeta potentials of these minerals are not sufficiently high at natural pH to produce required dispersion of fines prior to selective flocculation.

Nonionic polymers can adsorb on particles by formation of hydrogen bonds with the surface oxygen species of the mineral. Flocculation by interparticle bridging follows such adsorption of polymers when the electrical double layer repulsion between the particles is not very strong.

Selective adsorption of polymers can also be achieved if adsorption is due to covalent bonding between the active groups of the polymer and the cations of the mineral surface. Such flocculation of kaolin by polyacrylamides owing to the formation of salt-type compounds by reaction between the polymer and the Ca^{+2} ions present in the kaolin has been reported by Michaels and Morelos (24).

Kinetics of Adsorption

The kinetics and nature of adsorption of polymers on particles are dependent on a number of interrelated properties of the polymer, the suspending medium, and the particles (23).

The kinetics of adsorption of polymeric molecules on mineral particles are controlled mostly by the rates of diffusion of these molecules to the surface of the particles and are, therefore, influenced by agitation.

We have observed that even the concentration of the polymer has a major role in determining the kinetics of its adsorption (see fig 4) (26). The

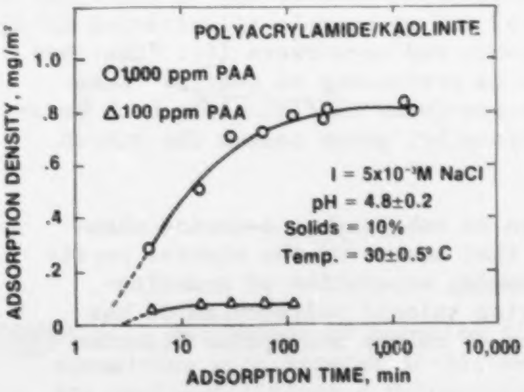

FIGURE 4. - Adsorption kinetics of polyacrylamide on kaolinite (26).

suspending medium, being a solvent for the polymer molecules, has a very important role in determining rates of adsorption of these molecules on the suspended mineral particles.

When a poor solvent is used, the rate of adsorption of the polymer is greater, owing to the weak interaction between the polymer molecules and the solvent. The kinetics and extent of adsorption are dependent also on the specific surface area and chemical nature of the particles. Adsorption rates are lower for porous particles with large specific surface, and equilibrium is, therefore, established slowly (18, 37).

Selective Adsorption and Flocculation

Selective adsorption of polymer molecules on particles can be achieved by (1) adjusting the chemical composition of the suspending medium (determines surface charge on the mineral) in order to exploit the dependence of adsorption of ionic polymers on surface charge, (2) introducing into the polymer active functional groups that will form complexes or salts with the metal atoms on the surface of the desired mineral, and (3) using depressants such as sodium silicate that would adsorb on the undesired mineral surface, thereby preventing adsorption of polymer, or using activators that induce adsorption of polymers on desired minerals.

Kuzkin and Nebera proposed that adsorption of ionic polymers on similarly charged mineral surfaces cannot take place if the interfacial potential is sufficient to introduce electrostatic repulsions arising from double layer interactions (19). A noteworthy example of the application of this principle is the selective flocculation of hematite from its mixtures with quartz using anionic polyacrylamide (30). Even though adsorption of the polymer on quartz particles is expected on account of the dominance of amide groups in it, the strong electrostatic repulsion between negatively charged quartz particles and the polymer apparently prevented its adsorption on quartz surface.

It is well known that adsorption of froth flotation collectors and modifiers on particles depends on active groups present in the collector or modifier molecules. The chemical aspects of polymer adsorption are, in several ways, similar to those of collectors. Thus in the past, selectivity has been obtained by incorporating active groups such as carboxylate, sulfonate, and mercaptan (2-4, 16). Incorporation of an improper active group, on the other hand, can also result in loss of selectivity, and an example illustrating this is that of modified starches discussed by Cooke and co-workers (4). Starches have been well known to flocculate hematite in preference to quartz. Cornstarch modified to contain aminoethyl group was found to flocculate both hematite and quartz, because the presence of aminoethyl group causes the starch to adsorb on quartz particles as well.

Response of minerals to flocculation can be enhanced or retarded when necessary by the addition of metal cations that adsorb on the mineral particles and activate or depress them. For example, separation of hematite-quartz mixture by selective flocculation using anionic polyacrylamide has been reported to be effective after addition of calgon and sodium fluoride (31).

Also Attia and Kitchener have reported the possibility of depressing flocculation of heavy minerals by xanthates using depressants such as sodium sulfide, polyphosphates, and polyacrylates (2).

Interparticle Bridging and Surface Coverage

Interparticle bridging, preceded by adsorption of polymer species, results in the progressive buildup of the fine particles into three-dimensional networks. A complete surface coverage of the particles by polymer molecules is reported to result in stabilization of the suspension by protected colloid action (17, 23). Stability of suspension resulting due to complete coverage of the particles by adsorbed polymer molecules is called steric stabilization and can be avoided only if the net change in Gibbs free energy due to interpenetration of the polymeric chains is negative (25). For flocculation to proceed, the increase in entropy due to release of solvent molecules should outweigh the loss of entropy due to interpenetration of polymeric chains and increase in enthalpy due to increased degrees of freedom attained by the released solvent molecules.

The fraction of solid surface covered by polymer molecules is dependent on the time of reagentizing of the mineral with the polymer solution at a given polymer concentration. Figure 5 shows the flocculation response of hematite towards Separan AP-30 as a function of time of conditioning the mineral with the polymer solution (36). Results shown in this figure indicate that the

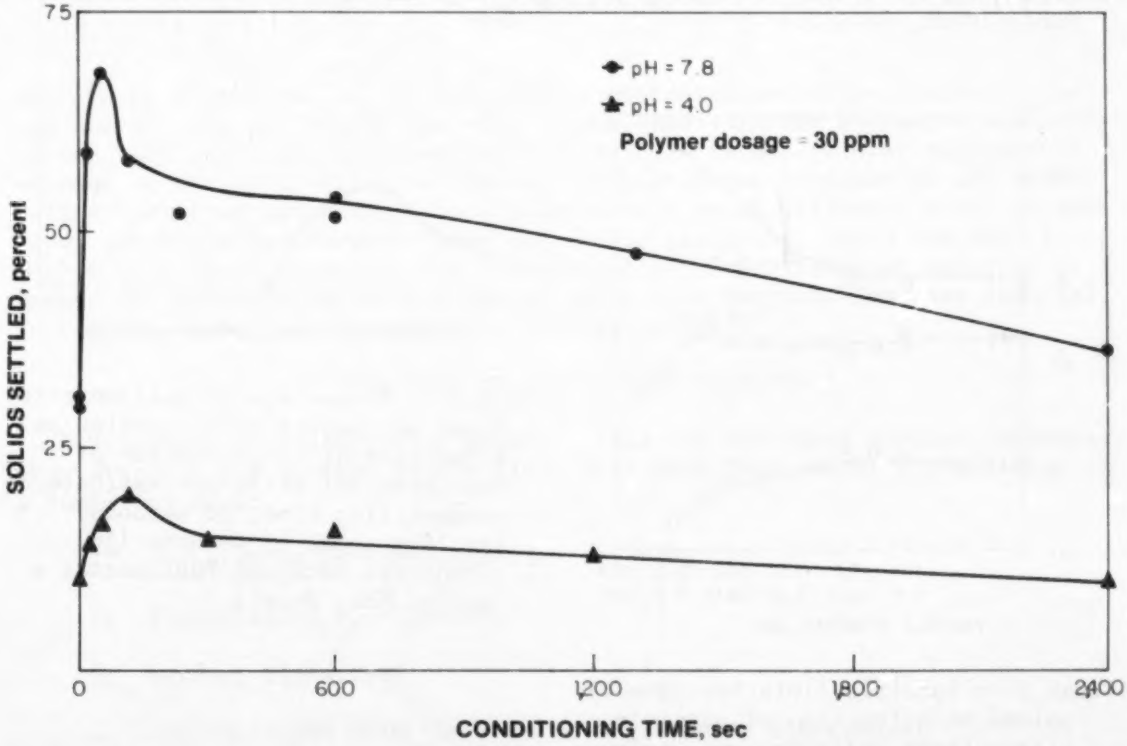

FIGURE 5. - Percentage of hematite fines settled as a function of time of reagentizing with Separan AP-30; settling time, 45 seconds (36). (*Courtesy, Nacional-Publicacoes e Publicidade, Brasil.*)

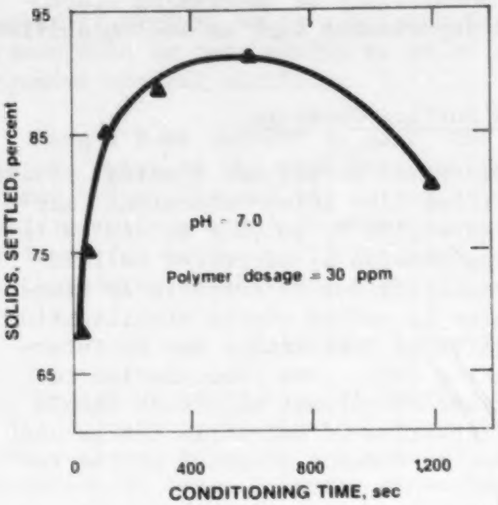

FIGURE 6. - Percentage of quartz fines settled as a function of time of reagentizing with Separan AP-30; settling time, 45 seconds (36). (*Courtesy, Nacional-Publicacoes e Publicidade, Brasil.*)

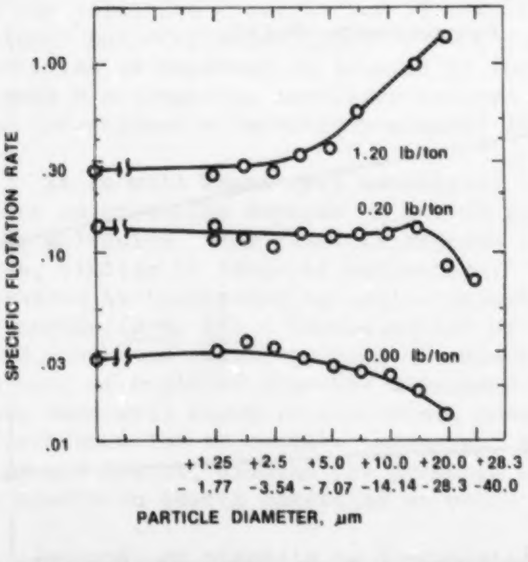

FIGURE 7. - Specific flotation rate of galena as a function of particle size without collector and at two concentrations of potassium ethylxanthate (12). (*Courtesy, American Chemical Society.*)

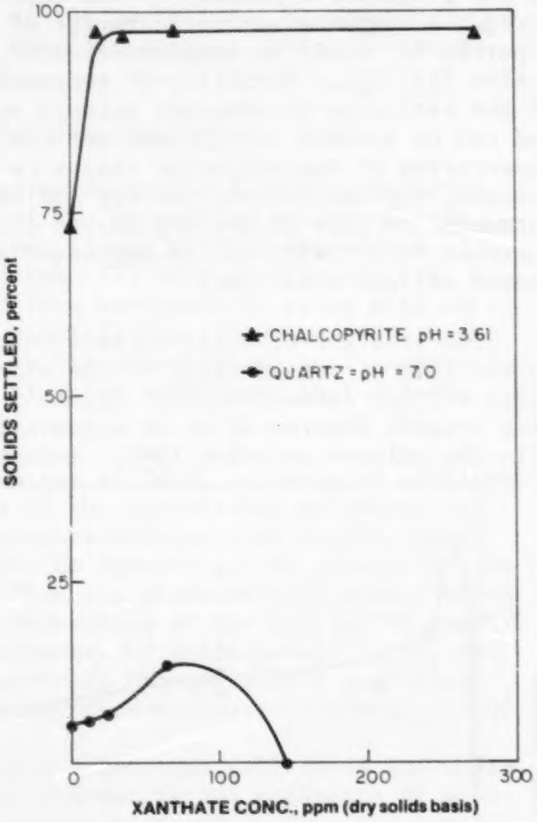

FIGURE 8. - Percentage of chalcopyrite fines and quartz fines settled as a function of concentration of hydroxypropyl cellulose xanthate; reagentizing time, 30 seconds; settling time, 45 seconds (36). (*Courtesy, Nacional Publicacoes e Publicidade, Brasil.*)

metastable state corresponding to maximum flocculation is reached within short periods of reagentizing. Prolonged reagentizing causes redispersion of the flocculated mass. In the case of quartz, however, maximum flocculation is obtained only at relatively longer periods (fig. 6). Such differences in time for maximum flocculation can be used profitably in achieving selective flocculation.

The interparticle bridging might be more effective if polymer molecules have an extended chain conformation. Polymers generally assume a highly coiled conformation at their isoelectric points, and a slight excess of either the positive or negative sites can sufficiently extend the polymer chain; this might improve the polymer's ability to produce interparticle bridging.

Hydrodynamic Aspects

Under most practical conditions, the probability for adhesion during collision can be enhanced by providing sufficient kinetic energy by stirring. Flocculation assisted by such external forces is known as orthokinetic flocculation. Under turbulent conditions, particles undergo collisions with each other due either to diffusion while entrained in eddies or to inertia. For colloidal particles Levich's (20) theory predicts the collision rate under turbulent conditions, J_{turb}, to be

$$J_{turb} = 12\pi\beta r^3 n_i^2 \left(\frac{\varepsilon_0}{\nu}\right)^{1/2} \tag{2}$$

where β is a constant, n_i is the initial concentration of particles, ε_0 is the energy loss per second per unit volume, and ν is the kinematic viscosity. Warren (40) has examined the role of equation 2 in determining aggregation between particles of different radii. Of particular interest is his observation that even under conditions selected for equal collision rates between fines and fines and between fines and coarse particles, rapid coating of coarse with fines occurred. He concluded that probablility of adhesion is larger for collision between a coarse and a fine particle (as that expected in carrier flotation) than between fine particles.

SELECTIVE AGGREGATION OF SULFIDES

Selective flocculation of mineral fines, as mentioned earlier, appears promising for application in the finer size range and can be accomplished in a number of ways:

1. coagulation by inorganic electrolytes;
2. flocculation by polymers;
3. carrier flotation;
4. agglomeration with the help of hydrophobic substances.

To the author's knowledge, selective flocculation has been tried only with sulfides; hence, this method will receive emphasis here. However, other techniques have been successfully tried, at least on a laboratory scale, for oxides, and for silicates or salt-type minerals, and there is a need to determine their application for sulfides. For example, Pugh and Kitchener have obtained some selective coagulation in rutile/quartz and hematite/quartz systems by adjusting the pH and ionic strength so that only hematite or rutile coagulated (27-29). Similar coagulation has also been obtained for colored impurities from kaolin (15, 22). Beneficiation of clay using carrier flotation on a commercial scale by Engelhard Minerals and Chemical Corp. is well known (13). Very little is known, however, about the mechanism by which this process works, and without further research it is difficult to predict whether it would have any application in sulfide systems.

Agglomeration with the help of oil has been used by Puddington and coworkers for graphite, chalk, zinc sulfide, coal, iron ore, and tin ore in aqueous solutions (7, 33). In this process, the fines are tumbled in an aqueous solution containing an immiscible liquid to form capillary bridges between reagentized particles and causes their aggregation. In a similar process, Warren Spring Laboratory is reported to have obtained good separations from a lead/zinc ore (32) owing to hydrophobic bonding between reagentized slime particles. Here a slime fraction of the ore was dispersed by a combination of sodium silicate-sodium carbonate and a polyacrylate; the fraction was subsequently conditioned with copper sulfate, and then potassium amyl xanthate was added. Floccs formed were cleaned twice for improving the separation. Formation of floccs was attributed to similar reasons that gave Gaudin and Malozemoff (11) selective aggregation of galena slimes in the presence of xanthates. The observation by Gaudin and co-workers (12) that, below a critical particle size of 4 µm all particles of galena were floatable to the same extent (fig. 7) has in fact been attributed to flocculation of the fines.

Selective Flocculation

Selective flocculation has been successfully used during the last 2 years on a commercial scale for the beneficiation of low-grade iron ore by the Cleveland-Cliffs Iron Ore Co. (6) and for that of potash by a Cominco plant in Saskatchewan (32). While selective flocculation has been attempted on a laboratory scale for a number of nonsulfide minerals, investigation on its use for systems containing sulfides have been limited (2, 35-36, 39, 42). Usoni and co-workers (39), for example, have studied the separation of a number of metal sulfides such as galena and sphalerite from associated quartz using both nonionic and anionic polymers as flocculants. They found prediction of selective flocculation on the basis of the results from single-mineral tests to agree with the results obtained for pyrite-quartz and sphalerite-quartz mixtures using a nonionic polymer (Separan), but to fail for mixtures of galena-quartz and sphalerite-quartz using anionic Aerofloc or Hercules CMC and for the mixture of Smithsonite-quartz even with Separan--which had worked for all other mixtures (see table 1). The reason for this discrepancy is not known. This problem (analogical to that in the flotation area) needs careful and systematic study. Selective flocculation of galena

TABLE 1. - Predicted possibilities for selective flocculation of pyrite from its mixtures of various minerals and comparison with separation obtained with actual mineral mixtures (41)

Separable pair	Flocculant	Conc, g/l	pH	Separation obtained with mineral mixtures
Galena-quartz.	Aerofloc R 550.	10^{-2}	5	No
	......do.......	10^{-3}	7	No
	......do.......	10^{-2}	9	No
	Hercules CMC...	10^{-3}-10^{-2}	5	No
	......do.......	10^{-1}	7	No
	......do.......	10^{-2}-10^{-1}	9	No
	Separan NP 10..	10^{-3}	7	-
	......do.......	10^{-3}-10^{-2}	9	-
Pyrite-quartz.	Aerofloc R 550.	10^{-3}	7	-
	......do.......	10^{-1}	9	-
	Separan NP 10..	10^{-2}	9	Yes
Sphalerite- quartz......	Aerofloc R 550.	10^{-1}	5	No
	......do.......	10^{-2}	7	No
	......do.......	10^{-2}	[illegible]	No
	Hercules CMC...	10^{-2}	[illegible]	No
	......do.......	10^{-1}	7	No
	......do.......	10^{-2}-10^{-1}	9	No
	Separan NP 10..	10^{-3}	7	Yes
	......do.......	10^{-3}-10^{-2}	9	Yes
Smithsonite- quartz......	Aerofloc R 550.	10^{-2}	7	No
	......do.......	10^{-2}	9	No
	Hercules CMC...	10^{-1}	7	No
	......do.......	10^{-2}-10^{-1}	9	No
	Separan NP 10..	10^{-3}	9	No
Galena- calcite.....	Hercules CMC...	10^{-1}	7	-
	Nalco 600......	10^{-1}	9	-
Sphalerite (alope).....	Hercules CMC...	10^{-1}	7	-
	Nalco 600......	10^{-2}	7	-
	......do.......	10^{-2}-10^{-1}	9	-
Pyrite- calcite.....	Nalco 600......	10^{-2}	9	-
Smithsonite- calcite.....	Hercules CMC...	10^{-1}	7	-
	Nalco 600......	10^{-1}	9	-

from quartz and calcite has been obtained by Yarar and Kitchener (42). Selectivity was found in this case to depend significantly upon the ions present in the suspension. Presence of divalent cations such as Ca^{+2} or Cu^{+2} rendered quartz to flocculation with anionic polymer reagents.

As mentioned earlier, selective adsorption of the polymer is the key for the successful application of this technique. An obvious way to generate selectivity is by incorporating complexing or chelating agents. Attia and Kitchener (2) have made some interesting studies in this regard. They have considered the possibilities of synthesizing flocculants with chelating groups specific to each metal.

The selectivity of both short-chain and long-chain organic compounds containing mercaptan or thiol group in adsorption on sulfide minerals is well illustrated by the extensive use of xanthates as collectors for the flotation of sulfide minerals. Tests with hydroxypropyl cellulose xanthate (synthesized by reacting 1 mole of hydroxypropyl cellulose with 3 moles of carbon disulfide and 3 moles of potassium hydroxide) containing mercaptan as the active group was found in our work to produce good flocculation of chalcopyrite with little effect on quartz (see fig 8) (35-36). The results of tests with synthetic mixtures of these minerals are shown in figure 9 as a function of concentration of hydroxypropyl cellulose xanthate. Both grade and recovery of

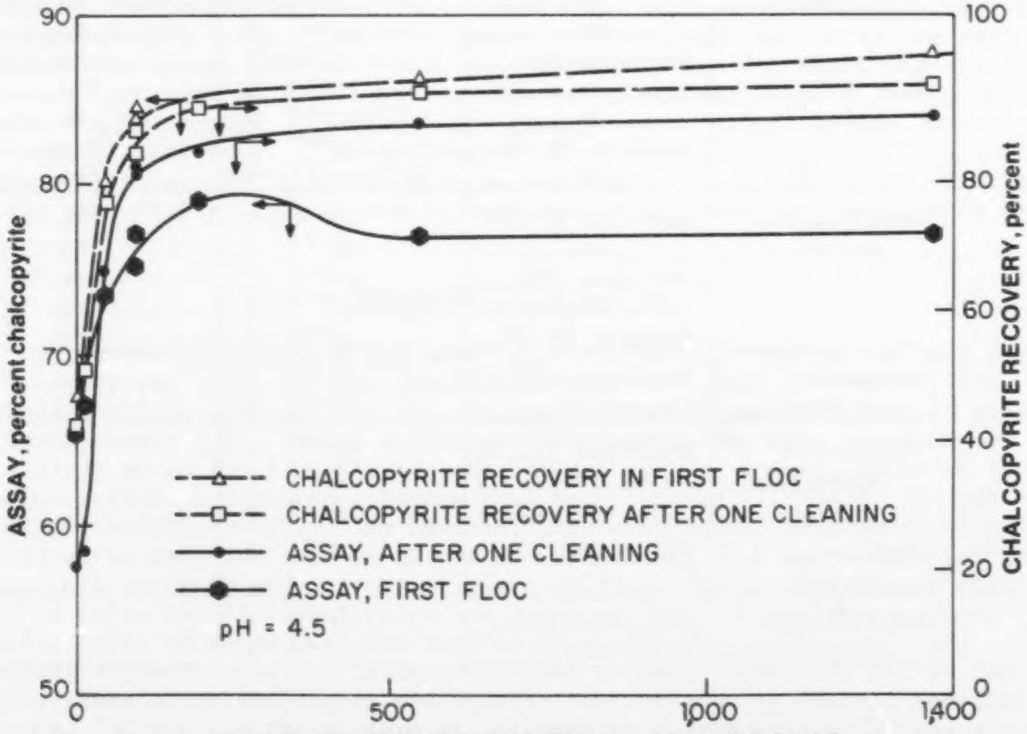

FIGURE 9. - Recovery and grade (chalcopyrite) of the concentrate from selective flocculation of chalcopyrite-quartz mixture as a function of concentration of hydroxypropyl cellulose xanthate; reagentizing time, 30 seconds; settling time, 45 seconds (35). (*Courtesy, CRC Press.*)

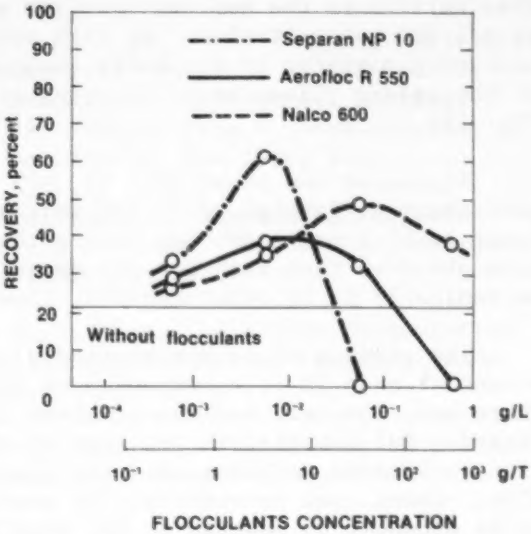

FIGURE 11. - Flotation recovery of sphalerite in the presence of different flocculants with potassium amylxanthate as collector and Dowfroth frother at pH 9 (39).

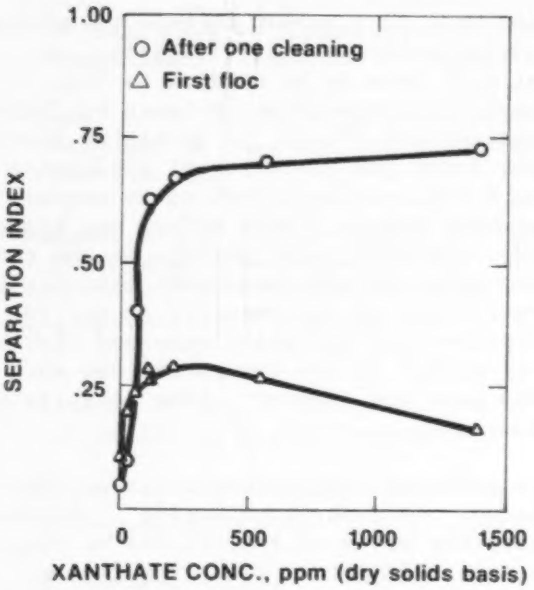

FIGURE 10. - Separation index achieved from selective flocculation of chalcopyrite-quartz mixture as a function of concentration of hydroxypropyl cellulose xanthate; reagentizing time, 30 seconds; settling time, 45 seconds.

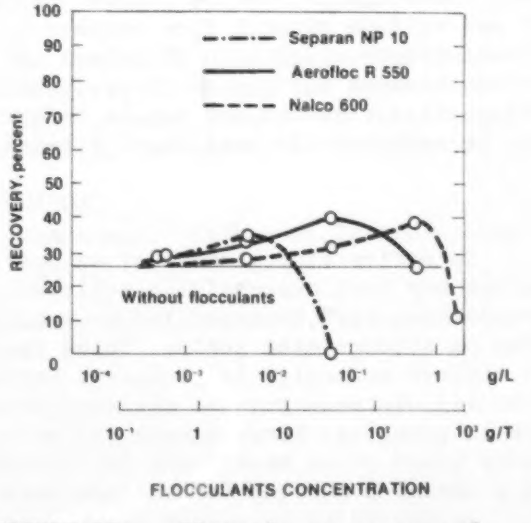

FIGURE 12. - Flotation recovery of sphalerite in the presence of different flocculants with potassium amylxanthate as collector and Dowfroth frother at pH 7 (39).

chalcopyrite in the sediment portion were observed to improve with increase in polymer concentration. At high concentrations of polymer, however, entrapment of the quartz by the bulky chalcopyrite flocculants did cause a lowering of the assay. Cleaning of the product improved the grade of sediment (see fig. 10).

Kitchener and co-workers (8, 42) and Read (30) have also considered the entrapment of foreign particles in the interstices of the selectively flocculants to be a major problem facing the successful use of this technique. They have observed that such trapped material can be released by gentle agitation mechanically or by countercurrent flow of washwater in an elutriator.

The process of selective flocculation does thus appear to hold tremendous potential when it is accompanied by flotation, elutriation, filtration, etc. There are, however, various problems that will have to be studied in this regard. For example, in the case of selective flocculation followed by flotation, polymeric reagents used for flocculation can affect the flotation operation. Usoni, and co-workers, for example, found the flotation of sphalerite to be enhanced by Separan NP 10, Aerofloc R 550, and Nalco 600 up to certain concentrations and to be depressed above those levels. This effect was higher at pH 9 than at pH 7 (see figs. 11 and 12). Possibly the increase at low concentrations is due to a fractional surface coverage and consequent flocculation. A more complete coverage at higher concentrations can be expected to retard flocculation and possibly collector adsorption on the particulates and thereby flotation. The reasons for the activating effect at low concentrations and depressing effect at higher concentrations have not, however, been established, and the problem warrants a systematic study.

Also, selective separation between various sulfide minerals has not yet been investigated, to the author's knowledge. As much as selective flotation of one sulfide mineral from another is possible owing to specificity of functional groups at certain pH values and reagent additions, selective flocculation between various sulfides should also be possible. However, both basic and applied research are needed before the technique of selective flocculation can be successfully used for the beneficiation of sulfides.

CLOSING REMARKS

Selective flocculation of oxides from oxides as well as of sulfides from oxides has been successfully achieved using polymers into which functional groups have been incorporated on a laboratory scale and, in the former case, also on a commercial scale. Using the same principle, it should be possible to achieve selective flocculation between sulfide slimes also. An understanding of the nature of the specificity of various polymers to sulfides and the interactions between such polymers and collectors and the related mechanisms would prove beneficial for the development of the selective flocculation as a useful technique for the processing of sulfide slimes.

ACKNOWLEDGMENTS

Support of this work by Particulate and Multiphase Processing Program of the National Science Foundation and the International Nickel Co. is gratefully acknowledged.

REFERENCES

1. Anathapadmanabhan, K. P., and P. Somasundaran. The Role of Unavoidable Chemical Species in Calcite/Apatite Flotation. AIME Annual Meeting, Atlanta, February 1977. Available upon request from P. Somasundaran, Mineral Engineering Dept., Columbia University, New York, N.Y.

2. Attia, Y. A., and J. A. Kitchener. Development of Complexing Polymers for the Selective Flocculation of Copper Minerals. Proc. 11th Internat. Miner. Proc. Cong., Cagliari, Italy, 1975, p. 1233.

3. Clauss, C. R. A., E. A. Appleton, and J. J. Vink. Selective Flocculation of Cassiterite in Mixtures with Quartz Using a Modified Polyacrylamide Flocculant. Internat. J. Miner. Proc., v. 3, 1976, p. 27.

4. Cooke, S. R. B., N. F. Schultz, and E. W. Lindross. The Effect of Certain Starches on Hematite and Quartz Suspensions. Trans. AIME, v. 193, 1952, p. 697.

5. Duggan, E. J. Fine-Grinding and Concentration at Climax. Mining and Metallurgy, June 1946, p. 323.

6. Engineering and Mining Journal. Tilden Based on Processing Breakthrough. v. 175, Nov. 1974, p. 140.

7. Farnand, J. R., H. M. Smith, and I. E. Puddington. Spherical Agglomeration of Solids in Liquid Suspension. Canad. J. Chem. Eng., v. 39, 1961, p. 94.

8. Friend, J. P., J. Iskra, and J. A. Kitchener. Cleaning a Selectively Flocculated Mineral Slurry. Trans. IMM, v. 83, 1973, p. C235.

9. Fuerstenau, D. W., S. Chander, and A. M. Abouzeid. The Concentration of Fine Particles. 1st Latin American Congress of Mining and Extractive Metallurgy, Chile, 1973. Available upon request from D. W. Fuerstenau, Dept. of Materials Science and Engineering, University of California, Berkeley, Calif.

10. Gaudin, A. M., J. O. Groth, and H. B. Henderson. Effect of Particle Size on Flotation. Trans. AIME, v. 96, 1931, p. 580.

11. Gaudin, A. M., and P. Malozemoff. Recovery by Flotation of Mineral Particles of Colloidal Size. J. Phys. Chem., v. 37, 1933, p. 579.

12. Gaudin, A. M., R. Schuhmann, and A. W. Schlechten. The Effect of Size on the Behavior of Galena Particles. J. Phys. Chem., v. 46, 1942, p. 902.

13. Greene, E. W., and J. B. Duke. Selective Froth Flotation of Ultrafine Particles of Slimes. Trans. AIME, v. 233, 1962, p. 389.

14. Hogg, R. T., W. Healy, and D. W. Fuerstenau. Mutual Coagulation of Colloid Dispersions. Trans. Faraday Soc., v. 62, 1966, p. 638.

15. J. M. Huber Corp. (by Robert N. Maynard, Bobby R. Skipper, and Nathan Millman). Clay Improvement. British Pat. 1,115,694, granted in 1968.

16. Iwasaki, I., W. J. Carlson, Jr., and S. N. Parmereer. The Uses of Starches and Starch Derivatives as Depressants and Flocculants in Iron Ore Beneficiation. Trans. AIME, v. 244, 1969, p. 88.

17. Kane, J. C., V. K. LaMer, and H. B. Linford. The Effect of Solid Contents on the Flocculation Behavior of Silica Suspensions. J. Phys. Chem., v. 68, 1964, p. 3539.

18. Kraus, G., and J. Dugone. Adsorption of Elastomer on Carbon Black. Ind. and Eng. Chem., v. 47, 1955, p. 1809.

19. Kuz'kin, S. K., and V. P. Nebera. Synthetic Flocculants in Dewatering Processes. National Lending Library of Science and Technology, Boston Spa, England, 1966, 344 p.

20. Levich, V. G. Physicochemical Hydrodynamics. Prentice-Hall, Englewood Cliffs, N.J., 2d ed, 1962, p. 213.

21. Lipatov, Yu. S., and L. M. Sergeeva. Adsorption of Polymers. John Wiley & Sons, New York, 1972.

22. Maynard, R. N., N. Millman, and J. A. Iannicelli. Removing Titanium Dioxide Impurities from Kaolin. Clays and Clay Miner., v. 17, No. 2, 1969, pp. 59-62.

23. Michaels, A. S. Aggregation of Suspensions by Polyelectrolytes. Ind. and Eng. Chem., v. 46, 1954, p. 1485.

24. Michaels, A. S., and O. Morelos. Polyelectrolyte Adsorption by Kaolinite. Ind. Eng. Chem., v. 47, 1955, p. 1801.

25. Napper, D. H. Flocculation Studies of Sterically Stabilized Polymers. J. Colloid and Interface Sci., v. 32, 1970, p. 106.

26. National Science Foundation. Adsorption from Flooding Solutions in Porous Media - A Study of Interactions of Surfactants and Polymers with Reservoir Minerals. Annual Report to NSA and a Consortium of Industrial Organizations. Columbia University, New York, 1977, p. 121. Available upon request from P. Somasundaran, Mineral Engineering Dept., Columbia University, New York, N.Y.

27. Pugh, R. J. Selective Coagulation in Quartz - Hematite and Quartz-rutile Suspensions. Colloid Polym. Sci., v. 252, 1974, p. 400.

28. Pugh, R. J., and J. A. Kitchener. Experimental Confirmation of Selective Coagulation in Mixed Colloidal Suspension. J. Colloid and Interface Sci., v. 38, 1972, p. 656.

29. ________. Theory of Selective Coagulation in Mixed Colloidal Suspensions. J. Colloid and Interface Sci., v. 35, 1971, p. 656.

30. Read, A. D. Selective Flocculation Separations Involving Hematite. Trans. IMM, v. 80, 1971, p. C24, C208.

31. ________. The Use of High Molecular Weight Polyacrylamides in the Selective Flocculation Separation of a Mineral Mixture. Brit. Polym. J., v. 4, 1972, p. 253.

32. Read, A. D., and C. T. Hollick. Selective Flocculation Techniques for Recovery of Fine Particles. Miner. Sci. Eng., v. 8, 1976, p. 202.

33. Sirianni, A. F., C. E. Capes, and I. E. Puddington. Recent Experience With the Spherical Agglomeration Process. Canad. J. Chem. Eng., v. 47, 1969, p. 166.

34. Slater, W., J. P. Clark, and J. A. Kitchener. Chemical Factors in the Flocculation of Mineral Slurries with Polymeric Flocculants. Proc. Brit. Cer. Soc., v. 13, 1969, p. 1.

35. Sresty, G. C., A. Raja, and P. Somasundaran. Selective Flocculation of Mineral Slimes Using Polymers. Recent Advances in Separation Science, v. 4, CRC Press, West Palm Beach, Fla., 1978, p. 93.

36. Sresty, G. C., and P. Somasundaran. Beneficiation of Mineral Slimes Using Modified Polymers as Selective Flocculants. XIIth Internat. Miner. Proc. Cong., partly in special publication v. I, Sao Paulo, Brazil, 1977, p. 160. Available upon request from P. Somasundaran, Mineral Engineering Dept., Columbia University, New York, N.Y.

37. Stromberg, R. R. and G. M. Kline. Adsorption of Polymers on Glass and Other Substances. Modern Plastics, v. 38, No. 8, 1961, p. 123; v. 38, No. 9, 1961, p. 241.

38. Trahar, W. J., and L. J. Warren. The Floatability of Very Fine Particles - A Review. Internat. J. Miner. Process, v. 3, 1976, p. 103.

39. Usoni, L., G. Rinelli, A. M. Marabini, and G. Ghigi. Selective Properties of Flocculants and Possibilities of Their Use in Flotation of Fine Minerals. Ind. Mineraria, v. 20, No. 4, 1969, pp. 167-169.

40. Warren, L. J. Slime Coating and Shear Flocculation in the Scheelite-Sodium Oleate System. Trans. IMM, v. 84, 1975, p. C99.

41. Wiese, G. R., and T. W. Healy. Effect of Particle Size on Colloid Stability. Trans. Faraday Soc., v. 66, 1970, p. 490.

42. Yarar, B., and J. A. Kitchener. Selective Flocculation of Minerals. Trans. IMM, v. 79, 1970, p. C23.

SUMMARY OF SYMPOSIUM

by

Maurice C. Fuerstenau[1] and Booker W. Morey[2]

This symposium addressed effectively the critical variables that influence sulfide flotation. The application of thermodynamics was treated in detail, as these concepts have brought us to our present level of understanding in sulfide flotation.

Thermodynamics is an equilibrium state, of course, and does not provide detailed mechanisms of interaction between the collector and sulfide surface. Clearly, additional techniques are required to learn these mechanisms, and electrochemical and chemical physics techniques have proven useful.

With respect to the paper on "Thermodynamics of Reagent Mineral Interactions," Dr. Douglas W. Fuerstenau described how adsorption affects interfacial phenomena and ultimately controls flotation. Adsorption can be either electrostatic in nature, or can involve a chemical reaction between the collector and mineral surface.

Chemisorption is one of the major phenomena responsible for selectivity in sulfide systems. A number of examples were shown where heats of reaction of known chemical reactions correlate very well with observed heats of adsorption in flotation systems. As pointed out by Dr. Douglas W. Fuerstenau, the use of Eh-pH diagrams is extremely useful in selecting conditions of chemisorption.

Detailed adsorption studies aimed at elucidating the complex system, oxygen-sulfide mineral-thiol collector, were summarized by Dr. Maurice C. Fuerstenau from work sponsored by the National Science Foundation and carried out at the South Dakota School of Mines and Technology as well as from data in the technical literature. In a system that is virtually free from oxygen, that is, containing less that 10^{-6} mole fraction oxygen in inert nitrogen and less that 5 ppb oxygen in water, chemisorption of xanthate occurs on sulfide surfaces.

---

[1] South Dakota School of Mines and Technology, Rapid City, S. Dak.
[2] Envirotech Corp., Menlo Park, Calif.

In the presence of oxygen, sulfide minerals are floated either by chemisorption of xanthate or by electrochemical formation and adsorption of dixanthogen. Chalcocite, galena, and sphalerite are floated by chemisorption of xanthate, while pyrite clearly requires electrochemical oxidation of xanthate to dixanthogen.

Dr. Paul E. Richardson described partial results aimed at understanding the electrochemical mechanism of the interaction of oxygen with semiconducting sulfide minerals. These kinds of charge transfer studies have provided insight into surface reactions that cannot be obtained by other means.

From combined capacitance, photovoltage, and electrochemical measurements, it was found that the reduction of oxygen on the surface is a two-electron process and occurs independently of whether the galena is n- or p-type.

The rate of oxygen reduction is first order with respect to oxygen concentration, with the "apparent" kinetics strongly affected by the exact partition of the potential between the solid and the electrolyte phases.

Future studies that will include xanthate in the system should provide a much more complete picture than has been previously available. We look forward to learning these results.

Dr. Frank F. Aplan showed a number of interesting effects that the semiconducting properties of galena exhibit on the flotation properties of this mineral. For example, n-type galena responds to flotation much better than p-type galena when dixanthogen is added as collector.

In oxides, the deliberate change in concentration of holes affects the PZC in predictable ways that are confirmed by flotation response. Dr. Aplan used nickel oxide as the subject of his study. In discussing this paper, Professor Nathaniel Arbiter suggested that the wide range in observed cassiterite floatability might easily be caused by substitution of iron, molybdenum, and titanium in the cassiterite.

Activation and deactivation in sulfide flotation were reviewed by Dr. Douglas W. Fuerstenau. A very clear picture emerged that activation is controlled by ion exchange substitution of metal ions that form less soluble sulfides than the host mineral. Copper and silver activation of sphalerite and copper activation of pyrrhotite were presented.

Deactivation follows the same thermodynamic principles. However, the kinetics of reaction suggest that other phenomena may be involved.

The use of sulfite and sulfur dioxide as depressants in sphalerite flotation was presented by Dr. Garrett R. Hyde. From his detailed work, he concluded that depression was caused by the formation and adsorption of a sulfide precipitate on the sphalerite surface.

Dr. George W. Poling pointed out a critical double standard in use of existing flotation knowledge in creating environmental constraints in the operation of a concentrator. While the adsorption of metal ions and reagents on mineral surfaces has been known and used for years, existing pollution control regulations discount such phenomena as having any effect on the aqueous concentration of these reagents. A number of examples were presented to show the effect of removing metal ions from solution by adsorption on naturally occurring tailings.

The disposal of tailings into water bodies in certain instances can be environmentally safe and dependable. The example of Island Copper shows that generalized legislation prohibiting this form of disposal is unnecessary and unrealistic.

In discussing Industrial Flotation Research and its Interface with Academics, Professor Nathaniel Arbiter described the traditional roles of each group and was disappointed at the wide gulf between them. Specific examples were cited where research has had a significant impact on industrial practice. Some of these include: the application of hydrodynamics to flotation machinery; creation of specific collectors for sulfide minerals; application of control theory to mill performance, and finally, the invention and application of selective flocculation of iron ores.

He felt very encouraged that the new body of fundamental flotation information, as discussed in the symposium, could have a significant impact in the future on flotation operations. A number of examples were cited to illustrate this point.

Dr. P. Somasundaran presented data to show the decrease in flotation recovery in sulfide particles smaller than 10 µm. He attributed this effect to smaller mass as well as increased surface oxidation. Dr. Somasundaran outlined conditions required for selectivity in flotation or agglomeration and outlined procedures for creating selective adsorption. He identified kinetics, dosage, chemical properties of reagent and zeta potential of the mineral as controllable variables. These variables were illustrated with chalcopyrite and quartz.

The goal of the symposium was to discuss current and emerging problems in flotation to define areas that need to be emphasized in future fundamental research. The incentive is to increase the recovery of the nation's mineral resources.

In the case of copper, 15 to 20 percent of the copper mined and milled is lost because flotation is not efficient. Losses are even higher in the case of molybdenum.

Some of the research needs in flotation fundamentals that must be met include:

1. Further studies of the role that oxygen assumes in sulfide flotation to provide a firm understanding of mechanisms in sulfide-thiol systems.

2. The surface properties of the copper and molybdenum sulfide minerals that do not respond to flotation must be established.
3. How can surfaces of oxide copper minerals be made hydrophobic and floatable? Present losses of these minerals are very high.
4. The fundamental limitations of fine particle flotation must be determined. For example, what are the trade-offs between chemical and physical phenomena that can affect fine particle flotation?
5. Can concepts of selective flocculation be applied to flotation?

To our knowledge, this symposium is one of the first that has been devoted to a rather narrow but extremely important area of the domestic mineral industry. This symposium has provided a thorough state-of-the-art review and an excellent forum for the consideration and extension of these concepts. On behalf of the participants, we would like to congratulate the Symposium Committee and would hope that similar symposia might be arranged on other timely topics.

☆U.S. GOVERNMENT PRINTING OFFICE: 1980-603-102/17